Coherence Dynamics in non-Markovian Quantum Brownian Motion

THESIS SUBMITTED FOR THE DEGREE OF DOCTOR OF PHILOSOPHY

Mehsati Sapphire Lally

URN: 6553764

UNIVERSITY OF SURREY

Supervisors:

Prof. Jim Al-Khalili

Dr Andrea Rocco

Quantum Biology Doctoral Training Centre

University of Surrey

November 2021

Abstract

We present a perturbative non-Markovian extension to the Caldeira-Leggett system + environment model of quantum Brownian motion, valid for general potentials and high temperatures. By expanding the Laplace transforms of the noise and dissipation kernels, we derive a master equation which describes the evolution of the reduced density matrix of a system of interest. By using a Fourier transform approach combined with the method of characteristics, an analytic solution is derived for the free particle case. The solution is plotted and discussed. The decoherence process is altered only slightly by the introduction of non-Markovianity, which we explain with a timescale argument. A new phenomenon which we term "lateral coherence" is observed. This is found to correspond to a resurgence of the l_1-norm of coherence, at times much later than the decoherence time. We find that the coherence resurgence causes a transient reduction in the von Neumann entropy, and link this to an increasing body of work which makes links between non-Markovianity and entropy decrease. We show that this effect is independent of the high-frequency behaviour of the spectral density. Finally, we make some speculations about the relevance of our results in quantum biology, and suggest future avenues of research.

Declaration

This thesis and the work to which it refers are the results of my own efforts. Any ideas, data, images or text resulting from the work of others (whether published or unpublished) are fully identified as such within the work and attributed to their originator in the text, bibliography or in footnotes. This thesis has not been submitted in whole or in part for any other academic degree or professional qualification. I agree that the University has the right to submit my work to the plagiarism detection service TurnitinUK for originality checks. Whether or not drafts have been so-assessed, the University reserves the right to require an electronic version of the final document (as submitted) for assessment as above.

Signature:

Date: 25/11/21

"I don't like it, and I'm sorry I ever had anything to do with it."

—Erwin Schrödinger on quantum mechanics

Acknowledgements

No woman is an island, and over the duration of my PhD I have felt deeply supported in many ways, and by many people. First and foremost, my thanks go to my supervisors Prof Jim Al-Khalili and Dr Andrea Rocco, not only for the intellectual and emotional bolstering, but for the opportunity to spend the last three years asking wonderful questions about wonderful topics. My colleagues at the Leverhulme Quantum Biology Doctoral Training Centre have provided companionship and solidarity as well as countless discussions about work; thanks especially go to Lester Buxton, who has shared many of my frustrations and joys.

The University of Surrey has been a fantastic academic home for the last three years - in no small part thanks to the food at Young's Kitchen. My undergraduate institution, the University of Manchester, will always have a place in my heart for helping bring my love of physics from daydream to reality. In particular, I fondly remember the days I spent there working with Gabriel Hawkins-Pottier and Prof Niels Walet, taking my first steps as an independent researcher.

No words can describe the gratitude I feel towards my family and friends for their continued love in the face of more than three years of late-night conversations about quantum physics. To my parents, who have always been there when I needed them, my partner, who has seen all angles of this process and stuck with me throughout, and my friends, who have been an invaluable source of laughter and wine: from the bottom of my heart, thank you.

Finally, I would like to note that any remaining typos in this work are almost certainly the result of my cat walking ruthlessly all over my laptop. She makes no apology, and neither do I.

Contents

Chapter 1

Introduction

Quantum mechanics is the theory that describes how matter behaves at the smallest scale. The world it describes - the quantum realm - is very different from the macroscopic classical world we interact with; it describes probabilities, rather than definite values, and imposes hard restriction on how precisely we can define systems. Quantum systems demonstrate a range of unique behaviours, including superposition between states, tunnelling across barriers, and entanglement between systems. These quantum effects are observed on a macroscopic scale only in very particular systems, such as superconductors, micromechanical resonators, and Bose-Einstein condensates [1]. However, because quantum effects are responsible for nuclear and atomic phenomena, hence much of physics and chemistry as we understand them, the world we interact with is underpinned by the rules of quantum mechanics - meaning that classical physics emerges from quantum physics. Despite this, many conceptions of quantum physics require a sharp boundary to be drawn between objects and systems that must be described using quantum physics, and those that are described by classical physics. An original description of the theory by Niels Bohr requires a classical measurement apparatus which is capable of interacting with the quantum system, but does not itself display any quantum properties [2]. The drive to understand how quantum behaviour transitions to classical behaviour, in a deterministic and prescriptive way, led to celebrated thought experiments such as Schrödinger's cat [3] and Wigner's friend [4].

In the 1980s, Wojciech Zurek pioneered an approach to the quantum-classical transition that focused on a property called quantum coherence [5–7]. When a system possesses coherence, it is able to behave in a fundamentally quantum way, maintaining superpositions between classically distinct states. But coherence is, like energy or information, a property that can be dissipatively

lost from a system by interaction with a large environment. The loss of coherence, which typically happens very rapidly, is called decoherence, and provides a physical mechanism for the transition between quantum and classical behaviours [8]. It is no longer necessary to invoke a classical measurement apparatus which obeys fundamentally different rules - instead, the measurement apparatus can be described as a large reservoir of quantum mechanical systems [9, 10]. Coherence spreads out in the reservoir and is diluted. Macroscopic quantum effects are also suppressed by decoherence, explaining the emergence of systems which can be described by classical, rather than quantum, physics.

1.1 Quantum Biology

When quantum systems are in contact with their surrounding environments, they typically retain coherence best when those environments are at very low temperatures, and thermal fluctuations do not dominate over quantum fluctuations. Biological systems do not display ideal conditions for persistent quantum coherence as they involve large numbers of large molecules, interacting at high temperatures. However, there are several processes in biological systems that seem to show evidence of non-trivial quantum mechanisms, which have macroscopic effects [11, 12]. The term "quantum biology" refers to the study of these mechanisms, such as coherent transport in photosynthesis [13–16], spin entanglement in avian magnetoreception [17–21], and tunnelling by electrons and protons in a variety of biological contexts [22–25]. A brief discussion of quantum mechanics in these biological contexts is presented below. This is not an exhaustive review of the study of quantum mechanisms in biological processes; additional proposals include the entanglement of living bacteria with incident light [26] and coherent transport in ion channels [27, 28]. A thorough and up-to-date review of the field can be found in Ref. [12].

1.1.1 Photosynthesis

In photosynthetic organisms, light is harvested using a transport network of chromophores, which are linked to a reaction centre [12]. Chromophores typically consist of a protein scaffold structure, surrounded by an array of pigments which are capable of supporting an excitation. The excitation is transported to the reaction centre with efficiency approaching 100 %. Within each complex, there are both weakly and strongly interacting components. The weak interactions can be fairly well described by FRET (Förster Resonance Energy Theory), which describes

a series of classical hops. However, because the complex also contains strongly coupled components, FRET is not alone sufficient to describe the process. Random energy transfer between pigments would lead to far lower efficiency than observed, as the excitations decay in a time shorter than the average transfer time [13]. Some particularly densely arranged complexes, for example the LH2 of purple bacteria, display excitations that are not localised but spread over multiple pigments. These considerations led to hypotheses that the transport takes place via coherent quantum mechanical mechanisms, rather than classical hopping.

Delocalised excitations in the purple bacteria LH2 were probed using 2DES (2D electron spectroscopy) [15], and a phenomenon called quantum beating was identified. This is a characteristic oscillation in the intensity of emitted radiation from a molecule due to it being in a time-dependent superposition state. The quantum beating in the LH2 light harvesting complex of purple bacteria was attributed to electronic coherences between chromophores in the system [12]. A theoretical exciton creation/annihilation model of the LH2 complex predicted similar quantum beating [14], which provides evidence for the hypothesis that quantum transport is responsible for the efficiency of light harvesting.

1.1.2 Avian Magnetoreception

The navigatory ability of European robins was found to be magnetically sensitive by observing the behaviour of caged birds in geological and induced magnetic fields [17]. A mechanism has been proposed to explain this phenomenon which involves the interaction of incident photons with the light receptor molecule cryptochrome. The mechanism utilises the so-called radical pair mechanism, which involves a pair of entangled (or correlated) electrons oscillating in a way that is sensitive to the Earth's magnetic field.

A radical, or a free radical, is a biological molecule with an unpaired electron [12]. In general, radicals are highly chemically reactive. Because electrons have spin, they are sensitive to magnetic fields, and correlations between electrons are particularly sensitive to magnetic fields. Therefore, a radical pair - consisting of radicals which have entangled electrons - can also display magnetic field sensitivity. In the radical pair mechanism, incident light excites two radicals, which become entangled. They oscillate in a superposition of singlet and triplet spin states [19] for a characteristic relaxation time, before decohering to either a singlet or a triplet

state. The singlet state will cause a different product than the triplet, so the ratio of singlet-triplet products conveys information about the direction of the incident magnetic field. In this case, decoherence is essential for the mechanism to work, as the pair need to relax in order for the information to be conveyed [21]. However, the molecular and chemical mechanisms are not yet well understood, so a definitive test of the radical pair hypothesis for avian magnetoreception is not currently possible.

1.1.3 Tunnelling in Nucleotides

In the Watson-Crick model of DNA [29], genetic information is stored in the hydrogen bonds between four distinct molecules called nucleotides: adenine (A), cytosine (C), guanine (G), and thymine (T). The molecules are paired together between the two strands of DNA such that the A-T pair is joined by two hydrogen bonds, and the G-C pair is joined by three bonds. These pairs involve the canonical forms of the nucleotides, displayed in Figure 1.1. However, less common tautomeric forms of the nucleotides, denoted by a star, can also occur despite being energetically less favourable. These occur when the hydrogen bonds are mismatched, which is demonstrated in Figure 1.2. When a base pair is tautomerized, it can cause mismatches: for example, tautomeric adenine, A*, pairs to canonical cytosine [22]. The DNA replication process then propagates this error: when the strand is split and replicated, the C that was previously paired to A* will be re-paired to a G. This means there is a new DNA strand with a G, where there was previously an A. This single-nucleotide error is referred to as a point mutation, and can cause errors in genetic coding.

A hydrogen bond can be modelled by a proton in a "double-well" potential, such that the minima of the potential represent possible configurations of the proton; typically one well is deeper than the other, and this represents the stable state. If a proton were to tunnel from the deeper well to the shallow well, it would cause a transition from the canonical to the tautomeric form of the base pair [22]. This was first suggested by Löwdin, and recent work has shown that quantum tunnelling is a likely contributor to tautomerization in the G-C base pair [30].

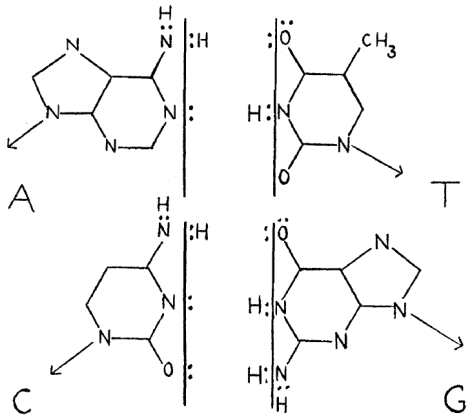

Figure 1.1: The canonic base pairs found in the DNA molecule [22]. Adenine is paired to thymine by an upper hydrogen bond localised to the adenine side, and a lower hydrogen bond localised to the thymine side. The G-C base pair has three hydrogen bonds, all localised to either the left or right.

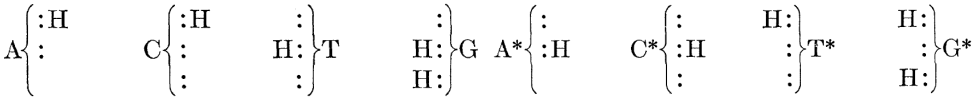

Figure 1.2: (a) the placement of hydrogen bonds in the canonical base pairs. (b) the placement of hydrogen bonds in the tautomeric base pairs. Note that in tautomerised adenine, the hydrogen bond is now in the middle position, meaning that it can pair with canonical cytosine [22].

1.2 Open Quantum Systems

Quantum biology presents a conceptual problem for those quantum physicists concerned with mechanisms for decoherence and the quantum-classical transition. If coherence is lost so rapidly that macroscopic quantum effects are suppressed - typically on femtosecond scales [2] - how is it possible that biological processes, which typically occur over timescales of microseconds or longer [12], are able to manipulate coherent effects? This is the question underpinning the work in this thesis, which aims to explore physical mechanisms for delaying decoherence and therefore extending the timescale over which non-trivial quantum effects can occur.

The natural mathematical approach to describe and develop models of decoherence is open quantum systems [9]. The standard Schrödinger formulation of quantum mechanics describes a wavefunction evolving deterministically according to the Schrödinger equation, in a closed system: no exchange of energy, information, or probability with the outside world is possible. However, decoherence involves a quantum system which interacts and exchanges energy, information, and coherence with a great many other systems. The motivation for developing

a theory of open quantum systems is to generalise our understanding of quantum physics to include systems that decohere.

The general principle underpinning open quantum systems is to define a system, its environment, and the interaction between them [9]. It is important that the system and the environment are distinct. The dynamics can usually be separated into a term that describes the isolated system, a term that describes the isolated environment, and a term that describes the interaction between them. Standard quantum mechanics - i.e. the Schrödinger equation - can be used to find the equation of motion for the complete system. A variety of mathematical techniques can be used to *reduce* the dynamics, by integrating out the irrelevant environment degrees of freedom, leaving only an equation of motion for the system that we are interested in, in the presence of its environment. This reduction is what allows the system to undergo non-Schrödinger dynamics. As the system builds up correlations with the environment, coherence is dissipated via each of the correlations. Because the environment is very large compared to the system of interest, the coherence dilutes through the environment rapidly, causing decoherence.

Quantum Brownian motion is a successful model of open quantum systems [9, 31] and is inspired by classical Brownian motion, which describes the random motion of a particle suspended in a fluid. Brownian motion is a model of stochastic dissipation: via random interactions with many particles that make up the fluid, the Brownian particle experiences a friction-like force that causes it to lose energy, while thermal fluctuations prevent it from coming entirely to rest. This is a good start for building a model capable of describing decoherence. In a quantum analogue of Brownian motion, the dissipative nature of the interaction causes decoherence, and the fact that the particle never comes to rest entirely will prevent violations of the uncertainty principle.

The model of quantum Brownian motion is a system in a general potential, coupled linearly in position to an infinite reservoir of non-interacting quantum harmonic oscillators. The high-temperature limit ($\hbar\omega \ll kT$) ensures that quantum fluctuations of the particle have much smaller magnitude than the thermal fluctuations of the oscillator environment. The spectral density, which describes the features of the environment, is Ohmic, meaning that it is linearly dependent on the frequency of environment oscillators. This imposes a condition called Marko-

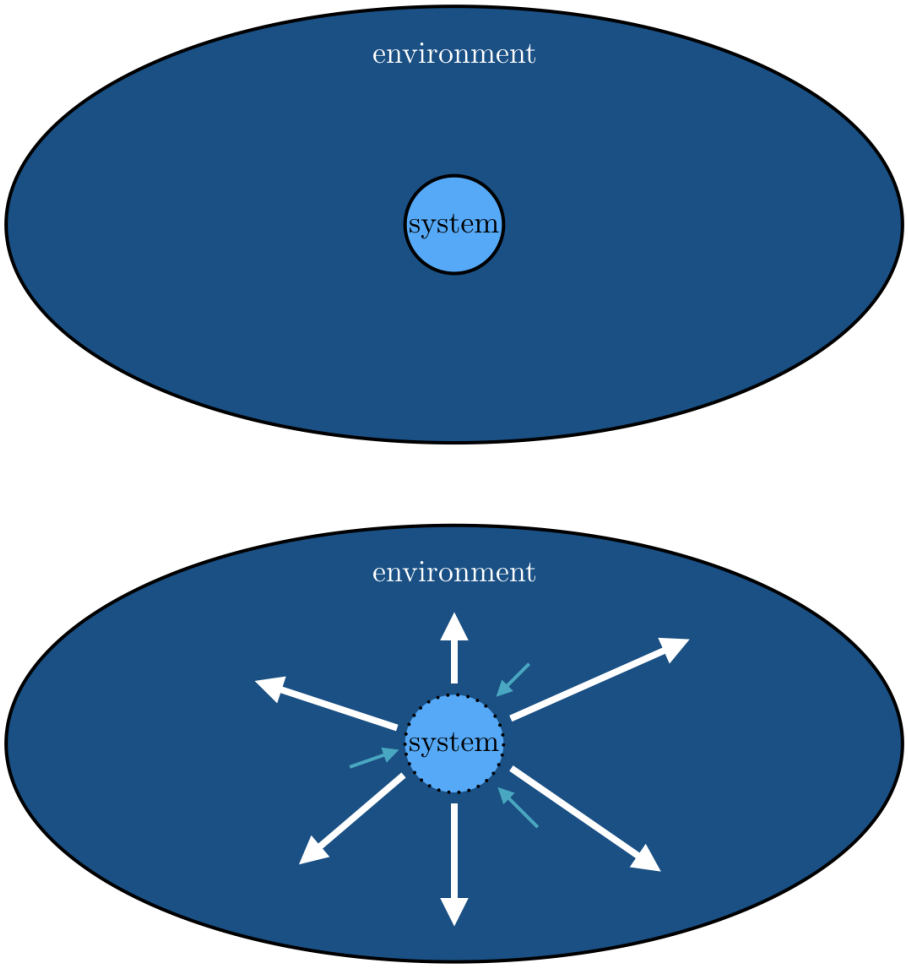

Figure 1.3: (Top) A closed quantum system. It may be in the presence of an environment, but there is no interaction between the two systems. (Bottom) An open quantum system. Interaction between the system and environment is present. Energy, information, and coherence can be transferred from system to environment (and vice versa, with lower probability).

vianity onto the interaction. In essence, this means that the system has no memory of its previous states.

Quantum Brownian motion describes very rapid decoherence. However, it is a good baseline model for exploring the problem of decoherence in quantum biology: it is valid for physiological temperatures and general potentials, and the final equation of motion for the quantum system depends only on quantities that are in principle experimentally determinable. In this thesis, we will attempt to relax the strict Markovianity condition of the quantum Brownian motion model and explore the ramifications on the decoherence time.

Open quantum systems approaches have been used in quantum biology in a variety of contexts. A Markovian model of the radical pair mechanism [20] displays interesting coherence behaviour, where even numbers of nuclei in the radical molecule preserve coherence via the hyperfine interaction, but odd numbers of nuclei do not. A recent study using Markovian quantum Brownian motion has found that tunnelling in the G-C base pair is a significantly more likely cause of tautomerization than any other process [30]. The polaron representation has been used to show that resonances between system and bath frequencies can extend coherence in light-harvesting complexes [32, 33], and a Markovian open quantum systems approach has been shown to accurately model features of cellular membrane transport [34]. In this thesis, we aim to provide a more general understanding of non-Markovian open quantum systems, which will be applicable across a wide range of biological processes.

1.3 Hypothesis

We hypothesise that extending the model of quantum Brownian motion [31] to include Ohmic spectral densities with cut-off functions will introduce non-Markovianity into the resultant dynamics, and therefore increase the predicted lifetime of quantum coherences in the system of interest, allowing non-trivial quantum behaviours to occur over longer timescales. When biologically relevant parameters are applied, our predictions will have relevance for assessing the credibility of hypotheses in quantum biology, including in situations which involve proton tunnelling in a double-well potential. We hypothesise that our model will predict long-lived coherence systems with biologically relevant parameters, and therefore provide evidence for non-trivial quantum effects in biology. We further hypothesise that the more non-Markovian the interaction between system and bath, the longer quantum coherence will persist in the system. This is based on an argument from quantum information theory that describes decoherence as a loss of quantum information from the system of interest to the environment, and characterises non-Markovian dynamics by the presence of information backflow [35], meaning that quantum information is localised in non-Markovian systems for a longer period of time.

1.4 Aim

We aim to construct an extended model of quantum Brownian motion as initially described in [31] to include the general class of Ohmic spectral densities. We will follow the derivation laid out by Caldeira and Leggett and build on the perturbative expansion approach pioneered by Werren [36, 37] to obtain an equation of motion for the reduced dynamics of a system interacting with a finite Ohmic bath, described by a spectral density of the general Ohmic class. In contrast to the Hu, Paz, and Zhang [38] description of non-Markovian quantum Brownian motion, the master equation will not be restricted to harmonic oscillator potentials, but will instead describe a system which experiences an arbitrary potential. We expect that introducing non-Markovianity into the model will affect the reduced dynamics of the system in such a way to non-trivially modify the coherence dynamics, and in order to explore this we will use an appropriate metric of coherence [39] to calculate how much coherence is present in the system as it evolves according to the equation of motion. We then propose some interesting avenues for further investigation, including schemes for the application of this work in quantum biology.

1.5 Outline

The remainder of this thesis is structured as follows:

In Chapter 2, we cover the theoretical background required for the topics discussed in this thesis. We start by reviewing some foundational concepts in quantum mechanics, then move on to the topic of open quantum systems. This includes the properties and uses of the density matrix. Then we discuss its evolution via various models of open quantum systems. Some key topics in open quantum systems are spectral densities, decoherence, and positivity. We include a brief overview of some topics in quantum thermodynamics, and how they are applied to open quantum systems. Chapter 3 introduces the Caldeira-Leggett model of open quantum systems in detail [31]. The resulting dynamics are discussed, as well as the corresponding Fokker-Planck equation in the classical limit. In Chapter 4 we describe the mathematical formulation of non-Markovianity, including its quantification via the so-called RHP (Rivas, Huelga, and Plenio [40]) and trace distance measures, and we review current approaches to non-Markovian open quantum systems.

In Chapter 5, the non-Markovian extension to quantum Brownian is derived, following the approach pioneered by Werren [36, 37]: an Ohmic spectral density with harsh cut-off is inserted into the Caldeira-Leggett propagator, and the exact description of the system dynamics is truncated to yield a first-order non-Markovian master equation. The resulting master equation is given an exact solution in the free particle case, which is used to calculate the l_1 norm of coherence across the evolution of the system. The steady state of the system is obtained. A quantum thermodynamical argument is used to explain the results and situate our work in the context of the wider literature. The purity and uncertainty of the system are calculated as a check on consistency. The Wigner equation which corresponds to the non-Markovian master equation is derived, and connections are made between the non-Markovian master equation and a different class of master equations.

In Chapter 6, we generalise the analysis performed in Chapter 5 to include various cut-off functions of the Ohmic spectral density. A pattern is noticed and demonstrated by fully generalising the analysis to an arbitrary Ohmic spectral density (subject to a small number of algebraic constraints). A general non-Markovian Ohmic master equation is obtained and the dynamics compared to the harsh cut-off case. Some connections to relevant results in the literature are discussed, and tentative connections are made to concepts from renormalisation.

In Chapter 7, we consolidate the discussion points raised in Chapters 5 and 6, as well as making several suggestions for future avenues of research. We consider practical applications of the work undertaken in this thesis, with particular focus on the field of quantum biology.

Chapter 2

Theory of Open Quantum Systems

2.1 Quantum States and Operators

In the standard formulation of quantum mechanics, the familiar time-dependent Schrödinger equation

$$-\frac{\hbar^2}{2m}\frac{\mathrm{d}^2}{\mathrm{d}x^2}\Psi(x,t)+\hat{\mathrm{V}}(x)\Psi(x,t)=i\hbar\frac{\mathrm{d}}{\mathrm{d}t}\Psi(x,t) \tag{2.1.1}$$

describes unitary evolution of the wavefunction $\Psi(x,t)$ of a quantum system in the presence of a real potential $\hat{\mathrm{V}}(x)$, and the time-independent Schrödinger equation

$$-\frac{\hbar^2}{2m}\frac{\mathrm{d}^2}{\mathrm{d}x^2}\Psi(x,t)+\hat{\mathrm{V}}(x)\Psi(x,t)=E\Psi(x,t) \tag{2.1.2}$$

describes the stationary states of the wavefunction. The wavefunction is a mathematical representation of all the accessible information about the position, energy, and other properties of the system, and can be used to determine expectation values and probabilities associated with measurements on the system. Unitary evolution has the property that inner products are preserved, such that

$$|\Psi(t)|^2=|\Psi(0)|^2 \tag{2.1.3}$$

This means that evolution under the Schrödinger equation conserves probability.

Using Dirac bra-ket notation, the state is represented as a ket, $|\Psi\rangle$ in the complex Hilbert space $\mathcal{H}$, with the wavefunction formally written as the inner product $\Psi(x,t)=\langle x|\Psi(t)\rangle$. The

state $|\Psi\rangle$ has unit norm, i.e. $\langle\Psi|\Psi\rangle = 1$, and the dynamics described by the Schrödinger equation do not change the norm [41]. An important concept is the overlap between two states, which is given by the inner product, i.e. the overlap between $|\Phi\rangle$ and $|\Psi\rangle$ is $\langle\Phi|\Psi\rangle$. The overlap gives a measure of how easy it is to discern between two states, or how likely it is that two states would give you the same measurement results.

By introducing a complete basis, i.e. a collection of orthonormal states which span the Hilbert space in which the state lives, we can write the state $|\Psi\rangle$ as a superposition:

$$|\Psi\rangle = \sum_n c_n |n\rangle , \tag{2.1.4}$$

where the coefficients obey $\sum_n |c_n|^2 = 1$. Orthonormal states have the property $\langle n_i|n_j\rangle = \delta_{ij}$, i.e. they do not have any overlap with other states in the basis, and their overlap is normalised to 1.

Operators act on states in the Hilbert space. They are given by the outer product of two state vectors $|A_1\rangle$, $|A_2\rangle$, such that the result of applying an operator to a state vector is always another state vector:

$$\begin{aligned} \hat{\mathrm{A}} &= |A_1\rangle\langle A_2| \\ \implies \hat{\mathrm{A}}\,|\Psi\rangle &= (\langle A_2|\Psi\rangle)\,|A_1\rangle . \end{aligned} \tag{2.1.5}$$

The Schrödinger equation can be written as an operator equation

$$\hat{H}\,|\Psi\rangle = i\hbar \frac{\mathrm{d}}{\mathrm{d}t}\,|\Psi\rangle , \tag{2.1.6}$$

where the Hamiltonian operator is

$$\hat{H} = -\frac{\hbar^2}{2m}\nabla^2 + \hat{\mathrm{V}}. \tag{2.1.7}$$

In this expression, the first term represents kinetic energy, with $\nabla^2 = \sum_i \frac{\partial^2}{\partial x_i^2}$, and the second term represents potential energy, via the potential operator $\hat{\mathrm{V}}$. The solution of the Schrödinger equation is

$$|\psi(t)\rangle = \mathrm{e}^{-iHt/\hbar}\,|\psi(0)\rangle , \tag{2.1.8}$$

where $\exp\{-\frac{iHt}{\hbar}\}$ is often referred to as the unitary operator, $\hat{U}(t)$. Because the solution of the Schrödinger equation describes unitary evolution, the operator $\hat{U}$ has the property that $U^{-1} = U^{\dagger}$ - i.e. the inverse is equal to the Hermitian conjugate.

With a choice of orthonormal basis, an operator can be written as the matrix

$$\hat{\mathrm{A}}_{nm} = \langle n|\hat{\mathrm{A}}|m\rangle\,, \tag{2.1.9}$$

and this is referred to as selecting a representation for the operator. Given a representation, we can define the trace of an operator as

$$\mathrm{Tr}(\hat{\mathrm{A}}) = \sum_n \langle n|\hat{\mathrm{A}}|n\rangle\,. \tag{2.1.10}$$

In a continuous basis (like position), the sum is replaced by an integral:

$$\mathrm{Tr}(\hat{\mathrm{A}}) = \int \mathrm{d}x\, \langle x|\hat{\mathrm{A}}|x\rangle\,, \tag{2.1.11}$$

The trace is basis-independent: any selected basis will give the same result.

We can use operators acting on states to obtain information about the quantum system we are interested in. In general, an operator is associated with an observable - a measurable property of the system - like energy, momentum, or position. Each operator has a preferred basis called the eigenbasis, which is made up of eigenstates. The effect of an operator acting on one of its eigenstates is to multiply it by an eigenvalue,

$$\hat{\mathrm{A}}\,|n\rangle = a_n\,|n\rangle\,. \tag{2.1.12}$$

For example, the Hamiltonian operator $\hat{\mathrm{H}}$ is associated with energy, and the eigenvalues E_n of the Hamiltonian operator are the allowed energies of the system; eigenstates are states of constant and definite energy.

The result of a measurement $\hat{\mathrm{A}}$ on a state $|\Psi\rangle$ with eigenbasis decomposition given by Eq. (2.1.4) will be one of the eigenvalues in the decomposition, and the superposition of states will

be collapsed to the corresponding eigenstate. The probability of the measurement result being a_m is the state overlap between $|\Psi\rangle$ and $|m\rangle$, i.e.

$$\begin{aligned} \mathrm{P}(a_m) &= |\langle m|\Psi\rangle|^2 \\ &= |\langle m| \left(\sum_n c_n |n\rangle \right)|^2 \\ &= |c_m|^2. \end{aligned} \tag{2.1.13}$$

The expectation value of an operator is defined, in either Dirac notation or wavefunction notation, as

$$\begin{aligned} \langle \hat{\mathrm{A}} \rangle &= \langle \Psi | \hat{\mathrm{A}} | \Psi \rangle \\ &= \int \Psi^*(x) \hat{\mathrm{A}} \Psi(x) \mathrm{d}x. \end{aligned} \tag{2.1.14}$$

A particularly useful class of operators called projection operators are given by the outer product of a ket with itself,

$$\hat{P}_\Psi = |\Psi\rangle\langle\Psi| . \tag{2.1.15}$$

By inserting the completeness identity

$$\sum_n |n\rangle\langle n| = \hat{I}, \tag{2.1.16}$$

expectation values and state overlaps can be written in terms of a trace of the projection operator,

$$\begin{aligned} \langle\Psi| \hat{\mathrm{A}} |\Psi\rangle &= \langle\Psi| \hat{\mathrm{A}} \sum_n |n\rangle\langle n| |\Psi\rangle \\ &= \sum_n \langle n| \left(|\Psi\rangle\langle\Psi| \hat{\mathrm{A}} \right) |n\rangle \\ &= \mathrm{Tr}(\hat{P}_\Psi \hat{\mathrm{A}}), \end{aligned} \tag{2.1.17}$$

and

$$\begin{aligned} |\langle\Phi|\Psi\rangle|^2 &= \langle\Phi|\Psi\rangle \langle\Psi| \sum_n |n\rangle\langle n| |\Phi\rangle \\ &= \sum_n \langle n| \left(|\Phi\rangle\langle\Phi| |\Psi\rangle\langle\Psi| \right) |n\rangle \\ &= \mathrm{Tr}(|\Phi\rangle\langle\Phi| P_\Psi). \end{aligned} \tag{2.1.18}$$

This demonstrates that the projection operator $|\Psi\rangle\langle\Psi|$ contains the same information as the wavefunction $\Psi(x)$, and can be manipulated to yield the same predictions about measurement outcomes. We can then use it to define a more general class of states, called mixed states. A mixed state is a statistical ensemble of states described by a weighted sum, referred to as the density operator. We denote this [9] by

$$\rho = \sum_k p_k \left|\Psi_k\right\rangle\!\left\langle\Psi_k\right| . \tag{2.1.19}$$

The density operator refers to a set of states $|\Psi_k\rangle = \sum_n c_n^{(k)} |n\rangle$, prepared with (classical) probabilities p_k [42]. In the eigenstate decomposition, we can write

$$\rho = \sum_{k,n,m} p_k c_n^{(k)} c_m^{(k)*} \left|n\right\rangle\!\left\langle m\right| . \tag{2.1.20}$$

The probabilities, or weights, are restricted by $\sum_k p_k = 1$. When there is only one term in the summation, or equivalently when $p_k = 1$ for some value of k, then the density operator describes a pure state - i.e. a state that can be described using a single wavefunction. Otherwise, the density operator cannot be described using a single wavefunction.

The density matrix is constructed by choosing a representation for the density operator. The position representation is particularly useful, in analogue to the wavefunction $\Psi(x)$. This is found by taking matrix elements:

$$\begin{aligned} \rho(x,y) &= \langle x| \rho |y\rangle \\ &= \sum_k p_k \langle x|\Psi_k\rangle \langle\Psi_k|y\rangle \\ &= \sum_k p_k \Psi_k(x) \Psi_k^*(y). \end{aligned} \tag{2.1.21}$$

A useful property of the density matrix is that the trace is equal to one. This is equivalent to the statement that $\sum_k p_k = 1$. Further to this, pure states have the property that $\rho = \rho^2$, and so

$$\mathrm{Tr}(\rho^2) = \mathrm{Tr}(\rho) = 1. \tag{2.1.22}$$

This can be used to identify when a state is pure, and in fact the purity of the density matrix

is a property defined by

$$\mu(\rho) = \mathrm{Tr}(\rho^2). \tag{2.1.23}$$

This is fixed between $(0, 1]$, and can be used to determine the degree of mixedness of a density matrix: the closer to 1, the more pure it is, and the closer to 0 the more mixed.

The equation describing unitary dynamics of the density operator can be derived by generalising the unitarily evolving wavefunction:

$$\begin{aligned} |\Psi(t)\rangle &= \mathrm{e}^{-\frac{iHt}{\hbar}} |\Psi(0)\rangle \\ \implies \rho(t) &= \left(\mathrm{e}^{-\frac{iHt}{\hbar}} |\Psi(0)\rangle\right) \left(\langle\Psi(0)| \, \mathrm{e}^{\frac{iHt}{\hbar}}\right) \\ &= \hat{U}(t)\rho(0)\hat{U}^\dagger(t). \end{aligned} \tag{2.1.24}$$

It is sometimes said that the unitary operators are acting forwards or backwards, depending on if they act on a ket ($|\Psi\rangle$) or bra ($\langle\Psi|$) state. The $\dagger$ refers to the Hermitian conjugate of the operator, and essentially tells it to "act backwards", because the Hermitian conjugate is equal to the *inverse* of U. The equation of motion corresponding to this evolution is the Liouville-von Neumann equation

$$\frac{\mathrm{d}}{\mathrm{d}t}\rho(t) = -\frac{i}{\hbar}[H, \rho], \tag{2.1.25}$$

which is analogous to the Schrödinger equation for wavefunctions.

The effect of measurement on the density matrix is to isolate only the elements which refer to classical probabilities and eliminating elements which refer to superposition between basis states. This is analogous to the process of collapsing the wavefunction, the key effect of which is also to eliminate superposition. Because the density matrix also represents statistical uncertainty, the information about all possible measurement outcomes is kept:

$$\rho = \sum_k p_k \, |\Psi_k\rangle\langle\Psi_k| \to \left(\sum_{n,k} p_k |a_n^{(k)}|^2\right) |n\rangle\langle n| \, . \tag{2.1.26}$$

The sum over n reflects that, in general, we do not necessarily have information about which eigenstate was obtained in a measurement.

2.1.1 Vectors and Matrices

Orthonormal states are sometimes written as unit column vectors, i.e. in a 2-dimensional system the basis states can be written as

$$|1\rangle = \begin{pmatrix} 1 \\ 0 \end{pmatrix}, \qquad |2\rangle = \begin{pmatrix} 0 \\ 1 \end{pmatrix} \tag{2.1.27}$$

Then, any possible state can be written as a vector,

$$\begin{aligned} |\psi\rangle &= c_1 |1\rangle + c_2 |2\rangle \\ &= \begin{pmatrix} c_1 \\ c_2 \end{pmatrix}. \end{aligned} \tag{2.1.28}$$

This notation can be used to find overlaps of state vectors with one another. For example,

$$\langle 1|2\rangle = \begin{pmatrix} 1 & 0 \end{pmatrix} \begin{pmatrix} 0 \\ 1 \end{pmatrix} = 0, \tag{2.1.29}$$

which is the result we expect for the inner product of two orthonormal states. In contrast, the outer product gives a matrix. For example,

$$|1\rangle\langle 2| = \begin{pmatrix} 0 \\ 1 \end{pmatrix} \begin{pmatrix} 1 & 0 \end{pmatrix} = \begin{pmatrix} 0 & 0 \\ 1 & 0 \end{pmatrix}. \tag{2.1.30}$$

Therefore, operator representations can also be explicitly written as matrices. For example, in two dimensions we would have

$$\hat{A} = \begin{pmatrix} A_{11} & A_{12} \\ A_{21} & A_{22} \end{pmatrix}, \tag{2.1.31}$$

and using matrix/vector terminology it is very clear that an operator acting on a state returns another state, e.g.

$$\begin{pmatrix} A_{11} & A_{12} \\ A_{21} & A_{22} \end{pmatrix} \begin{pmatrix} c_1 \\ c_2 \end{pmatrix} = \begin{pmatrix} A_{11}c_1 + A_{12}c_2 \\ A_{21}c_1 + A_{22}c_2. \end{pmatrix} \tag{2.1.32}$$

The density matrix can also be written as a matrix. For example, let's consider the state which is an equally weighted superposition of the eigenstates $|1\rangle$ and $|2\rangle$

$$|\psi\rangle = \frac{1}{\sqrt{2}} \left(|1\rangle + |2\rangle \right). \tag{2.1.33}$$

The density operator corresponding to this state is

$$\begin{aligned}\rho_1 &= |\psi\rangle\langle\psi| \\ &= \frac{1}{2}\left(|\psi_1\rangle\langle\psi_1| + |\psi_1\rangle\langle\psi_2| + |\psi_2\rangle\langle\psi_1| + |\psi_2\rangle\langle\psi_2|\right).\end{aligned} \tag{2.1.34}$$

When we use the vector representation of the states, we see that

$$\rho_1 = \frac{1}{2}\begin{pmatrix}1 & 1\\ 1 & 1\end{pmatrix}. \tag{2.1.35}$$

In contrast, when we construct a density operator which represents only the statistical mixture of the eigenstates $|1\rangle$ and $|2\rangle$, we obtain

$$\begin{aligned}\rho_2 &= \frac{1}{2}\left(|\psi_1\rangle\langle\psi_1| + |\psi_2\rangle\langle\psi_2|\right) \\ &= \frac{1}{2}\begin{pmatrix}1 & 0\\ 0 & 1\end{pmatrix}.\end{aligned} \tag{2.1.36}$$

This contrast shows that the off-diagonal and diagonal elements of the density matrix have very different meanings. The density matrix ρ_1 which represents a pure state with superposition between eigenstates has non-zero off-diagonal components, whereas the mixed state ρ_2 with no superposition has only 0 in the off-diagonal components. Therefore, the off-diagonal elements of the density matrix represent superposition between eigenstates in the chosen basis. The diagonal components are present in both cases, and represent the possible measurement outcomes.

As discussed, the effect of measurement on a density matrix is to remove the elements which refer to superposition, and isolate the elements which refer to classical probabilities. Therefore, we can identify that ρ_2 is in fact the post-measurement outcome of ρ_1. Therefore, we can say that the effect of measurement is to remove the off-diagonal elements of the density matrix.

2.2 Open Quantum Systems

The fundamental description of quantum physics, presented in the last section, assumes that a quantum system is evolving as a closed, isolated system. However, as first realised by Zeh [42], this is not a realistic way of modelling real world quantum systems, which are likely to interact with large environments. This is particularly true in quantum biology, which considers quan-

tum systems submerged in cellular environments at physiological temperatures. Open quantum systems is an umbrella term for models which describe a quantum system which interacts with its surroundings (referred to as the reservoir or environment) in some way. Open quantum systems approaches are common in quantum optics, concerned with how atoms interact with the electromagnetic field [9], in the study of mesoscopic systems [43], and in the study of two-level systems [44].

In order to describe systems which are in contact with an environment, exchanging energy and information, we take a "system plus reservoir" approach [10]. We first define the Hilbert space we are interested in as a tensor product between the Hilbert space of the system and of the environment (reservoir),

$$\mathcal{H} = \mathcal{H}_{\mathrm{S}} \otimes \mathcal{H}_{\mathrm{E}}, \tag{2.2.1}$$

and then define the total density matrix of the system and environment, $\rho(t)$. The Hamiltonian of the system plus reservoir is given by the general form

$$\hat{H} = \hat{H}_{\mathrm{S}} + \hat{H}_{\mathrm{I}} + \hat{H}_{\mathrm{E}}, \tag{2.2.2}$$

where $\hat{H}_{\mathrm{S}}$ is a Hamiltonian associated with the system of interest, $\hat{H}_{\mathrm{E}}$ the Hamiltonian associated with the environment, and $\hat{H}_{\mathrm{I}}$ is the interaction between them.

The general procedure is to evolve the total density matrix $\rho(t)$ according to the Hamiltonian $\hat{H}$, and then perform a partial trace to isolate only the dynamics of the system of interest [9]. The partial trace is defined by

$$\begin{aligned} \tilde{\rho}_{\mathrm{S}}(t) &= \mathrm{Tr}_E\left(\rho(t)\right) \\ &= \sum_{n_E} \langle n_{\mathrm{E}}|\rho(t)|n_{\mathrm{E}}\rangle\,, \end{aligned} \tag{2.2.3}$$

where $|n_{\mathrm{E}}\rangle$ is a basis set associated with the environment. In a continuous basis (like position), the partial trace is given by

$$\begin{aligned} \tilde{\rho}_{\mathrm{S}}(t) &= \mathrm{Tr}_E\left(\rho(t)\right) \\ &= \int \mathrm{d}\mathbf{R}\,\langle \mathbf{R}|\rho(t)|\mathbf{R}\rangle\,, \end{aligned} \tag{2.2.4}$$

with $\mathbf{R}$ the coordinate of the environment. This procedure is the mathematical equivalent of the statement that the environment dynamics are unimportant. The partial trace sums all environment configurations which correspond to the same system configuration, and this allows us to obtain the probabilities associated with the system configuration only.

After applying the partial trace, we obtain the equation of motion for the reduced dynamics of the system of interest:

$$\frac{\partial \tilde{\rho}}{\partial t} = -\frac{i}{\hbar}\mathrm{Tr}_{\mathrm{E}}\left([\hat{H}, \rho(t)]\right). \tag{2.2.5}$$

The partial trace is what allows this expression to describe non-unitary dynamics, as information about the exact dynamics of the system have been lost.

Equations of the type Eq. (2.2.5), which describe the dynamics of a reduced density matrix, are referred to as master equations.

2.2.1 Timescale Separation in Open Quantum Systems

The open quantum systems approach presented above relies on making a clear distinction between the system and the environment. This is summarised by the Born-Markov approximation [9]. The Born approximation states that the effect of the system on the reservoir is small; while the Markov approximation states that the reservoir has very many degrees of freedom and relaxes very rapidly. This allows us to write

$$\rho(t) \approx \rho_{\mathrm{S}}(t) \otimes \rho_{\mathrm{E}}. \tag{2.2.6}$$

This does not imply there are no reservoir excitations at all, simply that the excitations decay over times that are short enough to have no impact on the system dynamics. This requires an effective coarse-graining of the system dynamics: they are only accurate over timescales much longer than τ_{E}, a timescale associated with reservoir (environment) relaxation times, and imposes a timescale separation $\tau_{\mathrm{S}} \gg \tau_{\mathrm{E}}$ between the system and the environment; this is the Markov approximation. Here, τ_{S} is a general label denoting a timescale associated with dynamics in the system of interest; there are two such timescales that we need to take note of. First, the timescale associated with the underlying Hamiltonian dynamics - i.e. those which would occur in the absence of coupling to an environment. Second, the timescale associated

with environment-induced relaxation - which is typically controlled by the coupling strength of the system to the environment. The latter condition means that the Born approximation typically relies on an assumption of weak coupling; not only do we require that for a coupling strength γ, the relation $\gamma^{-1} \gg \tau_{\mathrm{E}}$ holds, but also that the statement "the environment is not significantly perturbed by the interaction with the system" is sensible in the regime of interest. The Born and Markov approximations are very closely linked together, as extreme timescale separation is often how the Born approximation is implemented.

2.2.2 Dissipation and Stochasticity

One of the most important consequences of the partial trace description of open quantum systems is that it allows us to describe dissipative dynamics in quantum systems [10]. In the classical regime, dissipative systems, which irreversibly lose energy to an environment, are described by Langevin equations, which take the form

$$m\ddot{x} + \eta(t)\dot{x} + \mathrm{V}(x) = F(t), \tag{2.2.7}$$

with $\eta(t)$ a frictional damping function and $F(t)$ a fluctuating stochastic force. Although in principle, the dynamics of the dissipative system could be computed exactly, it is in practice impractical to do this as the environment will have very many degrees of freedom. Instead, stochastic equations of the type Eq. (2.2.7) are used. The damping function characterises a smooth phenomenological frictional effect, and the fluctuating force accounts for the unpredictable interactions or collisions between the system and particles in the environment. The friction is described as phenomenological because there is often no complete understanding of the microscopic model of damping. The fluctuating force is often considered to obey the relations $\langle F(t) \rangle = 0$, i.e. collisions are equally likely in all directions, and $\langle F(t)F(t') \rangle = \delta(t-t')$, i.e. collisions at different times are not correlated. When these conditions are met the fluctuating force can be identified with Gaussian white noise. When $F(t)$ describes Gaussian noise, and the damping is time-independent, i.e. $\eta(t) = \eta$, Eq. (2.2.7) describes Brownian motion.

Dissipative dynamics are characterised by a loss of energy to the environment, and a gradual slowing down or stopping of the system dynamics [10]. It is a challenging problem to reconcile this with the process of quantization, which puts strict limits on the allowed values on energy

possessed by a system. In particular, the energy of the quantum system cannot be precisely 0 at long times as is the case for classical dissipative systems due to the constraint imposed by the uncertainty principle. It is also not possible in general to write down a Hamiltonian (which is time-reversible) to describe dynamics which are dissipative, and therefore irreversible.

Early efforts to describe dissipative quantum systems include non-linear Schrödinger equations, for example those developed by Kostin [45] and Yasue [46], the canonical quantization of Dekker [47], and the system + reservoir approach used by Senitsky to study damped electromagnetic field modes [48]. The motivation of the Caldeira-Leggett dissipative model of quantum Brownian motion, which will be discussed in detail in Section 3, is to find the master equation for a quantum system in a classically accessible region, i.e. at "high" temperatures, in a way which is only dependent on quantities which are, in principle, experimentally accessible. The desired outcome is that the master equation for the reduced dynamics of the system density matrix will, in the classical limit, correspond to behaviour described by Eq. (2.2.7).

The Quantum Langevin Equation

The quantum Langevin equation was originally derived in order to describe the stochastic equation of motion of the position coordinate of a Brownian particle coupled to a heat bath (environment) [49]. The aim is to recover the classical Langevin equation for Brownian motion, i.e. Eq. (2.2.7). An outline of the derivation of the Langevin equation is presented below, as given in [50].

We start from the Hamiltonian of a one-dimensional system in a general potential coupled to an environment of non-interacting harmonic oscillators,

$$\hat{H} = \frac{\hat{p}^2}{2m} + \hat{\mathrm{V}}(x) + \sum_j \left[\frac{\hat{p}_j^2}{2m_j} + \frac{1}{2} m_j \omega_j^2 \left(\hat{q}_j - \frac{C_j}{m_j \omega^2} \hat{x} \right)^2 \right], \tag{2.2.8}$$

with $\{\hat{x}, \hat{p}\}$ the position and momentum operators of the system and $\{\hat{q}_j, \hat{p}_j\}$ the position and momentum operators of the j^{th} oscillator. The system mass is m and the oscillator masses and frequencies are $\{m_j, \omega_j\}$. The oscillators are colinearly coupled to the system with strength C_j.

Using the Heisenberg equation for the time evolution of an operator,

$$i\hbar\dot{O} = [O, H], \tag{2.2.9}$$

along with the canonical equal-time relations

$$[\hat{x}, \hat{p}] = i\hbar, \qquad [\hat{q}_j, \hat{p}_j] = i\hbar\delta_{ij}, \tag{2.2.10}$$

we can obtain equations of motion for the system and oscillators. For the system operators, we have

$$\begin{aligned} \dot{x} &= \frac{p}{m} \\ \dot{p} &= -\mathrm{V}'(x) + \sum_j m_j\omega_j^2 \left(q_j - \frac{C_j}{m\omega^2}x\right) \\ \implies m\ddot{x} &= -\mathrm{V}'(x) + \sum_j m_j\omega_j^2 \left(q_j - \frac{C_j}{m\omega^2}x\right), \end{aligned} \tag{2.2.11}$$

where $\mathrm{V}'(x) = \frac{\mathrm{d}V}{\mathrm{d}x}$, and for the environment oscillators we have

$$\begin{aligned} \dot{q}_j &= \frac{p_j}{m_j} \\ \dot{p}_j &= -m_j\omega^2 \left(q_j - \frac{C_j}{m_j\omega^2}x\right) \\ \implies m_j\ddot{q}_j &= -m_j\omega^2 \left(q_j - \frac{C_j}{m_j\omega^2}x\right). \end{aligned} \tag{2.2.12}$$

We solve the last line of Eq. (2.2.12) (via Laplace transform) to give [50]

$$q_j(t) = q_j(0)\cos\omega_j t + \frac{p_j(0)}{m_j\omega_j}\sin\omega_j t - \frac{C_j^2}{m_j\omega_j^2}\int_0^t \mathrm{d}t' \sin\omega_j(t-t')\dot{x}(t'). \tag{2.2.13}$$

This can then be substituted into the last line of Eq. (2.2.11), leading to the solution for $x(t)$:

$$\begin{aligned} m\ddot{x} = -\mathrm{V}'(x) &+ \sum_j \left[C_j q_j(0)\cos\omega_j t + \frac{C_j}{m_j\omega_j}p_j(0)\sin\omega_j t\right] \\ &+ \sum_j \frac{C_j}{m_j\omega_j^2}\int_0^t \sin\omega_j(t-t')x(t')\mathrm{d}t' - \frac{C_j}{m_j\omega_j^2}x(t). \end{aligned} \tag{2.2.14}$$

Using integration by parts on the convolution integral gives

$$\frac{C_j}{m_j\omega_j^2}\int_0^t \sin\omega_j(t-t')x(t')\mathrm{d}t' = \frac{C_j^2}{m_j\omega_j^2}\left[x(t)-x(0)\cos\omega_j t\right] - \frac{C_j^2}{m_j\omega_j^2}\int_0^t \cos\omega_j(t-t')\dot{x}(t')\mathrm{d}t' \tag{2.2.15}$$

Then, by defining the stochastic force operator as

$$F(t) = \sum_j C_j q_j(0)\cos\omega_j t + C_j\frac{p_j(0)}{m_j}\sin\omega_j t, \tag{2.2.16}$$

and a new function, called the memory kernel (or sometimes the damping function), as

$$\mu(t) = \sum_j \frac{C_j}{m_j\omega_j^2}\cos\omega_j t, \tag{2.2.17}$$

we can write

$$m\ddot{x} + \mathrm{V}'(x) + \int_0^t \mu(t-t')\dot{x}(t')\mathrm{d}t' + \mu(t)x(0) = F(t). \tag{2.2.18}$$

Eq. (2.2.18) is the quantum Langevin equation, which is the equation of motion for the quantum operator $x(t)$. It is nearly in the same form as Eq. (2.2.7). We still need to make the identification

$$\int_0^t dt'\mu(t-t')\dot{x}(t') = \eta\dot{x}(t). \tag{2.2.19}$$

This is achieved by making a phenomenological assumption, namely that

$$\mu(t) = 2\eta\delta(t). \tag{2.2.20}$$

The δ-function "kills" the time-correlation and selects the value of the function at t. This just leaves us with another term

$$2\eta(t)x(0); \tag{2.2.21}$$

this can be discarded as it only affects the dynamics for an infinitesimal time [51], and we obtain Eq. (2.2.7).

Now we have to make some deductions about the behaviour of the stochastic force operator,

$F(t)$. By using [50]

$$\langle \hat{A} \rangle = \frac{\mathrm{Tr}\left(\hat{A}\exp\left\{-\frac{\hat{H}}{kT}\right\}\right)}{\mathrm{Tr}\left(\exp\left\{-\frac{\hat{H}}{kT}\right\}\right)} \tag{2.2.22}$$

to find the expectation value of an operator, it can be shown that

$$\langle q_j(0)q_k(0)\rangle = \frac{\langle p_j(0)p_k(0)\rangle}{(m_j\omega_j)^2} = \delta_{jk}\frac{\hbar}{2m_j\omega_j}\coth\frac{\hbar\omega_j}{2kT} \tag{2.2.23}$$

and

$$\langle q_j(0)p_k(0)\rangle = -\langle p_j(0)q_k(0)\rangle = \frac{i\hbar}{2}\delta_{jk}. \tag{2.2.24}$$

When we substitute these expressions into Eq. (2.2.16), we obtain for the correlation of the stochastic force

$$\langle F(t)F(t')\rangle = \sum_j \frac{C_j^2}{2m_j\omega_j^2}\hbar\omega_j\coth\frac{\hbar\omega_j}{2kT}\cos\omega_j(t-t'). \tag{2.2.25}$$

In the limit $\hbar\omega \ll kT$ (i.e. the classical limit), we can substitute in the definition of $\mu(t)$, Eq. (2.2.17), to obtain

$$\begin{aligned}\langle F(t)F(t')\rangle &= kT\sum_j \frac{C_j^2}{m_j\omega_j^2}\cos\omega_j(t-t') \\ &= kT\mu(t-t').\end{aligned} \tag{2.2.26}$$

By substituting in Eq. (2.2.20), we finally obtain

$$\langle F(t)F(t')\rangle = 2\eta kT\delta(t-t'). \tag{2.2.27}$$

We therefore show that Eq. (2.2.18) can be made equivalent to Eq. (2.2.7) - the equation which describes a classical dissipative system - with the friction (damping) described by a function $\mu(t)$ and the fluctuating stochastic force shown to obey the conditions which describe Gaussian noise.

The derivation of the Langevin equation (Eq. (2.2.18)) shows several important points. First, that it is possible to describe a quantum system which behaves like a Brownian particle in the classical limit, i.e. a dissipative quantum system. We call dynamics described by Eq. (2.2.18) quantum Brownian motion. Second, that it is possible to reduce a full system + reservoir

description to a stochastic equation of motion. Third, that in such a stochastic reduction the damping is related (in the high temperature limit) to the correlation of the stochastic force via

$$\langle F(t)F(t')\rangle = kT\mu(t-t'). \tag{2.2.28}$$

This last point is the topic of the fluctuation-dissipation theorem [52], which applies to both quantum and classical systems: the damping dissipates the energy of the system, and the corresponding thermal stochastic force increases the system's energy. The two forces cannot be separated as they are both derived from the interaction of the system with the environment oscillators.

The Fokker-Planck Equation

Because a Langevin equation describes stochastic motion, for any given initial condition it will describe one of a series of possible paths taken by the Brownian particle. There is a corresponding probability distribution $P(x,p,t)$ which evolves over time, and this is described by the Fokker-Planck equation [53]. The Fokker-Planck equation is found by averaging over the quantities described by the Langevin equation, i.e.

$$\langle x\rangle = \int_{-\infty}^{\infty}\int_{-\infty}^{\infty} xP(x,p,t)\mathrm{d}x\mathrm{d}p, \tag{2.2.29}$$

and then expanding the integrals in $P(x,p,t)$ using the Kramers-Moyal expansion [53]. Detailed derivations of the Fokker-Planck equation can be found in Refs. [53–55].

When the Fokker-Planck equation has both position and momentum variables included, it is also called the Klein equation. It describes the phase space distribution corresponding to Brownian motion [31], and is given by

$$\frac{\partial P}{\partial t} = -\frac{p}{m}\frac{\partial P}{\partial x} + \mathrm{V}'(x)\frac{\partial P}{\partial p} + \frac{\eta}{m}\frac{\partial}{\partial p}(pW) + \eta kT\frac{\partial^2 P}{\partial p^2}. \tag{2.2.30}$$

This Fokker-Planck equation will prove to be useful because it enables us to compare the behaviour of different quantum systems in the classical limit.

2.2.3 Spectral Density

In the Langevin equation description of an open system dynamics, the correlation between forces $\langle F(t)F(t')\rangle$ and the damping function $\eta(t)$ are determined by properties of the distribution of oscillators in the environment; this manifested in the identification of a memory kernel defined by a distribution of oscillators

$$\mu(t) = \sum_j \frac{C_j^2}{m_j\omega_j^2}\cos\omega_j t \tag{2.2.31}$$

which determines the phenomenological damping,

$$\eta(t)\dot{x}(t) = \int_0^t \mathrm{d}t'\mu(t-t')\dot{x}(t'). \tag{2.2.32}$$

We can use this to define an object which contains all the relevant information about the environment oscillators. This object is called the spectral density, and it is defined by [10]

$$J(\omega) = \frac{\pi}{2}\sum_j \frac{C_j^2}{m_j\omega_j}\delta(\omega-\omega_j). \tag{2.2.33}$$

The spectral density is linked to the memory kernel via the integral

$$\mu(t) = \frac{1}{\pi}\int_0^\infty \frac{J(\omega)}{\omega}\cos\omega\tau. \tag{2.2.34}$$

This is very useful as it allows us to go from a discrete sum of oscillators to a continuum. We can also invert this expression to obtain the spectral density in terms of the memory kernel [10],

$$J(\omega) = \omega\int_0^\infty \mu(t)\cos\omega t\mathrm{d}t. \tag{2.2.35}$$

In the case we considered before, i.e. with the phenomenological assumption $\mu(t) = 2\eta\delta(t)$, we obtain

$$\begin{aligned} J(\omega) &= 2\eta\omega\int_0^\infty \delta(t)\cos\omega t\mathrm{d}t \\ &= \eta\omega. \end{aligned} \tag{2.2.36}$$

This is often called the Ohmic spectral density, and it corresponds to "frequency-independent" damping, as the Fourier transform of $\mu(t)$ is constant:

$$\tilde{\mu}(\omega) = 2\eta \int_0^\infty \mathrm{e}^{-i\omega t}\delta(t)\mathrm{d}t = \eta. \tag{2.2.37}$$

Therefore, we can see that quantum Brownian motion is described by frequency-independent damping and the Ohmic spectral density. It is worth emphasising that although the spectral density has a microscopic definition, it is a phenomenological choice to assign a smooth function such as $J(\omega) = \eta\omega$. The same choice is responsible for the form of $J(\omega)$ and $\mu(t)$.

If we return to the Langevin equation (Eq. (2.2.18)), we can see that the dynamics of the particle can be entirely determined by m, $\mathrm{V}(x)$, $J(\omega)$, and T. Therefore, the spectral density is a very useful tool in open quantum system as it allows the effects of the interaction with the environment to be summarised in one (usually fairly simple) function.

Although the Ohmic spectral density is a very common choice, it is also common to identify the spectral density with a more general algebraic function, e.g.

$$J(\omega) = \eta_s \omega^s, \tag{2.2.38}$$

with s the so-called "Ohmicity" parameter. When $s = 1$, the spectral density is Ohmic. When $s > 1$ ($s < 1$), the spectral density is called super- (sub-) Ohmic.

The spectral density is sometimes separated into a low-frequency part and a high-frequency part [10]. In particular, it is common to use a so-called Drude regularization (sometimes called a Lorentz-Drude cut-off) and write the spectral density as

$$J(\omega) = \frac{\eta\omega}{1 + \omega^2/\omega_{\mathrm{LD}}^2}. \tag{2.2.39}$$

This introduces an environment timescale $\tau_{\mathrm{E}} \approx \omega_{\mathrm{LD}}^{-1}$; when τ_{E} is much smaller than the system timescales, the timescale separation $\tau_{\mathrm{S}} \gg \tau_{\mathrm{E}}$ is upheld, but the Drude cut-off allows potentially divergent integrals to be avoided. The Drude cut-off is one of several choices, including a harsh cut-off, a Gaussian, or an exponential. In the strict timescale separation regime, the low-

frequency part of the spectral density is responsible for the behaviour of the system, whereas the high-frequency part is absorbed into parameters of the Hamiltonian [10, 56].

It is not a straightforward task to experimentally determine the spectral density of an environment. A recent study determined the spectral density by weakly coupling a condensed matter environment to an optical cavity and measuring the spectrum of the cavity output light [57]; they find a highly sub-Ohmic spectral density with $s \approx -2.5$. However, it is possible to analytically calculate the spectral density for a range of models. For example, the Debye model predicts a density of states corresponding to an Ohmic spectral density [58], a 3D Bose-Einstein condensate (BEC) has super-Ohmic spectral density [59], and in a 1D BEC the spectral density varies from Ohmic behaviour to super-Ohmic behaviour with dependence on the scattering length. It is, currently, unclear what is expected to be the spectral density of a biological or cellular environment.

2.2.4 Coherence and Decoherence

A central concept in open quantum systems is coherence: the property which allows quantum systems to maintain superposition, and fundamentally distinguishes quantum systems from classical ones. Coherence can be thought of as a measure of the strength of superposition between different eigenstates (in some basis) that the system is able to maintain. States which have superpositions between well-separated eigenstates are sometimes thought of as more coherent than those which have superpositions between adjacent eigenstates, and (as we shall see later) are more vulnerable to environment-induced destruction of coherence.

In the density matrix representation, we are able to give coherence a quantifiable definition by considering the off-diagonal elements, which represent superpositions between eigenstates [39]. The least coherent state will be one which is completely diagonal in some basis, as this represents a total lack of superposition. The two most general measures of coherence are the l_1-norm of coherence and the relative entropy of coherence.

The l_1-norm of coherence is defined as

$$C_{l_1}(\rho) = \sum_{n \neq m} |\rho_{nm}|, \tag{2.2.40}$$

with ρ_{nm} the matrix element which describes the strength of superposition between eigenstates $|n\rangle$ and $|m\rangle$. The sum is over only the off-diagonal elements. The l_1-norm is possibly one of the simplest measures of coherence, and is also very easy to compute. However, it does not introduce a weight, so that superpositions between delocalised basis states, and superpositions between adjacent basis states, i.e. between $|n\rangle$ and $|n+1\rangle$, contribute equally.

The relative entropy of coherence is defined with respect to the von Neumann entropy of a state (see Section 2.3), which is given by

$$S(\rho) = -k_B \mathrm{Tr}\left(\rho \ln \rho\right). \tag{2.2.41}$$

Then we have

$$C_{\mathrm{rel.ent}}(\rho) = -\left(S(\rho) - S(\rho_{\mathrm{diag}})\right), \tag{2.2.42}$$

where ρ_{diag} is the post-measurement density matrix, which has only the diagonal elements remaining. Therefore, the relative entropy of coherence can be interpreted as the increase in von Neumann entropy that would result after a measurement. Conversely, as the von Neumann entropy is also a measure of quantum information [60], the relative entropy of coherence can be interpreted as the information that is lost from the system after measurement. The von Neumann entropy of a pure state is 0, which reflects that entropy is a measure of statistical uncertainty, which manifests in the density matrix as "mixed-ness".

Both the relative entropy of coherence and the l_1-norm of coherence fulfil several important criteria [39]: they are zero for so called incoherent states, which do not have any superposition in a selected basis, and they do not increase when the state becomes more mixed, i.e. the purity decreases. However, these measures are basis-dependent. This means that they will give different values dependent on the selected basis, e.g. position or energy. We have to keep this in mind when discussing coherence: it has to remain within the context of a specific basis. In the following discussion, unless otherwise specified, we will use "coherence" to mean coherence in the position basis - states which are spatially delocalised.

Resource Theory of Coherence

Because the presence and quantification of coherence is an essential tool in quantum technologies, as well as in emerging fields like quantum biology and quantum thermodynamics, a theory that describes coherence as a physical resource has been developed over the past few years, originally by Winter and Yang [61]. The general aims of a resource theory are to study the "interconversion between resource states under free operations" [61]: in this case, the evolution of states containing coherence under dynamics which do not introduce additional coherence into the system. The authors introduce two important concepts: distillable coherence, which is the coherence that can be obtained from a mixed state, and coherence cost, which is the coherence lost during the creation of a mixed state. The distillable coherence coincides with the relative entropy of coherence:

$$C_{\text{distill}}(\rho) = C_{\text{rel.ent}}(\rho). \tag{2.2.43}$$

This is useful, because it provides an interpretation for the relative entropy of coherence: it is the number of maximally coherent states that could be produced from a density matrix ρ [62].

Decoherence

In a closed system undergoing unitary dynamics, coherence cannot be lost from the system. However, this is not the case for an open system. Coherence is destroyed by the interaction with the environment - in most cases very rapidly - in a process known as decoherence. This has the effect of diagonalising the density matrix in the so-called *pointer* basis [6, 7, 63]. Therefore, we can identify decoherence with the effect of measurement on the density matrix, as discussed in Section 2.1: wavefunction collapse is analogous to density matrix diagonalisation, and both processes are a form of decoherence. Although we will continue to discuss the "system + environment", much of the discussion can also be applied to the "system + measurement apparatus" found in quantum measurement theory [9].

It has been identified by Zurek [6] that the pointer basis is determined by the Hamiltonian describing the interaction between system and environment; more specifically, it is the eigenbasis of an operator $\hat{\Pi}$ which commutes with the interaction Hamiltonian (i.e. $[\hat{\Pi}, \hat{H}_{\text{I}}] = 0$). This basis is not perturbed by interaction with the environment, which allows for the eventual emergence of a steady state. This is described as *environment-induced superselection* [7],

where the environment is interpreted as constantly monitoring the system and preventing it from maintaining superposition (or correlation) in the pointer basis. This process is essentially irreversible, as correlation recurrence times are shown to be damped by a factor of $N^{-1/2}$, with N the number of states accessible to the environment. This is why it is sometimes said that a decohered state will behave classically: it is practically impossible for systems to display correlations after they have initially decayed, while the system is undergoing interaction with the same environment.

Because decoherence is effectively a consequence of indirect measurements on the system by the environment, it can also be described as a transfer of information from the system to the environment [63, 64]. In quantum mechanics, information cannot be destroyed, but is dissipated throughout the degrees of freedom of the system and environment. Another way of interpreting decoherence is as increasing entanglement between the system of interest and the environment degrees of freedom [64]. Coherence is diffused amongst the entanglements, leading to the slogan "the arrow of time is an arrow of increasing correlations" [65]: decoherence can be seen as a time-asymmetric process.

The l_1-norm of coherence and the relative entropy of coherence can be used to quantify decoherence and find the pointer states of a system [64]. Decoherence is associated with a decrease in coherence - often very rapid [7] - and, because the pointer states are robust to environmental interaction, they have constant (usually very low) coherence. For certain classes of models, it is possible to derive analytically a "decoherence function", which determines the decay of the off-diagonal elements of the density matrix [9]. An example of this is the two-level spin-boson model, the coherences of which can be written as

$$\rho_{10}(t) = \rho_{10}(0)\mathrm{e}^{\Gamma(t)}, \tag{2.2.44}$$

with

$$\Gamma(t) \approx -\frac{t}{\tau_{\mathrm{E}}}, \tag{2.2.45}$$

where $\tau_{\mathrm{E}} = {}^{1}/_{\pi k_B T}$. It is very common for Markovian systems, which have complete timescale separation between system and environment, to undergo exponential decoherence. For simple systems (such as two-level systems), the decoherence function can be directly calculated from

the equation of motion for the coherences.

Decoherence is often studied in the position-basis for an initial state that represents spatial delocalisation, i.e. a double-Gaussian "Schrödinger cat" state.

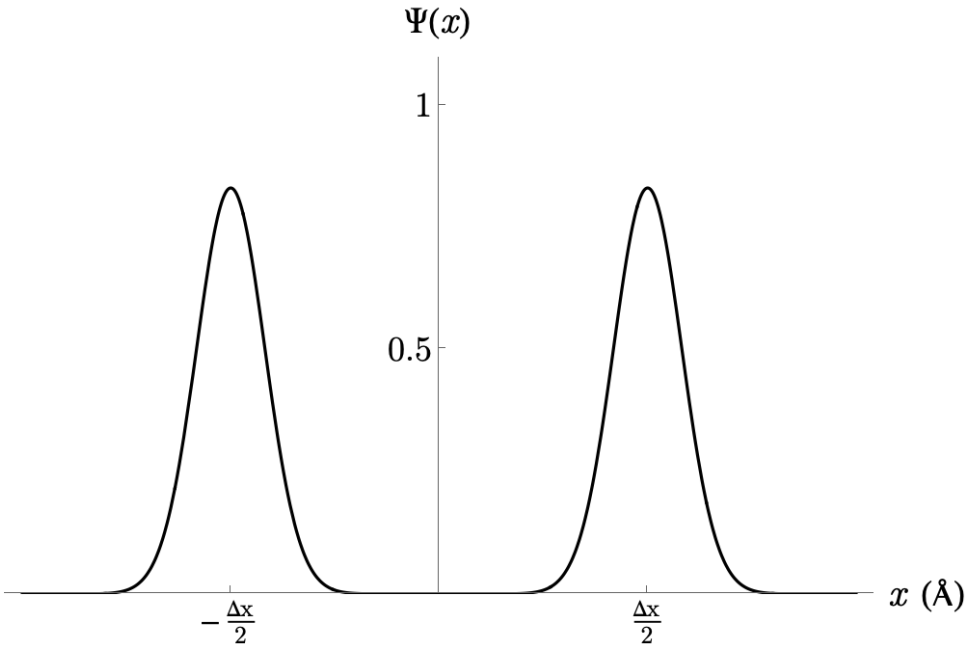

Figure 2.1: A Schrödinger cat pure state, or a double Gaussian. Each Gaussian peak is weakly localised, but the state itself represents delocalised spatial superposition.

Zurek derived an estimate of the ratio between the relaxation time and the decoherence time for a state of this type [7]:

$$\frac{\tau_{\mathrm{R}}}{\tau_{\mathrm{D}}} \approx \left(\frac{\Delta x}{\lambda_T}\right)^2, \tag{2.2.46}$$

with Δx the separation between the peaks, and $\lambda_T = \frac{\hbar}{\sqrt{2mk_BT}}$ the thermal wavelength of the system. For a macroscopic system at room temperature with mass 1g and separation 1cm, the ratio is approximately 10^{40}: decoherence happens much faster than any other dynamics associated with the system. For a mesoscopic system (such as might be found in biology) at physiological temperature, with mass 10^{-9}g and separation 1nm, the ratio is approximately 10^{16}. Although decoherence has slowed by several orders of magnitude compared to the macroscopic case, it is still the dominant feature of the quantum dynamics.

Decoherence is well-studied not only because of its significance in the quantum-classical transition, but because of its detrimental effects in quantum technologies [66], particularly in quantum computing [67–69]. However, it also presents one of the challenges faced in the field of

quantum biology [70, 71]: if decoherence is the dominant feature of the dynamics at mesoscopic, physiological temperatures, how can coherent behaviour survive in systems of this type?

2.2.5 Positivity

In mathematics, a positive map is one which maps positive elements to positive elements. This concept becomes important in quantum mechanics when we consider that some elements of the density matrix represent probabilities, and must therefore always be positive. For example, in the position basis, the diagonal elements of the density matrix represent the population density for the quantum system: this can at no point be negative, and the integral must be unity. Therefore, we need the function describing the time evolution of the density matrix to be a positive map, to ensure that no unphysical negative probabilities are obtained. Violations of positivity can also be associated with violations of the uncertainty principle [9].

It can be shown that a density matrix which evolves according to a Lindblad equation (see Section 2.2.6) will conserve positivity, meaning that there will never be negative contributions to the probability distribution [9, 72–74]. However, if a master equation cannot be expressed in Lindblad form, it is not guaranteed - or even expected - to conserve positivity in all regimes [75]. Positivity violations are expected in some regimes of the high-temperature Caldeira-Leggett equation (see Section 3), and have been addressed by introducing a "medium-temperature" correction [76].

This concept can be generalised to the stronger restriction of complete positivity, which requires positivity in the presence of a coupled environment - the situation we are most concerned with. Usually, complete positivity is taken to be a requirement for open quantum system dynamics [59]. However, it has been argued that complete positivity is not a necessary condition for reduced system dynamics [10, 77]. The argument against complete positivity is as follows. Suppose we have a system which obeys the restriction of complete positivity, along with two other restrictions. First, that mixtures are preserved (i.e. no state spontaneously becomes more pure). Second, that the trace of the reduced density matrix is preserved. Then, Pechukas has shown [77] that the only possible evolutions are product evolutions, i.e. $\Phi\rho = \Phi_{\mathrm{S}}\rho_{\mathrm{S}} \otimes \rho_{\mathrm{E}}$, with ρ_{E} a fixed state of the environment. Outside the Born approximation (weak coupling) regime, we expect to find evolutions which are not of this product form. Therefore, one of the

three restrictions (complete positivity, preservation of mixtures, and trace conservation) must be dropped; Pechukas argues that it should be the complete positivity restriction. However, this argument is not widely accepted, despite the emergence of exact models which are not in Lindblad form (and are therefore expected to violate positivity in some regimes) [38, 78]; it has been criticised by Alicki [79], and complete positivity is still regarded as an important criteria of physicality [80].

2.2.6 Models of Open Quantum Systems

There are many models of open quantum systems, some of which use specific features of the model, and some that are more general but subject to restrictive assumptions. In the following sections, brief overviews of a range of models are presented, to give an idea for the variety and flavour of the different approaches taken. Of particular interest is the Lindblad equation, which is often seen as the default description of open quantum system dynamics. However, none of the approaches presented below are of direct relevance to the approach used in this thesis, other than for comparison.

The Nakajima-Zwanzig Equation

The derivation of the Nakajima-Zwanzig equation is an example of a projection operator technique, which acts on the density operator rather than the density matrix [9, 81, 82]. The basic principle is isolate only the relevant part of the density operator

$$\hat{\rho}_{\mathrm{S}}(t) = \mathcal{P}\hat{\rho}(t), \tag{2.2.47}$$

where $\mathcal{P}$ is a projection operator which reduces the density operator to an operator which acts only in the space of relevant variables [10]. When we are working with the density *matrix*, the projection operator can be interpreted as the partial trace, $\mathcal{P}\rho(t) = \mathrm{Tr}(\rho(t)) \otimes \rho_{\mathrm{E}}$ [9]. The irrelevant part of the density operator is given by $(1-\mathcal{P})\hat{\rho}(t) = \mathcal{Q}\hat{\rho}(t)$, such that

$$\hat{\rho}(t) = \hat{\rho}_{\mathrm{S}}(t) + (1-\mathcal{P})\hat{\rho}(t). \tag{2.2.48}$$

We have the identities

$$\mathcal{P}^2 = \mathcal{P}, \tag{2.2.49}$$

$$(\mathcal{P} + \mathcal{Q}) = \mathcal{I}, \tag{2.2.50}$$

and

$$[\mathcal{P}, \mathcal{Q}] = 0. \tag{2.2.51}$$

To derive the Nakajima-Zwanzig equation, we start with a Hamiltonian

$$H = H_0 + \alpha H_{\mathrm{I}}, \tag{2.2.52}$$

where H_0 is the system Hamiltonian, H_{I} is an interaction Hamiltonian, and α characterises the strength of the interaction. The equation of motion is

$$\frac{\partial}{\partial t}\hat{\rho}(t) = -i\alpha[H_{\mathrm{I}}(t), \hat{\rho}(t)] = \alpha\mathcal{L}\hat{\rho}(t). \tag{2.2.53}$$

However, we are only interest in the "relevant" part:

$$\frac{\partial}{\partial t}\mathcal{P}\hat{\rho}(t) = \alpha\mathcal{P}\mathcal{L}(t)\hat{\rho}(t). \tag{2.2.54}$$

We use the corresponding equation for the irrelevant part,

$$\frac{\partial}{\partial t}\mathcal{Q}\hat{\rho}(t) = \alpha\mathcal{Q}\mathcal{L}(t)\hat{\rho}(t), \tag{2.2.55}$$

along with the identity $\mathcal{P} + \mathcal{Q} = I$, to write down coupled differential equations:

$$\begin{aligned} \frac{\partial}{\partial t}\mathcal{P}\hat{\rho}(t) &= \alpha\mathcal{P}\mathcal{L}(t)\mathcal{P}\hat{\rho}(t) + \alpha\mathcal{P}\mathcal{L}(t)\mathcal{Q}\hat{\rho}(t) \\ \frac{\partial}{\partial t}\mathcal{Q}\hat{\rho}(t) &= \alpha\mathcal{P}\mathcal{L}(t)\mathcal{P}\hat{\rho}(t) + \alpha\mathcal{P}\mathcal{L}(t)\mathcal{Q}\hat{\rho}(t). \end{aligned} \tag{2.2.56}$$

We can solve the second of these equations to give

$$\mathcal{Q}\hat{\rho}(t) = \mathcal{G}(t, t_0)\mathcal{Q}\hat{\rho}(t_0) + \alpha\int_{t_0}^{t} \mathrm{d}s\mathcal{G}(t, s)\mathcal{Q}\mathcal{L}(s)\mathcal{P}\hat{\rho}(s), \tag{2.2.57}$$

with $\mathcal{G}(t, s)$ a time-ordered propagator given by

$$\mathcal{G}(t, s) = \mathrm{T}_{\leftarrow}\exp\left[\alpha\int_{s}^{t}\mathrm{d}s'\mathcal{Q}\mathcal{L}(s')\right]. \tag{2.2.58}$$

This is substituted to solve the first of the coupled differential equations,

$$\frac{\partial}{\partial t}\mathcal{P}\hat{\rho}(t) = \alpha\mathcal{P}\mathcal{L}(t)\mathcal{G}(t,t_0)\mathcal{Q}\hat{\rho}(t_0) + \alpha\mathcal{P}\mathcal{L}(t)\mathcal{P}\hat{\rho}(t) + \alpha^2\int_{t_0}^{t}\mathrm{d}s\mathcal{P}\mathcal{L}(t)\mathcal{G}(t,s)\mathcal{Q}\mathcal{L}(s)\mathcal{P}\hat{\rho}(s). \quad (2.2.59)$$

This is the Nakajima-Zwanzig equation, which describes exactly the reduced dynamics of the system of interest. It is not subject to any restrictive assumptions about the strength of system coupling, or extreme timescale separation. However, the Nakajima-Zwanzig equation is very difficult to solve (either numerically or analytically), and perturbative approaches are often required [9], for example in the coupling strength α, which re-introduce approximations into the system.

The Lindblad Equation

The Lindblad equation [9] describes an open quantum system which obeys the Born-Markov approximation: the environment is not perturbed by the interaction with the system, and the interaction is memoryless (Markovian). This restricts it to describe weakly-coupled systems, but it is very useful because it can be used to describe a wide range of systems, and it is guaranteed to conserve positivity. An outline of its derivation is presented below.

The Lindblad equation is related to the concept of a quantum dynamical semigroup. An evolution of the reduced density matrix can be written by unitarily evolving the full density matrix and taking the partial trace over environment coordinates:

$$\rho_{\mathrm{S}}(t) = \mathrm{Tr}_{\mathrm{E}}\left(U(t,0)[\rho_{\mathrm{S}}(0)\otimes\rho_{\mathrm{E}}]U^{\dagger}(t,0)\right) = V(t)\rho_{\mathrm{S}}(0), \quad (2.2.60)$$

and this is equivalent to the action of the evolution operator $V(t)$, which is also called a dynamical map. If the evolution operator obeys the *semigroup property* [73]

$$V(t_1)V(t_2) = V(t_1+t_2), \quad t_2, t_1 \geq 0, \quad (2.2.61)$$

it is a Markovian dynamical map and the dynamics belong to a quantum dynamical semigroup.

The dynamical map can be associated to a generator $\mathcal{L}$, such that

$$\begin{aligned} V(t) &= \mathrm{e}^{\mathcal{L}t} \\ \implies \frac{\mathrm{d}}{\mathrm{d}t}\rho_{\mathrm{S}}(t) &= \mathcal{L}\rho_{\mathrm{S}}(t). \end{aligned} \tag{2.2.62}$$

We want to find out what the generator $\mathcal{L}$ will look like.

Using the definition of $V(t)$ given in Eq. (2.2.60), we can insert a spectral decomposition of the environment spectral density,

$$\rho_{\mathrm{E}} = \sum_{\alpha} \lambda_{\alpha} \left|\varphi_{\alpha}\right\rangle\!\left\langle\varphi_{\alpha}\right| \tag{2.2.63}$$

and perform the trace by inserting a resolution of identity in the states $|\varphi_{\beta}\rangle$ to obtain

$$V(t)\rho_{\mathrm{S}}(0) = \sum_{\alpha,\beta} W_{\alpha\beta}(t)\rho_{\mathrm{S}}(0)W^{\dagger}_{\alpha\beta}(t), \tag{2.2.64}$$

with

$$W_{\alpha\beta} = \sqrt{\lambda_{\beta}}\left\langle\varphi_{\alpha}\right|U(t,0)\left|\varphi_{\beta}\right\rangle. \tag{2.2.65}$$

With a set of N^2 basis operators F_i we re-write the dynamical map as

$$V(t)\rho_{\mathrm{S}}(0) = \sum_{i,j=1}^{N^2} c_{ij}(t)F_i\rho_{\mathrm{S}}(0)F_j^{\dagger}(t), \tag{2.2.66}$$

with

$$c_{ij}(t) = \sum_{\alpha\beta} \mathrm{Tr}\left(F_i W_{\alpha\beta}\right)\mathrm{Tr}\left(F_j W_{\alpha\beta}\right)^{*}. \tag{2.2.67}$$

We can see that

$$|c_{ij}(t)|^2 \geq 0, \tag{2.2.68}$$

which demonstrates the positivity of the dynamical map: positive elements of the density matrix

will only be mapped to positive elements. We can now define the generator:

$$\begin{aligned}\mathcal{L}\rho_{\mathrm{S}} &= \lim_{\varepsilon\to 0}\frac{V(\varepsilon)\rho_{\mathrm{S}}-\rho_{\mathrm{S}}}{\varepsilon}\\ &= \lim_{\varepsilon\to 0}\Big(\frac{1}{N}\frac{c_{N^2N^2}-N}{\varepsilon}\rho_{\mathrm{S}}+\frac{1}{\sqrt{N}}\sum_{i=1}^{N^2-1}\left(\frac{c_{iN^2}(\varepsilon)}{\varepsilon}F_i\rho_{\mathrm{S}}+\frac{c_{N^2i}(\varepsilon)}{\varepsilon}\rho_{\mathrm{S}}F_i^\dagger\right)\\ &\quad+\sum_{i,j=1}^{N^2-1}\frac{c_{ij}(\varepsilon)}{\epsilon}F_i\rho_{\mathrm{S}}F_j^\dagger\Big).\end{aligned} \tag{2.2.69}$$

By defining the Hermitian operator

$$H=\frac{1}{2i}\left(F^\dagger-F\right), \tag{2.2.70}$$

we can write

$$\mathcal{L}\rho_{\mathrm{S}}=-i[H,\rho_s]+\sum_{i,j=1}^{N^2-1}\left(\lim_{\varepsilon\to\epsilon}\frac{c_{ij}(\varepsilon)}{\epsilon}\right)\left(F_i\rho_{\mathrm{S}}F_j^\dagger-\frac{1}{2}\{F_j^\dagger F_i,\rho_{\mathrm{S}}\}\right). \tag{2.2.71}$$

By diagonalising the coefficient matrix

$$\lim_{\varepsilon\to\epsilon}\frac{c_{ij}(\varepsilon)}{\epsilon}=\gamma_j\delta_{ij} \tag{2.2.72}$$

with eigenvalues γ_j, the generator can be written in diagonal form

$$\mathcal{L}\rho_{\mathrm{S}}=-i[H,\rho_{\mathrm{S}}]+\sum_{j=1}^{N^2-1}\gamma_j\left(A_j\rho_{\mathrm{S}}A_j^\dagger-\frac{1}{2}A_j^\dagger A_j\rho_{\mathrm{S}}-\frac{1}{2}\rho_{\mathrm{S}}A_j^\dagger A_j\right), \tag{2.2.73}$$

where the operators A_j are appropriate linear combinations of the basis operators F_j. This is the Lindblad equation, which is the most general form of the generator of a quantum dynamical semigroup. When $\gamma_j\geq 0\ \ \forall j$, it represents completely positive, Markovian, weakly coupled open quantum system dynamics. The first term is the Liouville-von Neumann unitary dynamics, and the terms inside the sum represent the dissipative dynamics. The relaxation rates γ_j determine the strength of dissipation along each channel.

2.3 Quantum Thermodynamics

In classical systems, thermodynamics is the study of energy transfer between systems. This leads to concepts like heat, work, temperature, and entropy. Classical thermodynamics relies

on the ability to average over thermal fluctuations of large reservoirs of particles; this requires that the system is in the so-called thermodynamic limit, which is written in terms of the particle number N and the system volume V:

$$N \to \infty, \quad V \to \infty, \quad \frac{N}{V} = \text{const.} \tag{2.3.1}$$

Many quantum systems are much smaller than the scales at which the thermodynamic limit is valid [83], and can even be single-particle systems. Crucially, fluctuations can no longer be averaged out, and both quantum and thermal fluctuations can be dominant drivers of dynamics. Therefore classical thermodynamics is no longer a good description of these systems. Quantum thermodynamics aims to extend standard thermodynamics to quantum systems which may undergo significant quantum fluctuations, be out of equilibrium, and - in some cases - have sizes much smaller than the thermodynamic limit. Quantum thermodynamics can be closely linked to concepts in open quantum systems, such as quantum coherence and quantum information.

In this Section, we will introduce some core concepts in quantum thermodynamics and describe their relevance to open quantum systems. In order to describe the laws of thermodynamics in the quantum regime, we will follow Reference [83]. However, it is worth emphasising that a full quantum thermodynamic analysis of the systems we are interested in is outside the scope of this thesis, and therefore this is only a superficial overview of the topic. There are many introductions and reviews that provide thorough discussions of the state of the field, for example in Refs. [84–86], as well as focusing on specific topics within quantum thermodynamics, for example in Refs. [87–90].

2.3.1 Laws of Thermodynamics

For a quantum state ρ with Hamiltonian H, the internal energy is the expectation value of the Hamiltonian [83]:

$$U = \langle H \rangle = \text{Tr}\left(\rho H\right). \tag{2.3.2}$$

However, we know that energy can broken up into "useful" and "useless" categories - work and heat, respectively. The average heat absorbed by the system is

$$\langle Q \rangle = \int_0^t \mathrm{Tr}\left(\dot{\rho}(\tau) H(\tau)\right) \mathrm{d}\tau, \tag{2.3.3}$$

and the average work done on the system is

$$\langle W \rangle = \int_0^t \mathrm{Tr}\left(\rho(\tau) \dot{H}(\tau)\right) \mathrm{d}\tau, \tag{2.3.4}$$

such that no work can be done on or by the system if the Hamiltonian is not time dependent. Work is extracted when $-\langle W \rangle > 0$ and heat is dissipated when $-\langle Q \rangle > 0$. The first law of thermodynamics is then

$$\langle Q \rangle + \langle W \rangle = \mathrm{Tr}\left(\rho(t) H(t)\right) - \mathrm{Tr}\left(\rho(0) H(0)\right) = \Delta U. \tag{2.3.5}$$

The concept of heat, useless energy which is dissipated out of the system, allows irreversible dynamics to emerge. This is linked to the second law of thermodynamics, which states that

$$\Delta S \geq \int \frac{\langle \delta Q \rangle}{T}, \tag{2.3.6}$$

i.e., the change in entropy is bounded from below by the heat absorbed by the system divided by the temperature of the system. This can be reformulated as an upper bound on the extractable work,

$$\langle W_{\text{ext.}} \rangle \leq -\Delta U + T \Delta S. \tag{2.3.7}$$

The entropy used in quantum thermodynamics is the von Neumann entropy which we have used before,

$$S(\rho) = -\mathrm{Tr}\left(\rho \ln \rho\right). \tag{2.3.8}$$

It is still an open discussion whether this is a good choice; for states at equilibrium, the von Neumann information theoretic entropy is equal to the thermodynamics entropy, but not otherwise [83]. Some authors consider that the von Neumann is the logical extension to the thermodynamic entropy [91–93], whereas others believe it to be an inappropriate choice [94].

2.3.2 Thermodynamics and Information

The Maxwell's demon paradox provides a clear link between entropy and information. Consider a box which containing a gas at temperature T, with a partition that divides the box into two sections. If there is a very small "demon" inside the box who could open a gap in the divider, it could in principle let gas molecules through in only one direction, eventually creating a vacuum in one half of the box. Alternative versions of the paradox involve the demon separating the box between "slow-moving" and "fast-moving" particles, thereby creating a temperature gradient. This would lower the entropy of the gas without requiring any work to be applied, and therefore (apparently) violate the second law of thermodynamics. However, there is an information theory consideration which must be taken into account.

Landauer's principle states that the erasure of information has a fundamental entropy cost [88, 95]. To erase one "bit" of information (i.e. whether a given gas molecule is to the left or right of the divider) corresponds to a minimum heat dissipation of

$$\langle Q_{\text{erasure}} \rangle = k_B T \ln 2. \tag{2.3.9}$$

There is a corresponding work cost,

$$\langle W_{\text{erasure}} \rangle = -k_B T \ln 2, \tag{2.3.10}$$

and a corresponding entropy increase,

$$\Delta S_{\text{erasure}} = k_B \ln 2. \tag{2.3.11}$$

This concept can be used to effectively solve the Maxwell's demon paradox [96]. The only way the demon can sort the fast molecules from the slow ones is to be in possession of information about the system. Because information has a thermodynamic erasure cost, it cannot be thought of as a purely abstract concept, and must instead be a physical quantity that must be accounted for. Therefore, the demon's "brain" should be considered a secondary environment, which is capable of storing information, dissipating heat, and having an associated entropy.

When the demon makes a decision about whether to open the door, it is essentially an

information erasure task. It initially has one bit of information about a given molecule, i.e. which side of the box it is on. If the molecule is on the vacuum side of the box, the demon opens the door and lets it through to the entropic side of the box. If the molecule is on the entropic side of the box, the demon does not open the door. In both cases, the molecule ends up on the same side of the door, and the piece of information that differentiated two distinct possibilities has been erased. It may be temporarily stored in the demon's brain, but this is only a delay to its eventual erasure. Therefore, the act of opening the door eventually increases the entropy of the demon-box combined system enough to counteract the entropy decrease that results from the demon's actions.

Thermodynamics of Decoherence

Decoherence is an irreversible dissipative process which should have a corresponding thermodynamic interpretation. In fact, the decoherence predicted by the Caldeira-Leggett model [31] can be associated with a large rapid increase of entropy. This also has an information interpretation: information about the original coherences is erased, and therefore - according to Landauer's principle - the entropy of the system increases. To quantify this, consider the relative entropy of coherence of an arbitrary mixed state:

$$\begin{aligned} C_{\text{rel.ent.}}(\rho) &= -S(\rho) + S(\rho_{\text{diag}}) > 0 \\ &\implies S(\rho) < S(\rho_{\text{diag}}). \end{aligned} \tag{2.3.12}$$

Given that ρ_{diag} is the post-decoherence state, it is clear that the decoherence increases the entropy of the density matrix.

In principle, coherences represent extractable work. The maximum work that can be extracted in a given evolution from ρ_1 to ρ_2 can be determined from Eq. (2.3.7) (assuming the Hamiltonian is a constant of motion and the internal energy does not change [87]) to be

$$\langle W_{\text{ext.}} \rangle = -k_B T \left(S(\rho_1) - S(\rho_2) \right). \tag{2.3.13}$$

In the case where the evolution represents decoherence, i.e. an evolution from ρ to ρ_{diag}, the

maximum extractable work is then

$$\langle W_{\text{decoh.}} \rangle = C_{\text{rel.ent.}}(\rho) T. \tag{2.3.14}$$

However, decoherence represents a process where coherences are removed by the environment in a random, uncontrolled way, and no work can be extracted [83].

Chapter 3

The Caldeira-Leggett Model

In the following sections, we review the Caldeira-Leggett model of quantum Brownian motion, originally published in Ref [31]. The motivation of this paper is to explore dissipation in a quantum system in the classical regime - i.e. at high temperatures - in a way that does not violate the uncertainty principle. They do this by attempting to derive a master equation which will return to the Fokker-Planck equation for Brownian motion in the classical limit.

The approach is to apply the path integral formulation of quantum mechanics, fully developed by Feynman [97], to find the evolution of a system linearly coupled to a reservoir of harmonic oscillators. An integral propagator is initially constructed, which is then translated into a differential equation of motion, i.e. a master equation. Finally, the corresponding Fokker-Planck equation, which describes the dynamics in the classical limit, is found and shown to be equivalent to the Brownian motion Fokker-Planck equation.

The Caldeira-Leggett model produces a master equation in the coordinate representation for a quantum system in an arbitrary potential which is valid at high temperatures. This makes it particularly useful, as many other models are constrained to a specific potential [38, 98, 99], truncate the space of energy levels [100–102], or are only valid at low temperatures [103]. For exploring open system quantum dynamics in the classical regime - e.g. inside a cellular environment at high (physiological) temperatures - the Caldeira-Leggett model is a good place to start from.

3.1 Path Integrals

In classical physics, there are many situations in which is it useful to be able to calculate the trajectory of a particle in a potential. This technique uses the Lagrangian description of the system, which is conventionally defined by

$$L = T - V, \tag{3.1.1}$$

where T is the kinetic energy and V the potential. In general, L may be directly dependent on the time t, the path co-ordinate of the particle $x(t)$, and its time derivative $\dot{x}(t)$. From the Lagrangian, we define the action,

$$S(\dot{x}, x) = \int L(x, \dot{x}, t)\mathrm{d}t. \tag{3.1.2}$$

Then, the principle of least action is applied to find the trajectory: the change in action over a perturbation of the path, $\delta x(t)$, should be 0. This leads to the Euler-Lagrange equation,

$$\frac{\mathrm{d}}{\mathrm{d}t}\left(\frac{\partial L}{\partial \dot{x}}\right) = \frac{\partial L}{\partial x}, \tag{3.1.3}$$

which uniquely determines the classical path.

In quantum physics, a system cannot be said to follow one specific trajectory, but the action principle of classical mechanics can be generalised. The single trajectory is replaced with a functional integral over all allowed trajectories, with the contribution of each weighted by $\mathrm{e}^{iS/\hbar}$, where $S(\dot{x}(t), x(t))$ is the action along that path [104]. This is inspired by situations like the double slit experiment, where a quantum system may be said to take "more than one path" at the same time.

In this framework, the probability amplitude, or kernel, $K(b, a)$ for a system to move from an event a (with time t_a, $x(t_a) = x_a$)) to an event b (with time t_b, $x(t_b) = x_b$)) is a sum of the contributions $\phi[x(t)]$ from each path,

$$K(b, a) = \sum \phi_{a,\ b}[x(t)]. \tag{3.1.4}$$

The probability amplitude is related to the probability by

$$P(b,a) = |K(b,a)|^2. \tag{3.1.5}$$

Each possible path contributes to the probability amplitude with a phase which is determined by its action,

$$\phi_{a,\,b}[x(t)] = C\ \mathrm{e}^{iS[x(t)]/\hbar}, \tag{3.1.6}$$

with a constant C that will normalise $K(b,a)$ such that probability is correctly conserved. It is not immediately clear how you should go about performing this sum: in many situations, for example the free particle, the set of possible paths is infinite and continuous. Therefore, the sum over paths has to become a path integral.

The path integral concept can be explained as follows. Let's say we have two points $x_a = x(t_a)$ and $x_b = x(t_b)$. By breaking the time period $t_b - t_a$ into small time steps of width ε such that we have times $(t_a, t_1, t_2, ..., t_b)$, and assigning each time a position such that that we have coordinates $(x_a, x_1, x_2, ..., x_b)$, we select one of the many possible paths.

If we start with only one point between t_a and t_b, we can label it t_1, and define a path $x_a \to x_1 \to x_b$. However, the choice of x_1 is arbitrary, and any other choice x_1 would still form the path from x_a to x_b. Therefore, we can integrate out x_1:

$$\mathrm{path}(x_a \to x_b) = \int \mathrm{path}(x_a \to x_1 \to x_b)\mathrm{d}x_1. \tag{3.1.7}$$

This is the sum of all paths between x_a and x_b with one intermediary point. Similarly, with two points between t_a and t_b, we can integrate out the intermediate points to obtain

$$\mathrm{path}(x_a \to x_b) = \int\int \mathrm{path}(x_a \to x_1 \to x_2 \to x_b)\mathrm{d}x_1\mathrm{d}x_2. \tag{3.1.8}$$

The more intermediary points we take, the closer we get to approaching the continuum limit of a smooth path:

$$\mathrm{path}(x_a \to x_b) = \int ... \int\int \mathrm{path}(x_a \to x_1 \to x_2 \to ... \to x_N \to x_b)\mathrm{d}x_1\mathrm{d}x_2...\mathrm{d}x_N. \tag{3.1.9}$$

In the language of path integrals, we would write this as

$$K(b,a) \approx \int ... \int \int \phi_{a,\ b}[x(t)] \mathrm{d}x_1 \mathrm{d}x_2 ... \mathrm{d}x_N. \tag{3.1.10}$$

In the limiting case, we want to take as many points as possible, with a small width. So, we take times separated by the infinitesimal time ε, such that we have

$$\begin{aligned} t_1 &= t_a + \varepsilon, \\ t_2 &= t_1 + \varepsilon \end{aligned} \tag{3.1.11}$$

and so on. Therefore, the probability amplitude is

$$K(b,a) = \lim_{\varepsilon \to 0} C \ \int ... \int \int \mathrm{e}^{iS[x_a,\, x_b]/\hbar} \mathrm{d}x_1 \mathrm{d}x_2 ... \mathrm{d}x_N. \tag{3.1.12}$$

It is not known how to define the constant C in the general case [97], but it can be done in specific cases. For example, when

$$L = \frac{1}{2} m \dot{x}^2 - \mathrm{V}(x,t), \tag{3.1.13}$$

the constant C can be calculated as

$$\left(\frac{2\pi i \hbar \varepsilon}{m} \right)^{1/2}. \tag{3.1.14}$$

The full expression for the kernel, Eq. (3.1.12), is usually condensed into

$$K(b,a) = \int_a^b \mathrm{e}^{iS[x_a,\, x_b]/\hbar} \mathrm{D}x(t), \tag{3.1.15}$$

with the capital D distinguishing the path integral from an ordinary integral.

When there is a Hamiltonian H which corresponds to the Lagrangian L, we can recognise the probability amplitude $K(b,a)$ as the matrix element

$$K(b,a) = \langle x(b) | \mathrm{e}^{-\frac{iHt}{\hbar}} | x(a) \rangle \,, \tag{3.1.16}$$

and therefore we can identify matrix elements of the unitary operator as path integrals of the

corresponding action:

$$\langle x(b)|\mathrm{e}^{-\frac{iHt}{\hbar}}|x(a)\rangle = \int_a^b \mathrm{e}^{iS[x_a,\,x_b]/\hbar}\mathrm{D}x(t). \tag{3.1.17}$$

3.2 Application of Path Integrals

The evolution of the density matrix of a system with Hamiltonian H is described as in Eq. (2.1.24), by the unitary operator acting forwards and backwards:

$$\rho(t) = \mathrm{e}^{-\frac{iHt}{\hbar}}\rho(0)\mathrm{e}^{\frac{iHt}{\hbar}}. \tag{3.2.1}$$

In the co-ordinate (position) representation, we define system (x, y) and environment $(\mathbf{R}, \mathbf{Q})$ co-ordinates. The matrix elements of the density matrix undergoing this evolution are

$$\begin{aligned}\langle x\mathbf{R}|\,\rho(t)\,|y\mathbf{Q}\rangle &= \langle x\mathbf{R}|\,\mathrm{e}^{-\frac{iHt}{\hbar}}\rho(0)\mathrm{e}^{\frac{iHt}{\hbar}}\,|y\mathbf{Q}\rangle \\ &= \int \mathrm{d}x'\mathrm{d}y'\mathrm{d}\mathbf{R}'\mathrm{d}\mathbf{Q}'\,\langle x\mathbf{R}|\,\mathrm{e}^{-\frac{iHt}{\hbar}}\,|x'\mathbf{R}'\rangle\,\langle x'\mathbf{R}'|\,\rho(0)\,|y'\mathbf{Q}'\rangle\,\langle y'\mathbf{Q}'|\,\mathrm{e}^{\frac{iHt}{\hbar}}\,|y\mathbf{Q}\rangle\,.\end{aligned} \tag{3.2.2}$$

In this expression, the completeness identity has been inserted in the initial coordinates $(x', \mathbf{R}')$ and $(y', \mathbf{Q}')$. This has the effect of integrating out the initial states in the system and environment, as well as separating the expression out into tractable pieces. We can recognise the first and third terms in the integrand as kernels,

$$\begin{aligned}\langle x\mathbf{R}|\,\mathrm{e}^{-\frac{iHt}{\hbar}}\,|x'\mathbf{R}'\rangle &\equiv K(x, \mathbf{R}, t; x'\mathbf{R}', 0) \\ \langle y\mathbf{Q}|\,\mathrm{e}^{\frac{iHt}{\hbar}}\,|y'\mathbf{Q}'\rangle &\equiv K^*(y, \mathbf{Q}, t; y'\mathbf{Q}', 0).\end{aligned} \tag{3.2.3}$$

Using the path integral formulation described in the last section, the kernels are expressed by a path integral over the action of the system:

$$\begin{aligned}K(x, \mathbf{R}, t; x'\mathbf{R}', 0) &\equiv \int \mathrm{D}x\mathrm{D}\mathbf{R}\ \exp\left\{\frac{i}{\hbar}S[x, \mathbf{R}]\right\}; \\ K^*(y, \mathbf{Q}, t; y'\mathbf{Q}', 0) &\equiv \int \mathrm{D}y\mathrm{D}\mathbf{Q}\ \exp\left\{-\frac{i}{\hbar}S[y, \mathbf{Q}]\right\}.\end{aligned} \tag{3.2.4}$$

The action is found by integrating over the Lagrangian of the system, such that we have

$$S[x, \mathbf{R}] = \int_0^t L(x, \mathbf{R})\mathrm{d}t. \tag{3.2.5}$$

The capital D inside the integration of Eq. (3.2.4) refers to path integration [97], as described in Section 3.1.

Our aim is to obtain the reduced dynamics of just the system density matrix $\tilde{\rho}(x, y, t)$, and therefore we need to separate as far as possible the system and environment coordinates in order to perform a partial trace over the environment. We introduce a separated initial condition for the density matrix

$$\rho(x', y', \mathbf{R}', \mathbf{Q}', 0) = \tilde{\rho}(x', y', 0)\rho_{\mathrm{E}}(\mathbf{R}', \mathbf{Q}', 0). \tag{3.2.6}$$

This represents an interaction being "switched on" at time $t = 0$. Although widely used, this is not an uncontroversial choice [77, 105, 106].

In a system-plus-reservoir of the kind we are interested in modelling, the action can be broken up into contributions from the system, interaction, and environment Lagrangians:

$$L(x, \mathbf{R}) = L_{\mathrm{S}}(x) + L_{\mathrm{I}}(x, \mathbf{R}) + L_{\mathrm{E}}(\mathbf{R}), \tag{3.2.7}$$

such that

$$S = S_{\mathrm{S}}[x] + S_{\mathrm{I}}[x, \mathbf{R}] + S_{\mathrm{E}}[\mathbf{R}]. \tag{3.2.8}$$

We can re-write Eq. (3.2.2) as

$$\langle x,\ \mathbf{R}|\, \rho(t)\, |y,\ \mathbf{Q}\rangle = \int \mathrm{d}x'\mathrm{d}y'\mathrm{d}\mathbf{R}'\mathrm{d}\mathbf{Q}' \left(\int \mathrm{D}x\mathrm{D}\mathbf{R}\ \mathrm{e}^{\frac{i}{\hbar}S[x,\mathbf{R}]}\right)\left(\int \mathrm{D}y\mathrm{D}\mathbf{Q}\ \mathrm{e}^{-\frac{i}{\hbar}S[y,\mathbf{Q}]}\right) \langle x',\ \mathbf{R}'|\, \rho(0)\, |y',\ \mathbf{Q}'\rangle\,. \tag{3.2.9}$$

In order to obtain the reduced dynamics for the system alone, we trace over the environment coordinate:

$$\langle x|\, \rho(t)\, |y\rangle = \int \mathrm{d}\mathbf{R}\, \langle x,\ \mathbf{R}|\, \rho(t)\, |y,\ \mathbf{Q}\rangle\,, \tag{3.2.10}$$

where it is understood that the integrand is evaluated in $\mathbf{R}$ and $\mathbf{Q}$ prior to the trace being taken. We can rearrange the expression a little to separate out the system and environment

coordinates, and relabel the matrix elements as functions:

$$\begin{aligned}\tilde{\rho}(x,y,t) &= \int \mathrm{d}x'\mathrm{d}y'\mathrm{d}\mathbf{R}\mathrm{d}\mathbf{R}'\mathrm{d}\mathbf{Q}' \left(\int \mathrm{D}x\mathrm{D}\mathbf{R}\ \mathrm{e}^{\frac{i}{\hbar}(S_{\mathrm{S}}[x]+S_{\mathrm{I}}[x,\mathbf{R}]+S_{\mathrm{E}}[\mathbf{R}])}\right) \\ &\quad \times \left(\int \mathrm{D}y\mathrm{D}\mathbf{Q}\ \mathrm{e}^{\frac{i}{\hbar}(S_{\mathrm{S}}[q]+S_{\mathrm{I}}[q,\mathbf{Q}]+S_{\mathrm{E}}[\mathbf{Q}])}\right) \tilde{\rho}(x',y',0)\rho_{\mathrm{E}}(\mathbf{R}',\mathbf{Q}',0) \\ &= \int \mathrm{d}x'\mathrm{d}y'\tilde{\rho}(x',y',0)\int \mathrm{D}x\mathrm{D}y\ \mathrm{e}^{\frac{i}{\hbar}(S_{\mathrm{S}}[x]-S_{\mathrm{S}}[y])} \\ &\quad \times \int \mathrm{d}\mathbf{R}\mathrm{d}\mathbf{R}'\mathrm{d}\mathbf{Q}'\rho_{\mathrm{E}}(\mathbf{R}',\mathbf{Q}',0)\int \mathrm{D}\mathbf{R}\mathrm{D}\mathbf{Q}\mathrm{e}^{\frac{i}{\hbar}(S_{\mathrm{I}}[x,\mathbf{R}]-S_{\mathrm{I}}[x,\mathbf{Q}]+S_{\mathrm{E}}[\mathbf{R}]-S_{\mathrm{E}}[\mathbf{Q}])}\end{aligned} \tag{3.2.11}$$

These equations can be simplified to give the propagator equation for the reduced dynamics of the system,

$$\tilde{\rho}(x,y,t) = \int \mathrm{d}x'\mathrm{d}y' J(x,y,t;x',y',0)\tilde{\rho}(x',y',0), \tag{3.2.12}$$

with the propagator

$$J(x,y,t;x',y',0) = \int \mathrm{D}x\mathrm{D}y\ \mathrm{e}^{\frac{i}{\hbar}(S_{\mathrm{S}}[x]-S_{\mathrm{S}}[y])}\mathcal{F}[x,y] \tag{3.2.13}$$

and the influence functional

$$\mathcal{F}[x,y] = \int \mathrm{d}\mathbf{R}\mathrm{d}\mathbf{R}'\mathrm{d}\mathbf{Q}'\rho_{\mathrm{E}}(\mathbf{R}',\mathbf{Q}',0)\int \mathrm{D}\mathbf{R}\mathrm{D}\mathbf{Q}\mathrm{e}^{\frac{i}{\hbar}(S_{\mathrm{I}}[x,\mathbf{R}]-S_{\mathrm{I}}[x,\mathbf{Q}]+S_{\mathrm{E}}[\mathbf{R}]-S_{\mathrm{E}}[\mathbf{Q}])}. \tag{3.2.14}$$

The influence functional contains all the terms with environmental dependence. Eqs. (3.2.12)-(3.2.14) describe the exact reduced dynamics of a system interacting with an environment. In the next section, we will go from this general propagator equation to the specific case constructed by Caldeira and Leggett, and from there to a differential master equation.

3.3 The Caldeira-Leggett Model

The Caldeira-Leggett model [31] considers a one-dimensional system with co-ordinate x and mass m that experiences an arbitrary potential $\mathrm{V}(x)$. It is linearly coupled to an environment which is described by a collection of non-interacting harmonic oscillators with co-ordinates R_k, frequencies ω_k, and mass m_k; the coupling strength to each oscillator is C_k. Extensive justification for the harmonic oscillator model can be found in Appendix C of [103] and Section

2 of [107]. The Lagrangian of the total system is given by

$$\begin{aligned} L(x,\mathbf{R}) &= L_{\mathrm{S}}(x,t) + L_{\mathrm{I}}(x,\mathbf{R}) + L_{\mathrm{E}}(\mathbf{R},t) \\ &= \Big(\frac{p^2}{2m} - \mathrm{V}(x)\Big) - \Big(x\sum_k C_k R_k\Big) + \Big(\sum_k \frac{p_k^2}{2m_k} - \sum_k \frac{1}{2} m_k \omega_k^2 R_k^2\Big), . \end{aligned} \tag{3.3.1}$$

where $\{x,p\}$ ($\{R_k,p_k\}$) are the position and momentum of the system (environment oscillators), m (m_k) is the mass of the system (environment oscillator), ω_k is the frequency of the environment oscillator, and C_k is the coupling strength between the system and each environment oscillator. The influence functional and the propagator associated with this Lagrangian can be evaluated using the techniques outlined in Section 3.1 and fully explained in Ref [104]. We find that

$$J(x,y,t;x',y',0) = \int \mathrm{D}x\mathrm{D}y\ \mathrm{e}^{\frac{i}{\hbar}\left(\frac{1}{2}m(\dot{x}^2-\dot{y}^2)-[\mathrm{V}(x)-\mathrm{V}(y)]\right)}\mathcal{F}[x,y]. \tag{3.3.2}$$

The influence functional for a reservoir of harmonic oscillators is derived in Refs [97, 104], and we quote the result:

$$\mathcal{F}[x,y] = \mathrm{e}^{-\frac{1}{\hbar}\int_0^t\int_0^\tau [x(\tau)-y(\tau)][\alpha(\tau-\tau')x(\tau')-\alpha^*(\tau-\tau')y(\tau')]\mathrm{d}\tau'\mathrm{d}\tau}, \tag{3.3.3}$$

with the influence kernel

$$\alpha(\tau-\tau') = \sum_k \frac{C_k^2}{2m\omega_k}\Big(\mathrm{e}^{-i\omega_k(\tau-\tau')} + \frac{\mathrm{e}^{i\omega_k(\tau-\tau')}+\mathrm{e}^{-i\omega_k(\tau-\tau')}}{\mathrm{e}^{\hbar\omega/kT}-1}\Big). \tag{3.3.4}$$

This is calculated by inserting the known classical path of a damped harmonic oscillator into the action integrals, and assuming the reservoir of harmonic oscillators to be in a Gibbs distribution:

$$\langle \mathbf{R}'|\,\rho_E\,|\mathbf{Q}'\rangle = \prod_k \frac{1}{Z}\Big(\frac{m\omega_k}{2\pi\hbar\sinh\beta\hbar\omega_k}\Big)^{1/2}\exp\Big\{-\frac{m\omega_k}{2\hbar\sinh\beta\hbar\omega_k}\Big((R_k'^2+Q_k'^2)\cosh\beta\hbar\omega_k - 2R_k'Q_k'\Big)\Big\}, . \tag{3.3.5}$$

where Z is the partition function. However, details of these calculations are not included in this thesis as they can be found in full in Ref [97].

We can then insert the evaluated influence functional to write down the propagator in a

more useful form,

$$J(x,y,t;x',y',0) = \int \mathrm{D}x\mathrm{D}y\Big(\exp\left\{ \frac{i}{\hbar}(S_{\mathrm{S}}[x] - S_{\mathrm{S}}[y] - \int_0^t \int_0^\tau [x(\tau)-y(\tau)]\alpha_{\mathrm{I}}(\tau-\tau')[x(\tau')+y(\tau')]\mathrm{d}\tau'\mathrm{d}\tau \right\}$$
$$\times \exp\left\{ -\frac{1}{\hbar}\int_0^t \int_0^\tau [x(\tau)-y(\tau)]\alpha_{\mathrm{R}}(\tau-\tau')[x(\tau')-y(\tau')]\mathrm{d}s\mathrm{d}\tau \right\}. \tag{3.3.6}$$

In this expression, α_{R} and α_{I} are the real and imaginary parts of the influence kernel,

$$\begin{aligned} \alpha_R(\tau-\tau') &= \sum_k \frac{C_k^2}{2m\omega_k} \coth\frac{\hbar\omega_k}{2kT}\cos\omega_k(\tau-\tau') \\ \alpha_I(\tau-\tau') &= -\sum_k \frac{C_k^2}{2m\omega_k}\sin\omega_k(\tau-\tau'). \end{aligned} \tag{3.3.7}$$

These are often referred to as the noise kernel and the dissipation kernel, respectively [9]. When we take the high temperature limit $\hbar\omega \ll kT$ of the hyperbolic cotangent,

$$\coth\frac{\hbar\omega_k}{2kT} \approx \frac{2kT}{\hbar\omega_k}, \tag{3.3.8}$$

we can re-write these using the definition of the spectral density, Eq. (2.2.33):

$$\begin{aligned} \alpha_R(\tau-\tau') &= \frac{2kT}{\hbar\pi}\int_0^\infty \frac{J(\omega)}{\omega}\mathrm{cos}\omega(\tau-\tau')\mathrm{d}\omega; \\ \alpha_I(\tau-\tau') &= -\frac{1}{\pi}\int_0^\infty J(\omega)\mathrm{sin}\omega(\tau-\tau')\mathrm{d}\omega. \end{aligned} \tag{3.3.9}$$

It is worth noting that the high-temperature limit is where the Born approximation enters, and the timescale separation is imposed: the timescale of thermal fluctuations in the environment is much shorter than the timescale of any frequencies associated to the system.

In order to make the switch from a summation to an integral, the continuum limit has to be taken, which means we assume that the spectrum of oscillator frequencies is so smooth as to be continuous, from the point of view of the system. In addition, the Markov approximation is taken: the reservoir should have infinite size, such that the energy lost by the system should not return within a finite time. This choice is motivated by the desire to recover Markovian Brownian motion in the classical limit. With this in mind, the Ohmic spectral density is chosen

to describe the density of states and coupling strengths of the environment oscillators,

$$J(\omega) = \begin{cases} \eta\omega, & \omega < \Omega \\ 0, & \omega > \Omega. \end{cases} \tag{3.3.10}$$

When $\Omega \to \infty$, the Ohmic spectral density corresponds to frequency-independent damping (as demonstrated in Section 2.2.3), which is a Markovian process. This manifests in the Caldeira-Leggett propagator structure as the noise and dissipation kernels tend to δ-functions in the $\Omega \to \infty$, effectively killing off any time correlation:

$$\begin{aligned} \alpha_{\mathrm{R}}(\tau - \tau') &= \frac{2kT}{\hbar\pi} \int_0^{\Omega} \eta \cos\omega(\tau - \tau')\mathrm{d}\omega \\ &= \frac{2\eta kT}{\hbar\pi} \frac{\sin\Omega(\tau - \tau')}{(\tau - \tau')} \\ \implies \lim_{\Omega\to\infty} \alpha_{\mathrm{R}}(\tau - \tau') &= \lim_{\Omega\to\infty} \frac{2\eta kT}{\hbar\pi} \frac{\sin\Omega(\tau - \tau')}{(\tau - \tau')} \\ &= \frac{2\eta kT}{\hbar} \delta(\tau - \tau'). \end{aligned} \tag{3.3.11}$$

By identifying from Eq. (3.3.9) that

$$\alpha_{\mathrm{I}}(\tau - \tau') = \frac{\hbar}{2kT} \frac{\partial}{\partial(\tau - \tau')} \alpha_{\mathrm{R}}(\tau - \tau'), \tag{3.3.12}$$

we immediately write down

$$\lim_{\Omega\to\infty} \alpha_{\mathrm{I}}(\tau - \tau') = \eta \frac{\partial}{\partial(\tau - \tau')} \delta(\tau - \tau'). \tag{3.3.13}$$

This allows us to write the propagator as

$$\begin{aligned} J(x, y, t; x', y', 0) = \int \mathrm{Dx}\ \mathrm{Dy}\ \exp\left\{ \frac{\mathrm{i}}{\hbar} \left(S_S[x] - S_S[y] - \eta \int_0^t f_-(\tau) \int_0^{\tau} \frac{\mathrm{d}}{\mathrm{d}(\tau - \tau')} \delta(\tau - \tau') f_+(\tau')\mathrm{d}\tau'\mathrm{d}\tau \right) \right\} \\ \times \exp\left\{ -\frac{2\eta kT}{\hbar^2} \int_0^t f_-(\tau) \int_0^{\tau} \delta(\tau - \tau') f_-(\tau')\mathrm{d}\tau'\mathrm{d}\tau \right\}, \end{aligned} \tag{3.3.14}$$

with the notation $f_{\pm}(\tau) = [x(\tau) \pm y(\tau)]$. The nested integrals can be evaluated by utilising the

δ-function property. This is simple for the real integral,

$$\int_0^\tau \delta(\tau-\tau')f_-(\tau')\mathrm{d}\tau' = \frac{1}{2}f_-(\tau), \tag{3.3.15}$$

where the factor of $1/2$ is due to the condition $\delta(0)$ being met at the upper limit of integration, rather than in the integration interval. The imaginary integral is slightly more involved due to the derivative but we can approach it via integration by parts,

$$\begin{aligned}\int_0^\tau \frac{\mathrm{d}}{\mathrm{d}(\tau-\tau')}\delta(\tau-\tau')f_+(\tau')\mathrm{d}\tau' &= -[\delta(\tau-\tau')f_+(\tau')]_0^\tau + \int_0^\tau \delta(\tau-\tau')f'_+(\tau')\mathrm{d}\tau' \\ &= -\delta(0)f_+(\tau) + \frac{1}{2}f'_+(\tau').\end{aligned} \tag{3.3.16}$$

The $\delta(0)$ term is problematic, as it introduces an undefined and arbitrarily large constant into the dynamics, but this is justified by recalling that the δ-function is introduced via the $\Omega\to\infty$ limit of the exact form of the noise kernel, and therefore we make the replacement

$$\delta(0) = \frac{\sin\Omega\tau}{\tau}|_{\tau=0} = \frac{\Omega}{\pi}. \tag{3.3.17}$$

Therefore, the propagator can be re-written

$$\begin{aligned}J(x,y,t;x',y',0) = \int \mathrm{Dx}\ \mathrm{Dy}\ \exp\Big\{\frac{\mathrm{i}}{\hbar}\Big(S_S[x]-S_S[y] + \frac{\eta\Omega}{\pi}\int_0^t f_-(\tau)f_+(\tau)\mathrm{d}\tau \\ - \int_0^t \frac{\eta}{2}f_-(\tau)f'_+(\tau')\mathrm{d}\tau\Big)\Big\} \times\ \exp\Big\{-\frac{\eta kT}{\hbar^2}\int_0^t f_-^2(\tau)\mathrm{d}\tau\Big\},\end{aligned} \tag{3.3.18}$$

and when the $f_\pm(\tau)$ functions are expanded back into $x(\tau)$ and $y(\tau)$, this becomes

$$\begin{aligned}J(x,y,t;x',y',0) = \int \mathrm{Dx}\ \mathrm{Dy}\ \exp\Big\{\frac{\mathrm{i}}{\hbar}(S_\mathrm{R}[x]-S_\mathrm{R}[y]) \\ - \frac{iM\gamma}{\hbar}\int_0^t [x\dot{x}-y\dot{y}+x\dot{y}-y\dot{x}]\mathrm{d}\tau - \frac{2M\gamma kT}{\hbar^2}\int_0^t [x-y]^2\mathrm{d}\tau\Big\}.\end{aligned} \tag{3.3.19}$$

We have made the replacement $\eta = \frac{\gamma}{2m}$. The "renormalised action" S_R is given by

$$S_\mathrm{R}[x] = \int_0^t [\frac{1}{2}M\dot{x}^2 - \mathrm{V}(x)]\mathrm{d}\tau + \int_0^t \frac{1}{2}M(\Delta\omega)^2x^2\mathrm{d}\tau, \tag{3.3.20}$$

i.e. it is the action with the potential renormalised by the subtraction of a harmonic term with frequency $\Delta(\omega)^2 = \frac{4\gamma\Omega}{\pi}$. The shift comes from the integration by parts of the imaginary integral Eq. (3.3.16), where a term proportional to $\delta(0)$ is re-written as $\frac{\eta\Omega}{\pi}$. This renormalisation is conventionally understood to be unphysical, induced by coupling to oscillators with infinite frequency, and it is removed by the addition of a so-called "counter-term" in the Lagrangian [9]. This counter-term functions much like a UV cut-off in QFT [108]: it removes the predictions made in the regime where the model breaks down. For that reason, we drop the potential renormalisation here and continue as if we had removed it via the counter-term.

This propagator, when substituted back into Eq. (3.2.12), will give the evolution of the reduced dynamics of the system in terms of functional integrals. In order to go from the propagator to a master equation, we again follow a procedure laid out by Feynman [104] in which he derives the Schrödinger equation from a functional integral.

By considering the behaviour of the propagator over an infinitesimal time ϵ, we can write the evolution of the density matrix over this interval as

$$\tilde{\rho}(x, y, t+\varepsilon) = \int_{t}^{t+\varepsilon} \mathrm{d}x' \mathrm{d}y' J(x, y, t+\varepsilon; x', y', t)\tilde{\rho}(x', y', t). \tag{3.3.21}$$

Because ϵ is a small parameter, we write the left hand side as

$$\tilde{\rho}(x, y, t+\varepsilon) = \tilde{\rho}(x, y, t) + \varepsilon \frac{\partial}{\partial t}\tilde{\rho}(x, y, t) + O(\varepsilon^2). \tag{3.3.22}$$

Therefore, when the right hand side is expanded in terms of ε, the $O(1)$ terms should provide a normalisation condition, and the $O(\varepsilon)$ terms will become terms in the master equation.

Because we are only considering an infinitesimal time interval, we can approximate the integrand of the propagator as a straight line. The propagator is the value of the integrand

multiplied by a normalisation:

$$J(x,y,t+\varepsilon;x',y',t) \approx \frac{1}{A^2}\exp\Big\{\frac{\mathrm{i}}{\hbar}(\frac{1}{2}m\dot{x^2} - \frac{1}{2}m\dot{y}^2 - [\mathrm{V_R}(x) - \mathrm{V_R}(y)] \\ - \frac{iM\gamma}{\hbar}\int_0^t [x\dot{x} - y\dot{y} + x\dot{y} - y\dot{x}]\mathrm{d}\tau - \frac{2M\gamma kT}{\hbar^2}\int_0^t [x-y]^2\mathrm{d}\tau\Big\}. \tag{3.3.23}$$

We can also approximate the derivative terms as

$$\dot{x} \approx \frac{\beta_x}{\epsilon}, \tag{3.3.24}$$

with $\beta_x = x - x'$. Therefore, we have

$$\tilde{\rho}(x,y,t+\varepsilon) = \frac{1}{A^2}\int \mathrm{d}\beta_x \mathrm{d}\beta_y \exp\Big\{\frac{im}{2\varepsilon\hbar}(\beta_x^2 - \beta_y^2) - \frac{i\varepsilon}{\hbar}[\mathrm{V_R}\left(x - \frac{\beta_x}{2}\right) - \mathrm{V_R}\left(y - \frac{\beta_y}{2}\right)] \\ - \frac{im\gamma}{\hbar}\left(\left(x - \frac{\beta_x}{2}\right)\beta_y + \left(x - \frac{\beta_x}{2}\right)\beta_x - \left(y - \frac{\beta_y}{2}\right)\beta_y - \left(y - \frac{\beta_y}{2}\right)\beta_x\right) \\ - \frac{2m\gamma kT\varepsilon}{\hbar^2}(x-y)^2 - \frac{2m\gamma kT\varepsilon}{\hbar^2}(x-y)(\beta_x - \beta_y) - \frac{m\gamma kT\varepsilon}{\hbar^2}(\beta_x - \beta_y)^2\Big\} \\ \times \tilde{\rho}(x - \beta_x, y - \beta_y, t). \tag{3.3.25}$$

When the renormalised potential and initial condition terms are expanded around x or y, this integration can be performed. The first term, proportional to $O(\frac{1}{\varepsilon})$, is retained as an exponential. The other terms are expanded in powers of $O(\varepsilon)$, and the resulting integrals are Gaussian. When we evaluate this (see Appendix B for further details), we find that

$$A = \sqrt{\frac{2\pi\varepsilon\hbar}{m}}, \tag{3.3.26}$$

and

$$\frac{\partial\tilde{\rho}}{\partial t} = \frac{i\hbar}{2m}\left(\frac{\partial^2\tilde{\rho}}{\partial x^2} - \frac{\partial^2\tilde{\rho}}{\partial y^2}\right) - \frac{i}{\hbar}[\mathrm{V_R}(x) - \mathrm{V_R}(y)]\tilde{\rho} - \gamma(x-y)\left(\frac{\partial\tilde{\rho}}{\partial x} - \frac{\partial\tilde{\rho}}{\partial y}\right) - \frac{2m\gamma kT}{\hbar^2}(x-y)^2\tilde{\rho}. \tag{3.3.27}$$

The first two terms, with coefficients not proportional to γ, describe unitary evolution (kinetic and potential terms, respectively). The third term is responsible for environment-induced relaxation, and the final temperature-dependent term causes decoherence. The significance of these terms will be discussed in the next section.

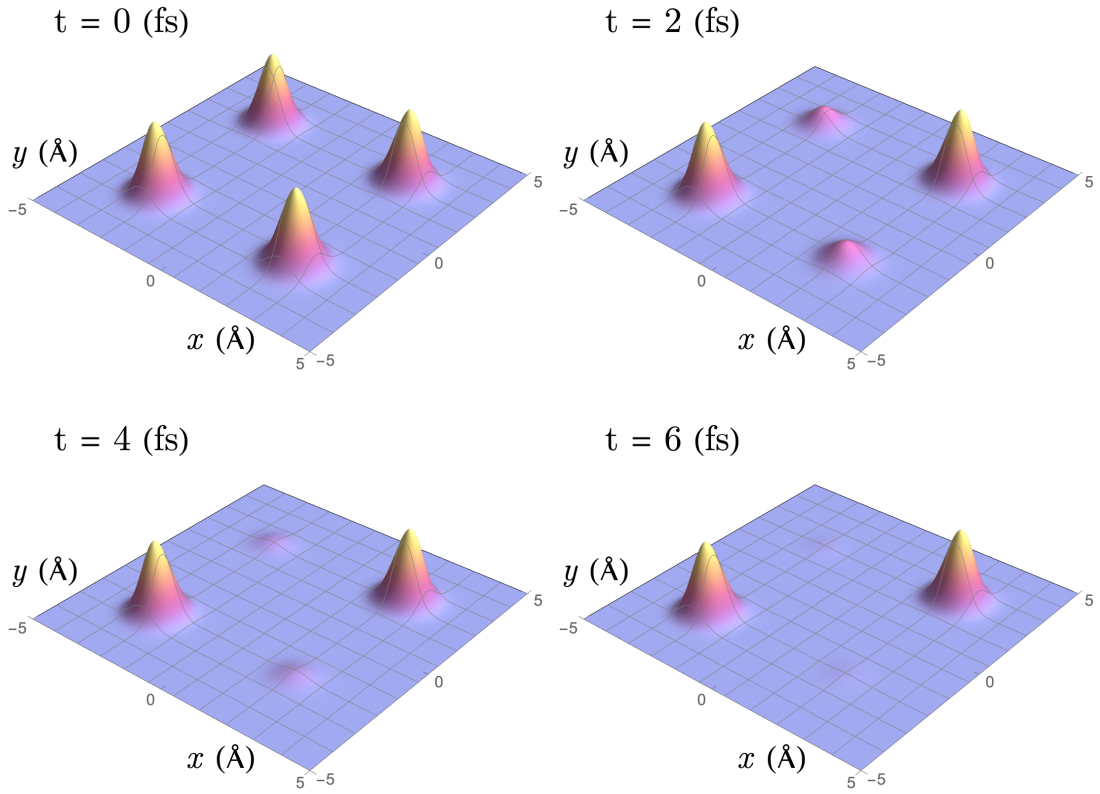

Figure 3.1: Evolution over 6fs of a proton in an initial double-Gaussian state with separation $5\mathring{A}$ and standard deviation $\frac{1}{\sqrt{6}}$ under the Markovian Caldeira-Leggett master equation, Eq. (3.3.27). The parameters are $T = 320\text{K}$, $\gamma = \frac{kT}{20\hbar}$, $m = M_p$ (the proton mass), and $\mathrm{V_R}(x) = 0$. Plots made using Eq. (5.2.8), the exact solution of the master equation, derived in Section 5.2.1. Decoherence is the dominant feature of the dynamics at this timescale.

3.3.1 Modelling Caldeira-Leggett Dynamics

The effects of the Caldeira-Leggett model can be demonstrated by considering an initial double Gaussian state. The short-time evolution for a proton in an initial double Gaussian state, with separation $5\mathring{A}$, is demonstrated in Figure 3.1. As predicted by Zurek [7], the decoherence process is the dominant feature over this timescale, with the on-diagonal peaks undergoing negligible evolution during the time that the off-diagonal peaks completely decohere.

Zurek also identified that the term responsible for decoherence is

$$\mathcal{L}_{\text{decoh.}} = \frac{2m\gamma kT}{\hbar^2}(x-y)^2, \tag{3.3.28}$$

and therefore the rate of decoherence is proportional to the temperature of the environment:

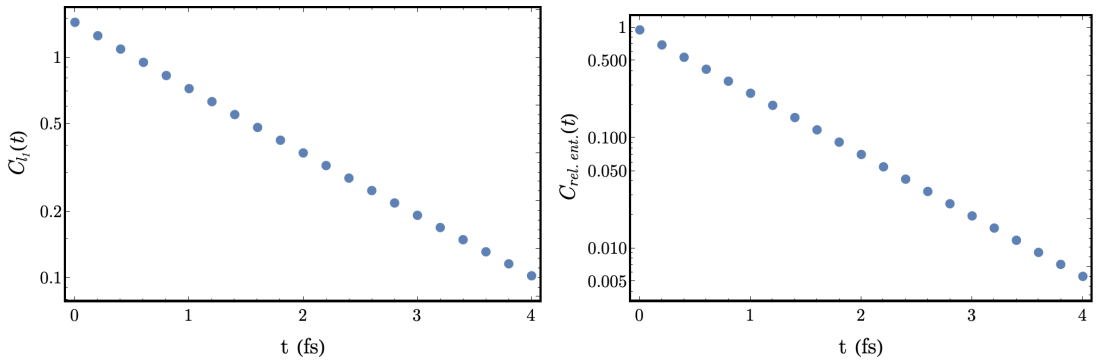

Figure 3.2: Decoherence in the Caldeira-Leggett master equation, measured using the l_1-norm (left) and the relative entropy (right) of coherence, demonstrated on a log-linear plot. The l_1-norm is calculated via Eq. (2.2.40) and the relative entropy of coherence is calculated via Eq. (2.2.42). The two measures do not match in scale, but in feature. The linear behaviour of the log-lin plot demonstrates exponential decoherence.

hotter environments cause quantum systems to decohere faster. Another feature of the decoherence term is that the strength of decoherence is proportional to the square of the distance from the diagonal: more delocalised superpositions are more susceptible to decoherence. Figure 3.2 demonstrates the decoherence quantified by the l_1-norm and the relative entropy of coherence previously discussed.

The term

$$\mathcal{L}_{\text{relax.}} = -\gamma(x-y)\left(\frac{\partial}{\partial x} - \frac{\partial}{\partial y}\right) \tag{3.3.29}$$

is the relaxation term, which spreads out the Gaussians on a timescale much longer than the decoherence time. Finally, the term

$$\mathcal{L}_{\text{L-vN}} = \frac{i\hbar}{2m}\left(\frac{\partial^2}{\partial x^2} - \frac{\partial^2}{\partial y^2}\right) - \frac{i}{\hbar}[\mathrm{V_R}(x) - \mathrm{V_R}(y)] \tag{3.3.30}$$

describes the unitary dynamics of the system. It can be shown [72, 109] that, for a free particle, the steady state of the system is

$$\rho_\infty = \frac{1}{\sqrt{2\pi}} \mathrm{e}^{-\frac{m\gamma T}{2\hbar^2}(x-y)^2}, \tag{3.3.31}$$

i.e. a Gaussian with temperature-dependent width.

3.3.2 Wigner Transform of the Caldeira-Leggett Equation

The Wigner phase-space distribution is an alternative formulation of quantum mechanics. It has an advantage over both the wavefunction and the density matrix in that it contains the distribution of both position q and momentum p [110]. Because phase space distributions exist for quantum and classical systems, it is much easier to compare a quantum system to its classical counterpart using the Wigner function, and therefore identify the dynamical differences between the two. The classical limit of the Wigner function is found by setting $\hbar = 0$, allowing for comparison between macroscopic dynamics of quantum systems, and classical dynamics. The Wigner equation can also be used to study the transition from quantum to classical behaviour [2, 111], via disappearing interference fringes which present a visualisation of the decoherence process [2].

The Wigner transform can be used to verify that the Caldeira-Leggett master equation corresponds to Brownian motion: in the classical limit $\hbar \to 0$, the equation of motion for the Wigner distribution becomes the Fokker-Planck equation [112].

The Wigner transform is defined for a general density matrix by

$$W_{\tilde{\rho}}(q,p) = \frac{1}{\hbar}\int \mathrm{d}u \ \exp\Big\{i\frac{pu}{\hbar}\Big\}\,\langle q - \frac{u}{2}|\tilde{\rho}|q + \frac{u}{2}\rangle\,, \tag{3.3.32}$$

and the probability distributions in q and p are found by calculating the marginals,

$$\begin{aligned}\langle q|\tilde{\rho}|q\rangle &= \int_{-\infty}^{\infty} W_{\tilde{\rho}}(q,p)\mathrm{d}p \\ \langle p|\tilde{\rho}|p\rangle &= \int_{-\infty}^{\infty} W_{\tilde{\rho}}(q,p)\mathrm{d}q.\end{aligned} \tag{3.3.33}$$

The Fokker-Planck, or Klein, equation corresponding to the Caldeira-Leggett master equation is [31]

$$\frac{\partial W}{\partial t} = -\frac{p}{m}\frac{\partial W}{\partial x} + \frac{\partial \mathrm{V}}{\partial x}\frac{\partial W}{\partial p} + 2\gamma\frac{\partial}{\partial p}(pW) + 2m\gamma kT\frac{\partial^2 W}{\partial p^2}, \tag{3.3.34}$$

with $W(x,p,t)$ the quantum probability distribution corresponding to $P(x,p,t)$ (see Section 5.3 for more details); recalling that $\eta = 2m\gamma$, we can see that this takes the same form as the Brownian motion Fokker-Planck equation, Eq. (2.2.30). Therefore, the Caldeira-Leggett

equation can be said to describe quantum Brownian motion, and is successful in describing a dissipative - irreversible - process.

3.4 Renormalisation Group Approach to the Caldeira-Leggett Model

The theory of renormalisation is most well-known for its application to quantum field theory (QFT) [98, 113, 114]. In QFT, it is used to "regularise" infinite values in the definition of quantities that are physically measurable, in particular the mass of fundamental particles, by subtracting the divergent contributions. However, it is also possible to consider the regularised theory as fundamental, which then becomes a theory of the effect of scaling on physical systems [115–117]. Here, scaling can be understood as the process of "zooming out", or "zooming in", to analyse the physical processes that dominate the dynamics at each scale. Scaling transformations form one part of the s-called renormalisation group, which by definition is the group of transformations under which a theory is universal. In this context, scale can refer to length, temperature, momentum, or energy, and one important feature that emerges from analysing scaling behaviour is phase transitions: there are special values of the scale parameters at which the behaviour of the system discontinuously changes. Examples are phase transitions between states of matter, such as boiling or melting, and separation between components of an alloy. The special values at which phase transitions occur are referred to as critical values. The Curie temperature of a ferromagnetic transformation is an example of a critical value.

Regularising the theory in the renormalisation group approach relies on choosing a "cut-off scale"; we understand that we do not expect a theory to be valid over all scales, and any infinite quantities arising from contributions at scales in which the theory is invalid should not be considered real predictions of the theory. For example, an ultraviolet (high frequency) cut-off is often imposed to reflect that QFT cannot tell us about Planck-scale physical phenomena. The resulting theory is often referred to as a Wilsonian effective theory [118]. The Caldeira-Leggett counter-term [9] is a form of UV cut-off, i.e a term which is artificially introduced into a theory in order to remove the divergent contribution from an unrealistically high-frequency contribution.

This Section provides an overview of some core concepts in renormalisation group approaches, as well as a review of their application to the Caldeira-Leggett model. We hope to present some interesting concepts which will be later used to suggest future research avenues.

Effective Field Theory

Effective field theory aims to formalise the ideas of coarse graining and cut-off scales such that these concept can be applied to a wide range of systems. It explicitly considers the case where some system has a characteristic energy scale k, and we are interested in modelling the physics at $\omega \ll k$ [116]. The system has an action, $S[\phi]$, which can be separated into a low-energy and a high-energy part: $S[\phi] = S[\phi_L, \phi_H]$ where $\phi_{H(L)}$ is valid for $\omega > k$ ($\omega < k$). The path integral of the action can be written as

$$\int \mathrm{D}\phi_L \mathrm{D}\phi_H \mathrm{e}^{\frac{i}{\hbar}S(\phi_L,\phi_H)} = \int \mathrm{D}\phi_L \mathrm{e}^{\frac{i}{\hbar}S_k(\phi_L)}, \tag{3.4.1}$$

where

$$\mathrm{e}^{\frac{i}{\hbar}S_k(\phi_L)} = \int \mathrm{D}\phi_H \mathrm{e}^{\frac{i}{\hbar}S(\phi_L,\phi_H)} \tag{3.4.2}$$

is known as the effective action, or sometimes the Wilsonian effective action. However, in principle we do not know exactly what the value of Λ will be, and we do not want the resulting physics to be dependent on an arbitrary selection of high-frequency cut-off. Varying Λ allows the Wilson equation to be written down:

$$\frac{\partial S_k}{\partial k} = \beta[S_k]. \tag{3.4.3}$$

The functional β can be found in Ref. [116]. It compensates the integration of high-momentum modes of the field in terms of an effective interaction. The Wilson equation defines a so-called renormalisation flow in an infinite dimensional space. The fixed points of this flow are critical points of the system of interest, and represent the low-energy physical content of the theory.

We can choose an ansatz for $S_k[\phi]$. The local potential approximation (LPA) [119] states that

$$S_k[\phi] = \int \mathrm{d}^D x V_k(\phi) + \frac{1}{2}\partial_\mu\phi\partial_\mu\phi, \tag{3.4.4}$$

where D is the dimension of the model. By considering a constant background field $\phi = \phi_0$, we

can write down

$$k\frac{\partial}{\partial k}V_k = \frac{\hbar k^D N_D}{2}\ln\left(k^2 + V_k''\right), \tag{3.4.5}$$

with N_D a constant that depends on the dimensionality.

Effective Field Theory in the Caldeira-Leggett Model

Previous attempts to apply renormalisation group techniques [120, 121] to the Caldeira-Leggett model have focused on the low-temperature tunnelling model (reference), and are primarily interested in analysing the quantum-classical transition. These attempts develop a framework in which the environment oscillators are thought of as modes in an infinite-dimensional field of the type described by quantum field theory.

Refs. [120, 121] start by identifying the contribution of the environment to the effective action experienced by the system of interest (coordinate q),

$$\Delta S_{\text{eff}}[q] = \int \mathrm{d}\tau \int \mathrm{d}\tau' q(\tau)\alpha(\tau-\tau')q(\tau'), \tag{3.4.6}$$

with the kernel defined (slightly differently to Eq. (3.3.7)) by

$$\begin{aligned}\alpha(\tau-\tau') &= \int \frac{\mathrm{d}\omega}{2\pi}\sum_j \frac{C_j^2}{2m_j}\frac{1}{\omega^2+\omega_j^2}\mathrm{e}^{i\omega(\tau-\tau')} \\ &= \int_0^\infty \frac{\mathrm{d}\omega}{2\pi} J(\omega)\mathrm{e}^{-\omega|\tau-\tau'|}.\end{aligned} \tag{3.4.7}$$

This action is separated into a local part, which contributes to the potential renormalisation, and a non-local part, which contributes to the genuine dissipative dynamics. The local part reads

$$\Delta S_{\text{L}} = -\tilde{\alpha}(0)\int \mathrm{d}\tau q^2(\tau), \tag{3.4.8}$$

with

$$\tilde{\alpha}(0) = \frac{1}{\pi}\int_0^\infty \frac{J(\omega)}{\omega}\mathrm{d}\omega, \tag{3.4.9}$$

and the non-local part is

$$\Delta S_{\text{NL}} = \frac{1}{2}\int \mathrm{d}\tau \int \mathrm{d}\tau' [q(\tau)-q(\tau')]^2\alpha(\tau-\tau'), \tag{3.4.10}$$

which can be written (after Fourier transform of the time variables) as

$$\Delta S_{\mathrm{NL}} = \frac{1}{2}\int \tilde{q}(\omega)\Sigma(\omega)\tilde{q}(\omega)\mathrm{d}\omega, \tag{3.4.11}$$

with

$$\Sigma(\omega) = -\frac{1}{2\pi}\int_0^\infty J(\omega')\frac{4\omega'}{\omega^2+\omega'^2}\mathrm{d}\omega'; \tag{3.4.12}$$

The "self-energy" $\Sigma(\omega)$ is the spectral density contribution to the dissipation.

Now, we replace ω - the environment oscillator frequency - with a cut-off scale k that describes the increasingly high-momentum modes of the environment. This step is just to re-label parameters according to convention, and the effective action of the system can be re-written as [121] as

$$S_k[q] = \frac{1}{2}\int M\dot{q}^2 + \int\Big(V_k(q) + \frac{1}{2}\Sigma_k q^2\Big). \tag{3.4.13}$$

From here, we use Eq. (3.4.5) to write down the LPA differential equation for the effective potential [119],

$$k\frac{\partial}{\partial k}V_k = \frac{k}{2\pi}\ln\Big(k^2 + \frac{\partial^2 V_k}{\partial q^2} + \Sigma_k\Big). \tag{3.4.14}$$

This is called the non-perturbative renormalisation group (NPRG) equation [122] or the Wenger-Houghton equation. This equation describes the effective potential V_k, felt by the system, as a result of the environment modes up to k. We can write down the boundary condition

$$\lim_{k\to 0} V_k[q] = V_0[q], \tag{3.4.15}$$

i.e. the effective potential when there are no environmental modes is equal to the bare potential of the system.

The Wegner-Houghton equation can then be solved to examine the dissipative effect of the non-local term. For example, Aoki and Horikoshi [120] look at the case of a bare double-well potential and note that as k increases, $V_k(q)$ becomes a single well potential, effectively halting any tunnelling between wells. Kovács et al [121] demonstrate numerically that for selected cut-off functions of the Ohmic spectral density, the critical exponent associated with correlation

length in the Caldeira-Leggett model is independent of the value and form of the frequency cut-off.

Chapter 4

Non-Markovianity

4.1 Markovian and Non-Markovian Dynamics

In previous sections, we have referred to the Markov approximation, which restricts open quantum systems to complete timescale separation between the system and the environment. In this Section, we describe the conditions which define Markovianity in more detail, as well as exploring the conditions which define *non*-Markovianity. Although the Markov approximation is used to model a wide range of systems, there are many situations in which the environment relaxation timescales are not separated well enough from the system relaxation and decoherence times [40, 59]. This can occur for small or structured environments, low temperatures, or strong coupling strengths. This manifests as memory effects in the dynamics, or non-monotonic decreases of properties which usually irreversibly dissipate.

The traditional definition of Markovianity comes from classical probability distributions [59], which cannot be directly translated into an appropriate definition for a quantum system. However, it is a useful tool to first discuss this. Suppose we have a classical variable X which takes values x_n at time t_n. It is Markovian if the value x_n and time t_n is dependent only on the value x_{n-1} at time t_{n-1}. This is formally expressed via the conditional probability equation

$$P(x_n, t_n|x_{n-1}, t_{n-1}; ...; x_0, t_0) = P(x_n, t_n|x_{n-1}, t_{n-1}), \tag{4.1.1}$$

i.e. the probability of the variable taking a value x_n at time t_n is only dependent on the "present" value of the variable x_{n-1} at time t_{n-1}, and not any "past" states of the system, x_{n-2}, x_{n-3}, etc.

The system dynamics are not dependent on its history, and the system is therefore described as "memoryless". From this we can derive the Chapman-Kolmogorov equation [40],

$$P(x_1, t_1|x_0, t_0) = \sum_{x' \in X} P(x_1, t_1|x', t')P(x', t'|x_0, t_0). \tag{4.1.2}$$

This can be interpreted as a path-independent probability: the intermediate points between t_0 and t_1 are integrated out. Therefore, we can say that Markov processes are path independent. Eqs. (4.1.1)-(4.1.2) fully determine a classical Markov process.

These conditions cannot be directly applied to quantum systems, because of the difficulty in determining the history of a similarly defined quantum variable. The analogous equation to Eq. (4.1.1) is [59]

$$P(x_n, t_n|x_{n-1}, t_{n-1}; ...; x_0, t_0) = \mathrm{Tr}\left(\mathcal{M}_{x_n} U(t_n, t_{n-1}) ... \mathcal{M}_{x_1} U(t_1, t_0)\rho(0)\right), \tag{4.1.3}$$

with $\mathcal{M}_{x_n}$ the operation corresponding to the measurement outcome x_n. In general, the RHS of this equation cannot be written in the form of the RHS of Eq. (4.1.1), meaning that this definition is insufficient for quantum systems. Although the Markov property is reflected by the semigroup property

$$V(t_1)V(t_2) = V(t_1 + t_2), \tag{4.1.4}$$

which defines quantum Markovian dynamics in the Lindblad equation, the best way to characterise non-Markovian dynamics in quantum systems is to study the memory effects induced by a given master equation. This allows us to avoid the effects of measurement choices and rely solely on the properties of the reduced density matrix $\rho_S(t)$. Several methods exist for doing so, and an overview of some of these is presented below.

4.1.1 Deviation from Complete Positivity

In a Markovian system, the dynamics can be described by a Lindblad equation, which ensures that the dynamics are completely positive (CP). However, in a non-Markovian system, some viewpoints assert that the dynamics will deviate from Lindblad form and therefore also deviate from being CP (although as discussed in Section 2.2.5, the necessity of CP-dynamics is still contested). Given the assumption that the more the dynamics deviates from CP, the more non-

Markovian it is, a measure of non-Markovianity can be constructed by quantifying the amount that a master equation deviates from CP. This approach was introduced by Rivas, Huelga, and Plenio [123] and is therefore referred to as the RHP measure of non-Markovianity.

For some evolution from t_0 to t_1 that goes through an intermediate point t', we can write

$$V(t_1, t_0) = V(t_1, t')V(t', t_0), \tag{4.1.5}$$

and we can use the inverse of the map to isolate the intermediate part:

$$V(t_1, t') = V(t_1, t_0)V^{-1}(t', t_0). \tag{4.1.6}$$

In a non-Markovian evolution, there must by some value of t' for which $V(t_1, t')$ is not completely positive (otherwise, it would be Markovian). The Choi theorem [124] states that

$$||V(t_1, t') \otimes |\Phi\rangle\langle\Phi| \, ||_1 = \begin{cases} = 1 & \text{iff V}(\mathrm{t}_1, \mathrm{t}')\text{CP} \\ > 1 & \text{else.} \end{cases} \tag{4.1.7}$$

A function $g(t)$ can be defined which signals non-CP behaviour:

$$g(t) = \lim_{\varepsilon \to 0} \frac{||V(t+\epsilon, t) \otimes |\Phi\rangle\langle\Phi| \, ||_1 - 1}{\varepsilon}, \tag{4.1.8}$$

such that $g(t) > 0$ for non-CP, non-Markovian behaviour. Therefore, we can construct the RHP measure of non-Markovianity:

$$\mathcal{N}_{\mathrm{RHP}} = \int g(t) \mathrm{d}t. \tag{4.1.9}$$

In this case, there is no need to specify a condition on the integral region, because the Markovian $g(t) = 0$ regions will not contribute.

4.1.2 Information Backflow and Trace Distance

In a Markovian system, information is constantly transferred from the system to the environment, as the environment continuously monitors - or makes weak measurements - on the system. However, in a non-Markovian system, information can return to the system, which typically introduces time correlations: the present state of the system is dependent on past states of the

system, via the information which left the system at an earlier time and then returned [125–129]. This idea can be formalised via the trace distance, which measures the distinguishability of two states, i.e. the probability of successfully distinguishing the states from one another [130, 131]. In a Markovian system, the trace distance should continuously decrease, as information about past states is irretrievably lost and both states evolve towards thermal equilibrium along the most direct path [132]. However, a non-Markovian system can have a non-monotonic trace distance between two states, as information about past states re-enters the system and increases the distinguishability.

For two density matrices $\rho_1(t)$ and $\rho_2(t)$, starting from different initial conditions and evolving according to the same master equation, the trace distance is defined by

$$D(\rho_1, \rho_2) = \frac{1}{2}\mathrm{Tr}\left|\rho_1 - \rho_2\right|, \tag{4.1.10}$$

with $|A| = \sqrt{A^\dagger A}$. When the master equation determining evolution of $\rho_1(t)$ and $\rho_2(t)$ is a Lindblad equation, it can be shown that [131]

$$D(\rho_1(t+\tau)\rho_2(t+\tau)) \leq D(\rho_1(t)\rho_2(t)), \tag{4.1.11}$$

and therefore the trace distance is decreasing for Markovian maps. Defining the rate of change of the trace distance as

$$\sigma(t, \rho_{1,2}(0)) = \frac{\mathrm{d}}{\mathrm{d}t}D(\rho_1, \rho_2), \tag{4.1.12}$$

any system for which $\sigma(t, \rho_{1,2}(0)) > 0$ for some value or values of t is non-Markovian. Therefore, a quantifier of non-Markovianity can be written down:

$$\mathcal{N}_{\text{trace dist.}} = \max_{\rho_{1,2}(0)} \int_{\sigma>0} \sigma(t, \rho_{1,2}(0))\mathrm{d}t. \tag{4.1.13}$$

This integral is optimised over the pair of initial states $\rho_1(0)$, $\rho_2(0)$ which maximise the value. The integral region is all time intervals for which $\sigma(t, \rho_{1,2}(0)) > 0$. For the Markovian case $\mathcal{N}_{\text{trace dist.}} = 0$, and it is bounded for all states which eventually thermalise.

The trace distance idea can be linked to the timescale separation expression of the Markov

approximation: information which is lost from the system to the environment introduces time correlations on the order of τ_{E}^{-1}, which is negligible in the coarse-graining necessary to uphold the Markov approximation. Therefore, these incredibly rapid fluctuations are washed out by the dominant processes of decoherence and relaxation [133].

The non-monotonic decrease of the trace distance is one way of using the characteristic information backflow to identify/quantify non-Markovian dynamics. We can also use the relative entropy between two states. Relative entropy signifies the information that is shared between two states [60]; it is given by

$$S(\rho||\sigma) = \mathrm{Tr}\left(\rho_1 \ln \rho_1\right) - \mathrm{Tr}\left(\rho_1 \ln \rho_2\right). \tag{4.1.14}$$

The relative entropy between two states ρ_1 and ρ_2 can also be used as a measure of the distinguishability; we have

$$S(\rho_1||\rho_2) = \mathrm{Tr}\left(\rho_1 \ln \rho_1\right) - \mathrm{Tr}\left(\rho_1 \ln \rho_2\right). \tag{4.1.15}$$

When $\rho_1 = \rho_2$, this vanishes. It can be shown that the relative entropy decreases under CP maps [134]:

$$S(V(\rho_1)||V(\rho_2)) \leq S(\rho_1||\rho_2). \tag{4.1.16}$$

Therefore, an increase in relative entropy between any two states signifies that the dynamics are non-Markovian in a similar way to the trace distance [40]. This can be extended to apply to the relative entropy of coherence: when we set $\rho_2 = \rho_{\mathrm{diag}}$ - i.e. the diagonalised state - we obtain the relative entropy of coherence, and therefore an increase in the relative entropy of coherence is a signifier of non-Markovian behaviour.

There are many other ways information backflow can be used as a signifier of non-Markovianity, for example by monitoring the flow of the quantum Fisher information [35], calculating the value of the Helstrom matrix norm [40], and finding an increase in the quantum discord [5]. Thorough reviews of these and other methods can be found in Refs. [40, 59].

4.2 The Hu-Paz-Zhang Model

The Hu-Paz-Zhang (HPZ) model presents the exact derivation of the master equation for a Brownian harmonic oscillator linearly coupled to an arbitrary environment [38]. Because the environment is not restricted to being Ohmic, the resulting equation is non-Markovian. However, it should be emphasised that although their work is valid for any choice of environment, they are restricted to the choice of a harmonic oscillator for the system. They follow the approach of Caldeira and Leggett [31], i.e. the path integral influence functional method for a system linearly coupled to an environment of harmonic oscillators. However, their method for going from an integral equation to a differential equation is considerably more involved. A brief overview of the derivation is presented below, with details in Appendix A; a more thorough derivation can be found in Refs. [38, 135].

The action of the combined system + environment is

$$\begin{aligned} S[x,R_k] &= S_{\rm S}[x] + S_{\rm I}[x,R_k] + S_{\rm E}[R_k] \\ &= \int_0^t {\rm d}s \left[\frac{1}{2}m(\dot{x}^2 - \omega_0^2 x^2) + \sum_k [\frac{1}{2}m_k(\dot{R}_k^2 - \omega_k^2 R_k^2] - \sum_k C_k x R_k \right], \end{aligned} \tag{4.2.1}$$

where, as in the Caldeira-Leggett action, x and R_k are the system and environment oscillator coordinates, m and m_k are the system and environment masses, and ω_0 and ω_k are the system and environment frequencies. We follow the Caldeira-Leggett approach up to the point of writing down the integral equation of motion, propagator, and influence functional (Eqs. (3.2.12)-(3.2.14)). After this, the derivation diverges. The propagator is re-defined via the effective action $A[x,y]$:

$$J(x,y,t;x',y',t_0) = \int {\rm D}x{\rm D}y \exp\left[\frac{i}{\hbar}A[x,y]\right], \tag{4.2.2}$$

with the influence functional similarly redefined with reference to the influence action $\delta A[x,y]$

$$\mathcal{F}[x,y] = \exp\left[\frac{i}{\hbar}\delta A[x,y]\right] \tag{4.2.3}$$

such that we have

$$A[x,y] = S_{\rm S}[x] - S_{\rm S}[y] + \delta A[x,y]. \tag{4.2.4}$$

The influence functional is written slightly differently to Eq. (3.3.3), but the character remains

essentially the same:

$$\mathcal{F}[x,y] = \exp\Bigg[-\frac{i}{\hbar}\int_0^t \mathrm{d}\tau \int_0^\tau \mathrm{d}\tau' f_-(\tau)\frac{\mathrm{d}}{\mathrm{d}(\tau-\tau')}\mu(\tau-\tau')f_+(\tau') \\ -\frac{1}{\hbar}\int_0^t \mathrm{d}\tau \int_0^\tau \mathrm{d}\tau' f_-(\tau)\left(\int_0^\infty \mathrm{d}\omega J(\omega)\coth\frac{\hbar\omega}{2kT}\cos\omega(\tau-\tau')\right) f_-(\tau')\Bigg], \tag{4.2.5}$$

with $f_\pm(\tau) = x(\tau) \pm y(\tau)$ as before. In general, the influence functional does not represent Markovian dynamics due to the non-local time correlation functions in the nested integrals. In the Caldeira-Leggett model of Markovian quantum Brownian motion, this is avoided by finding the condition under which these time correlations are δ-functions; the HPZ derivation leaves the non-locality in place in order to explicitly include non-Markovianity in the model.

The procedure continues by considering the propagation of the reduced density matrix over an infinitesimal time step. However, the method differs from the Caldeira-Leggett approach in that the authors define approximate paths for $x(t)$ and $y(t)$ and integrate over these. This allows the nested integrals to be evaluated without taking any approximations on the form of $\mu(\tau)$. The procedure is very involved and an overview can be found in Appendix A. However, it is worth emphasising that the paths defined for $(x(t), y(t))$ are dependent on the classical harmonic oscillator paths, and the final result is dependent on this; this is the step that restricts the validity of the HPZ equation to the harmonic oscillator. Although an analogous process could be performed for a specific choice of potential, this task is neither simple nor straightforward, and it is not possible to generalise this step.

The HPZ equation is obtained by performing the necessary integrations over the infinitesimal intervals and paths:

$$i\hbar\frac{\partial}{\partial t}\tilde{\rho}(x,y,t) = \Big[-\frac{\hbar^2}{2}\left(\frac{\partial^2}{\partial x^2} - \frac{\partial^2}{\partial y^2}\right) + \frac{1}{2}(\omega_0^2 + \delta\omega_0^2(t))(x^2 - y^2)\Big]\tilde{\rho}(x,y,t) \\ - i\hbar\Gamma(t)(x-y)\left(\frac{\partial}{\partial x} - \frac{\partial}{\partial y}\right)\tilde{\rho}(x,y,t) - i\Gamma(t)h(t)(x-y)^2\tilde{\rho}(x,y,t) \\ + \hbar\Gamma(t)f(t)(x-y)\left(\frac{\partial}{\partial x} + \frac{\partial}{\partial y}\right)\tilde{\rho}(x,y,t), \tag{4.2.6}$$

with time-dependent coefficients

$$\begin{aligned}
\Gamma(t) &= \frac{d_1(t)}{2\dot{u}_1(t)} \\
\delta\omega_0^2(t) &= d_2(t) - 2\Gamma(t)\dot{u}_2(t) \\
f(t) &= 2\frac{a_{12}(t)}{\dot{u}_2(0)} + \frac{e_2(t) - c_1(t)}{2\Gamma(t)\dot{u}_2(0)} \\
h(t) &= \dot{u}_2(t)f(t) + 8a_{11}(t) + \frac{e_1(t) - c_2(t)}{\Gamma(t)}.
\end{aligned} \tag{4.2.7}$$

Most of the time-dependent coefficients are dependent on $\mu(t)$; this is how the spectral density dependence enters into the master equation. This is an exact master equation which is valid for all temperatures, spectral densities, and does not involve any coarse-graining of time. However, it is not particularly "user-friendly"; computing the time-dependent coefficients is not a straightforward task. The non-Markovian character of the equation is contained in the time-dependent coefficients; in the Markovian case, the coefficients will lose their time dependence. The first two terms in the HPZ master equation are the standard Liouvillian-von Neumann dynamics, with the harmonic oscillator frequency shifted by a time-dependent phase. The relaxation and decoherence terms analogous to the Caldeira-Leggett relaxation and decoherence terms are the third and fourth terms, and the final term is an additional diffusive term.

4.3 Other non-Markovian Models

There are many varied approaches to non-Markovian dynamics in open quantum systems; a recent and thorough review can be found in Ref. [136]. Non-Markovian extensions to the Lindblad equation can be derived via the inclusion of time-dependent coefficients and Lindblad operators [35, 137] - in fact, it has been shown that the HPZ equation can be recovered from a time-dependent Lindblad approach [138]. The two-level spin-boson model has been given an exact non-Markovian master equation [139], and non-Markovian master equations of the form

$$\frac{\mathrm{d}\rho}{\mathrm{d}t} = \int_0^t \mathrm{d}t' k(t')\mathcal{L}\rho(t - t') \tag{4.3.1}$$

have been studied for qubit systems [140]. Approaches which do not involve deriving a master equation include stochastic Schrödinger equations (SSEs) [141, 142], Langevin equations [143, 144], and hierarchical equations of motion (HEOMs) [145].

Chapter 5

The non-Markovian Master Equation

In Chapter 3, we introduced the Caldeira-Leggett model [31] of quantum Brownian motion in some detail, and discussed its usefulness as a model valid for a general potential and high temperatures. We also considered a major limitation of the model, namely the Markov condition. In this Chapter, we will extend the model to investigate non-Markovian dynamics by relaxing the Markov condition, imposed in this framework by the limit $\Omega \to \infty$, and following the procedure described in the original model.

5.1 The Derivation of the non-Markovian Master Equation

The Caldeira-Leggett derivation of a quantum Brownian master equation considers the spectral density

$$J(\omega) = \begin{cases} \eta\omega & 0 < \omega < \Omega \\ 0 & \omega > \Omega, \end{cases} \tag{5.1.1}$$

in the limit $\Omega \to \infty$. The corresponding memory kernel, calculated according to Eq. (2.2.34), is

$$\begin{aligned} \mu(\tau) &= \lim_{\Omega\to\infty} \frac{\eta}{\pi} \int_0^\Omega \cos\omega\tau \mathrm{d}\omega \\ &= \eta\delta(\tau), \end{aligned} \tag{5.1.2}$$

and this represents the Markov condition. We consider the case in which this limit is relaxed[1]; Ω is no longer infinite but instead very large. This is a more realistic model of the thermal environment: there is a maximum oscillator frequency, and a finite timescale for effects in the environment [10]. This is in contrast to the Caldeira-Leggett spectral density, which assumes a bath with infinitely many oscillators at infinitely large frequencies, causing an infinite shift in the potential which is conventionally addressed by including a counter-term in the Lagrangian [9]. Introducing a high-frequency cut-off, Ω, into the spectral density means the potential shift is finite, and no such counter-term is required. Relaxing the limit is, in addition, equivalent to introducing non-Markovianity into the system: instead of the δ-function kernel (Eq. (3.3.11)) - which removes any time correlation - we will obtain a memory kernel which is only an approximation to a δ-function in the $\Omega \to \infty$ limit. This will introduce contributions to the master equation from correlations between times which are clearly separated. These time-correlations can be referred to as "memory", as the system dynamics are dependent on past states of the system. Another way of understanding the non-Markovianity of the system is to see that we have moved from the infinite heat bath of Caldeira-Leggett to a structured environment, with structure imposed by the cut-off frequency; this means that information backflow is to be expected [130, 146].

We can label $\tau_B = \Omega^{-1}$ as a timescale associated with dynamics in the bath: it is the period of the maximum oscillator frequency, which dominates the spectral density. The system relaxation time is $\tau_S = \gamma^{-1}$; this characterises the speed with which decoherence takes place. Then the condition $\Omega > \gamma$ means we will have the timescale separation $\tau_B < \tau_S$. Typically, for Markovian dynamics, we require that $\tau_S/\tau_B \gtrapprox 100$, whereas in the non-Markovian case we can consider timescales which have less strict separation. Maintaining a separation of timescales is an important part of the open quantum systems framework, as systems which are not separated in timescale are difficult to distinguish [9]: the open quantum systems framework relies on making a clear distinction between system and environment.

The new spectral density, representing a finite bath, is implemented in the model by re-

[1]This question was initially addressed by a previous student, Nicholas Werren. We worked collaboratively on making some corrections to obtain the master equation presented in this chapter. The work in Section 5.1 is a presentation of his derivation, and contains details and insights of my own; everything from Section 5.2 onwards is entirely my own work.

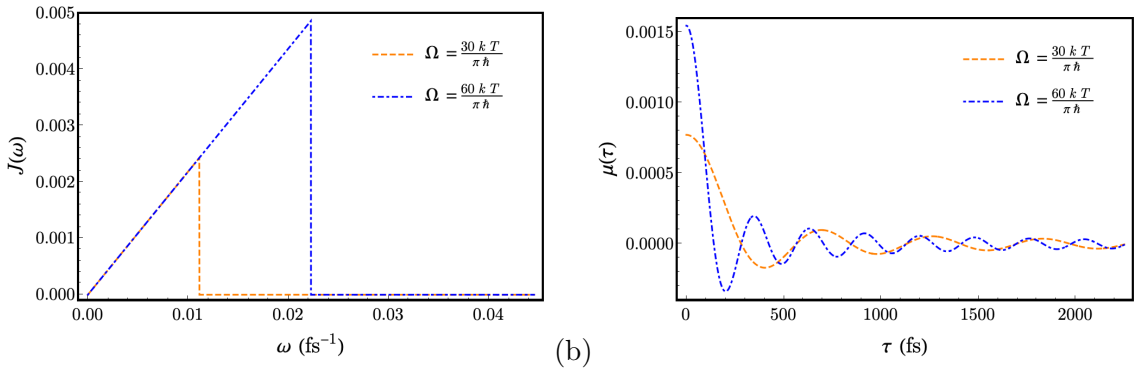

Figure 5.1: (a) The spectral density with $\gamma = \frac{kT}{20\hbar}\text{fs}^{-1}$ and a harsh cut-off with $\Omega = \{\frac{30kT}{\pi\hbar}, \frac{60kT}{\pi\hbar}\}$. (b) Memory kernel associated with the harsh cut-off spectral density, Eq. (5.1.6), with τ in fs. For the larger value of Ω, the memory kernel is a closer approximation of a δ-function.

calculating the Caldeira-Leggett propagator with a new memory kernel, and using the resulting expression to derive a master equation using the process outlined in Section 3.3. The Caldeira-Leggett propagator can be generalised by making the following correspondences between the the real and imaginary parts of the influence kernel and the memory kernel $\mu(t)$:

$$\begin{aligned}\alpha_{\text{R}}(\tau) &= \frac{2kT}{\hbar\pi}\int_0^\infty \frac{J(\omega)}{\omega}\cos\omega\tau\text{d}\omega \\ &= \frac{2kT}{\hbar}\mu(\tau)\end{aligned} \tag{5.1.3}$$

and

$$\begin{aligned}\alpha_{\text{I}}(\tau) &= -\frac{1}{\pi}\int_0^\infty J(\omega)\sin\omega\tau\text{d}\omega \\ &= \frac{\partial}{\partial\tau}\frac{1}{\pi}\int_0^\infty \frac{J(\omega)}{\omega}\cos\omega\tau\text{d}\omega \\ &= \frac{\partial}{\partial\tau}\mu(\tau).\end{aligned} \tag{5.1.4}$$

The memory kernel does not provide any information not contained in $\alpha_{\text{I}}(\tau)$ and $\alpha_{\text{R}}(\tau)$, but functions as a useful tool to summarise the effects of the spectral density in the propagator.

Therefore, we can re-write the Caldeira-Leggett propagator as

$$J(x,y,t;x',y',0) = \int \mathrm{Dx}\ \mathrm{Dy}\ \exp\left\{\frac{\mathrm{i}}{\hbar}\left(S_S[x] - S_S[y] - \int_0^t f_-(\tau)\int_0^\tau \frac{\mathrm{d}}{\mathrm{d}(\tau-\tau')}\mu(\tau-\tau')f_+(\tau')\mathrm{d}\tau'\mathrm{d}\tau\right)\right\}$$
$$\times \exp\left\{-\frac{2kT}{\hbar^2}\int_0^t f_-(\tau)\int_0^\tau \mu(\tau-\tau')f_-(\tau')\mathrm{d}\tau'\mathrm{d}\tau\right\}. \tag{5.1.5}$$

The memory kernel associated with the new spectral density is found by calculating

$$\begin{aligned}\mu_\Omega(\tau) &= \frac{\eta}{\pi}\int_0^\Omega \cos\omega\tau\mathrm{d}\omega \\ &= \frac{\eta}{\pi}\frac{\sin\Omega\tau}{\tau}.\end{aligned} \tag{5.1.6}$$

Substituting this result into Eq. (5.1.5) gives us

$$\begin{aligned}J(x,y,t;x',y',0) = \int \mathrm{Dx}\ \mathrm{Dy}\ \exp\Bigg\{\frac{\mathrm{i}}{\hbar}\Bigg(&S_S[x] - S_S[y] \\ &- \int_0^t f_-(\tau)\int_0^\tau \frac{\eta}{\pi}\frac{\mathrm{d}}{\mathrm{d}(\tau-\tau')}\frac{\sin\Omega(\tau-\tau')}{(\tau-\tau')}f_+(\tau')\mathrm{d}\tau'\mathrm{d}\tau\Bigg)\Bigg\} \\ \times \exp\Bigg\{&-\frac{2kT}{\hbar^2}\int_0^t f_-(\tau)\int_0^\tau \frac{\eta}{\pi}\frac{\sin\Omega(\tau-\tau')}{(\tau-\tau')}f_-(\tau')\mathrm{d}\tau'\mathrm{d}\tau\Bigg\}.\end{aligned} \tag{5.1.7}$$

The first step from here is to evaluate the two inner integrals over τ' containing the memory kernel. By noticing that these integrals have the form of a convolution, we can apply the Convolution Theorem for the Laplace transform to solve them:

$$\mathcal{L}\Big\{\int_0^\tau g_1(\tau-\tau')g_2(\tau')\mathrm{d}\tau'\Big\}(p) = \mathcal{L}\Big\{g_1(\tau)\Big\}(p)\times\mathcal{L}\Big\{g_2(\tau)\Big\}(p), \tag{5.1.8}$$

where

$$\mathcal{L}\Big\{g(\tau)\Big\}(p) = \int_0^\infty \mathrm{e}^{-p\tau}g(\tau)\mathrm{d}\tau. \tag{5.1.9}$$

Therefore, the first of the nested integrals can be written as an inverse Laplace transform:

$$\frac{\eta}{\pi}\int_0^\tau \frac{\sin\Omega(\tau-\tau')}{(\tau-\tau')}f_-(\tau')\mathrm{d}\tau' = \mathcal{L}^{-1}\Big\{\Big(\mathcal{L}\Big\{\frac{\eta}{\pi}\frac{\sin\Omega\tau}{\tau}\Big\}(p)F_-(p)\Big)\Big\}(\tau), \tag{5.1.10}$$

with $F_-(p)$ the Laplace transform of $f_-(\tau)$. In order to evaluate this, we first take the Laplace transform of the memory kernel:

$$\begin{aligned}\frac{\eta}{\pi}\int_0^\infty \mathrm{e}^{-p\tau}\frac{\sin\Omega\tau}{\tau}\mathrm{d}\tau &= \frac{\eta}{\pi}\arctan\Big(\frac{\Omega}{p}\Big)\\ &= \frac{\eta}{\pi}\Big(\frac{\pi}{2}-\arctan\Big(\frac{p}{\Omega}\Big)\Big),\end{aligned} \tag{5.1.11}$$

where the reciprocal property of the arctan function, valid for $p > 0$, has been used between the two lines.

To complete the evaluation of the first nested integral, we now have to take the inverse Laplace transform

$$\mathcal{L}^{-1}\Big\{\Big(\frac{\eta}{2}-\frac{\eta}{\pi}\arctan\Big(\frac{p}{\Omega}\Big)\Big)F_-(p)\Big\}(\tau). \tag{5.1.12}$$

If we utilise the Taylor expansion of the arctan function,

$$\arctan\Big(\frac{p}{\Omega}\Big) = \sum_{n=0}^{\infty}\frac{(-1)^n}{2n+1}\Big(\frac{p}{\Omega}\Big)^{2n+1}, \tag{5.1.13}$$

the expression

$$\mathcal{L}^{-1}\Big\{p^nF(p)\Big\}(\tau) = f^{(n)}(\tau) + \sum_{m=0}^{(n-1)}\Big[f^{(m)}(0)\delta^{(n-1)-m}(\tau)\Big]. \tag{5.1.14}$$

can be used to find the inverse Laplace transform. We write Eq. (5.1.12) as

$$\mathcal{L}^{-1}\Big\{\Big(\frac{\eta}{2}-\frac{\eta}{\pi}\arctan\Big(\frac{p}{\Omega}\Big)\Big)F_-(p)\Big\}(\tau) = \mathcal{L}^{-1}\Big\{\Big(\frac{\eta}{2}-\frac{\eta}{\pi}\sum_{n=0}^{\infty}\frac{(-1)^n}{2n+1}\Big(\frac{p}{\Omega}\Big)^{2n+1}\Big)F_-(p)\Big\}(\tau), \tag{5.1.15}$$

and therefore

$$\begin{aligned}&\frac{\eta}{\pi}\int_0^\tau\frac{\sin\Omega(\tau-\tau')}{(\tau-\tau')}f_-(\tau')\mathrm{d}\tau'\\ =&\frac{\eta}{2}f_-(\tau)-\frac{\eta}{\pi}\sum_{n=0}^{\infty}\frac{(-1)^n}{(2n+1)}\frac{1}{\Omega^{(2n+1)}}\Big(f_-^{(2n+1)}(\tau)+\sum_{m=0}^{(n-1)}f_-^{(m)}(0)\delta^{((n-1)-m)}(\tau)\Big).\end{aligned} \tag{5.1.16}$$

The first term on the right hand side contains the Markovian dynamics already in the Caldeira-Leggett equation. (We may refer to these terms as Caldeira-Leggett dynamics in following

discussions.) The non-Markovianity is contained in the second line of the right-hand side, represented by higher derivatives of the function $f_-(\tau)$. However, defining higher derivatives of a function requires more knowledge of the function at previous times. For example, the first derivative can be approximated in terms of finite differences using two time points,

$$f'(t_2) \approx \frac{f(t_2) - f(t_1)}{t_2 - t_1}, \tag{5.1.17}$$

whereas the second derivative approximated in the same way requires three time points:

$$f''(t_1) \approx \frac{f(t_2) - 2f(t_1) + f(t_0)}{(t_2 - t_1)^2}. \tag{5.1.18}$$

This reflects the non-Markovian behaviour described by the propagator we are deriving: more information about previous times is required. The more higher derivatives are included, the more non-Markovian the description of the system we obtain.

The choice to truncate the series after $n = 0$ is made on the justification that Ω is very large compared to γ, where $\gamma = \frac{\eta}{2M}$. Therefore, we retain terms to only leading order in $\frac{1}{\Omega}$. This is in line with the timescale arguments we have made previously; the condition $\Omega > \gamma$ implies that $\tau_B < \tau_S$ and that there is timescale separation between the system and the bath.

We (pre-emptively) neglect the δ-functions by following the Caldeira-Leggett procedure explained in Section 3.3 which moves the limits of integration from $[0, \tau]$ to $[t, t + 2\epsilon]$ in the transition from an integral propagator to a master equation. Therefore, in the appropriate limit,

$$\frac{\eta}{\pi} \int_0^\tau \frac{\sin \Omega(\tau - \tau')}{(\tau - \tau')} f_-(\tau') \mathrm{d}\tau' \approx \frac{\eta}{2} f_-(\tau) - \frac{\eta}{\pi\Omega} f'_-(\tau). \tag{5.1.19}$$

This could also have been directly obtained earlier in the process by identifying that

$$\frac{\eta}{2} - \frac{\eta}{\pi} \arctan\left(\frac{p}{\Omega}\right) \approx \frac{\eta}{2} - \frac{\eta}{\pi\Omega} p \tag{5.1.20}$$

and substituting this into Eq. (5.1.12). By comparing these two expressions, we see that the coefficients of $f_-(\tau)$ and $f'_-(\tau)$ in the approximate evaluation of the nested kernel are nothing more than the zeroth and first order Taylor coefficients of the Laplace variable p in the expansion

of the Laplace transform of the memory kernel, i.e.

$$\frac{\eta}{\pi}\int_0^\tau \frac{\sin\Omega(\tau-\tau')}{(\tau-\tau')}f_-(\tau')\mathrm{d}\tau' \approx \mathcal{L}\{\frac{\sin\Omega\tau}{\tau}\}(p)|_{p=0}f_-(\tau) - \frac{\partial}{\partial p}\mathcal{L}\{\frac{\sin\Omega\tau}{\tau}\}(p)|_{p=0}f'_-(\tau). \quad (5.1.21)$$

This is a natural result of the method we used to evaluate the integral: taking powers of the Laplace transform of the memory kernel and then truncating the series after first order. All the information retained about the system is contained in the zeroth- and first- order coefficients of the Laplace transform of the memory kernel.

The second integral we need to address can be evaluated with reference to another helpful property of the Laplace transform, which describes the transform of a derivative:

$$\mathcal{L}\Big\{g'(\tau)\Big\}(p) = pG(p) - g(0), \quad (5.1.22)$$

and therefore

$$\frac{\eta}{\pi}\int_0^\tau \frac{\mathrm{d}}{\mathrm{d}(\tau-\tau')}\frac{\sin\Omega(\tau-\tau')}{(\tau-\tau')}f_+(\tau')\mathrm{d}\tau' = \mathcal{L}^{-1}\Big\{\Big(\frac{\eta p}{2} - \frac{\eta p}{\pi}\arctan\Big(\frac{p}{\Omega}\Big) - \frac{\eta\Omega}{\pi}\Big)F_+(p)\Big\}(\tau). \quad (5.1.23)$$

Using the same justification and process as with the previous integral, we can approximate

$$\frac{\eta}{\pi}\int_0^\tau \frac{\mathrm{d}}{\mathrm{d}(\tau-\tau')}\frac{\sin\Omega(\tau-\tau')}{(\tau-\tau')}f_+(\tau')\mathrm{d}\tau' \approx -\frac{\eta\Omega}{\pi}f_+(\tau) + \frac{\eta}{2}f'_+(\tau) - \frac{\eta}{\pi\Omega}f''_+(\tau). \quad (5.1.24)$$

Once again, we see that the coefficients of $f'_+(\tau)$ and $f''_+(\tau)$ are the zeroth and first order Taylor coefficients of the Laplace variable p of the Laplace transform of the memory kernel. The first term on the right hand will contribute to the renormalised potential (as described by the Caldeira-Leggett model) and is given by $\mu_\Omega(0)$ - the value of the non-Markovian memory kernel, Eq. (5.1.6), at the origin. The second term is the Markovian Caldeira-Leggett dynamics, and the third term - which is Ω-dependent - contains the non-Markovian dynamics.

The non-Markovian propagator analogous to the Caldeira-Leggett propagator is then

$$J(x,y,t;x',y',0) = \int \mathrm{Dx}\ \mathrm{Dy}\ \exp\Big\{\frac{i}{\hbar}\Big(S_S[x] - S_S[y] + \frac{\eta\Omega}{\pi}\int_0^t f_-(\tau)f_+(\tau)\mathrm{d}\tau \\ - \frac{\eta}{2}\int_0^t f_-(\tau)f'_+(\tau)\mathrm{d}\tau + \frac{\eta}{\pi\Omega}\int_0^t f_-(\tau)f''_+(\tau)\mathrm{d}\tau\Big)\Big\} \\ \times \exp\Big\{-\frac{2kT}{\hbar^2}\Big(\frac{\eta}{2}\int_0^t f_-^2(\tau)\mathrm{d}\tau - \frac{\eta}{\pi\Omega}\int_0^t f_-(\tau)f'_-(\tau)\mathrm{d}\tau\Big)\Big\}. \tag{5.1.25}$$

For each Markovian term found in the Caldeira-Leggett equation, there is a corresponding non-Markovian term characterised by a $1/\Omega$ factor in the coefficient. As we have seen, the non-Markovian term in each case is multiplied by the coefficient of the Taylor expansion in the Laplace variable p of the Laplace transform of the memory kernel. Following the process outlined in Section 3.3 and described in detail in Appendix B, we consider the propagator evolution over an infinitesimal time interval

$$\tilde{\rho}(x,y,t+2\epsilon) = \int \mathrm{d}x'\mathrm{d}y' J(x,y,t+2\epsilon;x',y',0)\tilde{\rho}(x',y',t). \tag{5.1.26}$$

However, unlike in the original procedure we have to consider the propagation over two intervals to accommodate the second derivative, $f''_+(\tau)$ in the propagator. This becomes clear when we make the finite difference substitutions for $f'_\pm(\tau) = \dot{x}(\tau) \pm \dot{y}(\tau)$ and $f''_\pm(\tau) = \ddot{x}(\tau) \pm \ddot{y}(\tau)$. In the first interval, $x_0 \to x_1$ and $y_0 \to y_1$ as $t \to t+\varepsilon$ we have

$$\dot{x} \approx \frac{x_1 - x_0}{\epsilon} = \frac{\beta_{x_0}}{\epsilon}, \quad \dot{y} \approx \frac{y_1 - y_0}{\epsilon} = \frac{\beta_{y_0}}{\epsilon} \tag{5.1.27}$$

and in the second interval, $x_1 \to x_2$ and $y_1 \to y_2$ as $t+\varepsilon \to t+2\varepsilon$ we have

$$\dot{x} \approx \frac{x_2 - x_1}{\epsilon} = \frac{\beta_{x_1}}{\epsilon}, \quad \dot{y} \approx \frac{y_2 - y_1}{\epsilon} = \frac{\beta_{y_1}}{\epsilon} \tag{5.1.28}$$

The second derivatives cannot be separated across the 2ϵ integral as we have

$$\ddot{x} \approx \frac{(x_2 - x_1) - (x_1 - x_0)}{\varepsilon^2} = \frac{\beta_{x_1} - \beta_{x_0}}{\varepsilon^2}, \quad \ddot{y} \approx \frac{(y_2 - y_1) - (y_1 - y_0)}{\varepsilon^2} = \frac{\beta_{y_1} - \beta_{y_0}}{\varepsilon^2}. \tag{5.1.29}$$

This leads to a "quasi-Markovian" (QM) sub-propagator, J_{QM}, containing the first derivatives, which can be separated in β_{x_1} and β_{x_0} (and the corresponding y-variables), such that it has the

Chapman-Kolmogorov property [59]

$$\begin{aligned}&\int \mathrm{d}x_1\mathrm{d}y_1\mathrm{d}x_0\mathrm{d}y_0 J_{\mathrm{QM}}(x_2,y_2,t+2\epsilon;x_0,y_0,t)\rho(x_0,y_0,t)\\ &=\int \mathrm{d}x_1\mathrm{d}y_1 J_{\mathrm{QM}}(x_2,y_2,t+2\epsilon;x_1,y_1,t+\epsilon)\int \mathrm{d}x_0\mathrm{d}y_0 J_{\mathrm{QM}}(x_1,y_1,t+\epsilon;x_0,y_0,t)\rho(x_0,y_0,t),\end{aligned} \tag{5.1.30}$$

and a truly non-Markovian (NM) sub-propagator, J_{NM}, containing the second derivative, which cannot be separated over the intervals. Therefore, we can write

$$\begin{aligned}\tilde{\rho}(x,y,t+2\epsilon) &= \int \mathrm{d}x_0\mathrm{d}x_1\mathrm{d}y_0\mathrm{d}y_1\, J_{\mathrm{NM}}(x,y,t+2\epsilon;x_0,y_0,0)\,\tilde{\rho}\,(x_0,y_0,0)\\ &+\int \mathrm{d}x_1\mathrm{d}y_1\, J_{\mathrm{QM}}(x,y,t+2\epsilon;x_1,y_1,t+\epsilon)\int \mathrm{d}x_0\mathrm{d}y_0\, J_{\mathrm{QM}}(x_1,y_1,t+\epsilon;x_0,y_0,t)\,\tilde{\rho}\,(x_1,y_1,t+\epsilon)\,.\end{aligned} \tag{5.1.31}$$

After making this separation, it is a lengthy but straightforward procedure to perform the integration by substituting the Eqs. (5.1.27)-(5.1.29) into the propagator in Eq. (5.1.25) [36]. All the integrals are Gaussian, of the form

$$\int \mathrm{d}x(a_2x^2+a_1x+a_0)\mathrm{e}^{e_2x^2+e_1x+e_0} = \frac{\sqrt{\pi}(a_2e_1^2-2(a_2+a_1e_1)e_2+4a_0e_2^2)}{4(-e_2)^{5/2}}\mathrm{e}^{e_0-\frac{e_1^2}{4e_2}}. \tag{5.1.32}$$

Terms which are $O(\epsilon^2)$ or $O(1/\Omega^2)$ are truncated. More details about this calculation can be found in Ref. [36]. The resulting expression is collected in powers of ϵ, with the terms $O(\epsilon^0)$ forming the normalisation constant and terms $O(\epsilon)$ forming the master equation, analogously to Appendix B. After performing this procedure, we obtain

$$\begin{aligned}\frac{\partial}{\partial t}\tilde{\rho}(x,y,t) =&\hat{\mathrm{L}}_M\tilde{\rho}(x,y,t)\\ &+\frac{\gamma}{\pi\Omega}\Big[-\frac{4ikT}{\hbar}(x-y)\left(\frac{\partial}{\partial x}+\frac{\partial}{\partial y}\right)-\frac{i}{2\hbar}(x-y)\left(\frac{\partial \mathrm{V}_R}{\partial x}+\frac{\partial \mathrm{V}_R}{\partial y}\right)\\ &-2\gamma(x-y)\left(\frac{\partial}{\partial x}-\frac{\partial}{\partial y}\right)\Big]\tilde{\rho}(x,y,t),\end{aligned} \tag{5.1.33}$$

where

$$\begin{aligned}\hat{\mathrm{L}}_M =&-\frac{i\hbar}{2M}\left(\frac{\partial^2}{\partial x^2}-\frac{\partial^2}{\partial y^2}\right)+\frac{1}{i\hbar}\left(\mathrm{V}_R(x)-\mathrm{V}_R(y)\right)\\ &-\gamma(x-y)\left(\frac{\partial}{\partial x}-\frac{\partial}{\partial y}\right)-\frac{2M\gamma kT}{\hbar^2}(x-y)^2\end{aligned} \tag{5.1.34}$$

is the Caldeira-Leggett operator describing the Markovian dynamics. As conventional, we have

replaced η by $2M\gamma$. Eq. (5.1.33) is the non-Markovian master equation, obtained by extending the Caldeira-Leggett model to include contributions from leading order terms in $\frac{1}{\Omega}$.

The renormalised potential is retained in the non-Markovian case. In the original Caldeira-Leggett model, the potential renormalisation comes from the physically unrealistic coupling to infinite frequency modes of the bath, and is therefore removed from the final dynamics by including a counter-term in the Lagrangian of the system. However, this is not appropriate in this case: all bath modes have finite frequencies and the potential renormalisation contribution is from the dominant high, but finite, frequency bath oscillators. The renormalised potential, therefore, is retained as

$$\mathrm{V}_R(x) = \mathrm{V}(x) - \frac{1}{2}M(\Delta\omega)^2x^2, \tag{5.1.35}$$

with $(\Delta\omega)^2 = \frac{4\gamma\Omega}{\pi}$ now a well-defined finite harmonic shift.

An important feature of our new master equation is that, while the original Markovian Caldeira-Leggett terms are obtained without alteration, the new non-Markovian terms are all multiplied by the non-Markovianity factor

$$R_\Omega = \frac{\gamma}{\pi\Omega}. \tag{5.1.36}$$

This factor can be thought of as quantifying of how much non-Markovianity the system possesses: the larger Ω is, the closer to Markovian the system is. When $R_\Omega = 0$, the original Caldeira-Leggett equation is recovered. Conversely, the smaller Ω is, the further from Markovian the system dynamics will be.

The non-Markovianity factor can be linked to the Laplace transform of the spectral density, by noting that

$$-\frac{1}{2M}\frac{\partial}{\partial p}\mathcal{L}\{\mu_\Omega(\tau)\}(p)|_{p=0} = \frac{\gamma}{\pi\Omega}. \tag{5.1.37}$$

This explicitly links the non-Markovianity of the system dynamics to the properties of the spectral density of the surrounding bath, and we will discuss this relation further in Chapter 6.

The three new Liouvillian terms in the non-Markovian master equation can be categorised

as follows. There is an "orthogonal term", named for the '+' sign in the derivative bracket,

$$\hat{\mathrm{L}}_O = -\frac{4ikT}{\hbar}(x-y)\left(\frac{\partial}{\partial x}+\frac{\partial}{\partial y}\right), \tag{5.1.38}$$

a "potential term",

$$\hat{\mathrm{L}}_V = -\frac{i}{2\hbar}(x-y)\left(\frac{\partial \mathrm{V}_R}{\partial x}+\frac{\partial \mathrm{V}_R}{\partial y}\right), \tag{5.1.39}$$

which is also orthogonal in its derivative bracket, and a non-Markovian "relaxation term",

$$\hat{\mathrm{L}}_R = -2\gamma(x-y)\left(\frac{\partial}{\partial x}-\frac{\partial}{\partial y}\right). \tag{5.1.40}$$

The relaxation term has the same form as one of the Caldeira-Leggett terms, responsible for the diffusive behaviour in the Markovian dynamics.

In the following sections, we will explore the system dynamics induced by these terms.

5.2 Analysis of non-Markovian Dynamics

The non-Markovian master equation can be used to simulate the dynamics of a system in a finite heat bath and make predictions about coherence dynamics as well as observables of the system. In particular, we look in detail at the coherence dynamics of a free particle over short- and medium-long times. Our analysis is guided by our hypothesis: that non-Markovian spectral densities are able to extend coherence times and thereby enable quantum effects to take place over biological timescales. Therefore, over the short term, we investigate whether non-Markovian dynamics cause any changes to the initial rapid decoherence process, as described by Zurek [2]. Over the medium and long terms, we investigate whether there are any effects induced by information backflow from the bath.

5.2.1 Exact Solution of the Free Particle non-Markovian Master Equation

Deriving an analytic solution of the non-Markovian master equation will allow for rigorous and unambiguous analysis of the dynamics. Numerical uncertainty is removed and we are able to make exact calculations of the quantities we are interested in.

The simplest case is the free particle, i.e. $\hat{\mathrm{V}}_{\mathrm{R}}(x) = 0$, leading to the master equation

$$\begin{aligned}\frac{\partial}{\partial t}\rho(x,y,t) = \Bigg[&\frac{i\hbar}{2M}\left(\frac{\partial^2}{\partial x^2} - \frac{\partial^2}{\partial y^2}\right) - \gamma(x-y)\left(\frac{\partial}{\partial x} - \frac{\partial}{\partial y}\right) - \frac{2M\gamma kT}{\hbar^2}(x-y)^2 \\ &- \frac{4iR_\Omega kT}{\hbar}(x-y)\left(\frac{\partial}{\partial x} + \frac{\partial}{\partial y}\right) - 2\gamma R_\Omega(x-y)\left(\frac{\partial}{\partial x} - \frac{\partial}{\partial y}\right)\Bigg]\rho(x,y,t).\end{aligned} \tag{5.2.1}$$

We can obtain an exact analytical solution for this equation, and proceed by following the procedure outlined in Refs. [72, 109]: defining rotated variables, taking a Fourier transform, and solving the equation in Fourier space. We then go one step further and, for a double Gaussian initial state, inverse Fourier transform back into the rotated variables, then transform back into x and y, as described in detail in Appendix C.

The rotated variables are defined as

$$u = \frac{x+y}{2}, \qquad v = x - y. \tag{5.2.2}$$

and in the rotated co-ordinate system, the master equation is

$$\frac{\partial}{\partial t}\rho(u,v,t) = \left(\frac{i\hbar}{m}\frac{\partial^2}{\partial u \partial v} - \frac{4R_\Omega ikT}{\hbar}v\frac{\partial}{\partial u} - 2\gamma(1+2R_\Omega)v\frac{\partial}{\partial v} - \frac{2m\gamma kT}{\hbar^2}v^2\right)\rho(u,v,t). \tag{5.2.3}$$

We then Fourier transform with respect to u to reduce this equation to a first order differential equation in v, with the Fourier transform defined such that

$$\rho(u,v,t) = \frac{1}{\sqrt{2\pi}}\int_{-\infty}^{\infty} \mathrm{d}K\, \mathrm{e}^{iKu}\rho(K,v,t). \tag{5.2.4}$$

The Fourier transform gives us

$$\frac{\partial}{\partial t}\rho(K,v,t) + \left(\left(2\gamma(1+2R_\Omega)v + \frac{\hbar K}{m}\right)\frac{\partial}{\partial v} + \frac{2m\gamma kT}{\hbar^2}v^2 - \frac{4R_\Omega kT}{\hbar}Kv\right)\rho(K,v,t) = 0. \tag{5.2.5}$$

We solve this using the method of characteristics to obtain the solution in Fourier space,

$$\rho(K,v,t) = \rho_0(K,v_0)\exp\Big\{ -\frac{kT}{2m\gamma(1+2R_\Omega)^2}\Big[K^2(1+4R_\Omega+8R_\Omega^2)t \\ -\frac{mK}{\hbar}(1+4R_\Omega+8R_\Omega^2)[v-v_0] + \frac{m^2\gamma(1+2R_\Omega)}{\hbar^2}[v^2-v_0^2]\Big]\Big\}, \tag{5.2.6}$$

where

$$v_0 = -\frac{\hbar K}{2m\gamma(1+2R_\Omega)} + \left(v(t) + \frac{\hbar K}{2m\gamma(1+2R_\Omega)}\right)\mathrm{e}^{-2\gamma(1+2R_\Omega)t}. \tag{5.2.7}$$

It is important to note that this is a perfectly valid solution, and can be applied to find the evolution of any initial condition. However, we wish to transform back into x and y, and so we write the solution in a form that can be inverse Fourier transformed. Since the double Gaussian initial condition we are interested in (in (x,y) coordinates) is a sum of four Gaussian peaks, its Fourier transform is also a Gaussian. Therefore, Eq (5.2.6) is a completely Gaussian function for our initial condition. We inverse Fourier transform to obtain

$$\rho(x,y,t) = \frac{\mathrm{e}^{E_0}}{2\sqrt{2\pi}\left(1+\mathrm{e}^{-2b_1b_2^2}\right)}\sum_i \frac{1}{\sqrt{-2(E_2+C_2^i)}}\mathrm{e}^{C_0^i - \frac{(E_1+C_1^i - \frac{i(x+y)}{2})^2}{4(E_2+C_2^i)}}, \tag{5.2.8}$$

with the coefficients

$$E_2 = -\frac{kT}{2M\gamma(1+2R_\Omega)^2}\Big((1+4R_\Omega+8R_\Omega^2)t \\ + \frac{\mathrm{e}^{-2\gamma(1+2R_\Omega)t}-1}{2\gamma(1+2R_\Omega)}(1+4R_\Omega+8R_\Omega^2) - \frac{(\mathrm{e}^{-2\gamma(1+2R_\Omega)t}-1)^2}{4\gamma(1+2R_\Omega)}\Big), \\ E_1 = \frac{kT}{2M\gamma(1+2R_\Omega)^2}\frac{M(x-y)}{\hbar}\Big((1-4R_\Omega-8R_\Omega^2)(1-\mathrm{e}^{-2\gamma(1+2R_\Omega)t}) \\ - \mathrm{e}^{-2\gamma(1+2R_\Omega)t}(1-\mathrm{e}^{-2\gamma(1+2R_\Omega)t})\Big), \\ E_0 = -\frac{kT}{2M\gamma(1+2R_\Omega)^2}\frac{M^2\gamma(1+2R_\Omega)(x-y)^2}{\hbar^2}(1-\mathrm{e}^{-4\gamma(1+2R_\Omega)t}). \tag{5.2.9}$$

and

$$
\begin{aligned}
C_2^{\mathrm{p}\pm} &= -\frac{1}{8b_1} - \frac{b_1\hbar^2}{8M^2\gamma^2(1+2R_\Omega)^2}\left(1-\mathrm{e}^{-2\gamma(1+2R_\Omega)t}\right)^2 \\
C_1^{\mathrm{p}\pm} &= \pm ib_2 + \frac{b_1\hbar(x-y)}{2M\gamma(1+2R_\Omega)}\mathrm{e}^{-2\gamma(1+2R_\Omega)t}\left(1-\mathrm{e}^{-2\gamma(1+2R_\Omega)t}\right) \\
C_0^{\mathrm{p}\pm} &= -\frac{1}{2}b_1(x-y)^2\mathrm{e}^{-4\gamma(1+2R_\Omega)t}, \\
C_2^{\mathrm{c}\pm} &= -\frac{1}{8b_1} - \frac{b_1\hbar^2}{8M^2\gamma^2(1+2R_\Omega)^2}\left(1-\mathrm{e}^{-2\gamma(1+2R_\Omega)t}\right)^2 \\
C_1^{\mathrm{c}\pm} &= \frac{b_1\hbar\left(1-\mathrm{e}^{-2\gamma(1+2R_\Omega)t}\right)\left((x-y)\mathrm{e}^{-2\gamma(1+2R_\Omega)t}\pm 2b_2\right)}{2M\gamma(1+2R_\Omega)} \\
C_0^{\mathrm{c}\pm} &= -\frac{1}{2}b_1((x-y)\mathrm{e}^{-2\gamma(1+2R_\Omega)t}\pm 2b_2)^2.
\end{aligned}
\tag{5.2.10}
$$

The index i counts over $p^{\pm}$ and $c^{\pm}$, which refer to the population and coherent contributions respectively - such that the exact solution, Eq. (5.2.8) is a sum over the contributions from each of the four initial Gaussian peaks. However, it should be emphasised that Eq. (5.2.8) is a special case of the general solution Eq. (5.2.6), with a double Gaussian initial state inserted in order to take the inverse Fourier transform. Full detail on how to obtain the coefficients can be found in Appendix C.

Having the exact solution is very useful, as it allow to analyse the dynamics without relying on the accuracy of numerical simulations. What's more, it can be directly compared to the Caldeira-Leggett steady state solution [109, 147], which is given (in Fourier space) as

$$
\rho(K,v,t) = \rho_0(K,v)\exp\Big\{-\frac{kT}{2m\gamma}\Big[K^2t - \frac{mK}{\hbar}[v-v_0] + \frac{m^2\gamma}{\hbar^2}[v^2-v_0^2]\Big]\Big\}, \tag{5.2.11}
$$

with

$$
v_0 = \frac{\hbar K}{2m\gamma} + \left(v(t) - \frac{\hbar K}{2m\gamma}\right)\mathrm{e}^{-2\gamma t}. \tag{5.2.12}
$$

Not only is this derived in reference [109], it can be recovered from Eq. (5.2.6) by setting $R_\Omega = 0$. Additionally, the exact Caldeira-Leggett solution in coordinate space can be recovered from Eq. (5.2.8) by taking the $R_\Omega \to 0$ limit.

Steady State Free Particle Solution

In the limit $t = 0$, E_2 will diverge for all values of K not equal to 0. Therefore, we only need to consider the $K = 0$ terms: the density matrix is diagonalised in momentum at long times.

This effectively ensures it will becomes smoothed out in position, with no preferred value of u, in order to satisfy the uncertainty principle. The long-time solution, at $t \to \infty$ and $K = 0$, is

$$\begin{aligned}\rho(x, y, \infty) &= \frac{\mathrm{e}^{E_0(\infty)}}{2\sqrt{2\pi}\left(1 + \mathrm{e}^{-2b_1 b_2^2}\right)} \sum_i \exp\{C_0^i(\infty)\} \\ &= \frac{1}{\sqrt{2\pi}} \mathrm{e}^{-\frac{MkT}{2(1+2R_\Omega)\hbar^2}(x-y)^2}.\end{aligned} \tag{5.2.13}$$

When $R_\Omega \to 0$, this returns as expected to the Caldeira-Leggett steady state solution.

The steady state solution is presented in Figure (5.2). It bears great similarity to the Caldeira-Leggett steady state solution, which suggests that non-Markovian effects occur over short or medium time-scales, and are negligible in the long-time limit. The free-particle steady state is not normalised as the solution is spread out evenly over all space - much like the free particle Schrödinger solution.

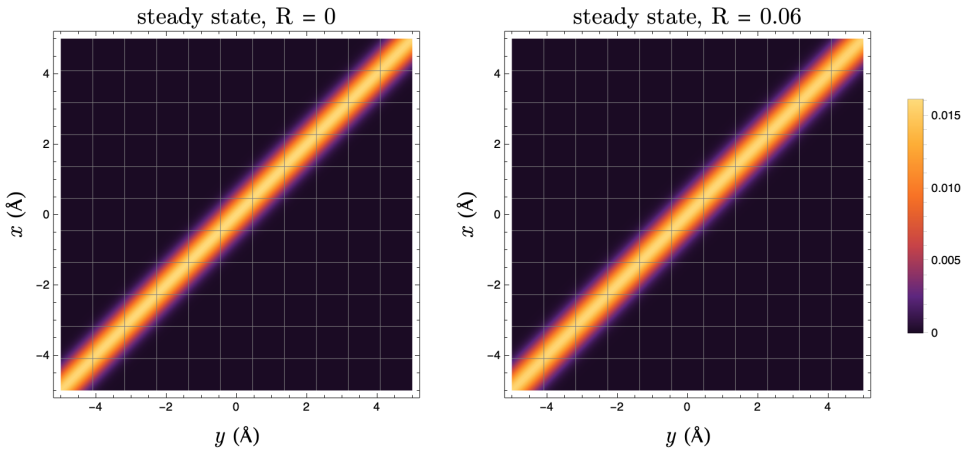

Figure 5.2: The steady state / thermal equilibrium state of the density matrix in the Caldeira-Leggett case (left) and the non-Markovian case (right) with $R_\Omega = 0.06$. The parameters are $T = 320$K, $\gamma = \frac{kT}{20\hbar}$, and $m = M_p$ (the proton mass). The steady states are almost indistinguishable from each other, which can be seen from the analytic expression Eq. (5.2.13).

5.2.2 Parameter Selection

In reference [148], Einsiedler et al. present a thorough analysis of the parameter space of quantum Brownian motion in the non-Markovian case, in which they examine the parameters temperature (T), characteristic frequency (ω_0), system-bath coupling (γ), and bath cut-off (Ω). An Ohmic spectral density with Lorenztian cut-off is chosen. They determine the degree of

non-Markovianity by using the trace distance (see Chapter 4.1) between two initial states [40],

$$D(\rho_1, \rho_2) = \frac{1}{2}\mathrm{Tr}|\rho_1 - \rho_2|, \tag{5.2.14}$$

which measures the indistinguishability of the states with respect to measurement.

Einsiedler et al. [148] calculate $\mathcal{N}_{\text{trace dist.}}$, Eq. (4.1.13), for various points in the parameter space $\{T, \omega_0, \gamma, \Omega\}$. In particular, they find that non-Markovianity is maximised when $\gamma = 0.1\omega_0$. They also present a "heat map" of non-Markovianity in $(\frac{T}{\omega_0}, \frac{\Omega}{\omega_0})$-space, for fixed $\gamma = 0.1\omega_0$, which demonstrates that non-Markovianity is maximised in the region $\Omega/\omega_0 \approx 1$, which corresponds to $R_\Omega > 0.03$, for all temperatures.

The parameter selection in the following sections is informed by the above. For the free particle, there is no characteristic frequency ω_0, but the relationships $\frac{T}{\omega_0}$ and $\frac{\gamma}{\omega_0}$ are used to derive a sensible choice of γ in terms of T. In particular, we want to avoid low-temperature effects: not only is the Caldeira-Leggett approach valid only in the high temperature regime, but we want to ensure that any deviation from Caldeira-Leggett dynamics is due to true non-Markovian effects, rather than low-temperature effects or regime violations. For that reason, we select the default value $\gamma = \frac{kT}{20\hbar}$, and choose R_Ω to be in the region $\gtrapprox 0.03$. This is to ensure that the perturbative approximation $\gamma \ll \Omega$ holds, while still being in a region of interesting non-Markovian effects.

The analytic solution derived in Section 5.2.1 allows us to restrict the parameter space further, because the regime in which the approximation, $\gamma < \Omega$, breaks down becomes apparent. By fixing $\{T, \gamma\}$, a maximum allowed value of R_Ω may be obtained. This works by noting that, for sufficiently large R_Ω, the real part of the $c\pm$ exponents along the anti-diagonal line are positive rather than negative for at least some values of t. This corresponds to a situation where the coherent elements of the density matrix diverge far from the diagonal, which is not a sensible physical scenario and represents a breakdown of the model. Therefore, the maximum value for which the exponents are negative for all t is the largest possible value of R_Ω for the fixed values of $\{T, \gamma\}$. This determination has to be made using numerical software such as Mathematica, as in general the exponent is too unwieldy to tackle this calculation analytically. The maximum values of R_Ω are, in general, not very large: for $T = 320\text{K}$, $\gamma = \frac{kT}{20\hbar}$ has a

maximum of $R_\Omega = 0.06$. However, as this is within the region identified by Einsiedler et al. as having high non-Markovianity, this should allow us to describe rich non-Markovian dynamics of the system.

The quantum Brownian motion framework is useful in quantum biology which is relevant at physiological temperatures. In order to explore the coherence dynamics of quantum physics in biological systems, the parameters we have chosen should be relevant. The temperature we have selected (320K) is physiological. The vibrational relaxation time of bulk water, which makes up much of the cellular environment [149], has been shown to be between 250fs and 500fs [150], and γ^{-1} falls in this range for the "default choice" of $\gamma = \frac{kT}{20\hbar}$ (we have $\gamma^{-1} = 477$fs). We consider a proton - which could correspond to a hydrogen bond across the DNA backbone, or a hydrogen ion in glycolysis - initially a double Gaussian state with peak separation of 5 Å, which is approximately the length of a hydrogen bond in a peptide [151]. Although we do not claim to represent any one specific biological system, our parameters have been chosen to be biologically relevant, and we can therefore use the analysis in the following sections to make some initial suggestions about the behaviour of non-Markovian quantum systems in biological contexts, albeit for a free particle.

Informed by the discussion presented by Einsiedler et al [148], we use a set of default parameters for our analysis. This set is $T = 320$K, $\gamma = \frac{kT}{20\hbar}$, and $m = M_p$, the proton mass. Unless otherwise stated, these are the parameters used in all discussions.

5.2.3 Free Particle Short Term Dynamics

In order to investigate the decoherence dynamics of the non-Markovian master equation, we select a double Gaussian state, i.e. a superposition of two spatially separated Gaussian wavefunctions. The double Gaussian state is selected because it has clearly distinguished coherent (off-diagonal) and classical (on-diagonal) components, and therefore by observing the decay of the off-diagonal peaks, we can study decoherence of the initial spatial superposition. The Caldeira-Leggett equation describes rapid decoherence of the two off-diagonal peaks, which represent the superposition. This means they decay in amplitude on a timescale much faster than the thermalisation timescale of the on-diagonal peaks, which represent the classical probabilities. In fact, during the decoherence process, there is almost no discernible evolution of the

on-diagonal peaks. It is well discussed that the decay of the off-diagonals is approximately exponential in the short time regime. In the two-level case, the decay is exactly exponential [9], but because in the continuous basis the rate of decoherence is proportional to the distance from the diagonal, there is a slight asymmetry in the decay of the Gaussian off-diagonal peak which prevents the decay from being exactly exponential [152, 153].

Fig. (5.3) presents a comparison of the Markovian and non-Markovian density matrices (real part) for $\gamma = \frac{kT}{20\hbar}$. The value $R_\Omega = 0.06$ has been chosen as it is close to the maximum allowed value for this choice of γ, and should therefore display the most deviation from the Markovian case. The non-Markovian dynamics very slightly deviate from the Markovian ones; at 6fs, the off-diagonal peaks are less decohered than their Markovian correspondents, but the effect is small. At fixed R_Ω, the 'decoherence delay' effect is weaker for larger γ and stronger for smaller γ. This can be explained by identifying that decreasing γ at fixed R_Ω corresponds to decreasing Ω, such that moving from larger to the smaller γ corresponds to considering a lower cut-off frequency. We would intuitively expect a lower cut-off frequency to demonstrate more significant non-Markovian effects. However, the delay of the decoherence is not particularly pronounced for any value of γ.

To examine the coherence dynamics more quantitatively, we use the l_1 norm of coherence [39]. In the discrete basis, this is defined as

$$C_{l_1} = \sum_{i \neq j} |\rho_{i,j}|, \tag{5.2.15}$$

which sums all the non-diagonal components of the density matrix, i.e. the truly quantum components. However, the definition is not so simple in the continuous basis, as it is not possible to define the "diagonal" unambiguously. Several choices are available, such as subtracting a diagonal segment with finite width, removing the on-diagonal peaks from the initial condition, or defining a weighting function for the density matrix that is 0 at the diagonal, 1 far from the diagonal, and transitions smoothly between these values with some characteristic length scale. However, each of these choices has drawbacks. Removing a diagonal segment with finite width requires a choice to be made about its width that is inherently subjective. This is particularly apparent when the separation between peaks is small compared to the variance of the peaks,

and it may become difficult to define a segment that removes the majority of the on-diagonal peak without also removing a significant portion of the off-diagonal peak.

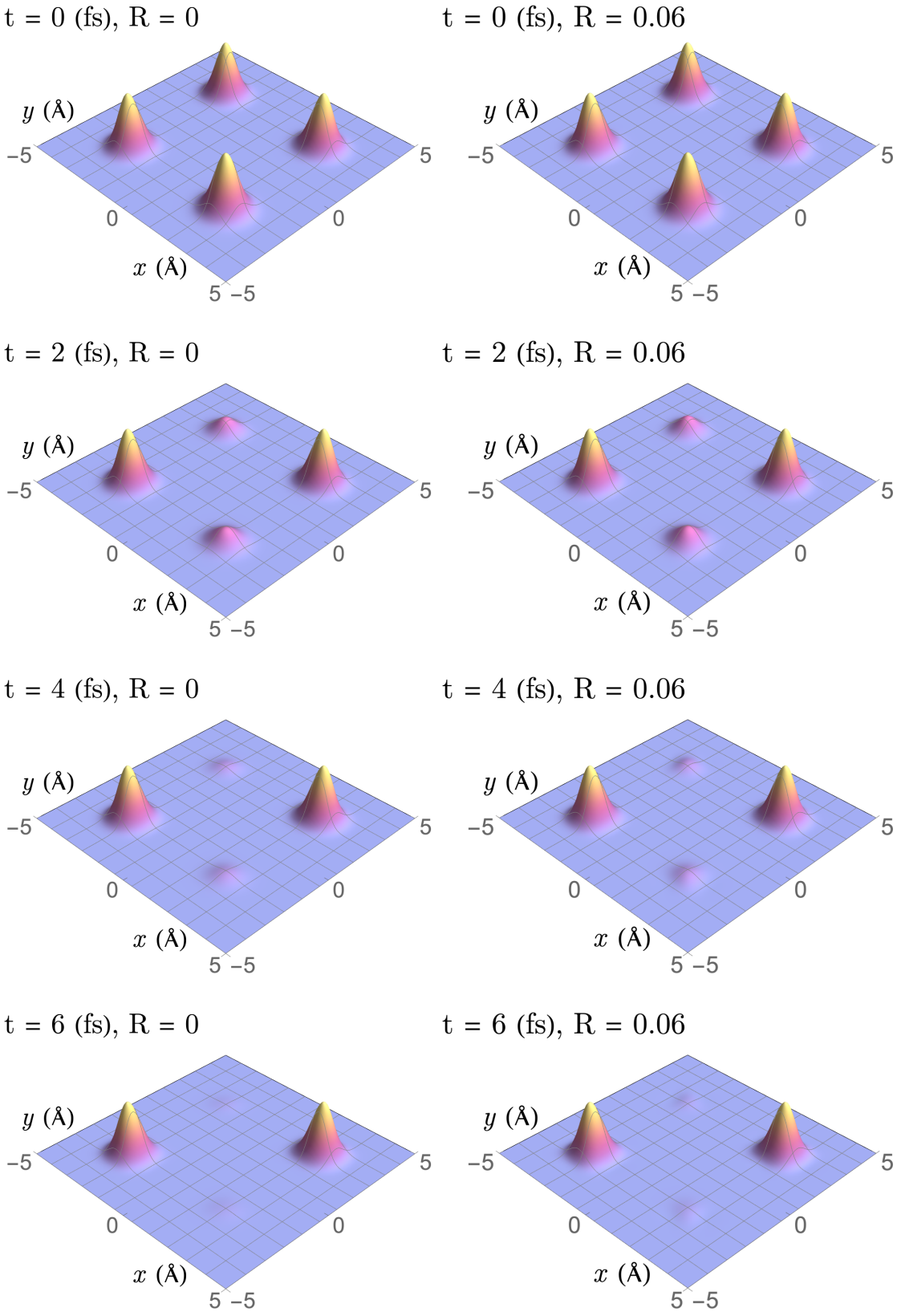

Figure 5.3: The density matrix evolving over 6fs in the Markovian case (left), and the non-Markovian case with $R_\Omega = 0.05$ (right). $T = 320$K and $\gamma = \frac{kT}{20\hbar}$. Deviation from the Markovian case is almost invisible.

Removing the on-diagonal peaks from the initial condition is a valid method for the exceedingly short timescales we are currently concerned with: as mentioned previously, the decoherence takes place on timescales short enough that no evolution of the on-diagonal peaks can occur. However, for longer timescales this will not be a sensible choice as any differences in the thermalisation pathway, potentially involving non-trivial coherence dynamics, between the Markovian and non-Markovian cases will not be detected. Finally, a weighting function could be used very effectively, but it is subject to many of the same criticisms as the diagonal segment: the coherence may be dependent on the choice one has made, and it may be necessary to define the weighting function with dependence on the initial condition.

Instead, we take the Markovian evolution of an initial condition without off-diagonal peaks to be a *time-dependent incoherent baseline*, i.e. a system that we would describe as decohered or incoherent, which can be removed from the density matrix to leave only the parts we can then describe as coherent. Therefore, the metric of coherence we use here is

$$C_{l_1}(t) = \int |\tilde{\rho}(t) - \tilde{\rho}^{\mathrm{M}}_{\mathrm{decoh}}(t)| \, \mathrm{d}x \, \mathrm{d}y, \tag{5.2.16}$$

where $\tilde{\rho}^{\mathrm{M}}_{\mathrm{decoh}}(t)$ denotes the time-dependent incoherent baseline. In the short time regime, the incoherent baseline method for determining the l_1 norm of coherence is practically equivalent to removing the on-diagonal peaks from the initial condition. The l_1-norm of coherence has been selected over the relative entropy of coherence largely because it is simpler to calculate. However, in Appendix D, the l_1-norm and relative entropy are benchmarked against each other to ensure that the qualitative features match up.

Fig. (5.4) shows the l_1 norm of coherence for the previously selected values of γ. (In Appendix D we compare this result to the relative entropy of coherence.) Since the result is plotted on a log-linear plot, it is also possible to see that the Markovian case has approximately exponentially decaying coherence, whereas the non-Markovian case deviates from this. The calculation of the l_1-norm confirms that the 'decoherence delay' effect is not large. This can be explained with a timescale argument. In the Markovian case, the bath has an infinitesimal response time: $\tau^{\mathrm{M}}_{\mathrm{E}} \to 0$. In fact, this is one of the characteristic features of Markovian systems. However, when non-Markovianity is introduced, this makes the response time finite:

$\tau_E^{NM} > 0$. If the non-Markovian bath response time is *greater* than the decoherence timescale $(\tau_E^{NM} > \tau_D)$, we should not expect any significant deviation from Markovian dynamics during the decoherence process: decoherence happens too quickly to be significantly affected by the non-Markovian dynamics.

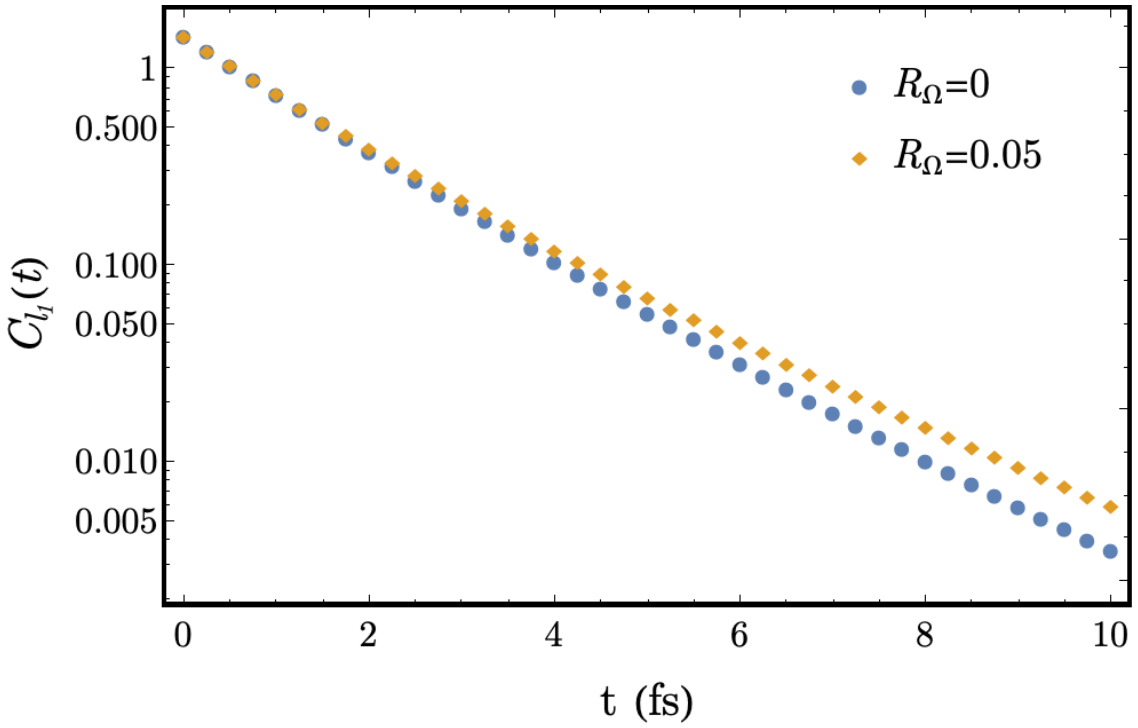

Figure 5.4: The l_1 norm of coherence, plotted on a log-linear plot in the case $\gamma = \frac{kT}{20\hbar}$, over an evolution of 10fs, found by numerically evaluating Eq. (5.2.16) for the exact solution. The non-Markovian case ($R_\Omega = 0.05$) clearly deviates from the Markovian case, but the effect is small.

As R_Ω has been maximised for the $\gamma = \frac{kT}{20\hbar}$ case, which should show the greatest deviation from Markovian dynamics, we can conclude that the perturbative expansion does not allow us to model more extreme cases of non-Markovian behaviour, including the region where $\tau_E^{NM} \approx \tau_D$. However, it is possible to speculate that in a non-perturbative approach that allows for greater values of R_Ω (or, equivalently, lower values of Ω), the non-Markovian bath response time could be made approximate to the decoherence timescale, and this would lead to interesting non-Markovian effects in the decoherence process.

Although the non-Markovian deviation is not significant in our expansion, it is still present, and interpreting it is an interesting task. In the next section, the role of the new non-Markovian Liouvillian operators will be explored in more detail.

5.2.4 Free Particle Medium-Long Term Dynamics

Because we have deduced that the non-Markovian bath response time - i.e. the time over which bath correlations decay - is longer than the decoherence timescale, the medium-long time dynamics are also of interest, as this is where we expect the non-Markovian dynamics to be more dominant. In standard Markovian Caldeira-Leggett dynamics, the thermalisation process takes place long after decoherence. The two on-diagonal peaks spread and merge along the diagonal until the density matrix is Gaussian along the diagonal, as in Figure (5.2). However, non-Markovian systems don't always progress to thermalisation along the most efficient route [132], and the system can move away from thermal equilibrium. By exploring the dynamics over longer timescales, we can investigate the routes taken to thermalisation by non-Markovian systems. For a free paricle, we know that the analytic steady state solution for a non-Markovian system varies very slightly (by a factor of $(1 + 2R_\Omega)$) from the Markovian solution.

Figures (5.5)-(5.6) show the evolution of the double Gaussian density matrix over 120fs. In this case, we have chosen $\gamma = \frac{kT}{20\hbar}$ as the default coupling strength, and $R_\Omega = 0.06$ as the maximum allowed value for this system. In contrast to the short timescale dynamics ($\leq$ 10fs), the deviation from non-Markovian dynamics is clearly visible and quite pronounced. In particular, between 20fs and 100fs, the Gaussian peak spreads along the diagonal *and* along the line orthogonal to the diagonal, forming a four-pointed star shape. Ripples form between the "points" of the star, which are necessarily off the diagonal. Looking at the analytic solution, it can be determined that the ripples take the form of a shifted cosine with Gaussian damping.

Since the new coherences emerge orthogonally from the diagonal, we call them *lateral coherences*. They are a weaker sign of quantum behaviour than the initial off-diagonal peaks, as they cannot represent a fully delocalised pure state, but they do nevertheless represent long lived ($\approx$ 100fs) quantum behaviour. It is therefore an interesting question to explore what kinds of quantum behaviour lateral coherences can promote that would not be possible in the Markovian case.

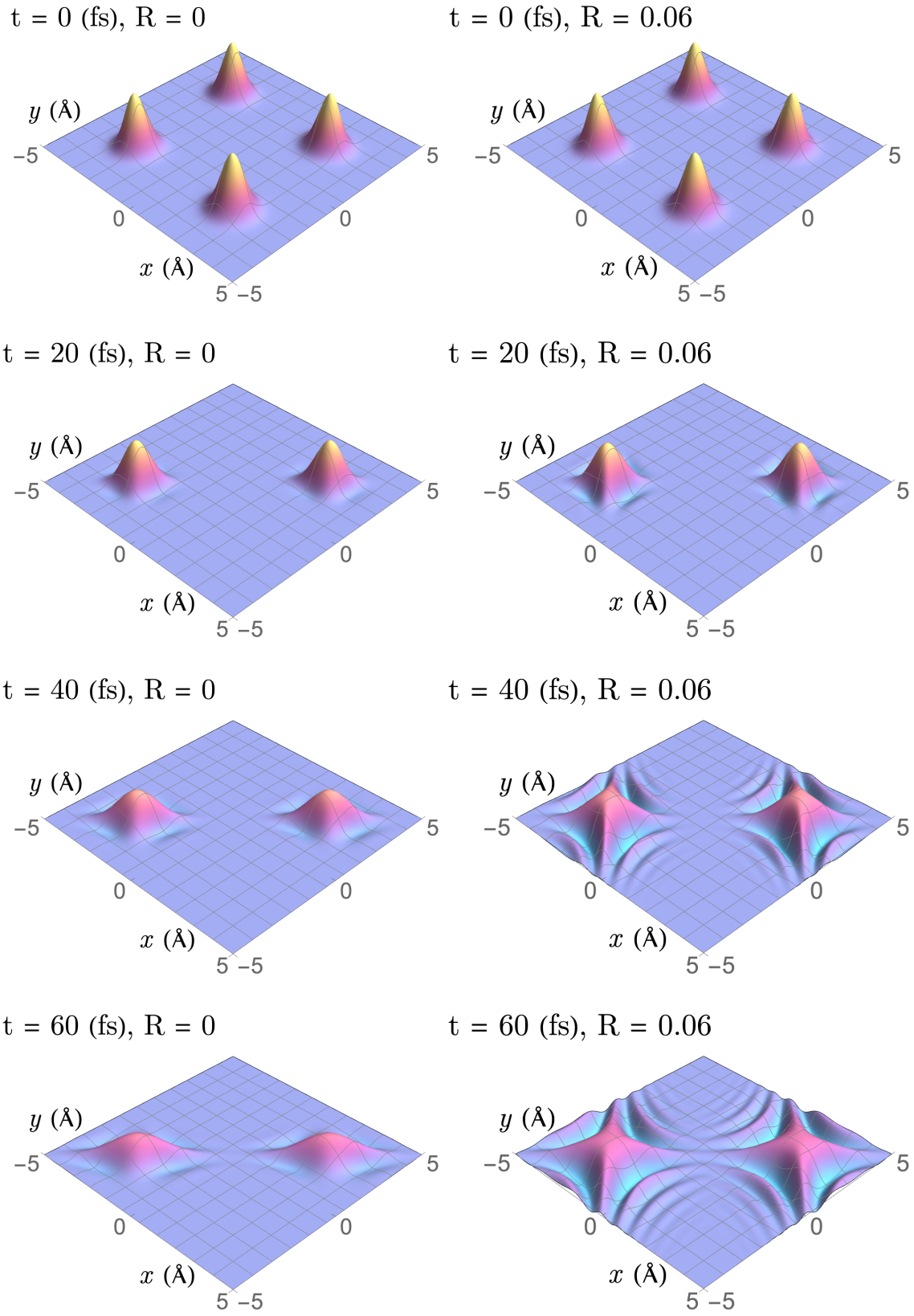

Figure 5.5: The real part of the density matrix evolving over 60fs in the Markovian case (left), and the non-Markovian case with $R_\Omega = 0.06$ (right). $T = 320$K and $\gamma = \frac{kT}{20\hbar}$ (the default parameters according to Section 5.2.2. Deviation from the Markovian case is clearly visible from 20fs.

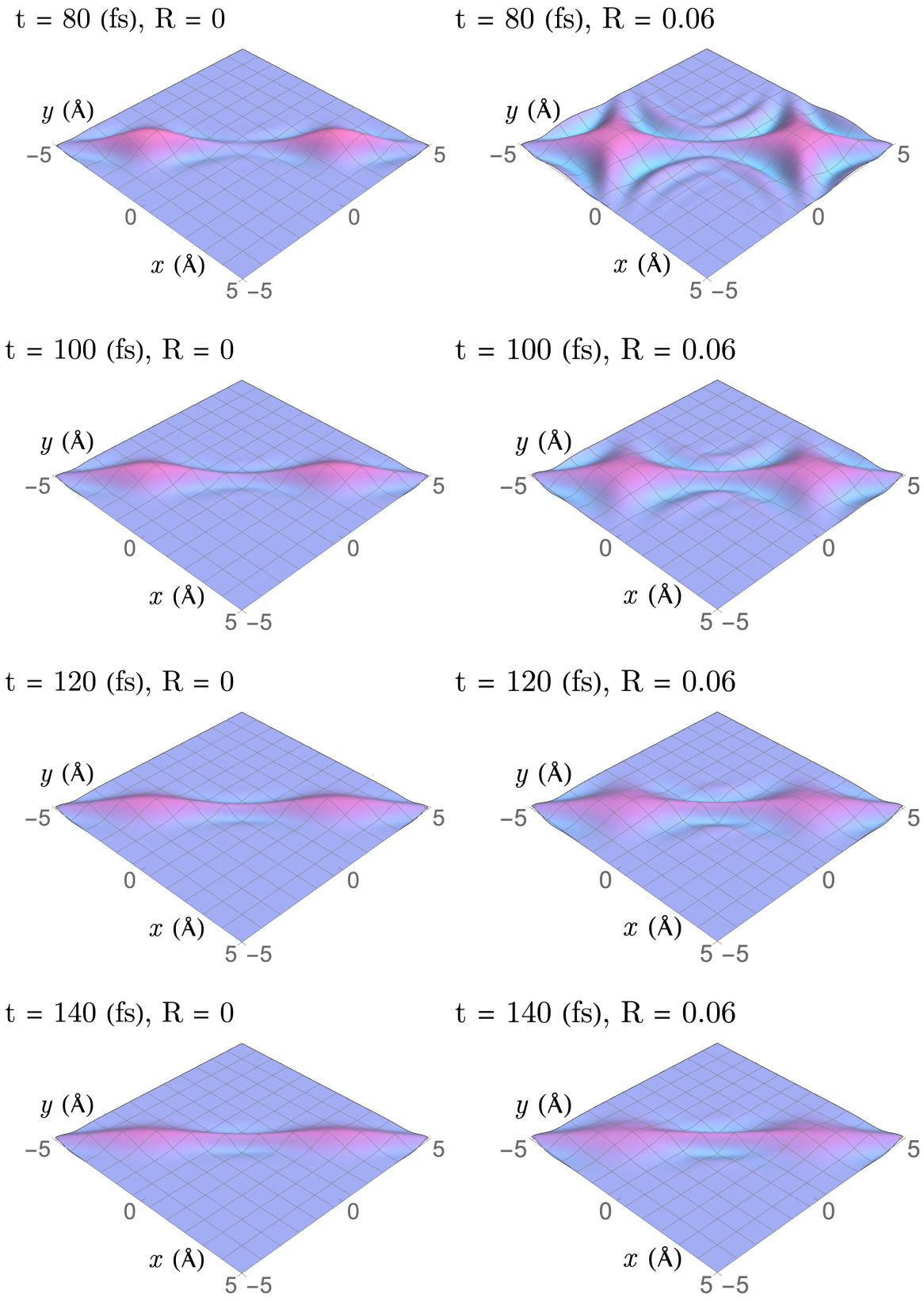

Figure 5.6: The real part of the density matrix evolving from 60fs to 140fsin the Markovian case (left), and the non-Markovian case with $R_\Omega = 0.06$ (right). $T = 320$K and $\gamma = \frac{kT}{20\hbar}$. Deviation from the Markovian case is clearly visible but decreases towards 140fs.

Because we are exploring the free particle case, the non-Markovian behaviours we see come from the orthogonal term, $\hat{L}_{\mathrm{O}}$. This is because there is no potential term, while the relaxation term only causes a slight amendment to the corresponding Caldeira-Leggett term, again by a factor $(1 + 2R_{\Omega})$. Therefore, the orthogonal term is the only new contribution. It is not therefore surprising that the term we labelled 'orthogonal' should be responsible for spreading of the density matrix orthogonal to the diagonal. The lines orthogonal to the diagonal, $x - y = 0$, are lines of constant $x + y$. So, it is reasonable that the term having an "orthogonal" derivative $(\frac{\partial}{\partial x} + \frac{\partial}{\partial y})$ induces dynamics that are orthogonal to the diagonal. As the orthogonal term is imaginary, it induces wave-like dynamics in both the real and imaginary parts of the density matrix, further boosting the coherence. Therefore, we can say that the novel non-Markovian dynamics are caused by the orthogonal term, $\hat{L}_{\mathrm{O}}$, which acts to cause orthogonal wave-like spreading of the density matrix. Now, we can revisit the cause of the non-Markovian deviations to the rapid decoherence process: the orthogonal term causes the off-diagonal peaks to spread parallel to the diagonal, which briefly increases their coherence (compared to the Markovian case with no spreading), but is not powerful enough to halt or reverse decoherence.

The emergence (and disappearance) of lateral coherence can be given a physical interpretation as follows. The phenomenon of decoherence is a constant effect by the environment to destroy quantum correlations that represent delocalised states. This is why the off-diagonal peaks decohere so quickly, and position superpositions at the macroscale are very rare. The effect of decoherence on the density matrix becomes stronger the further you travel from the diagonal. This is why some near-diagonal coherence can survive at long times (the steady state is a tight Gaussian function, not a delta function). The lateral coherences emerge due to the new orthogonal term, which acts to spread the density matrix away from the diagonal. This can be thought of as the non-Markovian effect of the environment sending information back into the system. However, decoherence is a continuous process and so it affects the lateral coherences too. Because they form much closer to the diagonal than the original off-diagonal peaks, they are not subject to such a strong decohering effect, and are not rapidly killed by decoherence. Instead, the orthogonal and decoherence terms compete for a time, until decoherence wins, the lateral coherences disappear, and the density matrix approaches the steady state.

Figures (5.5)-(5.6) also demonstrate the usefulness of the time-dependent incoherent base-

line method for calculating coherence. In particular, it can be seen that, along the diagonal, the non-Markovian solution is close to the Markovian solution. Away from the diagonal, it has additional contributions from the orthogonal spreading and rippling process - the lateral coherence contributions. Therefore, when we subtract the incoherent baseline from the non-Markovian solution, we will be left with only the new, coherent, contribution. This ensures that when we calculate the l_1 norm of coherence, we are only capturing the new lateral coherences originating from the non-Markovian dynamics. As with the short term dynamics, we calculate the l_1-norm of coherence to further explore the medium-long term coherence dynamics.

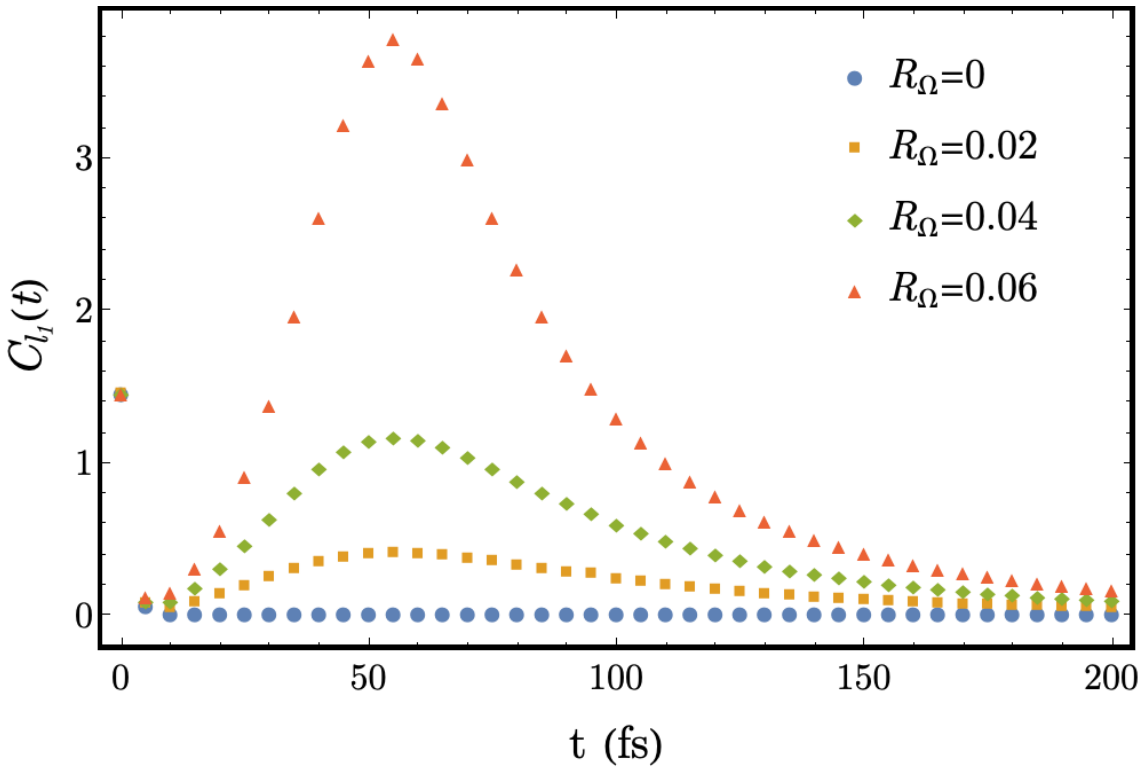

Figure 5.7: The l_1 norm of coherence in the case $\gamma = \frac{kT}{20\hbar}$, over an evolution of 200fs, found by numerically evaluating Eq. (5.2.16) for the exact solution. The non-Markovian cases ($R_\Omega = \{0.02, 0.04, 0.06\}$) clearly deviate from the Markovian case, with a resurgence of coherence which peaks around 60fs.

Figure (5.7) displays the l_1-norm of coherence, calculated as before with the incoherent baseline, up to 200fs. A range of values of R_Ω have been presented to demonstrate the increasing deviation from non-Markovian dynamics as R_Ω is increased. The initial rapid drop in the coherence plot can be interpreted as the short-time decoherence process discussed in the previous section. However, over the medium-long term, there is a much more noticeable and interesting feature: the l_1-norm of coherence rises as the lateral coherences emerge, peaking at times an order of magnitude longer than the length of the initial decoherence process. Not only

is there a resurgence of coherence in all non-Markovian cases, in the most extreme case the resurgence rises above the initial value. The implications of this will be further discussed in the next section. This is a clear indicator of significant non-Markovian deviations from the standard Caldeira-Leggett dynamics, occurring over significantly longer timescales than decoherence.

The concept of coherence being gained from interaction with a heat bath may seem counter-intuititive, especially as interaction with a heat bath is characterised by dissipative dynamics. However, work in the resource theory of coherence suggests that coherence can be generated by so-called thermal operations [132, 154]. These references highlight that coherence is primarily gained between degenerate energy eigenstates. This is particularly relevant for the free particle case, where energy is continuous. The amount of coherence that can be generated has been quantified [155], which demonstrates that the maximal possible coherence (in the energy basis) which can be generated via interaction with a heat bath increases with temperature. The initially counter-intuitive result that coherence is in fact gained by the system of interest during non-Markovian interaction with a heat bath is in agreement with literature [156].

Quantifying Coherence Resurgence

The coherence resurgence demonstrated by Figure (5.7) is for one particular choice of parameters. In order to understand the dependence of the coherence resurgence on the parameters γ, R_Ω, and T, we explore this further. In particular, we would like to have a better understanding of the time at which coherence may be maximised, and the amount that will be present in the system at this time. Although this will not present a full analysis - we are looking at the predictions made by the exact solution, rather than analysing the physical mechanisms behind the predictions - this will have relevance both in understanding the limits of the perturbative expansion and in exploring points made in the hypothesis, i.e. that a non-Markovian extension of the Caldeira-Leggett model will extend coherence times.

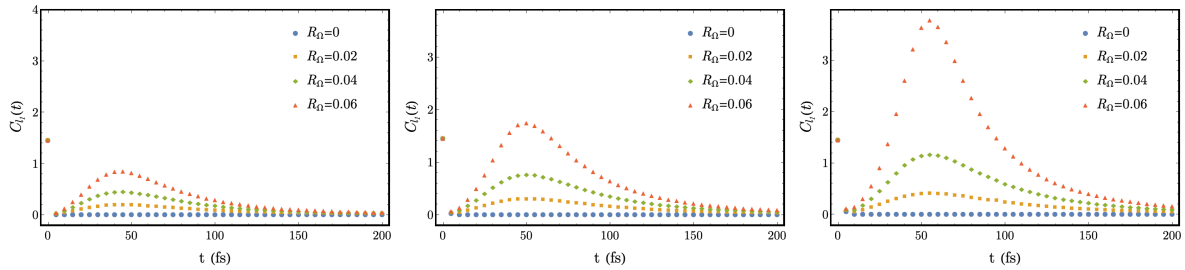

Figure 5.8: The l_1-norm of coherence over 200fs for (left to right): $\gamma = \frac{kT}{10\hbar}$, $\gamma = \frac{kT}{15\hbar}$, $\gamma = \frac{kT}{20\hbar}$, for the same range of R_Ω in each case, found by numerically evaluating Eq. (5.2.16) for the exact solution.

Figure (5.8) shows the difference in the coherence resurgence for a range of γ-values (decreasing from left to right). Two effects are apparent.

The first effect is that the magnitude of the coherence resurgence increases as γ decreases. This is only meaningful as a comparison, as coherence is not an unambiguously defined quantity and the absolute value carries little meaning, but it can be used to demonstrate that the strength of the coherence resurgence increases as the coupling to the bath gets weaker. This can be understood in two ways: firstly, that the weakened coupling to the bath decreases the strength of the decoherence, compared to the orthogonal term. Secondly, γ decreasing at fixed R_Ω corresponds to a bath reducing in size: we expect the system to be more non-Markovian as the bath size decreases, and this is supported by Figure (5.8). This figure suggests that R_Ω does not, by itself, quantify the non-Markovianity of the system. This corresponds to the conclusions of reference [148], which quantifies the non-Markovianity of a system defined by the parameters γ, T, Ω and notes that although the non-Markovianity is dependent on Ω, it is also dependent on the other parameters.

The second effect is that the time at which coherence is maximised is γ-dependent but not R_Ω-dependent. The coherence peak in each case moves to the right, i.e. the peak of coherence is at later times for weaker system-bath coupling. The weaker the coupling between system and bath, the longer it takes for coherence to return. This is intuitive; when γ^{-1} is seen as some kind of interaction timescale, a weaker coupling corresponds to a longer interaction time.

This allows us to address an assertion from the hypothesis, i.e. that the more non-Markovian the interaction between system and bath, the longer quantum coherence will persist in the sys-

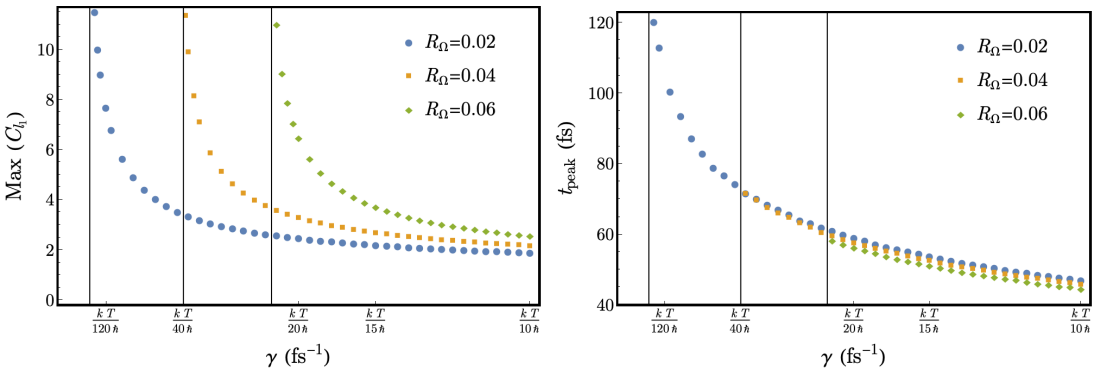

Figure 5.9: (Left) The value of coherence at the peak of the coherence resurgence, plotted against γ, with several values of R_Ω plotted. The points were found numerically by isolating the maximum of the l_1-norm of coherence with the initial coherence removed from the system. All cases have $T = 320$K. Divergent behaviour is seen in each case as the system enters a regime where the perturbation is invalid. (Right) The time at which the coherence resurgence is at its maximum, with several values of R_Ω plotted. The points were found numerically by isolating the maximum of the l_1-norm of coherence with the initial coherence removed from the system and extracting the time to which it corresponds. All cases have $T = 320$K. A clear γ-dependence is seen, but the R_Ω-dependence is weak.

tem. A full analysis of this point is beyond the scope of this thesis, as we have not implemented a quantifier of non-Markovianity, and we have seen that non-Markovianity is dependent on more than just R_Ω. However, when we vary R_Ω with all other parameters fixed, this functions as a crude proxy for degree of non-Markovianity. Varying R_Ω in this way does not correspond to a significant change in the time-dependence of the coherence: the peak of the resurgence happens at approximately the same time for every value of R_Ω (for fixed γ). Instead, the quantity of coherence present in the system at the peak is highly dependent on R_Ω, increasing as the system becomes more non-Markovian. The time for which quantum coherence persists in the system is much more dependent on the system-bath coupling.

Bringing this together gives an alternative result: the more non-Markovian the interaction between system and bath, the more coherence is present at long times during the coherence resurgence. Additionally, the weaker the coupling between system and bath, the longer quantum coherence persists in the system. Figure (5.9) provides a concrete demonstration of this result.

The question of thorough quantification of the coherence resurgence is an interesting avenue for future research. We have illustrated the dependence of the time of the peak of coherence on

γ, and the dependence of the magnitude of the peak of coherence on γ and R_Ω. However, there is more that could be done to understand the relationship between the coherence resurgence and the parameters. In addition, the quantification does not provide any explanatory power: we would in principle like to be able to predict the peak based on an understanding of the interplay between the decoherence and orthogonal terms of the master equation.

As discussed in Section 2.2.5, approximate approaches in modelling open quantum systems do not guarantee that the dynamics will not violate the uncertainty principle, or conserve positivity. So, despite the controversies associated with the requirements of complete positivity [38, 77, 78], it is sensible to check that the dynamics respect the constraints imposed by the theory of quantum mechanics. It is already known that the Caldeira-Leggett equation does not fully conserve positivity, but can be brought approximately into positivity-conserving Lindblad form [9, 76]. However, there is in principle no guarantee that this will also apply to the new non-Markovian equation, and it has been discussed that master equations of a similar form will not necessarily conserve positivity [75].

In order to perform a full analysis of the positivity of the dynamics, it would be necessary to diagonalise the matrix to find the eigenvalues, and verify that none of them become negative across the full evolution of the density matrix. However, this procedure is neither straightforward nor time-efficient, and so we select a different approach. The method presented in [72] uses a condition on the purity, namely that $\mathrm{Tr}(\tilde{\rho}^2) \leq 1$, and the Robertson-Schwinger uncertainty principle condition,

$$\sigma_x \sigma_p \geq \frac{\hbar}{2}, \tag{5.2.17}$$

where

$$\sigma_x \sigma_p = \sqrt{(\mathrm{Tr}(\tilde{\rho}x^2) - \mathrm{Tr}(\tilde{\rho}x)^2)(\mathrm{Tr}(\tilde{\rho}\hat{p}^2) - \mathrm{Tr}(\tilde{\rho}\hat{p})^2)}, \tag{5.2.18}$$

to present a necessary (but not sufficient) condition for the positivity of the dynamics. In addition, we confirm that the non-Markovian master equation conserves normalisation of the density matrix, i.e. that the trace satisfies $rmTr(\tilde{\rho}) = 1$.

We first calculate the trace and purity of the density matrix. Since we already have the

analytic solution, these quantities can be straightforwardly numerically integrated using

$$\mathrm{Tr}(\tilde{\rho}) = \int \mathrm{d}x \rho(x, x, t) \tag{5.2.19}$$

and

$$\mathrm{Tr}(\tilde{\rho}^2) = \int \mathrm{d}x \rho(x, x, t) \rho^*(x, x, t). \tag{5.2.20}$$

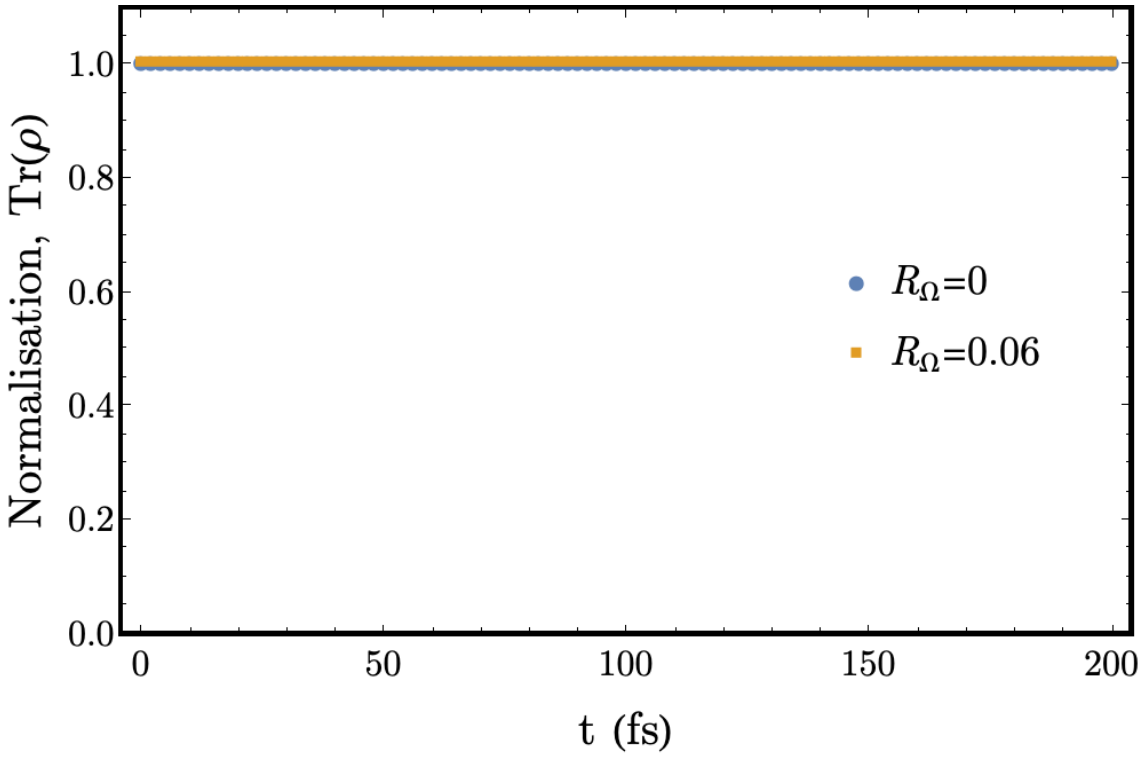

Figure 5.10: The trace of the density matrix in the Markovian $R_\Omega = 0$, and non-Markovian $R_\Omega = 0.06$ cases. $T = 320$K and $\gamma = \frac{kT}{20\hbar}$. The value of the trace is constant at 1, confirming that the non-Markovian master equation conserves normalisation.

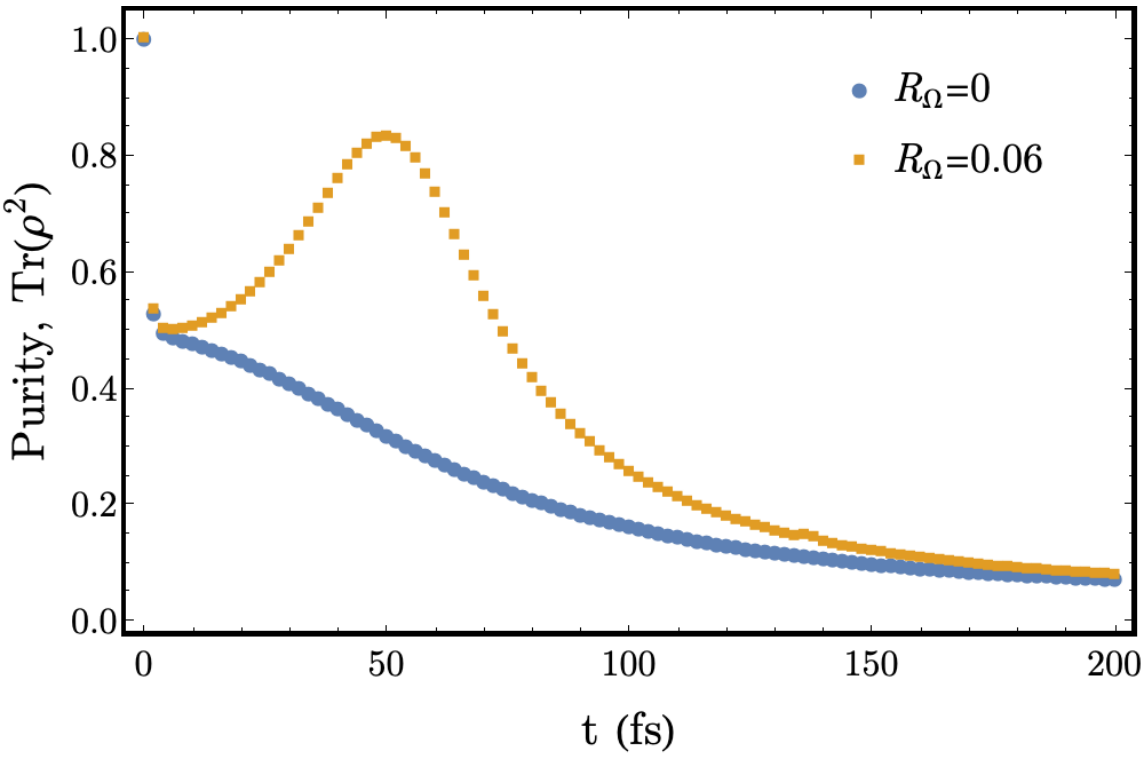

Figure 5.11: The purity of the density matrix in the Markovian $R_\Omega = 0$, and non-Markovian $R_\Omega = 0.06$ cases. $T = 320$K and $\gamma = \frac{kT}{20\hbar}$. The initial value is 1, which is expected for a pure state, and it never rises above 1 for $t > 0$. In the non-Markovian case there is a resurgence around 50fs. The Markovian and non-Markovian cases converge for large t; although the systems converge to slightly different steady states, the degree of mixedness in each case is equivalent.

Figure (5.11) displays that the purity never rises above 1 for $t > 0$, fulfilling the first condition. It is interesting to note that in the non-Markovian case, there is an increase in the purity starting very soon after the initial decoherence and peaking around 50fs, matching the timescales of the resurgence in coherence. This corresponds physically to a reduction in the degree of mixing of the density matrix, which reflects the non-Markovian information backflow [35, 157–159]; a pure state contains full information about the state, whereas a mixed state has incomplete information. As information flows back into the system, the degree of mixedness reduces.

The analytic solution makes it straightforward to compute the necessary terms to evaluate

the condition on the Robertson-Schwinger uncertainty:

$$\begin{aligned}
\mathrm{Tr}(\tilde{\rho}x) &= \int x\mathrm{d}x\tilde{\rho}(x,x,t) \\
\mathrm{Tr}(\tilde{\rho}x^2) &= \int x^2\mathrm{d}x\tilde{\rho}(x,x,t) \\
\mathrm{Tr}(\tilde{\rho}\hat{p}) &= -i\hbar\int \mathrm{d}x\mathrm{d}y\ \frac{\partial}{\partial x}\tilde{\rho}(x,y,t)\delta(x-y) \\
\mathrm{Tr}(\tilde{\rho}\hat{p^2}) &= -\hbar^2\int \mathrm{d}x\mathrm{d}y\ \frac{\partial^2}{\partial x^2}\tilde{\rho}(x,y,t)\delta(x-y).
\end{aligned} \tag{5.2.21}$$

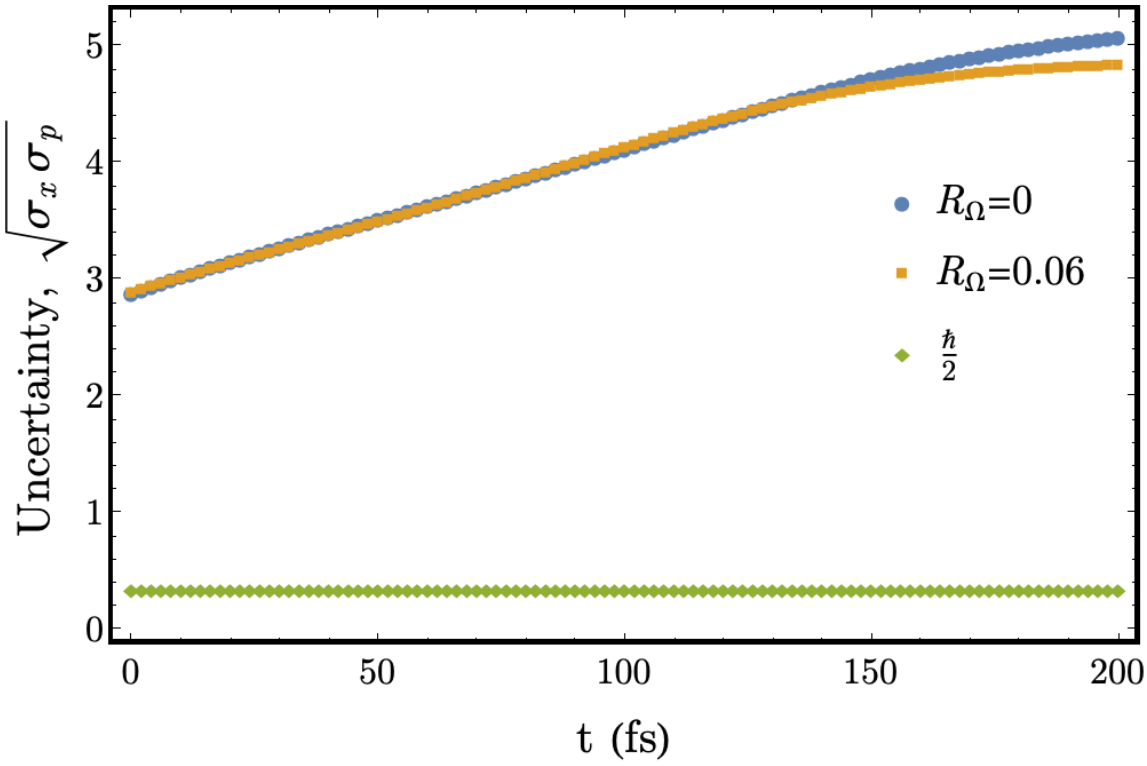

Figure 5.12: The uncertainty of the density matrix in the Markovian $R_\Omega = 0$, and non-Markovian $R_\Omega = 0.06$ cases. $T = 320$K and $\gamma = \frac{kT}{20\hbar}$. The minimum values $\hbar/2$ is also marked, and in neither the Markovian nor the non-Markovian case is the uncertainty principle violated. The non-Markovian cases converges to a slightly different value than the Markovian case, reflecting the difference in steady state.

Figure (5.12) displays the results of the uncertainty calculation, and it can clearly be seen that neither the Markovian nor non-Markovian case violates the uncertainty principle. The two cases tend towards slightly different final values, although there is no significant change in uncertainty resulting from the coherence resurgence. This reflects the fact that the diagonal elements are largely unchanged by the non-Markovian evolution, which means that operator expectation values will not greatly vary. However, the uncertainty of the final state is slightly different as the non-Markovian Gaussian steady state has a marginally different variance.

5.2.5 Quantum Thermodynamics and non-Markovianity

The coherence increase has implications for the entropy of the system. As discussed in Section 2.3, decoherence can be interpreted as an entropy-increasing process, and it is natural to then associate a coherence resurgence with a *decrease* of entropy. Further to this, the non-Markovian character of the dynamics means that the coherence resurgence is due to information backflow and, as we have discussed, information is closely related to entropy. Therefore, we explore this using concepts from quantum thermodynamics.

We approach a thermodynamic interpretation of the coherence resurgence by calculating the von Neumann entropy of the density matrix,

$$S_{\mathrm{vN}} = -k_B \mathrm{Tr}(\tilde{\rho} \ln \tilde{\rho}). \tag{5.2.22}$$

The form of the exact analytic solution in Eq. (5.2.8) remains a Gaussian state over time, just becoming more mixed. Because it is a Gaussian state, we can use the expression for the von Neumann entropy given in [160] as

$$\frac{S_{\mathrm{vN}}(\tilde{\rho})}{k_B} = \frac{1-\mu}{2\mu} \ln \frac{1+\mu}{1-\mu} - \ln \frac{2\mu}{1+\mu}, \tag{5.2.23}$$

with μ the purity, calculated as in the last section. The corresponding entropy production rate is

$$\frac{\dot{S}_{\mathrm{vN}}(\tilde{\rho})}{k_B} = -\frac{\dot{\mu}}{2\mu^2} \ln \frac{1+\mu}{1-\mu}, \tag{5.2.24}$$

where the derivative of the purity can be directly calculated from the analytic solution.

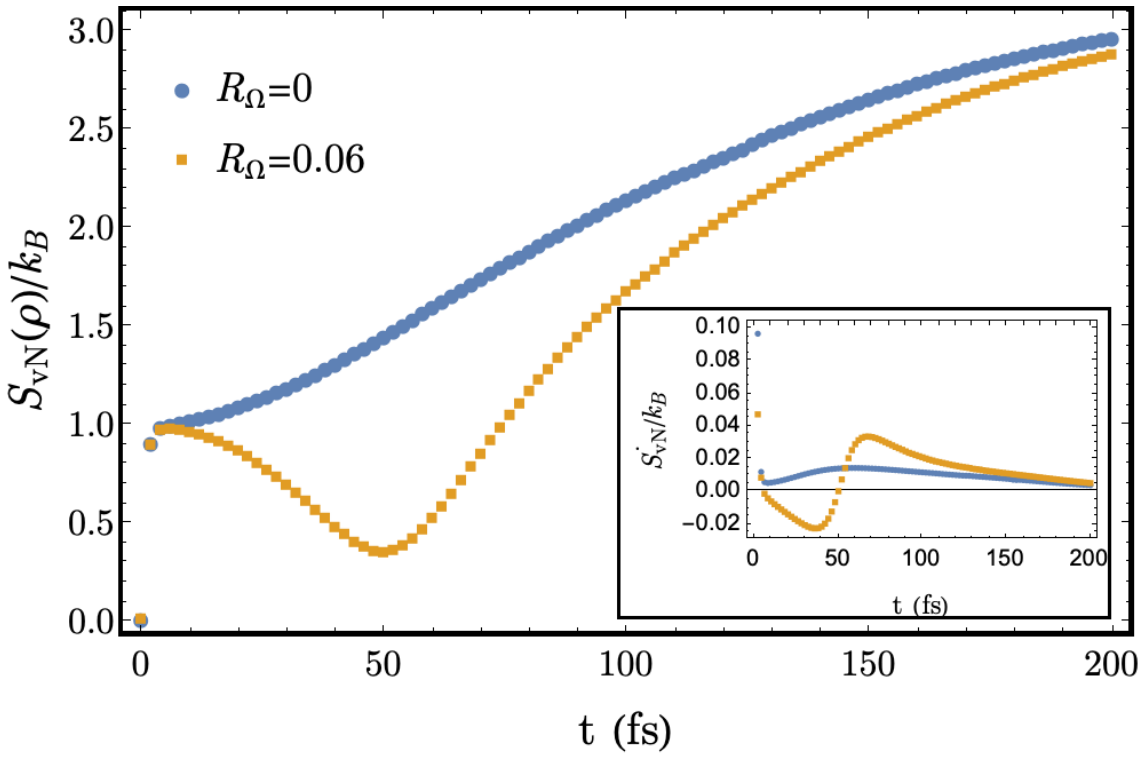

Figure 5.13: The von Neumann entropy of the density matrix in the Markovian $R_\Omega = 0$ and non-Markovian $R_\Omega = 0.06$ cases. $T = 320$K and $\gamma = \frac{kT}{20\hbar}$. There is a transient decrease in the non-Markovian case, but it never decreases below the initial value of 0 for the pure state. Inset: the corresponding von Neumann entropy production rate, which is transiently negative in the region that the entropy decreases.

Figure (5.13) displays the results of the von Neumann entropy calculation, as well as the entropy production rate. There is a transient decrease in entropy that corresponds with the regime in which the coherence resurgence occurs, and in the same region the entropy production rate becomes transiently negative. These transient negative entropy production rates are becoming understood as indicative of non-Markovian behaviour [125–129]. As the entropy never decreases below the original value, the second law of thermodynamics is never violated: at any point if the evolution were to be stopped, entropy would still have increased in the system.

It is natural to ask if different initial conditions, for example mixed states, could undergo dynamics which violate the second law. However, it has been shown in a variety of ways [51, 161, 162] that this is not possible for general non-Markovian dynamics, as there is a thermodynamic cost associated with preparing states, as well as removing the system from the bath. Despite this, we can still interpret the entropy decrease as a useful thermodynamic resource; this is further discussed in Section 7.1.2.

5.3 Wigner Functions

In the classical limit, the Caldeira-Leggett equation corresponds to Brownian motion; this was confirmed by comparing the Brownian motion Fokker-Planck equation to the $\hbar \to 0$ limit of the Wigner transform of the Caldeira-Leggett equation. We aim to derive the Fokker-Planck equation in the case of non-Markovian quantum Brownian motion. This will allow us to examine the dynamics of the system at the classical level and, in particular, to assess whether there are any new classical dynamics arising from the non-Markovian extension of the Caldeira-Leggett model.

In order to calculate the Wigner equation corresponding to Eq. (5.1.33), we need to apply the Wigner transformation in (3.3.32) to each term in the master equation,

$$\frac{\partial}{\partial t}\tilde{\rho}(x,y,t) = \left(\hat{\mathrm{L}}_M + R_\Omega\Big[\hat{L}_\mathrm{O} + \hat{L}_\mathrm{V} + \hat{L}_\mathrm{R}\Big]\right)\tilde{\rho}(x,y,t), \tag{5.3.1}$$

where, as before, the new terms are labelled by the Liouvillian operators $\hat{L}_\mathrm{O}$, $\hat{L}_\mathrm{V}$, and $\hat{L}_\mathrm{R}$:

$$\begin{aligned}
\hat{L}_\mathrm{O} &= -\frac{4ikT}{\hbar}(x-y)\left(\frac{\partial}{\partial x} + \frac{\partial}{\partial y}\right) \\
\hat{L}_\mathrm{V} &= -\frac{i}{2\hbar}(x-y)\left(\frac{\partial \mathrm{V}_R}{\partial x} + \frac{\partial \mathrm{V}_R}{\partial y}\right) \\
\hat{L}_\mathrm{R} &= -2\gamma(x-y)\left(\frac{\partial}{\partial x} - \frac{\partial}{\partial y}\right).
\end{aligned} \tag{5.3.2}$$

However, this cannot be done immediately as the master equation is in the coordinate representation. In order to apply the Wigner transform to the master equation, we need to transform it into the operator representation. This is because the Wigner transform selects a basis for the density matrix, i.e. by taking the matrix element $\langle q - \frac{u}{2}|\tilde{\rho}|q + \frac{u}{2}\rangle$. Once the master equation is in operator form, the transform can be applied to each term in the operator representation.

5.3.1 Operator Form of the Master Equation

We first transform the Liouvillians into operator representation. The Markovian term becomes [31]

$$\hat{L}_\mathrm{M}\tilde{\rho} = \frac{1}{i\hbar}[H_R, \tilde{\rho}] - \frac{i\gamma}{\hbar}[\hat{q}, \{\hat{p}, \tilde{\rho}\}] - \frac{2M\gamma kT}{\hbar^2}[\hat{q}, [\hat{q}, \tilde{\rho}]], \tag{5.3.3}$$

and the non-Markovian terms

$$\hat{L}_\mathrm{O}\tilde{\rho} = \frac{4kT}{\hbar^2}[\hat{q}, [\hat{p}, \tilde{\rho}]], \tag{5.3.4}$$

$$\hat{L}_{\mathrm{V}}\tilde{\rho} = \frac{1}{2\hbar^2}[\hat{q}, \{\tilde{\rho}, [\hat{p}, \hat{\mathrm{V}}_R]\}], \tag{5.3.5}$$

and

$$\hat{L}_{\mathrm{R}}\tilde{\rho} = -\frac{2i\gamma}{\hbar}[\hat{q}, \{\hat{p}, \tilde{\rho}\}]. \tag{5.3.6}$$

The operator forms can be verified by taking the matrix elements of the commutators. This is performed by multiplying out the commutator, inserting several resolutions of identity, and using the identities

$$\langle x|\hat{q}|y\rangle = x\delta(x-y) \tag{5.3.7}$$

$$\langle x|\hat{\mathrm{v}}_R|y\rangle = \hat{\mathrm{v}}_R(x)\delta(x-y) \tag{5.3.8}$$

and

$$\langle x|\hat{p}|y\rangle = -i\hbar\frac{\partial}{\partial x}\delta(x-y) = i\hbar\frac{\partial}{\partial y}\delta(x-y). \tag{5.3.9}$$

For example, the operator term $\hat{q}\hat{p}\tilde{\rho}$ can be translated into the position basis by using three resolutions of identity, referred to here by the dummy variables A_i:

$$\begin{aligned}\langle x|\hat{q}\hat{p}\tilde{\rho}|y\rangle &= \int \mathrm{d}A_1\mathrm{d}A_2\mathrm{d}A_3\, \langle x|\hat{q}|A_1\rangle \langle A_1|\hat{p}|A_2\rangle \langle A_2|\tilde{\rho}|y\rangle \\ &= i\hbar \int \mathrm{d}A_1\mathrm{d}A_2\mathrm{d}A_3\; x\delta(x-A_1)\frac{\partial}{\partial A_2}\delta(A_1-A_2)\langle A_2|\tilde{\rho}|y\rangle \\ &= -i\hbar\; x\frac{\partial}{\partial x}\tilde{\rho}(x,y,t).\end{aligned} \tag{5.3.10}$$

Integration by parts was used to move the derivative from the δ-function to the density matrix. All operator representations can be verified in the same way.

Although there is a certain amount of "trial-and-error" involved in finding these operator forms, it can largely by done using physical intuition: the factor $(x-y)$ will correspond to the position operator $\hat{q}$, a derivative bracket $(\frac{\partial}{\partial x} - \frac{\partial}{\partial y})$ will correspond to the momentum operator $\hat{p}$, and the potential also becomes an operator. Then it is simply a matter of finding the correct commutator bracket, which is done strategically by combining permutations of operators, then using commutator identities to condense the expression. More details about the procedure can be found in Appendix F.

We can then write the non-Markovian master equation in operator form as

$$\begin{aligned}\frac{\partial\tilde{\rho}}{\partial t} =&\frac{1}{i\hbar}\left[H_R,\tilde{\rho}\right]-\frac{i\gamma}{\hbar}[\hat{q},\{\hat{p},\tilde{\rho}\}]-\frac{2M\gamma kT}{\hbar^2}[\hat{q},[\hat{q},\tilde{\rho}]]\\ &+R_\Omega\left(\frac{4kT}{\hbar^2}[\hat{q},[\hat{p},\tilde{\rho}]]+\frac{1}{2\hbar^2}[\hat{q},\{\tilde{\rho},[\hat{p},\hat{\mathrm{V}}_R]\}]-\frac{2i\gamma}{\hbar}[\hat{q},\{\hat{p},\tilde{\rho}\}]\right),\end{aligned} \tag{5.3.11}$$

and this can now be Wigner transformed.

5.3.2 Wigner Transform of Operator Brackets

In order to obtain the Wigner function corresponding to the non-Markovian master equation, we need to take the Wigner transform of each operator bracket using the definition given by Eq. (3.3.32). We need to consider the Wigner transformation of several combinations of the operators $\hat{q}$, $\hat{p}$, $\hat{\mathrm{v}}_R$, and $\tilde{\rho}$. We take as given the Wigner transform of the Markovian terms [31]:

$$\left(\hat{L}_{\mathrm{M}}\tilde{\rho}\right)_W=-\frac{p}{M}\frac{\partial W}{\partial q}+\frac{\partial \mathrm{V}_R}{\partial q}\frac{\partial W}{\partial p}+2\gamma\frac{\partial}{\partial p}\left(pW\right)+2M\gamma kT\frac{\partial^2 W}{\partial p^2}, \tag{5.3.12}$$

and note that we can infer the Wigner transform of one of the non-Markovian terms which has the same form as the Caldeira-Leggett relaxation term,

$$\left(\hat{L}_{\mathrm{R}}\tilde{\rho}\right)_W=4\gamma\frac{\partial}{\partial p}(pW). \tag{5.3.13}$$

This term will not meaningfully change the dynamics of the system in the classical limit, especially as the values of R_Ω we are considering are much smaller than $1/\pi$ ($\gamma<\Omega$).

All that is left to do is find the Wigner transforms of the two remaining terms,

$$\left(\hat{L}_{\mathrm{O}}\right)_W=\frac{4kT}{\hbar^2}[\hat{q},[\hat{p},\tilde{\rho}]]_W \tag{5.3.14}$$

and

$$\left(\hat{L}_{\mathrm{V}}\right)_W=\frac{1}{2\hbar^2}[\hat{q},\{\tilde{\rho},[\hat{p},\hat{\mathrm{V}}_R]\}]_W. \tag{5.3.15}$$

We do this directly by expanding the operator brackets and inserting each term into the defini-

tion of the Wigner transform, i.e.

$$\begin{aligned}(\hat{q}\hat{p}\tilde{\rho})_W &= \frac{1}{\hbar}\int \mathrm{d}u \exp\Big\{-i\frac{pu}{\hbar}\Big\}\int \mathrm{d}A_1\mathrm{d}A_2 \,\langle q-\frac{u}{2}|\hat{q}|A_1\rangle\,\langle A_1|\hat{p}|A_2\rangle\,\langle A_2|\tilde{\rho}|q+\frac{u}{2}\rangle \\ &= -\frac{1}{\hbar}(i\hbar)\int \mathrm{d}u \exp\Big\{-i\frac{pu}{\hbar}\Big\} \\ &\qquad \times \int \mathrm{d}A_1\mathrm{d}A_2 \left(q-\frac{u}{2}\right)\delta\left(A_1-q+\frac{u}{2}\right)\frac{\partial}{\partial A_2}\delta\left(A_2-A_1\right)\langle A_2|\tilde{\rho}|q+\frac{u}{2}\rangle \\ &= \frac{1}{\hbar}(i\hbar)\int \mathrm{d}u \exp\Big\{-i\frac{pu}{\hbar}\Big\}\left(q-\frac{u}{2}\right)\left(\frac{1}{2}\partial_q-\partial_u\right)\langle q-\frac{u}{2}|\tilde{\rho}|q+\frac{u}{2}\rangle\,.\end{aligned} \tag{5.3.16}$$

Then, the relations for each of the operator terms are summed and the derivatives in ∂_q and ∂_u evaluated. Further details can be found in Appendix F. When all the terms in the commutator bracket are summed, we find that

$$[\hat{q},[\hat{p},\tilde{\rho}]]_W = \hbar^2\partial_p\partial_q W. \tag{5.3.17}$$

Therefore, the Wigner transform of the orthogonal term is

$$\begin{aligned}\left(\hat{L}_{\mathrm{O}}\right)_W &= \frac{4kT}{\hbar^2}(\hbar^2\partial_p\partial_q W) \\ &= 4kT\partial_p\partial_q W.\end{aligned} \tag{5.3.18}$$

There is no corresponding Markovian term of the same form, and therefore this will introduce new dynamics to the classical non-Markovian behaviour. As the effect of this term is temperature dependent, it should be significant at physiological temperatures.

We use the same process to determine the Wigner transform of the potential term, with the additional complication of the potential operator. Although the process is the same, terms of the form $\mathrm{V_R}(q\pm\frac{u}{2})$ require that an expansion in phase space is taken, i.e. to write that

$$\mathrm{V_R}(q\pm\frac{u}{2}) = \sum_{n=0}\frac{1}{n!}\frac{\partial^n}{\partial q^n}\mathrm{V_R}(q)\left(\frac{u}{2}\right)^n. \tag{5.3.19}$$

This leads to the Wigner transform

$$[\hat{q},\{\tilde{\rho},[\hat{p},\hat{\mathrm{V}}_{\mathrm{R}}]\}]_W = 2\hbar^2\sum_{n=0}\frac{1}{(2n)!}(-\hbar^2)^n\left(\frac{1}{2}\right)^2 n\frac{\partial^{2n+1}\mathrm{V_R}}{\partial q^{2n+1}}\frac{\partial^{2n+1}W}{\partial p^{2n+1}}, \tag{5.3.20}$$

and therefore

$$\left(\hat{L}_{\mathrm{V}}\right)_W = \sum_{n=0} \frac{1}{(2n)!}(-\hbar^2)^n \left(\frac{1}{2}\right)^2 n \frac{\partial^{2n+1}\mathrm{V_R}}{\partial q^{2n+1}} \frac{\partial^{2n+1} W}{\partial p^{2n+1}}. \tag{5.3.21}$$

In the $\hbar \to 0$ limit, this becomes

$$\lim_{\hbar\to 0}\left(\hat{L}_{\mathrm{V}}\right)_W = \frac{\partial \mathrm{V}_R(q)}{\partial q}\frac{\partial W}{\partial p}. \tag{5.3.22}$$

As with the relaxation term, this is of the same form as one of the terms already present in the Markovian Fokker-Planck equation. Therefore, this will not dramatically affect the dynamics, and the only effect is to amend the potential-dependent term in the Fokker-Planck equation by the factor $(1 + R_\Omega)$. As with the relaxation term, this will never dominate as we are limited to considering small R_Ω.

5.3.3 Wigner Transform and Fokker-Planck Equation

Combining these results for the Markovian, orthogonal, potential, and relaxation terms leads us to the Wigner transform of the whole master equation:

$$\begin{aligned}\frac{\partial W}{\partial t} =& -\frac{p}{M}\frac{\partial W}{\partial q} + \frac{\partial \mathrm{V}_R}{\partial q}\frac{\partial W}{\partial p} + 2\gamma\frac{\partial}{\partial p}(pW) + D\frac{\partial^2 W}{\partial p^2} \\ &+ R\left(4kT\frac{\partial^2 W}{\partial p \partial q} + \sum_{n=0}\frac{1}{(2n)!}(-\hbar^2)^n\left(\frac{1}{2}\right)^{2n}\frac{\partial^{2n+1}\mathrm{V}_R(q)}{\partial q^{2n+1}}\frac{\partial^{2n+1}W}{\partial p^{2n+1}} + 4\gamma\frac{\partial}{\partial p}(pW)\right).\end{aligned} \tag{5.3.23}$$

When we take the $\hbar \to 0$ limit of this result, we obtain the Fokker-Planck equation

$$\frac{\partial W}{\partial t} = \lim_{\hbar\to 0}\left[\hat{L}_{\mathrm{M}}\tilde{\rho} + R_\Omega\left(\hat{L}_{\mathrm{O}}\tilde{\rho} + \hat{L}_{\mathrm{V}}\tilde{\rho} + \hat{L}_{\mathrm{R}}\tilde{\rho}\right)\right]_W. \tag{5.3.24}$$

The only term containing $\hbar$ is the Wigner transform of the potential term. However, we take the $n = 0$ term of the sum to obtain

$$\lim_{\hbar\to 0}\left(\hat{L}_{\mathrm{V}}\right)_W = \frac{\partial \mathrm{V}_R(q)}{\partial q}\frac{\partial W}{\partial p}. \tag{5.3.25}$$

Therefore, the Fokker-Planck equation corresponding to the non-Markovian master equation is

$$\begin{aligned}\frac{\partial W}{\partial t} = -\frac{p}{M}\frac{\partial}{\partial q}W + (1+R_\Omega)\frac{\partial \mathrm{V}_R(q)}{\partial q}\frac{\partial W}{\partial p} + 2\gamma(1+2R_\Omega)\frac{\partial}{\partial p}(pW) \\ + 2M\gamma kT\frac{\partial^2 W}{\partial p^2} + 4kTR_\Omega\frac{\partial^2 W}{\partial p \partial q}.\end{aligned} \tag{5.3.26}$$

This result is strikingly similar to the Caldeira-Leggett Fokker-Planck equation, obtained by setting $R_\Omega = 0$. In fact, the only significant source of new dynamics is the term that arises from the orthogonal term, i.e. $4kTR_\Omega\partial_p\partial_q W$. The contributions to the potential and relaxation terms are negligible. The result indicates that there are novel and non-trivial non-Markovian classical dynamics which arise from this quantum system, and that this effect is largely system-independent - it is not strongly dependent on the potential.

5.4 Summary of this Chapter

In this section, we have followed the method developed in Refs. [36, 37] to derive a master equation which functions as a non-Markovian extension to the Caldeira-Leggett model of quantum Brownian motion. This involved using a Laplace transform technique to evaluate the nested convolution integrals in the Caldeira-Leggett propagator, and using an expansion in powers of $\frac{1}{\Omega}$ to isolate the leading order term in the expansion. The resulting approximate propagator is evaluated over two infinitesimal intervals, each of length ε, in order to account for the effects of higher-order derivatives. Following a process analogous to that outlined by Caldeira and Leggett [31], the master equation is recovered from the first-order terms in ε, and given as

$$\begin{aligned}\frac{\partial}{\partial t}\tilde{\rho}(x,y,t) =& \hat{\mathrm{L}}_M\tilde{\rho}(x,y,t) \\ &+R_\Omega\Big[-\frac{4ikT}{\hbar}(x-y)\left(\frac{\partial}{\partial x}+\frac{\partial}{\partial y}\right) - \frac{i}{2\hbar}(x-y)\left(\frac{\partial \mathrm{V}_R}{\partial x}+\frac{\partial \mathrm{V}_R}{\partial y}\right) \\ &\quad -2\gamma(x-y)\left(\frac{\partial}{\partial x}-\frac{\partial}{\partial y}\right)\Big]\tilde{\rho}(x,y,t),\end{aligned} \tag{5.4.1}$$

where

$$R_\Omega = \frac{\gamma}{\pi\Omega} \tag{5.4.2}$$

is a dimensionless ratio between the coupling strength and the cut-off frequency which stands in as an informal proxy for the non-Markovianity of the system.

We followed the approach outlined in Ref [109] to derive an analytic solution for the free particle, which was then used to examine the dynamics described by the non-Markovian master equation. While the initial rapid decoherence is only very slightly affected by the non-Markovian corrections, the medium-term dynamics show novel behaviour characterised by coherent rippling of the on-diagonal peaks away from the diagonal line. This corresponds to a resurgence of the l_1 norm of coherence and a transient decrease in von Neumann entropy. However, the entropy never reduces below its initial value, showing that the second law of thermodynamics is not violated. We have made connections between the observed coherence resurgence and a growing body of literature in quantum thermodynamics which describes transient negative entropy production rates as characteristic of non-Markovian processes.

Further checks were made to ensure that the uncertainty principle is not violated. We cannot state with complete confidence that the positivity condition is never violated, but we have shown that the purity and uncertainty conditions which are often used as a proxy for positivity are not violated in the regimes we are interested in. Finally, we have derived the corresponding Fokker-Planck equation, valid in the classical limit, by utilising the Wigner transform.

The content of this chapter has been written up as a paper which has been accepted for publication in Phys. Rev. A. [37].

Chapter 6

Frequency Rescaling of the non-Markovian Master Equation

In the previous chapter, we presented the derivation and analysis of a non-Markovian master equation, constructed by including a harsh cut-off in the spectral density. However, this is by no means the only possible amendment to the spectral density. While the harsh cut-off is the most straightforward way to introduce a frequency limit to the Caldeira-Leggett environment, it is not the most physically intuitive. In particular, it implies that the maximum of the spectral density is at the maximum allowed oscillator frequency. There are very few distributions for which this is true; the usual scenario is that there is some characteristic maximum frequency followed by a smoothly varying tail. We would like to be able to consider Ohmic spectral densities with a range of cut-off functions which reflect different kinds of high-frequency dependence. This will allow us to explore the space of possible spectral densities, and the dependence of the master equation on the spectral density.

In the previous chapter, the spectral density contributes to the master equation in a way that is clearly described by a Taylor approximation of the Laplace transform of the memory kernel:

$$\mathcal{L}\Big\{\mu_\Omega(\tau)\Big\}(p) \approx \frac{\eta}{2} - \frac{\eta}{\pi\Omega}p. \tag{6.0.1}$$

The linear form of this approximation is due to the perturbative expansion used. For this to hold, we require that $\frac{p}{\Omega} \ll 1$.

By examining the propagator given by Eq. (5.1.25), we identified that the first term (the zeroth order) of the Laplace transform induces the standard Markovian dynamics derived by Caldeira-Leggett and that the second term (the first order) is responsible for the non-Markovian dynamics. In fact, we can explicitly link the first order term of the Laplace transform to the non-Markovianity factor

$$R_\Omega = \frac{\gamma}{\pi\Omega} = -\frac{1}{2M}\frac{\partial}{\partial p}\mathcal{L}\Big\{\mu_\Omega(\tau)\Big\}(p)|_{p=0}. \tag{6.0.2}$$

The spectral density also induces a renormalization of the potential via

$$\mu_\Omega(0) = \frac{\eta\Omega}{\pi} = (\Delta\omega)^2, \tag{6.0.3}$$

as described in the Caldeira-Leggett model. All the information in the master equation that comes from the spectral density can be found in these listed quantities. This means that, in principle, we should be able to apply this process to find the corresponding quantities of other spectral densities to obtain similar master equations to Eq. (5.1.33).

6.1 A Library of Cut-Off Functions

Our goal is to examine non-Markovian Ohmic spectral densities other than the harsh cut-off spectral density. Therefore, we broaden our definition to

$$J(\omega) = \eta\omega f(\omega, \omega_f), \tag{6.1.1}$$

where $f(\omega, \omega_f)$ is a so-called "cut-off" function which describes the tail of the spectral density, and ω_f is a characteristic frequency which controls the transition from low-frequency Ohmic behaviour to high-frequency non-Ohmic behaviour. We refer to this as the Ohmic class of spectral densities.

We want the spectral density to be purely Ohmic in low frequencies and drop to zero at high frequencies. As with the harsh cut-off case, this will represent a finite bath, but in a more physically realistic way. The maximum of the spectral density will not be at the highest frequency, but will instead be determined by some characteristic frequency that describes the transition

from purely Ohmic to Ohmic decaying behaviour. This reflects the fact that the spectral density contains information about the distribution of frequencies as well as how strongly they are coupled to the environment; we do not expect the most densely occupied frequency to be the highest one. To reflect these physical considerations, we require cut-off functions to start at 1 and monotonically decay to 0 with dependence on an environmental characteristic frequency ω_f. In the same way that Ω^{-1} can be considered a timescale of the environment, so too can ω_f^{-1}. When $f_\Omega(\omega, \Omega) = \Theta(\Omega - \omega)$, the Heaviside step function, we should obtain the results of the previous section.

As discussed above, all the terms in the master equation that are induced by the spectral density can be obtained from the first order Taylor expansion of the Laplace transform of the memory kernel, and the potential renormalisation is given by the origin of the memory kernel. With this in mind, we can generalise the method of the previous section for Ohmic spectral densities of the form given by Eq. (6.1.1). We start with the memory kernel, defined for the Ohmic class of spectral densities as

$$\mu_f(\tau) \equiv \frac{\eta}{\pi} \int_0^\infty \frac{J(\omega)}{\omega} \cos\omega\tau = \frac{\eta}{\pi} \int_0^\infty f(\omega, \omega_f) \cos\omega\tau, \tag{6.1.2}$$

and take the Laplace transform to obtain

$$\mathcal{L}\Big\{\mu_f(\tau)\Big\}(p) = \int_0^\infty \mathrm{e}^{-p\tau} \mu_f(\tau) \mathrm{d}\tau. \tag{6.1.3}$$

We then want to look at the first order expansion of the Laplace transform,

$$\mathcal{L}\Big\{\mu_f(\tau)\Big\}(p) \approx \mathcal{L}\Big\{\mu_f(\tau)\Big\}(p)|_{p=0} + p\Big(\frac{\partial}{\partial p}\mathcal{L}\Big\{\mu_f(\tau)\Big\}(p)\Big)|_{p=0}. \tag{6.1.4}$$

By doing this, we should be able to construct a master equation for each choice of cut-off function and then examine the dependence of the dynamics on the choice of cut-off function.

We have collected a "library" of cut-off functions selected from literature, which are summarised in the Table 6.1 and graphically represented in Figure 6.1. Our goal is to repeat the process of Section 5.1, for the spectral densities described by the cut-off functions in Table 6.1.

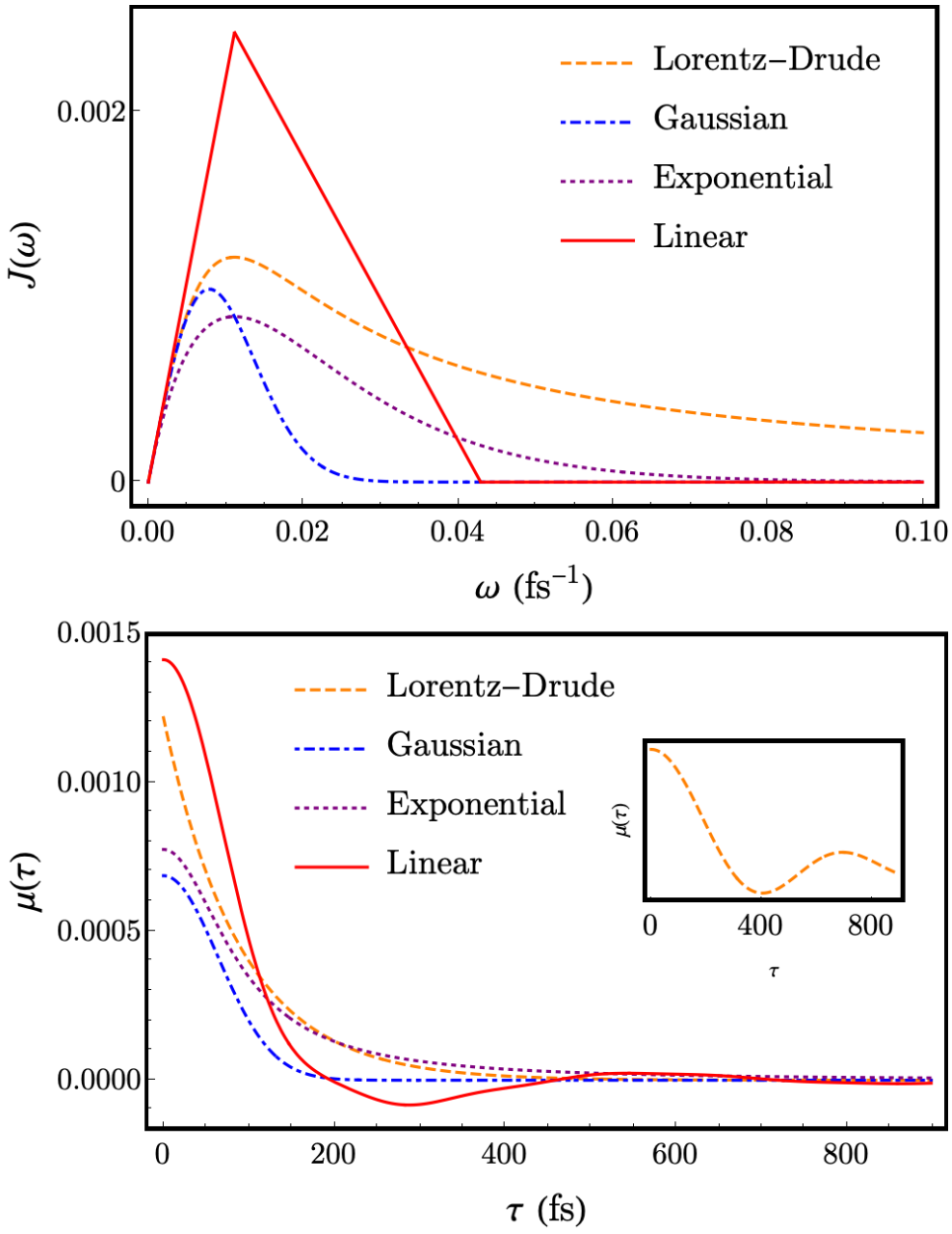

Figure 6.1: (Top) The library of spectral densities with different cut-off functions. ω is in units fs^{-1}. In each case, $\gamma = \frac{kT}{20\hbar}$, $\Omega = \frac{5kT}{6\pi\hbar}$ (such that $R_\Omega = 0.06$). (Bottom) The memory kernels corresponding to the library of cut-off functions. Inset: memory kernel corresponding to harsh cut-off function.

Type of function	Label	$f(\omega, \omega_f)$
Lorentz-Drude	LD, $\omega_f \to \omega_{\mathrm{LD}}$	$\dfrac{1}{1+\frac{\omega^2}{\omega_{\mathrm{LD}}^2}}$
Gaussian	G, $\omega_f \to \omega_{\mathrm{G}}$	$\mathrm{e}^{-\frac{\omega^2}{\omega_{\mathrm{G}}^2}}$
Linear	L, $\omega_f \to \omega_{\mathrm{L}}$	$\begin{cases} 1, & 0 < \omega < \omega_{\mathrm{L}} \\ -m + (m+1)\frac{\omega_{\mathrm{L}}}{\omega}, & < \omega_{\mathrm{L}} < \omega < \frac{(m+1)}{m}\omega_{\mathrm{L}} \\ 0, & \frac{(m+1)}{m}\omega_{\mathrm{L}} < \omega < \infty, \end{cases}$
Exponential	E, $\omega_f \to \omega_{\mathrm{E}}$	$\mathrm{e}^{-\frac{\omega}{\omega_{\mathrm{E}}}}$

Table 6.1: Library of cut-off functions considered and the labels attached to them. The Lorentz-Drude cut-off function is derived from the Drude model of electrons. The linear cut-off has an additional degree of freedom m; this characterises the speed of linear decay.

6.1.1 Lorentz-Drude Cut-Off

The Lorentz-Drude cut-off function [9, 75, 163] is derived from the Drude model of electrical conduction, sometimes called the Lorentz-Drude model, which predicts an electrical conductivity [164] with real part

$$\sigma(\omega) = \frac{\omega_0}{1+\omega^2\tau^2}. \tag{6.1.5}$$

The Lorentz-Drude cut-off is correspondingly given by

$$f_{\mathrm{LD}}(\omega, \omega_{\mathrm{LD}}) = \frac{1}{1+\frac{\omega^2}{\omega_{\mathrm{LD}}^2}}, \tag{6.1.6}$$

in analogue with the Lorentz-Drude conductivity.

We begin the process outlined in the previous section by calculating the memory kernel,

$$\begin{aligned} \mu_{\mathrm{LD}}(\tau) &= \frac{\eta}{\pi}\int_0^\infty \frac{1}{1+\frac{\omega^2}{\omega_{\mathrm{LD}}^2}}\cos\omega\tau \mathrm{d}\omega \\ &= \frac{\eta\omega_{\mathrm{LD}}}{2}\mathrm{e}^{-\omega_{\mathrm{LD}}\tau}. \end{aligned} \tag{6.1.7}$$

Taking the Laplace transform of this gives

$$\mathcal{L}\Big\{\mu_{\mathrm{LD}}(\tau)\Big\}(p) = \frac{\eta\omega_{\mathrm{LD}}}{2}\frac{1}{p+\omega_{\mathrm{LD}}}, \tag{6.1.8}$$

and taking the first order Taylor expansion in orders of p/ω_{LD}, we obtain

$$\mathcal{L}\Big\{\mu_{\mathrm{LD}}(\tau)\Big\}(p) \approx \frac{\eta}{2} - \frac{\eta}{2\omega_{\mathrm{LD}}}p. \tag{6.1.9}$$

This is strikingly similar to the result for the harsh cut-off, given by Eq. (6.0.1), if the harsh cut-off frequency is rescaled to $\widetilde{\Omega}_{\mathrm{LD}} = \frac{2\omega_{\mathrm{LD}}}{\pi}$. We can use this re-scaling of the frequency to directly obtain the master equation

$$\begin{aligned}\frac{\partial}{\partial t}\rho(x,y,t) =& \hat{L}_M\rho(x,y,t) \\ &+ \frac{\gamma}{2\omega_{\mathrm{LD}}}\Big[- \frac{4ikT}{\hbar}(x-y)\left(\frac{\partial}{\partial x} + \frac{\partial}{\partial y}\right) - \frac{i}{2\hbar}(x-y)\left(\frac{\partial \mathrm{V}_R}{\partial x} + \frac{\partial \mathrm{V}_R}{\partial y}\right) \\ &- 2\gamma(x-y)\left(\frac{\partial}{\partial x} - \frac{\partial}{\partial y}\right)\Big]\rho(x,y,t)\end{aligned} \tag{6.1.10}$$

for the Lorentz-Drude cut-off for the Ohmic spectral density. This is obtained by following the derivation presented in the previous section, with the substitution $\Omega \to \tilde{\Omega}_{\mathrm{LD}}$. We also obtain

$$\mu_{\mathrm{LD}}(0) = \frac{\eta\omega_{\mathrm{LD}}}{2} = \frac{\eta\tilde{\Omega}_{\mathrm{LD}}}{\pi}. \tag{6.1.11}$$

for the term that will renormalise the potential. Again, we note that this is equivalent to the result for the harsh cut-off with the frequency rescaled to $\tilde{\Omega}_{\mathrm{LD}}$.

This means that the Lorentz-Drude cut-off function induces Markovian Caldeira-Leggett dynamics, contained in the $\frac{\eta}{2}$ term, as well as non-Markovian dynamics of the same form as the harsh cut-off spectral density, with an effective frequency rescaling. The only effect of the cut-off function is to change the coefficient of the non-Markovian dynamics by a constant factor. Therefore, the Lorentz-Drude spectral density with characteristic frequency ω_{LD} is equivalent to the harsh cut-off spectral density with cut-off frequency $\frac{2\omega_{\mathrm{LD}}}{\pi}$.

6.1.2 Gaussian cut-off function

For the Gaussian cut-off function [56],

$$f_{\mathrm{G}}(\omega,\omega_{\mathrm{G}}) = \exp\{-\omega^2/\omega_{\mathrm{G}}^2\}, \tag{6.1.12}$$

we obtain the memory kernel

$$\begin{aligned}\mu_{\mathrm{G}} &= \frac{\eta}{\pi}\int_0^\infty \mathrm{e}^{-\omega^2/\omega_{\mathrm{G}}^2}\cos\omega\tau\mathrm{d}\omega \\ &= \frac{\eta\omega_{\mathrm{G}}}{2\sqrt{\pi}}\mathrm{e}^{-\omega_{\mathrm{G}}^2\tau^2/4},\end{aligned} \tag{6.1.13}$$

which has Laplace transform

$$\mathcal{L}\Big\{\mu_{\mathrm{G}}(\tau)\Big\}(p) = \frac{\pi}{2}\mathrm{e}^{p^2/\omega_{\mathrm{G}}^2}\int_{\frac{p}{\omega_{\mathrm{G}}}}^\infty \mathrm{e}^{-t^2}\mathrm{d}t. \tag{6.1.14}$$

We can use the Leibniz integral rule and take the first order expansion in p/ω_{G} to obtain

$$\mathcal{L}\Big\{\mu_{\mathrm{G}}(\tau)\Big\}(p) \approx \frac{\eta}{2} - \frac{\eta}{\sqrt{\pi}\omega_{\mathrm{G}}}p. \tag{6.1.15}$$

In this case, we again recover the harsh cut-off case (Eq. (6.0.1)) with a rescaled frequency $\widetilde{\Omega}_{\mathrm{G}} = \frac{1}{\sqrt{\pi}}\omega_{\mathrm{G}}$, meaning that we can write down the master equation:

$$\begin{aligned}\frac{\partial}{\partial t}\rho(x,y,t) =& \hat{L}_M\rho(x,y,t) \\ &+ \frac{\gamma}{\sqrt{\pi}\omega_{\mathrm{G}}}\Big[-\frac{4ikT}{\hbar}(x-y)\left(\frac{\partial}{\partial x}+\frac{\partial}{\partial y}\right) - \frac{i}{2\hbar}(x-y)\left(\frac{\partial \mathrm{V}_R}{\partial x}+\frac{\partial \mathrm{V}_R}{\partial y}\right) \\ &- 2\gamma(x-y)\left(\frac{\partial}{\partial x}-\frac{\partial}{\partial y}\right)\Big]\rho(x,y,t).\end{aligned} \tag{6.1.16}$$

Once again, this is the harsh cut-off equation with rescaled frequency. We can also find the potential renormalisation to be

$$\mu_{\mathrm{G}}(0) = \frac{\eta}{2\sqrt{\pi}}\omega_{\mathrm{G}}. \tag{6.1.17}$$

However, in this case, this is not equal to $\frac{\eta\tilde{\Omega}_{\mathrm{G}}}{\pi}$.

6.1.3 Linear cut-off function

The linear cut-off function

$$f(\omega,\omega_{\mathrm{L}}) = \begin{cases} 1, & 0<\omega<\omega_{\mathrm{L}} \\ -m+(m+1)\frac{\omega_{\mathrm{L}}}{\omega}, & <\omega_{\mathrm{L}}<\omega<\frac{(m+1)}{m}\omega_{\mathrm{L}} \\ 0, & \frac{(m+1)}{m}\omega_{\mathrm{L}}<\omega<\infty, \end{cases} \tag{6.1.18}$$

is defined piece-wise, but as in the previous cases we can still define a memory kernel. In this case, we obtain

$$\begin{aligned}\mu_{\mathrm{L}}(\tau) &= \frac{\eta}{\pi}\int_0^{\omega_{\mathrm{L}}}\cos\omega\tau\mathrm{d}\omega - \frac{\eta m}{\pi}\int_{\omega_{\mathrm{L}}}^{\frac{(m+1)}{m}\omega_{\mathrm{L}}}\cos\omega\tau\mathrm{d}\omega + \frac{\eta(m+1)}{\pi}\omega_{\mathrm{L}}\int_{\omega_{\mathrm{L}}}^{\frac{(m+1)}{m}\omega_{\mathrm{L}}}\frac{\cos\omega\tau}{\omega}\mathrm{d}\omega.\\ &= \frac{\eta(1+m)}{\pi}\frac{\sin\omega_{\mathrm{L}}\tau}{\tau} - \frac{\eta m}{\pi}\frac{\sin\frac{(m+1)}{m}\omega_{\mathrm{L}}\tau}{\tau} + \frac{\eta(m+1)}{\pi}\omega_{\mathrm{L}}\Big(\mathrm{Ci}[\frac{m+1}{m}\omega_{\mathrm{L}}\tau] - \mathrm{Ci}[\omega_{\mathrm{L}}\tau]\Big),\end{aligned} \tag{6.1.19}$$

with $\mathrm{Ci}[x]$ the cosine integral function. We proceed to the Laplace transform,

$$\begin{aligned}\mathcal{L}\Big\{\mu_{\mathrm{L}}(\tau)\Big\}(p) =& \frac{\eta(1+m)}{\pi}(\frac{\pi}{2} - \arctan\frac{p}{\omega_{\mathrm{L}}}) - \frac{\eta m}{\pi}(\frac{\pi}{2} - \arctan\frac{m}{(m+1)}\frac{p}{\omega_{\mathrm{L}}})\\ &-\frac{\eta(m+1)}{\pi}\omega_{\mathrm{L}}\frac{\ln\left(\frac{m^2p^2}{(m+1)^2\omega_{\mathrm{L}}^2}+1\right) - \ln\left(\frac{p^2}{\omega_{\mathrm{L}}^2}+1\right)}{2p},\end{aligned} \tag{6.1.20}$$

which can be expanded (using the reciprocal arctan relation) to first order in p/ω_{L} as

$$\mathcal{L}\Big\{\mu_{\mathrm{L}}(\tau)\Big\}(p) \approx \frac{\eta}{2} - \frac{\eta}{2\pi}\frac{2m+1}{m+1}\frac{p}{\omega_{\mathrm{L}}}. \tag{6.1.21}$$

In the limit of $m \to \infty$, we obtain exactly the harsh cut-off result, and in the finite m case we once again obtain Eq. (6.0.1) - the harsh cut-off master equation - with frequency re-scaled to $\widetilde{\Omega}_{\mathrm{L}} = \frac{2(m+1)}{2m+1}\omega_{\mathrm{L}}$. We calculate that the potential is renormalised by

$$\mu_{\mathrm{L}}(0) = \frac{\eta(m+1)}{\pi}\omega_{\mathrm{L}}\log\Big(\frac{m+1}{m}\Big). \tag{6.1.22}$$

This is approximately equal to $\frac{\eta\tilde{\Omega}_{\mathrm{L}}}{\pi}$ for all values of m excepting those very close to 0. So in the case $m > 0$, the potential renormalisation also tends to the harsh cut-off expression with rescaled frequency.

6.1.4 Exponential cut-off function

Let us consider one more cut-off function: $f(\omega, \omega_{\mathrm{E}}) = \mathrm{e}^{-\omega/\omega_E}$ [163, 165, 166], common in the quantum optical regime [9]. We perform the usual procedure, starting with the evaluation of

the memory kernel

$$\begin{aligned}\mu_{\mathrm{E}}(\tau) &= \frac{\eta}{\pi}\int_0^\infty \mathrm{e}^{-\frac{\omega}{\omega_{\mathrm{E}}}}\cos\omega\tau\mathrm{d}\omega \\ &= \frac{\eta}{\pi}\frac{\omega_{\mathrm{E}}}{1+\omega_{\mathrm{E}}^2\tau^2}.\end{aligned} \tag{6.1.23}$$

When we attempt to take the Laplace transform, we find it is expressed in terms of the sine and cosine integrals,

$$\begin{aligned}\mathcal{L}\Big\{\mu_{\mathrm{E}}(\tau)\Big\}(p) &= \frac{\eta}{\pi}\int_0^\infty \mathrm{e}^{-p\tau}\frac{\omega_{\mathrm{E}}}{1+\omega_{\mathrm{E}}^2\tau^2}\mathrm{d}\tau \\ &= \frac{\eta}{\pi}\Big(-\sin\frac{p}{\omega_{\mathrm{E}}}\int_{\frac{p}{\omega_{\mathrm{E}}}}^\infty \frac{\cos t}{t}\mathrm{d}t + \cos\frac{p}{\omega_{\mathrm{E}}}\int_0^\infty \frac{\sin t}{t}\mathrm{d}t\Big).\end{aligned} \tag{6.1.24}$$

However, taking the expansion in p/ω_{E} leads to a problem: the cosine integral term is divergent at the origin. Although this is regulated by the sine term in the zeroth order of the expansion, it causes a divergence in the first order. We are unable to obtain a master equation for this cut-off in the same way as for the others we have considered. This is interesting, as exponential decay is numerically very similar to Gaussian decay. It is important for us to understand where this divergency comes from, and what it tells us about the choice of cut-off function and its physical significance.

Despite the issues we have identified with the exponential cut-off function, it is a popular choice in the literature of authors wishing to select a realistic Ohmic spectral density [102, 165, 167–169]. It will be discussed in the next section what the implications of the divergency arising from this cut-off function are.

6.2 Effect of a General Cut-Off Function

We have obtained an interesting pattern, with one notable exception. However, it would be wise to construct a convincing argument that this should be true for all sensible cut-off functions - as well as some criteria that must be fulfilled to make a cut-off function "sensible". We would also like to be able to characterise the rescaling of the frequency. Our hypothesis is that, for a sensible choice of cutoff function $f(\omega, \omega_f)$, the first order Taylor expansion of the Laplace

transform should read

$$\mathcal{L}\Big\{\mu_f(\tau)\Big\}(p) \approx \frac{\eta}{2} - \frac{\eta}{\pi\tilde{\Omega}}p, \tag{6.2.1}$$

where $\tilde{\Omega}$ is an expression which is dependent on the specific choice of $f(\omega, \omega_f)$.

We can take the Laplace transform of a general memory kernel,

$$\mathcal{L}\Big\{\mu_f(\tau)\Big\}(p) = \frac{\eta}{\pi}\int_0^\infty \mathrm{e}^{-p\tau}\int_0^\infty f(\omega,\omega_f)\cos\omega\tau\mathrm{d}\omega\mathrm{d}\tau. \tag{6.2.2}$$

Changing the order of integration using Fubini's theorem, we re-write this as

$$\mathcal{L}\Big\{\mu_f(\tau)\Big\}(p) = \frac{\eta}{\pi}\int_0^\infty \frac{p}{p^2+\omega^2}f(\omega,\omega_f)\mathrm{d}\omega. \tag{6.2.3}$$

Using integration by parts gives us

$$\mathcal{L}\Big\{\mu_f(\tau)\Big\}(p) = -\frac{\eta}{\pi}\int_0^\infty f'(\omega,\omega_f)\arctan\Big(\frac{\omega}{p}\Big)\mathrm{d}\omega. \tag{6.2.4}$$

Again, we take advantage of the reciprocal property of the arctan function to write

$$\mathcal{L}\Big\{\mu_f(\tau)\Big\}(p) = -\frac{\eta}{2}\int_0^\infty f'(\omega,\omega_f)\mathrm{d}\omega + \frac{\eta}{\pi}\int_0^\infty f'(\omega,\omega_f)\arctan\Big(\frac{p}{\omega}\Big)\mathrm{d}\omega \tag{6.2.5}$$

So far, all of these results are exact. We can even evaluate the first term in the equality by noticing it is the integral of a derivative to obtain

$$-\frac{\eta}{2}\int_0^\infty f'(\omega,\omega_f)\mathrm{d}\omega = \frac{\eta}{2}. \tag{6.2.6}$$

We do not need to evaluate the second term exactly and just need to look at the zeroth and first order terms in p.

What a (first order) Taylor expansion of this integral actually entails is the evaluation of the limits

$$\frac{\eta}{\pi}\lim_{p\to 0}\int_0^\infty f'(\omega,\omega_f)\arctan\Big(\frac{p}{\omega}\Big)\mathrm{d}\omega$$

and

$$\frac{\eta}{\pi}\lim_{p\to 0}\frac{\partial}{\partial p}\int_0^\infty f'(\omega,\omega_f)\arctan\Big(\frac{p}{\omega}\Big)\mathrm{d}\omega.$$

To avoid actually doing these integrals in their current form, we want to exchange the order of limit and integration. This will vastly simplify the integration. The conditions for us to be able to exchange the limit and integral in each case should be the same, as a derivative can be considered a special case of a limit. We turn to the dominated convergence theorem [170], which allows the interchange of limits and integrals under the condition that the integrand is bounded by an integrable function. So, we need to ascertain whether

$$|f'(\omega,\omega_f)\arctan\Big(\frac{p}{\omega}\Big)|$$

is bounded by an integrable function in the domain $[0,\infty]$. We know that the arctan function is bounded in the range $[0,\frac{\pi}{2}]$, and we know that $f'(\omega,\omega_f)$ is an integrable function (because it is a derivative). So the integrand is in fact bounded by the integrable function

$$\frac{\pi}{2}f'(\omega,\omega_f),$$

and we can perform the limit-integral interchange. Therefore, we write down that

$$\begin{aligned}\frac{\eta}{\pi}\lim_{p\to 0}\int_0^\infty f'(\omega,\omega_f)\arctan\Big(\frac{p}{\omega}\Big)\mathrm{d}\omega &= \frac{\eta}{\pi}\int_0^\infty f'(\omega,\omega_f)\lim_{p\to 0}\arctan\Big(\frac{p}{\omega}\Big)\mathrm{d}\omega\\ &= 0,\end{aligned} \tag{6.2.7}$$

and

$$\begin{aligned}\frac{\eta}{\pi}\lim_{p\to 0}\frac{\partial}{\partial p}\int_0^\infty f'(\omega,\omega_f)\arctan\Big(\frac{p}{\omega}\Big)\mathrm{d}\omega &= \frac{\eta}{\pi}\int_0^\infty f'(\omega,\omega_f)\lim_{p\to 0}\frac{\partial}{\partial p}\arctan\Big(\frac{p}{\omega}\Big)\mathrm{d}\omega\\ &= \frac{\eta}{\pi}\int_0^\infty \frac{f'(\omega,\omega_f)}{\omega}\mathrm{d}\omega.\end{aligned} \tag{6.2.8}$$

Substituting these results back into the Laplace transform, we obtain

$$\mathcal{L}\Big\{\mu_f(\tau)\Big\}(p)\approx\frac{\eta}{2}+\frac{\eta p}{\pi}\int_0^\infty\frac{f'(\omega,\omega_f)}{\omega}\mathrm{d}\omega. \tag{6.2.9}$$

The second term can be evaluated a little further. If we consider that all the cut-off functions we have considered have been dependent on the characteristic frequency as a ratio, $f(\omega, \omega_f) = f(\omega/\omega_f)$, then we can write the integral part of the second term as

$$\int_0^\infty \frac{f'(\frac{\omega}{\omega_f})}{\omega} \mathrm{d}\omega = \frac{1}{\omega_f} \int_0^\infty \frac{f'(u)}{u} \mathrm{d}u, \tag{6.2.10}$$

where $u = \frac{\omega}{\omega_f}$ is the substitution used to define the dummy variable u. Therefore,

$$\mathcal{L}\Big\{\mu_f(\tau)\Big\}(p) \approx \frac{\eta}{2} + \frac{\eta}{\pi\omega_f}\Big(\int_0^\infty \frac{f'(u)}{u}\mathrm{d}u\Big)p. \tag{6.2.11}$$

This is exactly the result we were looking for; we have shown that (to first order in the expansion of p/ω_f, the choice of cut-off function affects the dynamics up to a constant multiplicative factor defined by

$$\int_0^\infty \frac{f'(u)}{u} \mathrm{d}u. \tag{6.2.12}$$

In fact, by comparing Eq. (6.2.11) to Eq. (6.0.1) we can say that the master equation given by Eq. (5.1.33) is valid for all appropriate cut-off functions, with the scaled frequency

$$\tilde{\Omega_f} = -\frac{1}{\int_0^\infty \frac{f'(u)}{u}\mathrm{d}u}\omega_f. \tag{6.2.13}$$

To be specific, we obtain the master equation

$$\begin{aligned}\frac{\partial}{\partial t}\rho(x,y,t) =& \hat{L}_M\rho(x,y,t) \\ &+ \frac{\gamma}{\pi\tilde{\Omega}}\Big[-\frac{4ikT}{\hbar}(x-y)\left(\frac{\partial}{\partial x}+\frac{\partial}{\partial y}\right) - \frac{i}{2\hbar}(x-y)\left(\frac{\partial \mathrm{V}_R}{\partial x}+\frac{\partial \mathrm{V}_R}{\partial y}\right) \\ &- 2\gamma(x-y)\left(\frac{\partial}{\partial x}-\frac{\partial}{\partial y}\right)\Big]\rho(x,y,t).\end{aligned} \tag{6.2.14}$$

It is worth noting that the negative sign in the definition of $\tilde{\Omega}$ is not surprising; we require that $f(\omega, \omega_f)$ is a monotonically decreasing function - and therefore it will have a negative derivative. The two negative contributions mean the rescaled frequency is always positive.

Now, let us refine what we mean when we say "appropriate cut-off functions". After evaluating the Laplace transform, we have a good condition for constraining the choice of cut-off function: we require that the integral in Eq. (6.2.12) is finite. To avoid a pole at the origin, we

require that the limit $\lim_{u\to 0}\frac{f'(u)}{u}$ is well-defined. We can see from the conditions of L'Hopital's rule that this will only converge when $f'(0) = 0$ (when the cut-off function has a stationary point at the origin). To ensure convergence at the upper limit of the integral, we also require

$$\lim_{u\to\infty} f'(u) = 0. \tag{6.2.15}$$

We have already specified that we want the cut-off function to asymptotically tend to 0 as $u \to \infty$, so this criteria is automatically fulfilled.

Looking back at the exponential cut-off function, $f(u) = \mathrm{e}^{-u}$, we obtained a memory kernel Laplace transform that did not have a finite Taylor expansion. We can see from this approach that this is due to the behaviour of the first derivative of the cut-off function at the origin where there is no stationary point. This now makes intuitive sense: the framework we are using is essentially an expansion around the Markovian dynamics. Therefore, the behaviour of the cut-off function for $\omega \ll \omega_f$ is important, as this should represent the Markovian regime. Essentially, we require the approximation

$$J(\omega) = \eta\omega f(\omega/\omega_f) \approx \eta\omega \tag{6.2.16}$$

to hold for $\omega < \omega_f$. That is, there should be a significant domain of ω for which the dynamics is essentially Markovian. When we take the Taylor expansion of the cut-off function, we write

$$J(\omega) = \eta\omega\Big(1 + f'(0)\frac{\omega}{\omega_f} + \frac{1}{2}f''(0)\frac{\omega^2}{\omega_f^2} + \ldots\Big). \tag{6.2.17}$$

The condition $f'(0) = 0$ means that the $\eta\omega$ term dominates for a bigger range of ω. This is because the condition $\omega^2 < \omega_f^2$ is stronger than the condition $\omega < \omega_f$. So in the case where $f'(0) = 0$, we can say with confidence that we are expanding around Markovian dynamics, and that there is a domain of ω that we can call the Markovian regime. In essence, we require that the spectral density is Markovian in the first order, and only admits non-Markovian corrections in the second order. The exponential cut-off function does not fulfil this, because $f'_{\mathrm{E}}(0) \neq 0$, and there is no clear Markovian regime for us to expand around. For authors who are not relying on an expansion around Markovian behaviour, e.g. the quantum optical community [9], the exponential cut-off will not pose the same issues as here. Therefore, we do not have to be

worried about any inconsistencies between this work and other approaches with regard to the exponential cut-off.

In two of the cases we considered - the harsh cut-off and the linear cut-off cases - we have used a piecewise definition of the cut-off function. This means we need to be careful about using a derivative argument, because it is not continuous everywhere. However, we simply split the integral in the domain $[0, \infty]$ into a sum of integrals with appropriate limits. Additionally, in both of these cases, the cut-off function is 1 for the domain $[0, \omega_f]$. This means we have a clearly defined Markovian regime, which is the condition we have just discussed. Therefore, there is no need to worry about choosing piecewise cut-off functions, as long as they satisfy the other conditions.

Finally, we should check that Eq. (6.2.13) is consistent with previous calculations, e.g. that we obtain the same scaled frequencies. The scaled frequency we want to calculate is

$$\tilde{\Omega}_f = -\frac{\omega_f}{\int_0^\infty \frac{f'(u)}{u} \mathrm{d}u}. \tag{6.2.18}$$

The results are presented in Table 6.2; we can see that in all cases the integral returns the rescaled frequency from our original calculations. Our method is consistent.

Cut-off Function	Rescaled Frequency Integral	Rescaled Frequency
Lorentz-Drude	$\tilde{\Omega}_{\mathrm{LD}} = -\frac{1}{\int_0^\infty -\frac{2}{(1+u^2)^2}\mathrm{d}u}\omega_{\mathrm{LD}}$	$\frac{2}{\pi}\omega_{\mathrm{LD}}$
Gaussian	$\tilde{\Omega}_{\mathrm{G}} = -\frac{1}{\int_0^\infty -2\mathrm{e}^{-u^2}\mathrm{d}u}\omega_{\mathrm{LD}}$	$\frac{1}{\sqrt{\pi}}\omega_{\mathrm{G}}$
Linear	$\tilde{\Omega}_{\mathrm{L}} = -\frac{1}{-\int_1^{(m+1)/m} \frac{m+1}{u^3}\mathrm{d}u}\omega_{\mathrm{L}}$	$\frac{2(m+1)}{2m+1}\omega_{\mathrm{L}}$

Table 6.2: Rescaled frequencies for the library of cut-off functions, using the integral result we derived. The exponential is omitted as the integral is not convergent.

6.2.1 Potential Renormalisation

Another important effect of the spectral density is to renormalise the potential by the subtraction of a harmonic term with frequency $\mu(0) = (\Delta\omega)^2$. We can express this using the cut-off

function as

$$\mu(0) = \frac{\eta\omega_f}{\pi}\int_0^\infty f(u)\mathrm{d}u. \tag{6.2.19}$$

We refer to this as "renormalising the potential", following the terminology of the Caldeira-Leggett quantum Brownian motion model [31]. More specifically and say that the environment induces a change in the potential that is equal to the subtraction of a harmonic term with frequency $\Delta\omega$, i.e.

$$V_R(x) = V(x) - \frac{1}{2}M(\Delta\omega)^2x^2. \tag{6.2.20}$$

As discussed in the previous section, the potential renormalisation in the original Caldeira-Leggett model is usually removed via a counter-term in the Lagrangian, because it is understood to arise from the physically unrealistic infinite bath. In that case, the potential is renormalised by the *infinite* frequency, Ω. In our case, there is no such issue arising from including arbitrarily strong coupling to infinite frequencies - especially in the harsh cut-off or linear cut-off cases - and therefore, the potential renormalisation must be retained.

It is worth noting that the amount by which a harmonic frequency is rescaled is proportional to the cut-off frequency ω_f. When the Markovian limit $\omega_f \to 0$ limit is taken, this will once again become infinite in the manner of the Caldeira-Leggett potential renormalisation.

6.2.2 Effect of the Rescaling

We have shown in the previous sections that, up to a rescaling of the frequency, all Ohmic spectral densities with appropriately defined cut-off values produce the same dynamics. We have also shown that in the Markovian limit $\omega_f \gg \gamma$, the Markovian Caldeira-Leggett dynamics are recovered. Therefore, the inclusion of a cut-off into the Ohmic spectral density does not immediately guarantee non-Markovian dynamics. It is also necessary that the limit $\omega_f \gg \gamma$ is relaxed to $\omega_f > \gamma$ in order to keep at least first order terms in the expansion in $\frac{\gamma}{\omega_f}$.

The choice of cut-off function affects the dynamics only be rescaling the harsh cut-off non-Markovianity factor, and in most cases the rescaling is of order unity. For example, a harsh cut-off function with characteristic frequency Ω induces a non-Markovianity factor $R_\Omega = \frac{\gamma}{\pi\Omega}$, whereas a Lorentz-Drude cut-off function with the same characteristic frequency induces non-Markovianity factor $R_{\mathrm{LD}} = \frac{\gamma}{2\Omega} = \frac{\pi}{2}R_\Omega$. For the Gaussian case, we obtain $R_{\mathrm{G}} = \sqrt{\pi}R_\Omega$. Figure

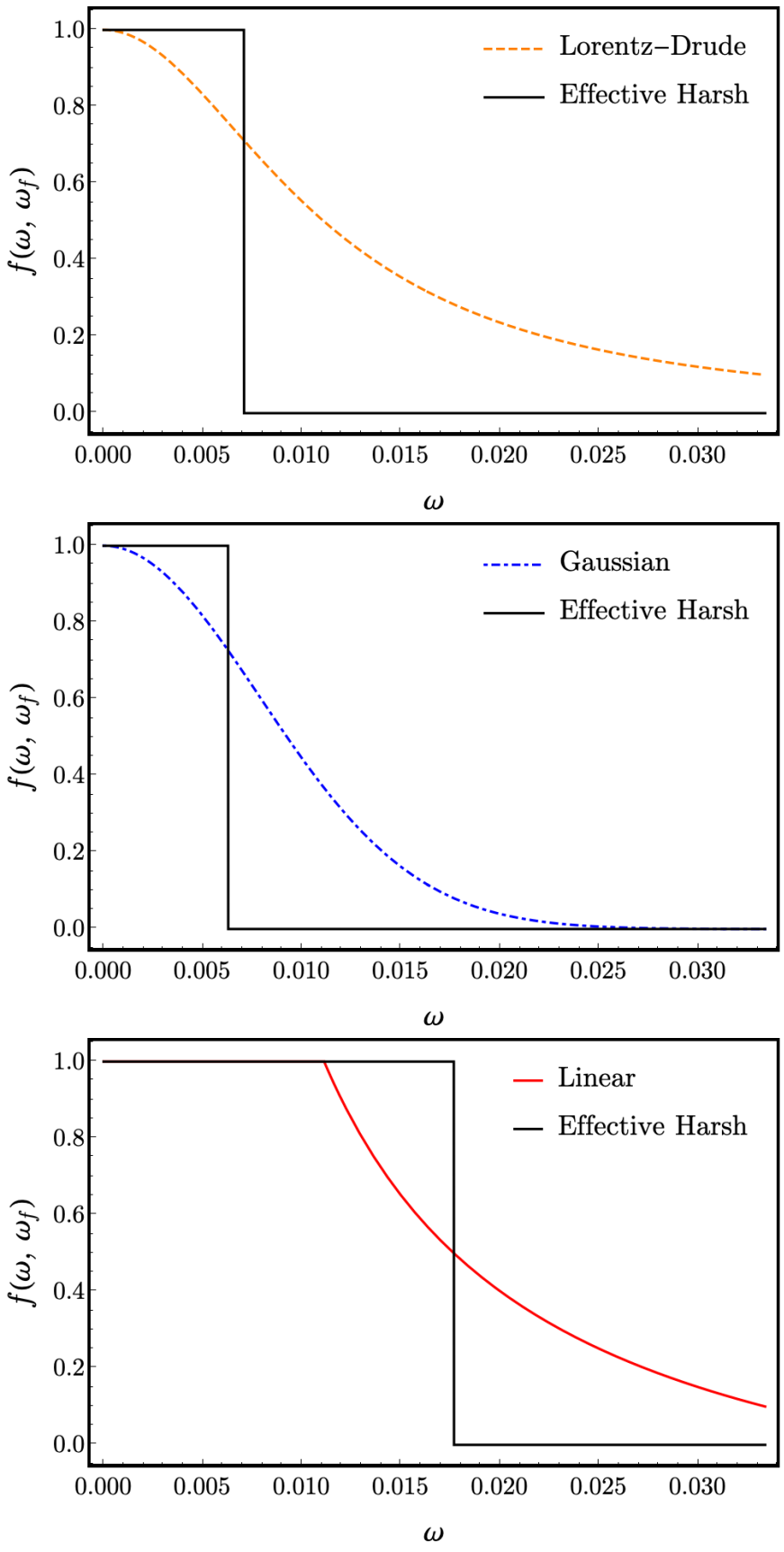

Figure 6.2: Each of the cut-off functions in our library compared to the step function that they are effectively equivalent to. ((Top) Lorentz-Drude, (Middle) Gaussian, (Bottom) Linear). In each case, the characteristic frequency is $\omega_f = \frac{5kT}{6\pi\hbar}$.

6.2 demonstrates each cut-off function (with the same cut-off frequency) compared to the harsh cut-off function to which it is effectively equal.

6.2.3 Relationship to Literature

This work is not the first to identify that the cut-off function of an Ohmic spectral density does not significantly affect the dynamics [56, 121]. However, Refs. [56, 121] have made this observation with no attempt to justify it. By using the framework described in the previous section, we have provided the first model-dependent justification of this phenomenon. This is not a particularly general result, as we are limited by the perturbative expansion approach we have used. This is evident in the consideration of the exponential cut-off; we find divergences when we attempt to find corrections to the Markovian dynamics, whereas quantum optics approaches [9] which absorb the spectral density into a number operator do not have the same issues. So our conclusion should be stated as follows: in the Markovian limit, all Ohmic spectral baths are equivalent, and in the leading order perturbative non-Markovian expansion, all Ohmic spectral baths are equivalent up to a frequency re-scaling.

The question we have explored here - what is the dependence of the final dynamics on the form of the spectral density? - has been explored by other authors in different contexts. In the Langevin framework, a paper by Spiechowicz and Luczka [171] explores the effect of the spectral density on the $T = 0$K dynamics. This work discusses the importance of the dissipation function - equivalent to what we have called the memory kernel - on the zero-point energy of a free particle in a thermal bath. The primary conclusion is that the zero-point energy depends solely on the cut-off function and the dimensionless parameter $c = \eta/m\omega_c^2$. One point raised in this paper is that the correlation function of the environment thermal noise, defined at $T = 0$ as

$$C(t) = \int_0^\infty \frac{\hbar}{2} J(\omega) \cos \omega t \, \mathrm{d}\omega, \tag{6.2.21}$$

is key to determining the variance of the noise, defined as $C(0)$. The corresponding high-temperature correlation function is just the memory kernel multiplied by the temperature;

$$C_T(t) = k_b T \mu(t). \tag{6.2.22}$$

This means that the significance of $\mu(0)$ is not limited to the potential renormalisation; it

determines the variance of the thermal noise, $F(t)$. Therefore, we can say that

$$\langle F^2(t)\rangle = \frac{2m\gamma kT}{\hbar}\int_0^\infty f(\omega,\omega_c)\mathrm{d}\omega. \tag{6.2.23}$$

This point is also discussed in Ref. [172]: the potential renormalisation, dependent on the cut-off function, can also be interpreted as a mass renormalisation effect. This feature is usually not considered to be of much interest, but in some cases the renormalised mass can become negative. This effect can become significant at low temperatures, which are outside the regime we are interested in.

A paper by Fraga et al [143] looks at the same problem, i.e. non-Markovian quantum Brownian motion with a spectral density of the form $J(\omega) = \eta\omega f(\omega,\omega_c)$, from the point of view of a Langevin equation analysis. In fact, the same cut-off functions are considered (harsh cut-off, exponential cut-off, Gaussian cut-off, and Lorentzian cut-off). They find that the Langevin equation for the system is

$$m\ddot{x} + \bar{\mathrm{V}}'(x) + 2\eta\int_0^t \mathrm{d}t'\mu_f(t-t')\dot{x}(t') = F(t), \tag{6.2.24}$$

with the modified potential

$$\bar{\mathrm{V}}'(x) = \mathrm{V}'(x) - 2\eta\mu_f(0)x(t). \tag{6.2.25}$$

However, the specific dependence of the cut-off is not probed: the authors conclude that the physics is much more dependent on the value of ω_c than the form of $f(\omega,\omega_c)$.

6.3 Connection to Renormalisation Group Approaches

As discussed in Section 3.4, renormalisation group approaches are often employed to deal with high-frequency cut-offs, or other scaling problems that involve making a choice of frequency or scale. It is common to apply this logic to the Caldeira-Leggett model by introducing a counter-term into the Lagrangian that removes the potential renormalisation from the contributions of infinitely high frequency oscillators [9]. We shall tentatively propose that the frequency rescaling we have observed is, in fact, a renormalisation group effect. The cut-off functions we have considered can be crudely approximated by a harsh, or step, cut-off function (at a rescaled

frequency), as demonstrated by Figure 6.2. The further you "zoom out" (i.e. lose resolution in the spectral density) the better this approximation will be.

6.3.1 Scope for application to our system

Previous attempts to apply renormalisation techniques [120, 121] have focused on the low-temperature tunnelling model, which usually considers a symmetric or nearly-symmetric double-well potential [103]. The approach used in the treatment of this model is different from that used in the quantum Brownian motion model, as it considers the density matrix $\rho(q, q', T)$ of a system trajectory from $q' = q(0)$ to $q = q(\tau)$. In general, the trajectory description is set up to describe either the presence or absence of tunnelling in the double well. The goal is to calculate a tunnelling rate, rather than derive a master equation, and therefore neither the results nor the process are directly comparable to the derivation of the non-Markovian master equation that underpins this work. The differences are manifest in the description of the action; in the low-temperature tunnelling model it is written down as

$$S_{\text{eff}} = \int \Big(\frac{1}{2}M\dot{q}^2 + V(q)\Big)\mathrm{d}\tau + \frac{1}{2}\int \mathrm{d}\tau\, \mathrm{d}\tau' \alpha(\tau - \tau')[q(\tau) - q(\tau')], \tag{6.3.1}$$

with

$$\alpha(\tau - \tau') = \sum_j \frac{C_j^2}{4m_j\omega_j} \mathrm{e}^{-\omega_j|\tau - \tau'|}. \tag{6.3.2}$$

Contrasting this to the corresponding expressions from the quantum Brownian motion Caldeira-Leggett model [31],

$$\begin{aligned} S_{\text{eff}} = \int \Big(\frac{1}{2}M\dot{x}^2 + V(x)\Big)\mathrm{d}\tau - \int \Big(\frac{1}{2}M\dot{y}^2 + V(y)\Big)\mathrm{d}\tau \\ -i\int \mathrm{d}\tau\, \mathrm{d}\tau' [x(\tau) - y(\tau)][\alpha(\tau - \tau')x(\tau') - \alpha^*(\tau - \tau')y(\tau')], \end{aligned} \tag{6.3.3}$$

with

$$\alpha(\tau - \tau') = \sum_k \frac{C^k}{2m\omega_k}\Big(\mathrm{e}^{-i\omega_k(\tau - \tau')} + \frac{\mathrm{e}^{-i\omega_k(\tau - \tau')} + \mathrm{e}^{i\omega_k(\tau - \tau')}}{\mathrm{e}^{\frac{\hbar\omega_k}{kT}} - 1}\Big), \tag{6.3.4}$$

we see that it is different not only in details (i.e. the form of the kernel, $\alpha(\tau - \tau')$), but in structure: there are contributions from the system coordinates x and y that are not separable, and we cannot straightforwardly derive a Wegner-Houghton equation (as in Eq. (3.4.14)) without further consideration on how to proceed.

For this reason, replicating the renormalisation group analyses in [120, 121] is not straightforward, and we have not attempted to do so. However, we believe that an analogous process could be carried out, with modifications made to the method where appropriate. There appear to be two options: either to understand how to express the effective action of the quantum Brownian motion Caldeira-Leggett model in a separated form, or to explore the Wegner-Houghton theory in two dimensions. It is not clear whether the quantum Brownian motion effective action can be understood as a two-dimensional field theory in the same way that the low-temperature tunnelling effective action can be understood as a one-dimensional field theory. It is also not clear what the critical phenomena of interest would be in this case, and it may well be a potential-dependent selection - i.e. by inserting a double-well potential, the transition from tunneling to no tunneling could be considered as a quantum-classical transition, with an associated critical value. In addition, previous studies have shown critical behaviour associated with the onset of non-Markovianity in two-level systems [136]. There are many interesting problems in quantum biology that can be modelled as double well tunnelling problems (see Section 1.1) and it is possible that by treating these problems as critical phenomena in the renormalisation group framework, a deeper understanding could arise.

Unfortunately, a full reckoning of this problem is beyond the scope of this thesis, and we would like to suggest that a future research project could examine the question of applying formal renormalisation group techniques to the quantum Brownian motion Caldeira-Leggett model. While the analysis presented in this Section has demonstrated that the effect of a cutoff function is to rescale - or renormalise - the frequency of an effective harsh cut-off, a renormalisation group approach could lead to further insight regarding the physical driver of this effect. Additionally, there is further scope to investigate non-Ohmic spectral densities and confirm whether any analogous relationships hold.

6.3.2 Summary of this chapter

We have generalised the master equation derivation of the previous section to include spectral densities in the so-called "Ohmic class", i.e. having the form

$$J(\omega) = \eta\omega f(\omega, \omega_f), \tag{6.3.5}$$

and we derived the general master equation

$$\begin{aligned}\frac{\partial}{\partial t}\rho(x,y,t) =&\hat{L}_M\rho(x,y,t)\\ &+\frac{\gamma}{\pi\tilde{\Omega}}\Big[-\frac{4ikT}{\hbar}(x-y)\left(\frac{\partial}{\partial x}+\frac{\partial}{\partial y}\right)-\frac{i}{2\hbar}(x-y)\left(\frac{\partial \mathrm{V}_R}{\partial x}+\frac{\partial \mathrm{V}_R}{\partial y}\right)\\ &-2\gamma(x-y)\left(\frac{\partial}{\partial x}-\frac{\partial}{\partial y}\right)\Big]\rho(x,y,t),\end{aligned} \tag{6.3.6}$$

where

$$\tilde{\Omega} = -\frac{1}{\int_0^\infty \frac{f(u)}{u}\mathrm{d}u}\omega_f. \tag{6.3.7}$$

We have determined conditions for which cut-off functions $f(\omega,\omega_f)$ are allowed, namely that $f(0)=1$, $\lim_{u\to\infty} f(u)=0$, and $f'(0)=0$.

We have also linked the renormalisation of the potential to the variance of the environment thermal noise, by referring to the paper by Spiechowicz and Luczka [171]. We find that it is determined by the integral of the cut-off function, bounded for all allowed cut-off functions.

Finally, we made some tentative links between the cut-off frequency rescaling and renormalisation techniques. Although fully exploring this connection is beyond the scope of this work, we propose that there is room for further research.

The result of this section is important, because it lends credibility to the conclusions drawn in the previous section: that a non-Markovian Ohmic bath leads to a coherence resurgence which is linked to a transient negative entropy production. When only the harsh cut-off was considered, it could have been argued that the result was due to the unrealistic bath spectral density considered. However, with the extension of this analysis to a range of spectral densities with physically realistic cut-off functions, the results are more compelling. Further work could focus on linking the magnitude of coherence resurgence, as well as the timescale at which it peaks, to the specific choice of cut-off frequency. This proposed work would provide a concrete numerical application for the results of this chapter.

Chapter 7

Discussion and Conclusions

7.1 Discussion

In this Chapter, we discuss the extent to which the hypothesis we proposed at the start of the thesis was accurate, and to what extent we achieved our aim, as well as consolidating discussion points that were raised during the research process.

7.1.1 Reviewing the Hypothesis

A major aim of this thesis was to extend the model of quantum Brownian motion to include Ohmic spectral densities representing reservoirs with physically intuitive cut-off functions. This was successfully carried out[1] in order to obtain a new master equation. The new master equation contained the original Caldeira-Leggett dynamics, as well as three new terms, each multiplied by a non-Markovianity factor, $R_\Omega = \gamma/\pi\Omega$, which we labelled orthogonal ($\hat{L}_\mathrm{O}$), potential ($\hat{L}_\mathrm{V}$), and relaxation ($\hat{L}_\mathrm{R}$) terms.

We hypothesised that this finite bath correction would introduce non-Markovianity into the system, and have shown that this hypothesis was correct. The non-Markovianity is evident in several ways: in the kernel structure of the propagator, which no longer contains δ-functions, in the finite bath size represented by the inclusion of terms which are first order in $\frac{1}{\Omega}$, and in the coherence resurgence and transient negative entropy production which are characteristic signs of the non-Markovian information backflow.

[1] As a collaborative effort led by a previous student, Nicholas Werren.

We hypothesised that including non-Markovian interactions would extend coherence times, and we initially expected that the decoherence process itself would be delayed or slowed. However, this turned out to be only partially correct. For the free particle, the initial decoherence process was slowed very slightly, due to the spreading of the off-diagonal peaks induced by the orthogonal term, but the effect was negligible. More significantly, we found a resurgence of the l_1-norm of coherence at much later times, leading to significant amounts of coherence being present in the system up to $t \approx 100$fs. We labelled this "lateral coherence", as it emerges from the diagonal populations rather than the off-diagonal coherences. The lateral coherence is closer to the diagonal, so cannot represent an extreme delocalised state in the same way as the double Gaussian density matrix, but its proximity to the diagonal allows it to persist for much longer than the off-diagonal peaks. In this way, it becomes a compromise between the orthogonal term, which acts to spread the populations away from the diagonal, and the decoherence term, which acts to decay any off-diagonal elements. We also benchmarked this feature by calculating the relative entropy of coherence (in Appendix D) to ensure that this feature was not isolated to the l_1-norm of coherence.

We also hypothesised that for biologically relevant parameters such as physiological temperatures, the predictions we made would have relevance for assessing the credibility of hypotheses in quantum biology. The prediction of coherence resurgence, described above, was obtained for biologically relevant parameters, and so this provides a promising initial result for the question of coherence in biological systems. However, we have not specifically applied our result to biological systems, e.g. a double well, so although we can be tentatively optimistic, we cannot make any direct claims about the application of this work to quantum biology.

One final hypothesis we made was that *the more non-Markovian the interaction, the longer quantum coherence will persist.* This was not a simple question to answer as the non-Markovianity of the system is dependent on all parameters and not just R_Ω. We also did not implement any measures of non-Markovianity in order to rigorously quantify the interaction. However, we found that the length of time for which coherence persists is strongly dependent on the coupling strength between the system and the bath, and the amount of coherence present in the resurgence is dependent on the bath size and the coupling strength. Therefore, we have a situation whereby the weaker the coupling between the system and bath, the longer coherence

persists and the more it is present in the system. This can be understood with reference to the form of the decoherence term, which is proportional to the coupling strength, and so decoherence is slower for weaker couplings.

7.1.2 Further Discussion

Timescale Restriction

A crucial element of the open quantum system framework is a separation of timescales between the system of interest and the environment, and this is summarised by the Born-Markov approximation. Although we relax the Markov approximation in this work, it is the timescale separation that underpins the perturbative expansion. The system relaxation time is usually defined as $\tau_S = \gamma^{-1}$, which describes the timescale of the *dissipative* dynamics, rather than the underlying Hamiltonian dynamics. The strength of both the relaxation and the decoherence processes are proportional to γ, and we therefore consider it to be the inverse timescale associated with relaxation from a pure state to a thermal mixture. In contrast, the timescale of the bath is (in the harsh cut-off case) determined by $\tau_E = \Omega^{-1}$, which is the period of the fastest and most dominant oscillators. This is also the most dominant oscillator in the bath. In the general cut-off case, this timescale is $\tilde{\Omega}^{-1}$, defined in Eq. (6.2.13), which is only changed from τ_E by a small multiplicative factor. The perturbative approach uses the approximation $\gamma < \Omega$, and therefore $\tau_S > \tau_E$: the timescale separation is reinforced by the perturbative approach, although it is relaxed compared to the Markovian case, and a non-perturbative approach would be needed to eliminate it entirely.

The timescale restriction means that the treatment of non-Markovian dissipative dynamics exists within a set of narrow conditions. The bath response time has to be long enough that it is no longer infinitesimal in comparison to the system relaxation time - the condition that defines non-Markovianity - but not so long that system-bath timescale separation fails. Therefore, this description is only appropriate for *weakly non-Markovian* systems. This distinction is analogous to weak-coupling or strong-coupling limits, which often require different treatments dependent on the strength of the coupling between the system and the bath. In order to describe strongly non-Markovian systems, it would be necessary to either take more terms in the expansion of $\frac{1}{\Omega}$, or find a way of evaluating the nested convolution integrals without resorting to an expansion at all.

A strongly non-Markovian system, with little to no separation between timescales, could exhibit very different dynamics from the system considered here. In particular, we observed that the time over which non-Markovian effects make a significant contribution to the dynamics is much longer than the time over which decoherence of the original off-diagonal peaks dominates. The decoherence process happens, essentially, too quickly for non-Markovian dynamics to kick in. If the condition $\tau_S \approx \tau_E$ could be reached, the non-Markovian dynamics may occur over a timescale similar to that of the decoherence dynamics of the system. This could potentially slow or halt the decoherence process in its tracks, allowing delocalised superpositions to occur over greatly extended timescales. However, this would require a very different approach, not requiring separation of timescales - i.e., fully rejecting the Born approximation, as well as relaxing the Markov approximation. It has been suggested elsewhere that a fully non-Markovian treatment requires going beyond the Born approximation [165, 173, 174].

The approximation $\tau_S > \tau_E$ is reflected in a restriction of the parameter space: we are only allowed to consider the regime where $\frac{\gamma}{\Omega} \lessapprox 0.1$, which reflects the regime in which the first order Taylor approximation we made is valid. This means that $R_\Omega < \frac{1}{\pi}$. However, this is not a well-defined restriction, and we see (as in Figure 5.9) that the model breaks down and gives unphysical results for values of R_Ω which are much smaller than the upper bound of $\frac{1}{\pi}$. An interesting conclusion we are forced to draw is that the maximum allowed value of R_Ω - the limit of the model - is γ dependent. This can be understood in the following way. Suppose we have two systems, coupled to their respective environments with strength $\gamma_1 = \frac{kT}{10\hbar}$ and $\gamma_2 = \frac{kT}{20\hbar}$. In each system, we impose $R_\Omega = 0.06$. This corresponds to cut-off frequencies of $\Omega_1 = \frac{6kT}{10\hbar}$ and $\Omega_2 = \frac{3kT}{10\hbar}$. So in the second instance, the cut-off frequency is half the size, and is far closer to the breakdown of the validity of the $\frac{1}{\Omega}$ expansion. We need to ensure that not only is R_Ω not too large, but that Ω is not too small. This is a result of the perturbative approach we have used.

Novel Non-Markovian Terms

The novel dynamics of the non-Markovian master equation, Eq. (5.1.33) are encapsulated by three novel terms: the orthogonal term $\hat{L}_O$, the potential term $\hat{L}_V$, and the relaxation term $\hat{L}_R$.

The relaxation term is the simplest to interpret, as it has the same form as the Caldeira-Leggett relaxation term,

$$\left(\hat{L}_{\mathrm{R}}\right)_{\mathrm{W}} = 4\gamma \frac{\partial}{\partial p}(pW). \tag{7.1.1}$$

This term is responsible for the difference between the Markovian (Caldeira-Leggett) and the non-Markovian steady states, with the non-Markovian steady state being a wider Gaussian than the Markovian case, and as such is the longest lived non-Markovian effect. This effect essentially makes the steady state more delocalised. However, the effect is very slight as we only allow very small values of R_Ω. In the Wigner transform, the relaxation term contributes to the original Caldeira-Leggett relaxation term, and so there are no novel effects at the classical level originating from this term.

The orthogonal term is responsible for the novel dynamics we observe, including the negligible slowing of decoherence and the coherence resurgence. This is because it acts to spread populations of the density matrix away from the diagonal, and spread coherences parallel to the diagonal. However, it is difficult to describe exactly the effect of the orthogonal term on the original off-diagonal coherences because the decoherence dynamics are so dominant.

In the Wigner transform, the orthogonal term becomes the mixed derivative term

$$\left(\hat{L}_{\mathrm{O}}\right)_{\mathrm{W}} = 4kT \frac{\partial^2 W}{\partial p \partial q}. \tag{7.1.2}$$

This is a new term in the Wigner equation, suggesting that the classical dynamics are meaningfully changed by the inclusion of a non-Markovian interaction between the system and bath.

The potential term has not been investigated in this thesis since the free particle case had the simplest analytic solution and proved to contain plenty of interesting dynamics to analyse. However, the non-Markovian master equation, as well as the corresponding Wigner equation, are valid for a general choice of potential. All the potential-dependent terms in the non-Markovian master equation are given by

$$\frac{1}{i\hbar}[\mathrm{v_R}(x) - \mathrm{v_R}(y)] + \frac{R_\Omega}{2i\hbar}(x-y)\left(\frac{\mathrm{dv_R}}{\mathrm{d}x} - \frac{\mathrm{dv_R}}{\mathrm{d}y}\right).$$

For the harmonic oscillator, this becomes

$$\frac{(1+R_\Omega)}{i\hbar}[\mathrm{v_R}(x)-\mathrm{v_R}(y)],$$

and the non-Markovian contribution from the potential to the dynamics is negligible, equal to a very slight shift in frequency. However, this is not true for the general case. For example, in the case of a double well potential with general form $\mathrm{V_R}(x)=(x-a)^2(x+a)^2$, we obtain

$$\frac{(1+R_\Omega)}{i\hbar}[\mathrm{V_R}(x)-\mathrm{V_R}(y)]+\frac{R_\Omega}{i\hbar}(x+y)(x-y)^3,$$

such that the original Markovian term is retained, multiplied by the factor $(1+R_\Omega)$, and a new term is gained. This will have non-trivial effects for the dynamics of the density matrix.

However, in the corresponding Fokker-Planck equation, the non-Markovian potential term has the same form as the Markovian potential term,

$$\left(\hat{L}_\mathrm{V}\right)_\mathrm{W}=\frac{\partial \mathrm{V_R}(q)}{\partial q}\frac{\partial W}{\partial p}. \tag{7.1.3}$$

Therefore no novel potential-dependent dynamics in the classical limit are obtained in the non-Markovian case.

Relationship to Other Master Equations

It is interesting that our results (the non-Markovian master equation and the corresponding Fokker-Planck equation) bear similarity to other results in different contexts. In particular, we will discuss some of the many papers that set out to describe the dissipative Markovian dynamics of the damped or driven quantum harmonic oscillator, e.g. a damped or driven harmonic oscillator which interacts with a Caldeira-Leggett-type heat bath [38, 75, 175–180]. These papers use a variety of methods and are not in general restricted by the high temperature approximation of Caldeira and Leggett [31]. In addition, we will discuss a paper by Diosi [76] that aims to generalise the Caldeira-Leggett master equation to medium or intermediate temperatures.

It has been noted by several authors [38, 75, 175–180] that the Fokker-Planck equation of

the damped harmonic oscillator at arbitrary temperature can be given by

$$\partial_t W = -\frac{p}{m}\partial_q W + k(t)q\partial_q W + \gamma(t)\partial_p(pW) + D_{pp}\partial_p^2 W + D_{qp}\partial_q\partial_p W, \tag{7.1.4}$$

with different approaches taken to determine the diffusion coefficients D_{pp} and D_{pq}. This is of note because the final term, $D_{qp}\partial_q\partial_p W$, has the same form as the orthogonal term in our non-Markovian Fokker-Planck equation, which is responsible for the novel dynamics we observe.

This equation was first derived by Adelman [175], motivated by the effect of non-Markovian Gaussian noise in the quantum Langevin equation for the Brownian harmonic oscillator [112]. The non-Markovianity enters in a time dependence of the friction function, and coefficients are given in terms of the memory function: non-Markovianity is represented via time-dependent coefficients. The free-particle case can be found by setting the harmonic oscillator frequency, ω, to 0; in this case the coefficient D_{qp} is given in the Markovian limit by

$$D_{qp} = -\frac{kT}{m}. \tag{7.1.5}$$

The persistence of this term in the Markovian limit implies that the mixed derivative term itself does not here represent non-Markovian dynamics. Schramm et al [176] noticed that the same equation, with slightly different time-independent coefficients, can be exactly derived in a Markovian case with coloured (non-Gaussian) noise. In this case the mixed derivative coefficient at $\omega = 0$ is given by

$$D_{qp} = -\frac{\langle\hat{p}^2\rangle}{m}, \tag{7.1.6}$$

which is again negative and non-vanishing.

Unruh and Zurek [178] independently derive the master equation in order to explore the decoherence dynamics of the dissipative harmonic oscillator dynamics, with particular focus given to the selection of the pointer basis. In their approach, they couple the harmonic oscillator to a scalar field, and describe the emergence of the mixed derivative term as a small non-Markovian correction to the underlying Markovian dynamics. However, they go on to say that this term is negligible, and can be safely neglected in almost all regimes. Hu, Paz, and Zhang [38] derive the same mixed derivative term via their exact path integral approach, again describing the

non-Markovianity of the term in the time-dependence of the coefficient. There are many other approaches to the dissipative quantum oscillator that result in terms of the same form appearing, including those in [75, 138, 177, 179, 181].

We will single out one paper, by Dillenschneider and Lutz [180], in order to directly compare the coefficient of their mixed derivative to ours. Here, the authors present a general derivation of the equation via Green's functions solutions of the damped quantum harmonic oscillator Langevin equation. The time-independent coefficients are derived by expanding the convolution kernels expressed by Eq. (3.3.9) in powers of $\hbar$. They obtain

$$D_{qp} = \frac{\gamma^2\hbar^2}{12kT}, \tag{7.1.7}$$

in the free particle limit. Because of the simple form of this coefficient, it is tempting to simply compare the coefficient of this term to our coefficient, i.e. to set

$$4R_\Omega kT = \frac{\gamma^2\hbar^2}{12kT'}, \tag{7.1.8}$$

where we allow the coefficients to act at different temperatures: the actual temperature T, and an "effective" temperature T'. Via this crude comparison, we can say that the effects of the non-Markovian term $4R_\Omega kT\partial_q\partial_p W$ would be felt equivalently by a damped harmonic oscillator interacting with a Markovian heat bath at temperature

$$kT' = \frac{\gamma^2\hbar^2}{48R_\Omega kT}. \tag{7.1.9}$$

For our default parameters, e.g. $T = 320\text{K}$, $\gamma = \frac{kT}{20\hbar}\text{fs}^{-1}$, and $R_\Omega = 0.06$ (see Section 5.2.2), we find that $T' = 0.0278\text{K}$, which is close to absolute zero. Therefore, in this sense our non-Markovian orthogonal term can be mapped to an equivalent term in the dynamics of an ultra-low temperature harmonic oscillator undergoing Markovian evolution. This hints at a connection between ultra-low temperature Markovian dynamics and medium-high temperature non-Markovian dynamics.

Another relevant paper is by Diosi [76], and aims to generalise the Caldeira-Leggett master equation to medium or intermediate temperatures. This paper is particularly relevant as it

is for a general potential, in contrast to the approaches presented above which focus on the harmonic oscillator. The procedure is to relax the strict approximation $\hbar\omega \ll kT$, which is what enables Caldeira and Leggett to cast the convolution kernel into δ-function form, such that the convolution kernel is instead taken to be

$$\alpha_R(\tau) = \frac{4m\gamma kT}{\hbar}\delta(\tau) - \frac{m\gamma\hbar}{3kT}\delta''(\tau). \tag{7.1.10}$$

The Markovian approximation is kept by applying the restriction $t \gg \Omega^{-1}$, such that the resultant dynamics are coarse-grained with respect to a high frequency cut-off, and discarding any terms of $O(\frac{1}{\Omega})$ or higher. Although the only the operator representation master equation is derived in this paper, it is simple to translate from this to the Fokker-Planck equation using the methods presented in the previous sections. The Diosi Fokker-Planck equation is

$$\partial_t W = -\frac{p}{m}\partial_q W + \partial_q V \partial_p W + 2\gamma\partial_p(pW) + 2m\gamma kT\partial_p^2 W + \frac{\gamma\hbar^2}{6mkT}\partial_q^2 W + \frac{\gamma\Omega\hbar^2}{6\pi kT}\partial_q\partial_p W. \tag{7.1.11}$$

This equation also has the mixed derivative term (although some other new terms are also present). In this case, the coefficient D_{qp} along with D_{qq} ensure positivity of the density matrix, as well as enabling the model to be valid at lower temperatures.

It has also been noted that in the general case of the Caldeira-Leggett model (i.e. not a specific choice of potential or a lowered temperature), it would be technically correct to include a term of the form

$$\frac{2\gamma kT}{\hbar^2\Omega}\partial_q\partial_p W, \tag{7.1.12}$$

in the Markovian limit $\Omega \gg \gamma$, but that this term is negligible in the limit considered and so is usually neglected [9, 64]. This can be interpreted as follows: the non-Markovian term of the same form is responsible for information backflow into the system. However, in the Markovian case, it is not true that there is no information backflow into the system, just that the *average* information backflow into the system is zero [133]. This information backflow is a negligible effect, due to fluctuations, and is washed out by the overall dynamics. Therefore, the presence of this term as a negligible contribution in the Markovian limit is not in contradiction to its function as a significant source of information backflow in the non-Markovian case.

The purpose of this section has been to note that in a variety of different situations: non-Markovian Gaussian noise [175], Markovian non-Gaussian noise [176], non-Markovian coupling to a scalar field [178], the exact path integral approach [38], and in the medium-temperature correction to the Caldeira-Leggett model [76], the same mixed derivative term appears. Some of these approaches describe the term as Markovian, others as non-Markovian. It is tempting to conclude that the mixed derivative term describes dynamics that are inherently non-Markovian but of negligible magnitude in most cases, as described by several authors [9, 64, 178], and therefore do not describe a significantly non-Markovian dynamics. To support this, we compare the magnitude of our coefficient (of the mixed derivative term) to coefficients derived in other works.

For our "default" set of parameters (see Section 5.2.2), the coefficient of the term in our case is

$$C_{\mathrm{NM}} = \frac{6}{25}kT. \tag{7.1.13}$$

Therefore, the ratio of coefficients between the mixed derivative term and the decoherence term, which is known to dominate the dynamics in most regimes, is

$$\frac{C_{\mathrm{NM}}}{C_{\mathrm{decoh}}} \approx 0.2. \tag{7.1.14}$$

We see that although decoherence is still the dominant factor, it dominates by less than an order of magnitude (in this crude method of describing the dynamics). In the other cases discussed, we have

$$\begin{aligned} C_{\mathrm{Adelmann}} &= -\frac{1}{m}kT \approx 0.01 C_{\mathrm{NM}} \\ \implies \frac{C_{\mathrm{Adelmann}}}{C_{\mathrm{decoh}}} &\approx 0.002, \end{aligned} \tag{7.1.15}$$

$$\begin{aligned} C_{\mathrm{Dillenschneider}} &= \frac{1}{4800}kT \approx 0.0005 C_{\mathrm{NM}} \\ \implies \frac{C_{\mathrm{Dillenschneider}}}{C_{\mathrm{decoh}}} &\approx 0.0001 \end{aligned} \tag{7.1.16}$$

and

$$\begin{aligned} C_{\mathrm{Diosi}} &= \frac{1}{144\pi^2}kT \approx 0.0002 C_{\mathrm{NM}} \\ \implies \frac{C_{\mathrm{Diosi}}}{C_{\mathrm{decoh}}} &\approx 0.00004. \end{aligned} \tag{7.1.17}$$

In each of these cases, the decoherence effect is much more dominant, compared to the mixed derivative term, than in our non-Markovian master equation - by several orders of magnitude. This explains why a coherence resurgence has not been observed in any of the other contexts mentioned; the mixed derivative term is simply incapable of dominating the dynamics at any point.

The mixed derivative term we derive in the non-Markovian master equation is not novel in the literature, but its effect seems to be significantly magnified in this case, allowing it to temporarily dominate the dynamics and produce a non-trivial effect, e.g. the coherence resurgence. However, the physical meaning of this term is not as well discussed as the decoherence or relaxation terms. Further avenues for investigation of this topic are raised in Section 7.2.4.

Quantum Thermodynamics

In Section 5.2.5, we observed that the coherence resurgence phenomenon is associated with a transient negative entropy production rate. This can be interpreted with particular reference to the argument set out in [182]. A summary of the argument follows. The thermodynamic entropy can be understood as a measure of how much thermal energy of a system is available to perform useful work, whereas the information theoretic entropy is a measure of how much information in that system is accessible [60]. It has been shown that it is possible to use quantum information to do work [183, 184], e.g. via a so-called Szilard engine [185] - an extension of the Maxwell's demon idea. So, as shown by Landauer's principle [88], when information is lost or erased, the entropy increases and there is a work cost: the ability of the system to do work decreases [92]. We can think of the information lost as being information about the internal degrees of freedom of the system which describe its thermal energy. This unites the information theoretic and thermodynamic frameworks. But a characteristic feature of non-Markovianity is information backflow [125–129], i.e. flow of information from the environment back into the system. This can therefore be interpreted as a new source for work, and there must be a corresponding entropy decrease to accommodate the system's increased thermodynamic capability. This argument shows that, if information backflow is taken to be characteristic of non-Markovianity, then non-Markovian dynamics must lead to transient negative entropy production.

It should be further pointed out that, despite the phenomenon of work-locking [62, 90],

quantum coherence can be used as a source of work [186–189]. Without having to resort to an information theoretic framework, this allows us to see straight away that an increase in coherence should be associated with an increase of thermodynamic power. Therefore, by considering either the coherence resurgence, the information backflow, or the transient decrease in entropy, the evolution described by the non-Markovian master equation, Eq. (5.1.33), can be seen as a source of more efficient thermodynamics (i.e. more extractable work) than the Markovian counterpart.

Although it has been identified that a decrease in von Neumann entropy can correspond to non-Markovian effects, the exactness of the correspondence is still an open question. Some authors consider negative entropy production rates to be a thermodynamic signature of non-Markovianity [126–128]. However, reference [158] asserts that von Neumann entropy can decrease for reasons unrelated to memory effects, and even if the "quantumness" reduces, i.e. via decay of entanglements. However, despite this subtlety, the conclusion of reference [158] is that non-Markovianity increases the extractable work of the system, effectively boosting the thermodynamic power. This analysis is made by considering the quantum correlations that build up between the system and an observer.

The quantum thermodynamical arguments presented here establish with confidence that the information backflows which are characteristic of non-Markovian dynamics, and present in our model of non-Markovian quantum Brownian motion, should enable more work to be extracted from the system of interest, over times much longer than the decoherence time. This is in line with work in the resource theory of coherence [61], which introduces the concept of a "coherence cost" that must be paid to create certain states: the coherence resurgence we observe enables that cost to be paid at later times. Essentially, we conclude from the coherence resurgence and the transient negativity of the von Neumann entropy production rate that non-trivial quantum behaviours can emerge at later times, powered by the increased extractable work or, equivalently, powered by the increased coherence resource present in the system. The quantification of the extractable work is an intriguing subject for future research, as is the question of which quantum behaviours could emerge.

7.2 Future Work

This work naturally suggests many avenues for further research. The identification and thermodynamic interpretation of a coherence resurgence in the free particle case is only the first stage in fully exploring these rich and counter-intuitive dynamics.

7.2.1 Application to Quantum Biology

The motivation of this work was a collection of hypotheses in quantum biology; the idea was to explore a model that could predict long-lived coherence in physiological temperature systems. While our initial results are promising, the non-Markovian master equation should be applied to specific systems in order to make predictions about coherence lifetime and tunnelling rates. For example, a collection of problems falling roughly under the umbrella "the biological tunnelling problem" [22, 24, 30, 190] could be investigated by inserting a double-well potential into the non-Markovian master equation. Although solving this analytically may present a challenge, direct simulation of either the master equation or the Fokker-Planck equation is possible.

7.2.2 Further Exploration of the Coherence Resurgence

We have begun exploring the quantification of the coherence resurgence, making connections between the parameters γ, R_Ω, T and the coherence peak time and value. However, as discussed, the actual value of the l_1-norm of coherence is not as meaningful as the general trends it displays, because coherence is not unambiguously defined, and different coherence measures give different values. Despite this, there are many interesting questions about the coherence resurgence that remain. Although a thorough classification of the parameter space - i.e. calculating the maximum value of the coherence and the time at which coherence is maximised for a wider range of values in the parameter space formed by γ, R_Ω, T - is a valid target, it would be more interesting and physically meaningful to be able to predict these quantities from a physical understanding of how the decoherence and orthogonal terms interact with each other, similar to Zurek's estimation [7] of the ratio $\frac{\tau_R}{\tau_D}$ (discussed in Section 2.2.4).

Additionally, we have only investigated the free particle case. Further work should investigate a range of potentials - for example, a harmonic oscillator, a double-well, or a particle in a box - in order to investigate whether the coherence resurgence is a system-independent phe-

nomenon. By placing the system into a context, the question of usefulness may also be answered. For example, the coherence resurgence may promote long-lived superpositions between energy states of the harmonic oscillator, novel tunnelling behaviour, or coherent transport across a lattice. Currently, this is just speculation, but I believe this to be an interesting question meriting further exploration.

7.2.3 Quantum Thermodynamics

A more thorough thermodynamic analysis of the dynamics described by the non-Markovian master equation presents an interesting and timely challenge. Our approach only extended as far as calculating the von Neumann entropy, and the rate of change of the von Neumann entropy, and making some interesting qualitative conclusions. However, this is a connection that could be further developed.

For example, the definition of entropy production that we used ($\dot{S}_{\mathrm{vN}}(\rho)$) was fairly crude. Instead, the relative entropy can be utilised to define the irreversible contribution to the entropy production [127],

$$\langle \Sigma \rangle = S(\rho(0)||\rho_\infty) - S(\rho(t)||\rho_\infty), \tag{7.2.1}$$

and the corresponding instantaneous entropy production rate

$$\sigma(t) = -\frac{\mathrm{d}}{\mathrm{d}t} S(\rho(t)||\rho_\infty). \tag{7.2.2}$$

In addition, the calculation of maximum extractable work - i.e. $\langle W_{\mathrm{max.extr.}} \rangle = \Delta U + T\Delta S$ - is an interesting question in the context of non-Markovianity. A similar analysis has been undertaken in Ref [127] in the context of the spin-boson model, and the work in Ref. [158] show that the work extraction is highly dependent on non-Markovianity. The thermodynamic analysis of the non-Markovian master equation will be enlightening, not only for our understanding of the behaviour of non-Markovian quantum systems, but also for our understanding of non-Markovian quantum thermodynamics.

The development of thermodynamics to model systems which exchange heat allowed a much deeper understanding of fundamental limits to be developed, e.g. the Carnot limit which sets a firm upper bound on the efficiency of an engine. Similarly, modelling quantum biological

systems using techniques from quantum thermodynamics could provide an interesting insight on which processes are allowed, and which may be ruled out by thermodynamic considerations. For example, upper limits can be set on the amount of work that can be extracted from a given system in terms of the initial coherence and the amount of non-Markovianity present, and we can calculate the work cost of certain tasks (e.g. proton tunnelling across the DNA backbone). It should be possible to determine necessary and sufficient conditions on the initial coherence of the system and the non-Markovianity of the system-environment interaction that must be met before this task can be achieved.

The field of quantum thermodynamics is rapidly developing. A new framework to model non-equilibrium single-particle systems has been developed by Ali et al [191]; the authors propose the definition of "dynamical temperature":

$$T(t) = \frac{\partial Q}{\partial S}. \tag{7.2.3}$$

In the free particle case, we can see that the heat flow is constant (see Appendix E), and therefore when the rate of change of entropy takes on a negative value, the dynamical temperature will also become negative. Ref. [191] associates this behaviour of the dynamical temperature with a phase change. An interesting question is to explore the dynamics of our system in terms of the dynamical temperature.

7.2.4 Information Flow Analysis

In Section 7.1.2, we discussed the connection between our non-Markovian Fokker-Planck equation and other Fokker-Planck equations which also present a mixed-derivative term. In the current situation, it is unclear whether this mixed derivative term presents inherently non-Markovian dynamics, or whether this is dependent on the other terms present and the magnitude and sign of the coefficient. One option for investigation of this question is an "information channel" method as described in a paper which by Lu et al [35]. In this work, the authors lay out a method for breaking down the total information flow of the dynamics described by a master equation into sub-flows described by each operator. Any operator which corresponds to a negative information sub-flow - i.e. information flow back into the system - corresponds to non-Markovian dynamics.

Although the initial formulation looks at the quantum Fisher information, it could be generalised to consider the von Neumann entropy. In this case, we can make the crude initial approach of substituting a general master equation,

$$\dot{\rho}(t) = \sum_i \hat{L}_i \rho(t), \tag{7.2.4}$$

with some general Liouvillian operators $\hat{L}_i$, in the rate of change of the von Neumann entropy,

$$\dot{S} = -k_B \mathrm{Tr}\left[\dot{\rho}(t) \ln \rho(t)\right], \tag{7.2.5}$$

to obtain a sum of information subflows

$$\dot{S} = \sum_i \dot{S}_i, \tag{7.2.6}$$

given by

$$\dot{S}_i = -k_B \mathrm{Tr}\left[(\hat{L}_i \rho(t)) \ln \rho(t)\right]. \tag{7.2.7}$$

By inserting the exact solution into this expression, we could determine the information flow along each channel, represented by the different Liouvillians. The parameter dependence could also be probed. This would enable us not only to determine whether the mixed derivative term is inherently or conditionally non-Markovian, and also to analyse the information flows more generally.

7.2.5 Structured Spectral Densities

The work undertaken in this thesis is largely involved with the extension of quantum Brownian motion to include interactions with finite baths. This introduces structure to the bath in the form of a characteristic frequency, and therefore a bath response time. However, this is not the only way of introducing structure, or accurately reflecting physically realistic environments. Environments may have preferred frequencies, or quantised modes, that differ from a smooth Ohmic spectral density. Models of this kind have been explored in various contexts [32, 33, 192–194], many quantum biological, and typically find that coupling to a quantised mode can promote coherent dynamics at long times. These quantised modes could refer to vibrational

or rotational modes of the particles which make up the bath, or modes to which the system is more strongly coupled.

An extension of this work would be to introduce spectral densities of the form

$$J(\omega) = J_{\mathrm{CM}}(\omega) + \sum_i J^i_{\mathrm{QM}}(\omega), \tag{7.2.8}$$

with the continuous mode part given by a finite Ohmic bath, and the quantised mode part given by a sum of (e.g.) Lorentzian spikes [194],

$$J^i_{\mathrm{QM}}(\omega) = \eta \sum_i g_i \omega_\delta^2 \omega_i \frac{\omega}{(\omega^2 - \omega_i^2)^2 + \omega_\delta^2 \omega^2}. \tag{7.2.9}$$

In this expression, ω_i is a privileged frequency of the environment and ω_δ is the parameter determining the width of the mode. It couples to the system with a strength g_i.

Contributions from a linear combination of spectral density components would form a linear combination of terms in the integral propagator. Therefore, the quantised mode spectral density can be treated independently. The same process can be followed, i.e. taking the Laplace transform of the memory kernel. For each quantised mode contribution, we have

$$\mu_i(\tau) = \frac{\eta g_i \omega_\delta^2 \omega_i}{\pi} \int_0^\infty \frac{\cos \omega\tau}{(\omega^2 - \omega_i^2)^2 + \omega_\delta^2 \omega^2} \mathrm{d}\omega. \tag{7.2.10}$$

This can be evaluated using the integral identity [195]

$$\int_0^\infty \frac{\cos ax}{x^4 + 2b^2 x^2 \cos 2t + b^4} \mathrm{d}x = \frac{\pi}{2b^3} \exp\{-ab\cos t\} \frac{\sin(t + ab \sin t)}{\sin 2t}, \tag{7.2.11}$$

after making the identifications $x \to \omega$, $a \to \tau$, and $b \to \omega_i$. By expanding out the denominator,

$$(\omega^2 - \omega_i^2)^2 + \omega_\delta^2 \omega^2 = \omega^4 + (\omega_\delta^2 - 2\omega_i^2)\omega^2 + \omega_i^4, \tag{7.2.12}$$

we can see that $\cos 2t = \frac{\omega_\delta^2}{2\omega_i^2} - 1$. This also limits the choice of frequencies, such that $\omega_\delta^2 < 4\omega_i^2$. For convenience here, we define here the ratio of frequencies $A = \omega_\delta / 2\omega_i$. Then, trigonometric

identities can be used to determine that

$$\begin{aligned}\cos t &= \frac{\omega}{2\omega_i} = A,\\ \sin t &= \sqrt{1-A^2},\\ \sin 2t &= 2A\sqrt{1-A^2}.\end{aligned} \tag{7.2.13}$$

We can also expand out the sin term in the identity to give

$$\begin{aligned}\sin(t + ab\sin t) &= \sin(t)\cos(ab\sin t) + \cos(t)\sin(ab\cos t)\\ &= \sqrt{1-A^2}\cos\Big(\sqrt{1-A^2}\omega_i\tau\Big) + A\sin\Big(\sqrt{1-A^2}\omega_i\tau\Big).\end{aligned} \tag{7.2.14}$$

Using all of this, we can write

$$\begin{aligned}\mu_i(\tau) &= \frac{2\eta g_i\omega_\delta^2\omega_i}{\pi}\frac{\pi}{2\omega_i^3}\exp\{-A\omega_i\tau\}\frac{\sqrt{1-A^2}\cos\Big(\sqrt{1-A^2}\omega_i\tau\Big) + A\sin\Big(\sqrt{1-A^2}\omega_i\tau\Big)}{2A\sqrt{1-A^2}}\\ &= 2\eta g_i A^2\exp\{-A\omega_i\tau\}\Big(\frac{\cos\Big(\sqrt{1-A^2}\omega_i\tau\Big)}{2A} + \frac{\sin\Big(\sqrt{1-A^2}\omega_i\tau\Big)}{2\sqrt{1-A^2}}\Big).\end{aligned} \tag{7.2.15}$$

This can be Laplace transformed using the identities

$$\begin{aligned}\int_0^\infty \mathrm{e}^{-p\tau}\mathrm{e}^{-\alpha\tau}\sin\omega\tau\mathrm{d}\tau &= \frac{\omega}{(p+\alpha)^2+\omega^2},\\ \int_0^\infty \mathrm{e}^{-p\tau}\mathrm{e}^{-\alpha\tau}\cos\omega\tau\mathrm{d}\tau &= \frac{p+\alpha}{(p+\alpha)^2+\omega^2}.\end{aligned} \tag{7.2.16}$$

Therefore, with the appropriate substitutions, we obtain

$$\mathcal{L}\Big\{\mu(\tau)\Big\}(p) = \eta g_i A\frac{p+2A\omega_i}{p^2+2pA\omega_i+\omega_i^2}. \tag{7.2.17}$$

The goal then is to evaluate

$$\mathcal{L}^{-1}\{\frac{p+2A\omega_i}{p^2+2pA\omega_i+\omega_i^2}F_\pm(p)\}(\tau) \tag{7.2.18}$$

such that it can be substituted back into the propagator. There are several options for how to proceed. In the derivation of the non-Markovian master equation with Ohmic finite bath, we used an expansion in powers of $\frac{1}{\Omega}$, and truncated it after the first order. This meant our analysis was restricted to very large Ω. However, we do not wish to restrict the choice of

preferred frequencies in the same way, and therefore expanding in $\frac{1}{\omega_i}$ is not a good choice. There is a choice to expand around $p = \omega_i$, but it is not clear that this is a physically meaningful choice, as p is a Laplace variable rather than a real frequency. Further work could explore the most sensible approach to deal with a spectral density of this form, whether this involves taking to take an expansion much earlier in the process (e.g. before calculating the memory kernel), to use a different quantised mode function like a δ-function or an approximate δ-function, to include many more powers of $\frac{1}{\omega_i}$, or to come up with another scheme for evaluating the inverse Laplace transform.

7.2.6 Renormalisation Group Approach

As discussed in Section 6.3, we believe a functional renormalisation group analysis of the high-temperature non-Markovian Caldeira-Leggett model should be possible, by writing the effective action of the system in the form of an effective action and following the standard procedure of analysis. It may be possible to avoid any perturbative expansions of the memory kernel in this approach, which would allow for a strongly non-Markovian system to be described. This may prove an interesting topic for future research. In particular, renormalisation theory techniques have been used in Refs. [120, 121] to analyse the "quantum-classical transition" in the double-well potential, i.e. the transition from tunnelling behaviour to no tunnelling behaviour. Not only does the inclusion of the non-Markovian memory kernel provide a natural extension to the analysis of these papers, it could be applied to the biological tunnelling problem to gain new insights about the conditions under which tunnelling can happen.

7.3 Conclusions

Motivated by the feasibility of hypotheses in quantum biology, the purpose of this project has been to extend the model of quantum Brownian motion [31] to include spectral densities which describe realistic, finite environments. This was achieved in Chapter 5 by following the Caldeira-Leggett derivation and inserting an Ohmic spectral density with a finite cut-off Ω, in contrast to the original model which has no cut-off. The effect of this was to replace the δ-function kernels in the original derivation with kernels which only weakly approximate a δ-function. This meant there were contributions to the Caldeira-Leggett propagator from the nested integrals which relied on past times: i.e. the propagator represented a non-Markovian evolution. The nested

integrals were evaluated using the Laplace transform, and the exact representation in powers of $\frac{1}{\Omega}$ was truncated after the first order. This introduced higher spatial derivatives into the propagator, and two time intervals were required to translate the propagator equation into a master equation. Additional terms proportional to $\frac{1}{\Omega}$ were found in the master equation, representing the new non-Markovian dynamics.

The dynamics of the free particle were thoroughly explored, initially by finding the exact solution (analogously to a paper by Roy [109]). The exact solution was plotted over short times to investigate decoherence in the non-Markovian case, and it was found that the non-Markovian corrections did not significantly impact decoherence. This was explained with a timescale argument: a non-Markovian bath has a finite response time, and when this is longer than the decoherence time, it should not be expected that decoherence would be slowed. This can also be understood via the information theory argument: there is a finite time for information to flow back into the system. The medium-long term dynamics were probed and the striking results of lateral coherence emergence and coherence resurgence were obtained: at times an order of magnitude longer than decoherence times, lateral coherences emerge from the incoherent diagonal parts of the density matrix and this leads to a resurgence of the l_1-norm of coherence. This effect persists to around 100fs before decohering, and the density matrix thermalises in manner very similar to the Caldeira-Leggett density matrix.

In order to further understand the coherence resurgence, the von Neumann entropy and von Neumann entropy production rate were calculated. It was found that the coherence resurgence corresponded to a transient reduction in von Neumann entropy. However, the second law of thermodynamics is never violated as the *total* entropy production is always positive. A thermodynamic interpretation of the result was given: as information flows back into the system from the environment, which is the characteristic feature of non-Markovian interactions in open quantum systems, and the entropy is lowered due to the inverse relationship between entropy and information.

The purity and uncertainty were calculated as a proxy for checking that positivity of the density matrix is not violated, and we confirmed that the dynamics obey $\mathrm{Tr}\left(\tilde{\rho}^2\right) < 1$ and $\sigma_x\sigma_p < \frac{\hbar}{2}$. Although this cannot completely confirm that there are no positivity violations, it

is a strong signal.

In Chapter 6, the derivation of the previous chapter was generalised to include all Ohmic spectral densities with cut-off functions. This was motivated by justified criticisms of the harsh cut-off: it is not a particularly realistic model for a bath of oscillators occurring in a non-engineered environment. Several cut-off functions were examined (Lorentz-Drude, Gaussian, and linear, each with a characteristic frequency that described the transition from low frequency Ohmic to high-frequency non-Ohmic behaviour) and it was found that the master equations in each case were identical up to a rescaling of the characteristic frequency. The exponential cut-off function was also analysed and it was found that the frequency rescaling was divergent.

This was generalised to an arbitrary cut-off function $f(\omega, \omega_f)$ and an expression for the frequency rescaling in terms of the cut-off function was obtained. Conditions on the cut-off function were also obtained. Crucially, it was found that the cut-off function must have a turning point at the origin: this is to ensure there is a fully Ohmic (or Markovian) regime to be expanded about before the transition begins. This explained why we could not use the exponential cut-off: the transition from Ohmic to non-Ohmic behaviour begins too "quickly" for the perturbative approach.

It was tentatively proposed that the equivalence of all Ohmic spectral densities is a renormalisation group effect, and an avenue was suggested to explore this effect. We used the analysis of Refs [120, 121], which apply renormalisation theory to the low-temperature dissipative Caldeira-Leggett model, as a template for this idea. The influence functional can be re-imagined as a Wilsonian effective action [118], and this can be used to derive a differential Wegner-Houghton equation [116] for the effective potential felt by the system. Then, the dissipative effects can be absorbed into the effect of an effective potential, which may not be physical.

The parameters used in this work were chosen to be biologically relevant, and therefore to provide insight into the feasibility of quantum processes occurring within biological environments. Although our focus has been on the free particle, and cannot be immediately applied to questions in quantum biology, the work presented in this thesis provides a convincing demonstration of coherence persisting in non-Markovian systems at physiological temperatures over times

between one and two orders of magnitude longer than decoherence times in analogous Markovian systems. This should represent significant progress towards building an understanding of how open quantum systems may protect and even create coherences, and therefore promote quantum effects such as tunnelling or entanglement. This work also provides the framework for exploring specific scenarios in quantum biology in more detail.

Finally, there may also be implications in quantum thermodynamics and quantum technology design. As quantum thermodynamics is a rapidly growing field, there is still no definitive interpretation of coherence in a thermodynamic framework. The work presented in this thesis contributes to a growing body of literature which associates non-Markovian dynamics with transient negative entropy production rates. Additionally, the emergence of lateral coherence in a finite Ohmic bath is of interest in the field of reservoir engineering, which aims to design systems in which quantum coherences are protected from the decohering effects of the environment.

Appendices

Appendix A

The Hu-Paz-Zhang Model

The action of the combined system + environment is

$$\begin{aligned} S[x,R_k] &= S_{\rm S}[x] + S_{\rm I}[x,R_k] + S_{\rm E}[R_k] \\ &= \int_0^t {\rm d}s \left[\frac{1}{2} m(\dot{x}^2 - \omega_0^2 x^2) + \sum_k [\frac{1}{2} m_k (\dot{R}_k^2 - \omega_k^2 R_k^2] - \sum_k C_k x R_k \right], \end{aligned} \tag{A.1}$$

where, as in the Caldeira-Leggett action, x and R_k are the system and environment oscillator coordinates, m and m_k are the system and environment masses, and ω_0 and ω_k are the system and environment frequencies. The spectral density is assumed to be of the form

$$J(\omega) = \frac{\eta}{\pi} \omega \left(\frac{\omega}{\Omega} \right)^{n-1} {\rm e}^{-\frac{\omega^2}{\Omega^2}}, \tag{A.2}$$

i.e. a spectral density of algebraic form, with a Gaussian cut-off at the characteristic frequency Ω. We follow the Caldeira-Leggett approach up to the point of writing down the integral equation of motion, propagator, and influence functional (Eqs. 3.2.12-3.2.14). After this, the derivation diverges. The propagator is re-defined via the effective action $A[x,y]$:

$$J(x,y,t;x',y',t_0) = \int {\rm D}x {\rm D}y \exp\left[\frac{i}{\hbar} A[x,y] \right], \tag{A.3}$$

with the influence functional similarly redefined with reference to the influence action $\delta A[x,y]$

$$\mathcal{F}[x,y] = \exp\left[\frac{i}{\hbar} \delta A[x,y] \right] \tag{A.4}$$

such that we have

$$A[x,y] = S_{\rm S}[x] - S_{\rm S}[y] + \delta A[x,y]. \tag{A.5}$$

The influence functional is written slightly differently to Eq. (3.3.3), but the character remains essentially the same:

$$\begin{aligned}\mathcal{F}[x,y] = \exp\Bigg[&-\frac{i}{\hbar}\int_0^t \mathrm{d}\tau \int_0^\tau \mathrm{d}\tau' f_-(\tau)\frac{\mathrm{d}}{\mathrm{d}(\tau-\tau')}\mu(\tau-\tau')f_+(\tau') \\ &-\frac{1}{\hbar}\int_0^t \mathrm{d}\tau \int_0^\tau \mathrm{d}\tau' f_-(\tau)\left(\int_0^\infty \mathrm{d}\omega J(\omega)\coth\frac{\hbar\omega}{2kT}\cos\omega(\tau-\tau')\right) f_-(\tau')\Bigg],\end{aligned} \tag{A.6}$$

with $f_\pm(\tau) = x(\tau) \pm y(\tau)$ as before. In general, the influence functional does not represent Markovian dynamics due to the non-local time correlation functions in the nested integrals. In the Caldeira-Leggett model of Markovian quantum Brownian motion, this is avoided by finding the condition under which these time correlations are δ-functions; the HPZ derivation leaves the non-locality in place in order to explicitly include non-Markovianity in the model.

The procedure continues analogously to the Caldeira-Leggett method, by considering the propagation of the reduced density matrix over an infinitesimal time step. However, in this case, there are two steps to the process. First, we take the propagation from 0 to $t+\varepsilon$ and break the path integrals into two parts, with an intermediary point x_m at time t. The path integral is re-written:

$$\int_{0;x+0}^{t+\varepsilon;x_f} \mathrm{D}x = \int_{-\infty}^{\infty} \mathrm{d}x_m \int_{0;x_0}^{t;x_m} \mathrm{D}\bar{x} \int_{t;x_m}^{t+\varepsilon;x_f} \mathrm{D}\tilde{x}, \tag{A.7}$$

where $\bar{x}$ and $\tilde{x}$ are the paths taken from $0 \to t$ and $t \to t+\varepsilon$ - also called histories. Therefore, we have

$$J(x_f, y, t+\varepsilon;, x_0, y_0, 0) = \int \mathrm{d}x_m \mathrm{d}y_m J(x_f, y_f, t+\varepsilon; x_m, y_m, t) J(x_m, y_m, t; x_0, y_0, 0). \tag{A.8}$$

The effective action can be written in terms of the new histories,

$$A[x,y] = A[\bar{x},\bar{y}] + A[\tilde{x},\tilde{y}] + A_i[\bar{x},\bar{y},\tilde{x},\tilde{y}], \tag{A.9}$$

with A_i a term which mixes the histories. This may be called a truly non-local or non-Markovian

term. The second step is to approximate the the infinitestimal $\tilde{x}$ paths along straight lines:

$$\tilde{x}(\tau) \approx x_m + (x_f - x_m)\frac{\tau - t}{\varepsilon} = x_m + \beta_x \frac{\tau - t}{\varepsilon}, \tag{A.10}$$

and

$$\tilde{y}(\tau) \approx y_m + (y_f - y_m)\frac{\tau - t}{\varepsilon} = y_m + \beta_y \frac{\tau - t}{\varepsilon}. \tag{A.11}$$

Therefore, we can write the propagator as

$$\begin{aligned} J(x_f, y_f, t; x_0, y_0, 0) &= \int_{0;x_0,y_0}^{t+\varepsilon;x_f,y_f} \mathrm{D}x\mathrm{D}y \mathrm{e}^{iA[x,y]} \\ &= N(t) \int \mathrm{d}x_m \mathrm{d}y_m \mathrm{e}^{iA[\tilde{x},\tilde{y}]} \int \mathrm{D}\bar{x}\mathrm{D}\bar{y} \mathrm{e}^{iA[\bar{x},\bar{y}]+iA_i[\bar{x},\bar{y},\tilde{x},\tilde{y}]}, \end{aligned} \tag{A.12}$$

with the normalising constant the time-dependent $N(t)$. From here, this is expanded to first order in ε. The action and mixing term become

$$A[\tilde{x}, \tilde{y}] = \frac{1}{2\varepsilon}(\beta_x^2 - \beta_y^2) - \frac{1}{2}\omega_0(x_f^2 - y_f^2)\varepsilon + O(\varepsilon^2), \tag{A.13}$$

and

$$A_i[\bar{x}, \bar{y}, \tilde{x}, \tilde{y}] = -\varepsilon \int_0^t \mathrm{d}\tau \frac{1}{2} J_+(\tau)\bar{f}_+(\tau) + i\varepsilon \int_0^t J_-(\tau)\bar{f}_-(\tau), \tag{A.14}$$

with

$$J_+(\tau) = (x_f - y_f)\frac{\mathrm{d}}{\mathrm{d}(t-\tau)}\mu(t-\tau) + O(\varepsilon^2) \tag{A.15}$$

and

$$J_-(\tau) = (x_f - y_f)\int_0^\infty \mathrm{d}\omega J(\omega) \coth\frac{\hbar\omega}{2kT}\cos\omega(\tau - \tau') + O(\varepsilon^2). \tag{A.16}$$

Substituting these expressions in allows us to write the total propagator as an integral of the infinitesimal part multiplying the part from 0 to t:

$$J(x_f, y_f, t+\varepsilon; x_i, y_i, 0) \approx N(t) \int \mathrm{d}\beta_x \mathrm{d}\beta_y \exp\left[\frac{i}{2\varepsilon}(\beta_x^2 - \beta_y^2\right] [1 - i\varepsilon\omega_0^2(x^2 - y^2)] J(x_m, y_m, t; x_0, y_0, 0), \tag{A.17}$$

with

$$J(x_m, y_m, t; x_0, y_0, 0) = \int \mathrm{D}\bar{x}\mathrm{D}\bar{y} \exp i \left[A[\bar{x}, \bar{y}] - \varepsilon \int_0^t \mathrm{d}\tau \frac{1}{2} J_+(\tau) f_+(\tau) + i\varepsilon \int_0^t \mathrm{d}\tau J_-(\tau) f_-(\tau) \right]. \tag{A.18}$$

From here, the propagator is further expanded in powers of β_x and β_y to obtain the derivative,

$$\begin{aligned} i\frac{\partial}{\partial t} J(x_f, y_f, t; x_0, y_0, 0) = \Bigg(& -\frac{1}{2}\left(\frac{\partial^2}{\partial x_f^2} - \frac{\partial^2}{\partial y_f^2}\right) + \frac{1}{2}\omega_0(x_f^2 - y_f^2) \\ & - [\frac{1}{2} d_1(t) f_+(0) f_-(t) + \frac{1}{2} d_2(t) f_+(t) f_-(t) - i[e_2(t) - c_1(t)] f_-(0) f_-(t) \\ & - i[e_1(t) - c_2(t)] f_-^2(t)] \Bigg) J(x_f, y_f, t; x_0, y_0, 0). \end{aligned} \tag{A.19}$$

This process is rather long and involved, and full details can be found in Reference [38]. The time-dependent coefficients are

$$c_1(t) = \int_0^t \int_0^t \int_0^t \mathrm{d}\tau \mathrm{d}\tau' \mathrm{d}\tau'' \frac{\mathrm{d}}{\mathrm{d}(t-\tau)} \mu(t-\tau) [G_{12}(\tau, \tau') + G_{21}(\tau', \tau)] \int \mathrm{d}\omega J(\omega) \coth \frac{\hbar\omega}{2kT} \cos\omega(\tau' - \tau'') u_i(\tau''), \tag{A.20}$$

$$d_i(t) = 2 \int_0^t \mathrm{d}\tau \frac{\mathrm{d}}{\mathrm{d}(t-\tau)} \mu(t-\tau) u_i(\tau), \tag{A.21}$$

and

$$e_i(t) \int_0^t \mathrm{d}\tau \int \mathrm{d}\omega J(\omega) \coth \frac{\hbar\omega}{2kT} \cos\omega\tau u_i(\tau), \tag{A.22}$$

where $u_1(\tau) = f_+(\tau) - f_+^{\mathrm{cl.}}(\tau)$ and $u_2(\tau) = f_-(\tau) - f_-^{\mathrm{cl.}}(\tau)$ are the differences between the paths and the classical harmonic oscillator paths, and G_{ij} are the elements of the matrix which is inverse to

$$\begin{pmatrix} 0 & \left[\frac{\mathrm{d}^2}{\mathrm{d}\tau^2} + \omega_0^2\right] \delta(\tau - \tau') + 2\Theta(\tau - \tau') \frac{\mathrm{d}}{\mathrm{d}(\tau - \tau')} \mu(\tau - \tau') \\ \left[\frac{\mathrm{d}^2}{\mathrm{d}\tau^2} + \omega_0^2\right] \delta(\tau - \tau') + 2\Theta(\tau' - \tau) \frac{\mathrm{d}}{\mathrm{d}(\tau - \tau')} \mu(\tau - \tau') & 2i \int \mathrm{d}\omega J(\omega) \coth \frac{\hbar\omega}{2kT} \cos\omega(\tau - \tau'). \end{pmatrix} \tag{A.23}$$

This is nearly the final step, but Eq. (A.19) is still dependent on the initial points of the paths $f_\pm(0)$. To address this, another time-dependent coefficient is introduced

$$a_{ij}(t) = \frac{1}{2} \int_0^t \mathrm{d}\tau \int_0^t \mathrm{d}\tau' u_i(\tau) \int \mathrm{d}\omega J(\omega) \coth \frac{\hbar\omega}{2kT} \cos\omega(\tau - \tau') u_2(\tau)' \tag{A.24}$$

to write

$$
\begin{aligned}
f_-(0)J(t,0) &= \left(\frac{\dot{u}_2(t)}{\dot{u}_2(0)}f_-(t) + \frac{i}{\dot{u}_2(0)}\frac{\partial}{\partial f_+(t)}\right)J(t,0) \\
f_+(0)J(t,0) &= \Big(-\frac{\dot{u}_2(t)}{\dot{u}_1(t)}f_+(t) - i\left(\frac{4a_11(t)}{\dot{u}_1(t)} + \frac{2a_{12}(t)\dot{u}_2(t)}{\dot{u}_1(t)\dot{u_2}(0)}\right)f_-(t) \\
&\quad - \frac{i}{\dot{u}(t)}\frac{\partial}{\partial f_-(t)} + \frac{2a_{12}(t)}{\dot{u}_1(t)\dot{u}_2(0)}\frac{\partial}{\partial f_+(t)}\Big)J(t,0).
\end{aligned}
\tag{A.25}
$$

This step is worth emphasising as it is where the explicit restriction that the system be a harmonic oscillator enters the model: the above relations are dependent on the well-known harmonic oscillator classical path [104] that determines the functions $u_i(t)$, and cannot therefore be easily generalised to arbitrary potentials. An analogous process could be performed for a specific choice of potential, but it is neither simple or straightforward to generalise.

Finally, the HPZ equation is obtained by multiplying Eq. (A.19) by $\tilde{\rho}(x,y,t)$ and integrating over the initial coordinates:

$$
\begin{aligned}
i\hbar\frac{\partial}{\partial t}\tilde{\rho}(x,y,t) = \Big[&-\frac{\hbar^2}{2}\left(\frac{\partial^2}{\partial x^2} - \frac{\partial^2}{\partial y^2}\right) + \frac{1}{2}(\omega_0^2 + \delta\omega_0^2(t))(x^2 - y^2)\Big]\tilde{\rho}(x,y,t) \\
&- i\hbar\Gamma(t)(x-y)\left(\frac{\partial}{\partial x} - \frac{\partial}{\partial y}\right)\tilde{\rho}(x,y,t) - i\Gamma(t)h(t)(x-y)^2\tilde{\rho}(x,y,t) \\
&+ \hbar\Gamma(t)f(t)(x-y)\left(\frac{\partial}{\partial x} + \frac{\partial}{\partial y}\right)\tilde{\rho}(x,y,t),
\end{aligned}
\tag{A.26}
$$

with time-dependent coefficients

$$
\begin{aligned}
\Gamma(t) &= \frac{d_1(t)}{2\dot{u}_1(t)} \\
\delta\omega_0^2(t) &= d_2(t) - 2\Gamma(t)\dot{u}_2(t) \\
f(t) &= 2\frac{a_{12}(t)}{\dot{u}_2(0)} + \frac{e_2(t) - c_1(t)}{2\Gamma(t)\dot{u}_2(0)} \\
h(t) &= \dot{u}_2(t)f(t) + 8a_{11}(t) + \frac{e_1(t) - c_2(t)}{\Gamma(t)}.
\end{aligned}
\tag{A.27}
$$

Appendix B

Deriving the Caldeira-Leggett Equation of motion

In order to go from the integral propagator equation

$$\tilde{\rho}(x,y,t) = \int \mathrm{d}x'\mathrm{d}y' J(x,y,t;x',y',0)\tilde{\rho}(x',y',0), \tag{B.1}$$

where

$$J(x,y,t;x',y',0) = \int \mathrm{Dx}\ \mathrm{Dy}\ \exp\Bigg\{\frac{\mathrm{i}}{\hbar}(S_R[x] - S_R[y]) \\ - \frac{im\gamma}{\hbar}\int_0^t [x\dot{x} - y\dot{y} + x\dot{y} - y\dot{x}]\mathrm{d}\tau - \frac{2m\gamma kT}{\hbar^2}\int_0^t [x-y]^2\mathrm{d}\tau\Bigg\}, \tag{B.2}$$

to a differential equation of motion, we consider an infinitesimal interval. Over small intervals, path integrals can be approximated as a straight line multiplied by a constant factor. So we have

$$\tilde{\rho}(x,y,t+\varepsilon) = \int \mathrm{d}x'\mathrm{d}y' J(x,y,t+\varepsilon;x',y',t)\tilde{\rho}(x',y',t) \tag{B.3}$$

and

$$J(x,y,t+\varepsilon;x',y',t) \approx \frac{1}{A^2}\exp\frac{i}{\hbar}\Big\{\int_t^{t+\varepsilon}(\frac{1}{2}m\dot{x}^2-\mathrm{V_R}(x))\;\mathrm{d}\tau-\int_t^{t+\varepsilon}(\frac{1}{2}m\dot{y}^2-\mathrm{V_R}(y))\;\mathrm{d}\tau \\ -\int_t^{t+\varepsilon} m\gamma[x\dot{x}-y\dot{y}+x\dot{y}-y\dot{x}]\;\mathrm{d}\tau\Big\}\times\exp-\frac{1}{\hbar^2}\int_t^{t+\varepsilon}2m\gamma kT[x-y]^2\;\mathrm{d}\tau \tag{B.4}$$

Making use of the expressions

$$\begin{aligned}\dot{x}&\approx\frac{x-x'}{\varepsilon}=\frac{\beta_x}{\varepsilon},\\ \dot{y}&\approx\frac{y-y'}{\varepsilon}=\frac{\beta_y}{\varepsilon},\end{aligned} \tag{B.5}$$

and

$$\int_t^{t+\varepsilon} f(x(\tau))\mathrm{d}\tau\approx\varepsilon f(\frac{x+x'}{2}), \tag{B.6}$$

we can evaluate the infinitesimal propagator term by term. We have for the kinetic term

$$\frac{i}{\hbar}\int_t^{t+\varepsilon}\frac{1}{2}m\dot{x}^2\mathrm{d}\tau\approx\int_t^{t+\varepsilon}\frac{im\beta_1^2}{\varepsilon^2}\mathrm{d}\tau=\frac{im\beta_1^2}{2\varepsilon\hbar}, \tag{B.7}$$

for the potential term

$$\frac{i}{\hbar}\int_t^{t+\varepsilon}\mathrm{V_R}(x)\mathrm{d}\tau\approx\frac{i\varepsilon}{\hbar}\mathrm{V_R}(\frac{x+x'}{2})=\frac{i\varepsilon}{\hbar}\mathrm{V_R}(x-\frac{\beta_1}{2}), \tag{B.8}$$

for the imaginary γ-dependent terms

$$\frac{im\gamma}{\hbar}\int_t^{t+\varepsilon}x\dot{x}\mathrm{d}\tau\approx\frac{im\gamma}{\hbar}\int_t^{t+\varepsilon}\frac{x\beta_1}{\varepsilon}\mathrm{d}\tau\approx\frac{im\gamma}{\hbar}(x-\frac{\beta_1}{2})\beta_1;\quad\text{(etc.)} \tag{B.9}$$

and for the temperature-dependent term

$$-\frac{2m\gamma kT}{\hbar^2}\int_t^{t+\varepsilon}x^2(\tau)-2x(\tau)y(\tau)+y^2(\tau)\approx\varepsilon\Big((x-\frac{\beta_1}{2})^2-2(x-\frac{\beta_1}{2})(y-\frac{\beta_2}{2})+(y-\frac{\beta_2}{2})^2\Big) \\ =-\frac{2m\varepsilon\gamma kT}{\hbar^2}\Big((x-y)^2-(x-y)(\beta_1-\beta_2)+\frac{1}{4}(\beta_1-\beta_2)^2\Big). \tag{B.10}$$

These terms can be reinserted into the infinitesimal propagator equation, such that

$$\begin{aligned}\tilde{\rho}(x,y,t+\varepsilon) = \frac{1}{A^2}\int \mathrm{d}\beta_1\mathrm{d}\beta_2\ \exp\Bigg\{ & \frac{im\beta_1^2}{2\varepsilon\hbar} - \frac{i\varepsilon}{\hbar}\mathrm{V_R}(x-\frac{\beta_1}{2}) - \frac{im\beta_2^2}{2\varepsilon\hbar} + \frac{i\varepsilon}{\hbar}\mathrm{V_R}(y-\frac{\beta_2}{2}) \\ & - \frac{im\gamma}{\hbar}(x-\frac{\beta_1}{2})\beta_2 + \frac{im\gamma}{\hbar}(y-\frac{\beta_2}{2})\beta_1 - \frac{im\gamma}{\hbar}(x-\frac{\beta_1}{2})\beta_1 + \frac{im\gamma}{\hbar}(y-\frac{\beta_2}{2})\beta_2 \\ & - \frac{2m\gamma kT\varepsilon}{\hbar^2}(x-y)^2 + \frac{2m\gamma kT\varepsilon}{\hbar^2}(x-y)(\beta_1-\beta_2) - \frac{m\gamma kT\varepsilon}{2\hbar^2}(\beta_1-\beta_2)^2 \\ & \times \tilde{\rho}(x-\beta_1, y-\beta_2, t)\Bigg\}\end{aligned} \tag{B.11}$$

with the change of variables

$$\beta_1 = x - x' \implies \mathrm{d}\beta_1 = -\mathrm{d}x'. \tag{B.12}$$

The equation can be written in a more convenient form as

$$\begin{aligned}\tilde{\rho}(x,y,t+\varepsilon) = \frac{1}{A^2}\int \mathrm{d}\beta_1\mathrm{d}\beta_2\ \exp\Big\{ & \frac{im}{2\varepsilon\hbar}(\beta_1^2-\beta_2^2) - \frac{i\varepsilon}{\hbar}[\mathrm{V_R}(x-\frac{\beta_1}{2}) - \mathrm{V_R}(y-\frac{\beta_2}{2})] \\ & - \frac{im\gamma}{\hbar}\Big[(x-y) - \frac{1}{2}(\beta_1-\beta_2)\Big](\beta_1+\beta_2) - \frac{2m\varepsilon\gamma kT}{\hbar^2}(x-y)^2 \\ & + \frac{2m\varepsilon\gamma kT}{\hbar^2}(x-y)(\beta_1-\beta_2) - \frac{m\varepsilon\gamma kT}{2\hbar^2}(\beta_1-\beta_2)^2\Big\}\tilde{\rho}(x-\beta_1, y-\beta_2, t).\end{aligned} \tag{B.13}$$

Looking at the factor $\exp\{{}^{im}/_{2\varepsilon\hbar}(\beta_1^2-\beta_2^2)\}$, it can be deduced that the main contribution comes from $\beta_1 \approx \beta_2 \approx ({}^{\varepsilon\hbar}/_{m})^{1/2}$. For all other $(\beta_1,\ \beta_2)$, this factor will oscillate with no finite contribution to the integral. By introducing rotated variables

$$\begin{aligned}\beta_1' &= \beta_1 - \varepsilon\gamma(x-y); \\ \beta_2' &= \beta_2 + \varepsilon\gamma(x-y),\end{aligned} \tag{B.14}$$

it can be seen that any terms depending on $\beta_1 - \beta_2$ will be at least $O(\varepsilon^2)$.

Rewriting the terms in β_1' and β_2', we obtain the following expressions. For the rapidly oscillating part of the exponent, we obtain

$$\frac{im}{2\varepsilon\hbar}(\beta_1^2-\beta_2^2) = \frac{im}{2\varepsilon\hbar}(\beta_1'^2-\beta_2'^2) + \frac{im\gamma}{\hbar}(x-y)(\beta_1'+\beta_2'). \tag{B.15}$$

For the potential dependent terms, we obtain

$$-\frac{i\varepsilon}{\hbar}(\mathrm{V_R}(x-{}^{\beta_1}\!/_2)-\mathrm{V_R}(y-{}^{\beta_2}\!/_2))=-\frac{i\varepsilon}{\hbar}\Big((\mathrm{V_R}(x)-\mathrm{V_R}(y))-\frac{1}{2}(\beta_1'\frac{\partial \mathrm{V_R}}{\partial x}-\beta_2'\frac{\partial \mathrm{V_R}}{\partial y}). \quad \text{(B.16)}$$

For the terms that come from the imaginary part of the influence kernel, we obtain

$$\begin{aligned}-\frac{im\gamma}{\hbar}\Big[(x-y)-\frac{1}{2}(\beta_1-\beta_2)\Big](\beta_1+\beta_2)=&-\frac{im\gamma}{\hbar}(x-y)(\beta_1'+\beta_2')\\&+\frac{im\gamma}{\hbar}\Big(\frac{1}{2}(\beta_1'-\beta_2')+\varepsilon\gamma(x-y)\Big)(\beta_1'+\beta_2'),\end{aligned} \quad \text{(B.17)}$$

and for the temperature dependent terms we obtain

$$\begin{aligned}&-\frac{2m\varepsilon\gamma kT}{\hbar^2}(x-y)^2+\frac{2m\varepsilon\gamma kT}{\hbar^2}(x-y)(\beta_1-\beta_2)-\frac{m\varepsilon\gamma kT}{2\hbar^2}(\beta_1-\beta_2)^2\\&=-\frac{2m\varepsilon\gamma kT}{\hbar^2}(1-\varepsilon\gamma)^2(x-y)^2+\frac{2m\varepsilon\gamma kT}{\hbar^2}(1-\varepsilon\gamma)(x-y)(\beta_1'-\beta_2')-\frac{m\varepsilon\gamma kT}{2\hbar^2}(\beta_1'-\beta_2')^2.\end{aligned} \quad \text{(B.18)}$$

The density matrix can be expanded around $\beta_1 \approx \beta_2 \approx 0$, such that

$$\begin{aligned}\tilde{\rho}(x-\beta_1,y-\beta_2,0)=&\tilde{\rho}(x,y,0)-\beta_1'\frac{\partial\tilde{\rho}}{\partial x}-\beta_2'\frac{\partial\tilde{\rho}}{\partial y}+\frac{1}{2}\beta_1'^2\frac{\partial^2\tilde{\rho}}{\partial x^2}+\frac{1}{2}\frac{\partial^2\tilde{\rho}}{\partial y^2}+\beta_1'\beta_2'\frac{\partial^2\tilde{\rho}}{\partial x\partial y}\\&-\varepsilon\gamma(x-y)\Big(\frac{\partial\tilde{\rho}}{\partial x}-\frac{\partial\tilde{\rho}}{\partial y}+\beta_1'\frac{\partial^2\tilde{\rho}}{\partial x^2}-\beta_2'\frac{\partial^2\tilde{\rho}}{\partial y^2}-(\beta_1'-\beta_2')\frac{\partial^2\tilde{\rho}}{\partial x\partial y}\Big)\\&+\varepsilon^2\gamma^2(x-y)^2\Big(\frac{\partial^2\tilde{\rho}}{\partial x^2}-\frac{\partial^2\tilde{\rho}}{\partial x\partial y}+\frac{\partial^2\tilde{\rho}}{\partial y^2}\Big)+O(\beta_1'^2,\beta_2'^2).\end{aligned} \quad \text{(B.19)}$$

We can also write

$$\tilde{\rho}(x,y,t+\varepsilon)\approx\tilde{\rho}(x,y,t)+\varepsilon\frac{\partial\tilde{\rho}}{\partial t}, \quad \text{(B.20)}$$

using the fact that ε is very small.

With the help of Equations (B.15-B.20), we can re-write Equation B.11, such that

$$\begin{aligned}\tilde{\rho}+\varepsilon\frac{\partial\tilde{\rho}}{\partial t} = \frac{1}{A^2}\int \mathrm{d}\beta_1'\mathrm{d}\beta_2'\,\exp\{-\frac{im}{2\varepsilon\hbar}(\beta_1'^2-\beta_2'^2)\}\\ \sum_m \frac{1}{m!}\Big(-\frac{i\varepsilon}{\hbar}[\mathrm{V_R}(x)-\mathrm{V_R}(y)]-\frac{i\varepsilon}{2\hbar}(\beta_1'\frac{\partial \mathrm{V_R}}{\partial x}-\beta_2'\frac{\partial \mathrm{V_R}}{\partial y})\\ +\frac{i\varepsilon^2\gamma}{2\hbar}(x-y)(\frac{\partial \mathrm{V_R}}{\partial x}+\frac{\partial \mathrm{V_R}}{\partial y})+\frac{im\gamma}{2\hbar}(\beta_1'^2-\beta_2'^2)+\frac{im\varepsilon\gamma^2}{\hbar}(x-y)(\beta_1'+\beta_2')\\ -\frac{2m\varepsilon\gamma kT}{\hbar}(1-\varepsilon\gamma)^2(x-y)^2+\frac{2m\varepsilon\gamma kT}{\hbar^2}(1-\varepsilon\gamma)(x-y)(\beta_1'-\beta_2')-\frac{m\varepsilon\gamma kT}{2\hbar^2}(\beta\_1'-\beta_2')^2\Big)^m\\ \times\Big(\tilde{\rho}(x,y,0)-\beta_1'\frac{\partial\tilde{\rho}}{\partial x}-\beta_2'\frac{\partial\tilde{\rho}}{\partial y}+\frac{1}{2}\beta_1'^2\frac{\partial^2\tilde{\rho}}{\partial x^2}+\frac{1}{2}\frac{\partial^2\tilde{\rho}}{\partial y^2}+\beta_1'\beta_2'\frac{\partial^2\tilde{\rho}}{\partial x\partial y}\\ -\varepsilon\gamma(x-y)\Big(\frac{\partial\tilde{\rho}}{\partial x}-\frac{\partial\tilde{\rho}}{\partial y}+\beta_1'\frac{\partial^2\tilde{\rho}}{\partial x^2}-\beta_2'\frac{\partial^2\tilde{\rho}}{\partial y^2}-(\beta_1'-\beta_2')\frac{\partial^2\tilde{\rho}}{\partial x\partial y}\Big)\\ +\varepsilon^2\gamma^2(x-y)^2\Big(\frac{\partial^2\tilde{\rho}}{\partial x^2}-\frac{\partial^2\tilde{\rho}}{\partial x\partial y}+\frac{\partial^2\tilde{\rho}}{\partial y^2}\Big)\Big).\end{aligned} \tag{B.21}$$

where the Taylor expansion of the exponential has been used. Neglecting terms of $O(\varepsilon^2)$, $O(\beta_1'-\beta_2')$, or $O(\varepsilon(\beta_1',\beta_2')$, we obtain a much simpler expression.

$$\begin{aligned}\tilde{\rho}+\varepsilon\frac{\partial\tilde{\rho}}{\partial t} = \frac{1}{A^2}\int \mathrm{d}\beta_1'\mathrm{d}\beta_2'\,\exp\{-\frac{im}{2\varepsilon\hbar}(\beta_1'^2-\beta_2'^2)\}\Big(\tilde{\rho}-\frac{\partial\tilde{\rho}}{\partial x}-\frac{\partial\tilde{\rho}}{\partial y}\\ +\frac{1}{2}\beta_1'^2\frac{\partial^2\tilde{\rho}}{\partial x^2}+\frac{1}{2}\beta_2'^2\frac{\partial^2\tilde{\rho}}{\partial y^2}+\beta_1'\beta_2'\frac{\partial^2\tilde{\rho}}{\partial x\partial y}-\frac{i\varepsilon}{\hbar}[\mathrm{V_R}(x)-\mathrm{V_R}(y)]\tilde{\rho}-\frac{2m\varepsilon\gamma kT}{\hbar^2}(x-y)^2\tilde{\rho}\Big).\end{aligned} \tag{B.22}$$

It is permissible to have made these approximations before performing the integrals, because the integral will only yield powers of $O(\varepsilon^n)$ and not $O(1/\varepsilon^n)$.

The integrals in β_1' and β_2' can then be performed. Writing the integral in more sensible groupings, we get

$$\begin{aligned}\tilde{\rho}+\varepsilon\frac{\partial\tilde{\rho}}{\partial t} = \frac{1}{A^2}\int \mathrm{d}\beta_1'\mathrm{d}\beta_2'\exp\{-\frac{im}{2\varepsilon\hbar}(\beta_1'^2-\beta_2'^2)\}\Big(\tilde{\rho}-\frac{i\varepsilon}{\hbar}[\mathrm{V_R}(x)-\mathrm{V_R}(y)]\tilde{\rho}\\ -\frac{2m\varepsilon\gamma kT}{\hbar^2}(x-y)^2\tilde{\rho}-\varepsilon\gamma(x-y)(\frac{\partial\tilde{\rho}}{\partial x}-\frac{\partial\tilde{\rho}}{\partial y})\Big)\\ +\frac{1}{A^2}\int \mathrm{d}\beta_1'\mathrm{d}\beta_2'\exp\{-\frac{im}{2\varepsilon\hbar}(\beta_1'^2-\beta_2'^2)\}\Big(\frac{1}{2}\beta_1'^2\frac{\partial^2\tilde{\rho}}{\partial x^2}-\beta_1'\frac{\partial\tilde{\rho}}{\partial x}+\beta_1'\beta_2'\frac{\partial^2\tilde{\rho}}{\partial x\partial y}-\beta_2'\frac{\partial\tilde{\rho}}{\partial y}+\frac{1}{2}\beta_2'^2\frac{\partial^2\tilde{\rho}}{\partial y^2})\Big).\end{aligned} \tag{B.23}$$

The process is to perform the integrals and compare coefficients on each side of the equation.

The first term of Equation B.23 can be evaluated by noticing the double Gaussian integral,

$$\int \mathrm{d}\beta_1'\beta_2' \exp\{-\frac{im}{2\varepsilon\hbar}\} = \frac{2\pi\varepsilon\hbar}{m}, \tag{B.24}$$

and therefore this term is

$$\frac{1}{A^2}\cdot\frac{2\pi\varepsilon\hbar}{m}\Big[\tilde{\rho} - \frac{i\varepsilon}{\hbar}[\mathrm{V_R}(x) - \mathrm{V_R}(y)]\tilde{\rho} - \frac{2m\varepsilon\gamma kT}{\hbar^2}(x-y)^2\tilde{\rho} - \varepsilon\gamma(x-y)(\frac{\partial\tilde{\rho}}{\partial x} - \frac{\partial\tilde{\rho}}{\partial y})\Big]. \tag{B.25}$$

In order to normalise the term containing only $\tilde{\rho}$, i.e. the first term in the previous expression, with the LHS of Equation B.23, the constant A must be such that

$$A^2 = \frac{2\pi\varepsilon\hbar}{m}. \tag{B.26}$$

The second term is more complex but can be evaluated with the help of the identities

$$\begin{aligned}
&\int_{-\infty}^{\infty} \exp\{-mx^2\}\mathrm{d}x = \sqrt{\frac{\pi}{m}} \\
&\int_{-\infty}^{\infty} x\exp\{-mx^2\}\mathrm{d}x = 0 \\
&\int_{-\infty}^{\infty} x^2\exp\{-mx^2\}\mathrm{d}x = \frac{\sqrt{\pi}}{2m^{3/2}}.
\end{aligned} \tag{B.27}$$

Taking first the integral in β_1', we can re-write the second term in Equation B.23 as

$$\frac{m}{2\varepsilon\pi\hbar}\int \mathrm{d}\beta_2' \exp\Big\{\frac{im}{2\varepsilon\hbar}\beta_2'^2\Big\}\int \mathrm{d}\beta_1'\Big(a\beta_1'^2 + b\beta_1' + c\Big)\exp\Big\{-\frac{im}{2\varepsilon\hbar}\beta_1'^2\Big\}, \tag{B.28}$$

where

$$\begin{aligned}
a &= \frac{1}{2}\frac{\partial^2\tilde{\rho}}{\partial x^2}; \\
b &= \beta_2'\frac{\partial^2\tilde{\rho}}{\partial x\partial y} - \frac{\partial\tilde{\rho}}{\partial x}; \\
c &= -\frac{\partial\tilde{\rho}}{\partial y}\beta_2' + \frac{1}{2}\beta_2'^2\frac{\partial^2\tilde{\rho}}{\partial y^2}.
\end{aligned} \tag{B.29}$$

Using the identities in Equation B.27, this becomes

$$\begin{aligned}\int \mathrm{d}\beta_2' \exp\Big\{\frac{im}{2\varepsilon\hbar}\beta_2'^2\Big\}\Big(&\frac{m}{4\varepsilon\pi^{1/2}\hbar}\Big(\frac{2\varepsilon\hbar}{im}\Big)^{1/2}\frac{\partial^2\tilde{\rho}}{\partial y^2}\beta_2'^2 - \frac{m}{2\varepsilon\pi^{1/2}\hbar}(\frac{2\varepsilon\hbar}{im}\Big)^{1/2}\frac{\partial\tilde{\rho}}{\partial y}\beta_2' \\ &+\frac{m}{8\varepsilon\pi^{1/2}\hbar}(\frac{2\varepsilon\hbar}{im}\Big)^{3/2}\frac{\partial^2\tilde{\rho}}{\partial x^2}\Big).\end{aligned} \tag{B.30}$$

We can perform this integral in β_2' in the same way, giving

$$\begin{aligned}&\frac{m}{4\varepsilon\pi^{1/2}\hbar}\Big(\frac{2\varepsilon\hbar}{im}\Big)^{1/2}\frac{\pi^{1/2}}{2}\Big(-\frac{2\varepsilon\hbar}{im}\Big)^{3/2}\frac{\partial^2\tilde{\rho}}{\partial y^2} + \frac{m}{8\varepsilon\pi^{1/2}\hbar}\Big(\frac{2\varepsilon\hbar}{im}\Big)^{3/2}\pi^{1/2}\Big(-\frac{2\varepsilon\hbar}{im}\Big)^{1/2}\frac{\partial^2\tilde{\rho}}{\partial x^2} \\ =&\frac{i}{\hbar}\frac{\hbar^2}{2m}\varepsilon\Big(\frac{\partial^2\tilde{\rho}}{\partial x^2} - \frac{\partial^2\tilde{\rho}}{\partial y^2}\Big).\end{aligned} \tag{B.31}$$

Having evaluated both terms, it is now possible to use Equation B.23 to obtain the equation of motion:

$$\begin{aligned}\tilde{\rho} + \varepsilon\frac{\partial\tilde{\rho}}{\partial t} =&\tilde{\rho} + \frac{\varepsilon}{i\hbar}[\mathrm{V_R}(x) - \mathrm{V_R}(y)]\tilde{\rho} - \frac{2m\varepsilon\gamma kT}{\hbar^2}(x-y)^2\tilde{\rho} \\ &-\varepsilon\gamma(x-y)(\frac{\partial\tilde{\rho}}{\partial x} - \frac{\partial\tilde{\rho}}{\partial y}) - \frac{1}{i\hbar}\frac{\hbar^2}{2m}\varepsilon\Big(\frac{\partial^2\tilde{\rho}}{\partial x^2} - \frac{\partial^2\tilde{\rho}}{\partial y^2}\Big).\end{aligned} \tag{B.32}$$

Comparing coefficients, we see that the $O(1)$ terms are $\tilde{\rho} = \tilde{\rho}$. Looking at the $O(\varepsilon)$ terms, we can read off the equation of motion,

$$\frac{\partial\tilde{\rho}}{\partial t} = \frac{i\hbar}{2m}\left(\frac{\partial^2\tilde{\rho}}{\partial x^2} - \frac{\partial^2\tilde{\rho}}{\partial y^2}\right) - \frac{i}{\hbar}[\mathrm{V_R}(x) - \mathrm{V_R}(y)] - \gamma(x-y)\left(\frac{\partial\tilde{\rho}}{\partial x} - \frac{\partial\tilde{\rho}}{\partial y}\right) - \frac{2m\gamma kT}{\hbar^2}(x-y)^2\tilde{\rho}. \tag{B.33}$$

This is the coordinate representation equation of motion for the reduced density matrix of a quantum system of interest under the Ohmic markovian scheme.

Appendix C

Derivation of the Exact Solution

We aim to derive an exact solution to the free particle non-Markovian master equation,

$$\frac{\partial}{\partial t}\rho(x,y,t) = \Bigg[\frac{i\hbar}{2M}\left(\frac{\partial^2}{\partial x^2} - \frac{\partial^2}{\partial y^2}\right) - \gamma(x-y)\left(\frac{\partial}{\partial x} - \frac{\partial}{\partial y}\right) - \frac{2M\gamma kT}{\hbar^2}(x-y)^2 \\ - \frac{4iR_\Omega kT}{\hbar}(x-y)\left(\frac{\partial}{\partial x} + \frac{\partial}{\partial y}\right) - 2\gamma R_\Omega(x-y)\left(\frac{\partial}{\partial x} - \frac{\partial}{\partial y}\right)\Bigg]\rho(x,y,t). \tag{C.1}$$

We begin by defining rotated variables as

$$u = \frac{x+y}{2}, \qquad v = x - y. \tag{C.2}$$

This is a useful step because it removes the dependence on second derivatives (the second derivatives in u and v cancel out) and leaves us with a partial differential equation that is only first order in both co-ordinates.

In the rotated co-ordinate system, the master equation is

$$\frac{\partial}{\partial t}\rho(u,v,t) = \left(\frac{i\hbar}{m}\frac{\partial^2}{\partial u \partial v} - \frac{4R_\Omega ikT}{\hbar}v\frac{\partial}{\partial u} - 2\gamma(1+2R_\Omega)v\frac{\partial}{\partial v} - \frac{2m\gamma kT}{\hbar^2}v^2\right)\rho(u,v,t). \tag{C.3}$$

We then Fourier transform with respect to u to reduce this equation to a first order differential equation in v, with the Fourier transform defined such that

$$\rho(u,v,t) = \frac{1}{\sqrt{2\pi}}\int_{-\infty}^{\infty} \mathrm{d}K \mathrm{e}^{iKu}\rho(K,v,t). \tag{C.4}$$

Note that here, $K = p' - p$, with p and p' the Fourier momentum variables associated with x and y respectively. Therefore, $K = 0$ represents the values diagonal in momentum-space, and delocalised in position-space, and $K \to \pm\infty$ represents a smearing out of momentum, and a corresponding localisation in position.

The Fourier transform gives us

$$\frac{\partial}{\partial t}\rho(K,v,t) + \left(\left(2\gamma(1+2R_\Omega)v + \frac{\hbar K}{m}\right)\frac{\partial}{\partial v} + \frac{2m\gamma kT}{\hbar^2}v^2 - \frac{4R_\Omega kT}{\hbar}Kv\right)\rho(K,v,t) = 0. \quad \text{(C.5)}$$

We address this differential equation using the method of characteristics. By introducing a parameterisation variable, s, such that $t = t(s)$, $v = v(s)$ and $\rho = \rho(s)$, we then assign the following equalities:

$$\begin{aligned} \frac{\partial t}{\partial s} &= 1, \\ \frac{\partial v}{\partial s} &= 2\gamma(1+2R_\Omega)v + \frac{\hbar K}{m}, \end{aligned} \quad \text{(C.6)}$$

and solve to obtain

$$\begin{aligned} t(s) &= s, \\ v(s) &= -\frac{\hbar K}{2m\gamma(1+2R_\Omega)} + \left(v_0 + \frac{\hbar K}{2m\gamma(1+2R_\Omega)}\right)\mathrm{e}^{2\gamma(1+2R_\Omega)s}, \end{aligned} \quad \text{(C.7)}$$

with $t(0) = 0$ and $v(0) = v_0$. Since

$$\frac{\mathrm{d}\rho}{\mathrm{d}s} = \frac{\partial\rho}{\partial t}\frac{\partial t}{\partial s} + \frac{\partial\rho}{\partial v}\frac{\partial v}{\partial s}, \quad \text{(C.8)}$$

this enables us to write the equation to be solved as

$$\frac{\mathrm{d}\rho}{\mathrm{d}s} + \left(\frac{2m\gamma kT}{\hbar^2}v^2 - \frac{4R_\Omega kT}{\hbar}Kv\right)\rho = 0, \quad \text{(C.9)}$$

which when we substitute in Eq. (C.7), has the solution

$$\rho = A_0 \exp\Big\{ -\frac{kT}{2m\gamma(1+2R_\Omega)^2}\Big[K^2(1+4R_\Omega+8R_\Omega^2)t \\ -\frac{2m}{\hbar}K(1+2R_\Omega+4R_\Omega^2)\Big(v_0+\frac{\hbar K}{2m\gamma(1+2R_\Omega)}\Big)\mathrm{e}^{2\gamma(1+2R_\Omega)t} \\ +\frac{m^2\gamma(1+2R_\Omega)}{\hbar^2}\Big(v_0+\frac{\hbar K}{2m\gamma(1+2R_\Omega)}\Big)^2\mathrm{e}^{4\gamma(1+2R_\Omega)t}\Big]\Big\}, \tag{C.10}$$

with A_0 a constant of integration. We can determine this constant by setting $t = 0$ and introducing an initial condition, $\rho_0(K, v_0)$. This gives us

$$\rho = \rho_0(K,v_0)\exp\Big\{ -\frac{kT}{2m\gamma(1+2R_\Omega)^2}\Big[K^2(1+4R_\Omega+8R_\Omega^2)t \\ -\frac{2m}{\hbar}K(1+2R_\Omega+4R_\Omega^2)\Big(v_0+\frac{\hbar K}{2m\gamma(1+2R_\Omega)}\Big)(\mathrm{e}^{2\gamma(1+2R_\Omega)t}-1) \\ +\frac{m^2\gamma(1+2R_\Omega)}{\hbar^2}\Big(v_0+\frac{\hbar K}{2m\gamma(1+2R_\Omega)}\Big)^2(\mathrm{e}^{4\gamma(1+2R_\Omega)t}-1)\Big]\Big\}, \tag{C.11}$$

which we can write in a much more simplified form by inserting the definition of $v(t)$ to remove the explicit time dependence from many of the terms.

Our solution in Fourier space is therefore

$$\rho(K,v,t) = \rho_0(K,v_0)\exp\Big\{ -\frac{kT}{2m\gamma(1+2R_\Omega)^2}\Big[K^2(1+4R_\Omega+8R_\Omega^2)t \\ -\frac{mK}{\hbar}(1+4R_\Omega+8R_\Omega^2)[v-v_0]+\frac{m^2\gamma(1+2R_\Omega)}{\hbar^2}[v^2-v_0^2]\Big]\Big\}, \tag{C.12}$$

where

$$v_0 = -\frac{\hbar K}{2m\gamma(1+2R_\Omega)} + \left(v(t)+\frac{\hbar K}{2m\gamma(1+2R_\Omega)}\right)\mathrm{e}^{-2\gamma(1+2R_\Omega)t}. \tag{C.13}$$

To accomplish the transform back into x and y, we must write the solution in a form that can be easily inverse Fourier transformed. In particular, we can use the Fourier and inverse Fourier transform of a Gaussian function:

$$\mathcal{F}_u[\exp\{a_2u^2+a_1u+a_0\}](K) = \frac{\mathrm{e}^{a_0}}{\sqrt{-2a_2}}\exp\left\{-\frac{(a_1+iK)^2}{4a_2}\right\}, \\ \mathcal{F}_K^{-1}[\exp\{a_2u^2+a_1u+a_0\}](u) = \frac{\mathrm{e}^{a_0}}{\sqrt{-2a_2}}\exp\left\{-\frac{(a_1-iu)^2}{4a_2}\right\}. \tag{C.14}$$

Because we are interested in x and y, not u, we can directly write the result of the inverse Fourier transform as

$$\frac{\mathrm{e}^{a_0}}{\sqrt{-2a_2}}\exp\left\{-\frac{(a_1-\frac{i(x+y)}{2})^2}{4a_2}\right\}. \tag{C.15}$$

We can similarly substitute $v=x-y$ wherever we find it now that the equation has been solved.

The time-dependent part of Eq. (C.12) is a Gaussian in K with time-dependent coefficients; we can write

$$\begin{aligned}\mathrm{e}^{E_2K^2+E_1K+E_0} = \exp\Big\{ &-\frac{kT}{2m\gamma(1+2R_\Omega)^2}\Big[K^2(1+4R_\Omega+8R_\Omega^2)t \\ &-\frac{mK}{\hbar}(1+4R_\Omega+8R_\Omega^2)[v-v_0]+\frac{m^2\gamma(1+2R)}{\hbar^2}[v^2-v_0^2]\Big]\Big\},\end{aligned} \tag{C.16}$$

with

$$\begin{aligned}E_2 &= -\frac{kT}{2M\gamma(1+2R_\Omega)^2}\Big((1+4R_\Omega+8R_\Omega^2)t \\ &\qquad +\frac{\mathrm{e}^{-2\gamma(1+2R_\Omega)t}-1}{2\gamma(1+2R_\Omega)}(1+4R_\Omega+8R_\Omega^2)-\frac{(\mathrm{e}^{-2\gamma(1+2R_\Omega)t}-1)^2}{4\gamma(1+2R_\Omega)}\Big), \\ E_1 &= \frac{kT}{2M\gamma(1+2R_\Omega)^2}\frac{M(x-y)}{\hbar}\Big((1-4R_\Omega-8R_\Omega^2)(1-\mathrm{e}^{-2\gamma(1+2R_\Omega)t}) \\ &\qquad -\mathrm{e}^{-2\gamma(1+2R_\Omega)t}(1-\mathrm{e}^{-2\gamma(1+2R_\Omega)t})\Big), \\ E_0 &= -\frac{kT}{2M\gamma(1+2R_\Omega)^2}\frac{M^2\gamma(1+2R_\Omega)(x-y)^2}{\hbar^2}(1-\mathrm{e}^{-4\gamma(1+2R_\Omega)t}).\end{aligned} \tag{C.17}$$

Now we address the initial condition. A generic normalised double Gaussian density matrix with width parameter b_1, centred at $\pm b_2$, is given by

$$\rho_0(x,y) = \frac{\sqrt{b_1}}{\sqrt{2\pi}\left(1+\mathrm{e}^{-2b_1b_2^2}\right)}\left(\mathrm{e}^{-b_1(x+b_2)^2}+\mathrm{e}^{-b_1(x-b_2)^2}\right)\left(\mathrm{e}^{-b_1(y+b_2)^2}+\mathrm{e}^{-b_1(y-b_2)^2}\right). \tag{C.18}$$

In this expression, there are four distinct linear terms, two of which represent the "classical", or on-diagonal, states, and two of which represent the "coherent", or off-diagonal states. These are constructed by multiplying out the brackets; the classical terms are those given by the product of

$$\mathrm{e}^{-b_1(x\pm b_2)^2}\mathrm{e}^{-b_1(y\pm b_2)^2}, \tag{C.19}$$

and the coherent terms are those given by the product

$$e^{-b_1(x\pm b_2)^2}e^{-b_1(y\mp b_2)^2}. \tag{C.20}$$

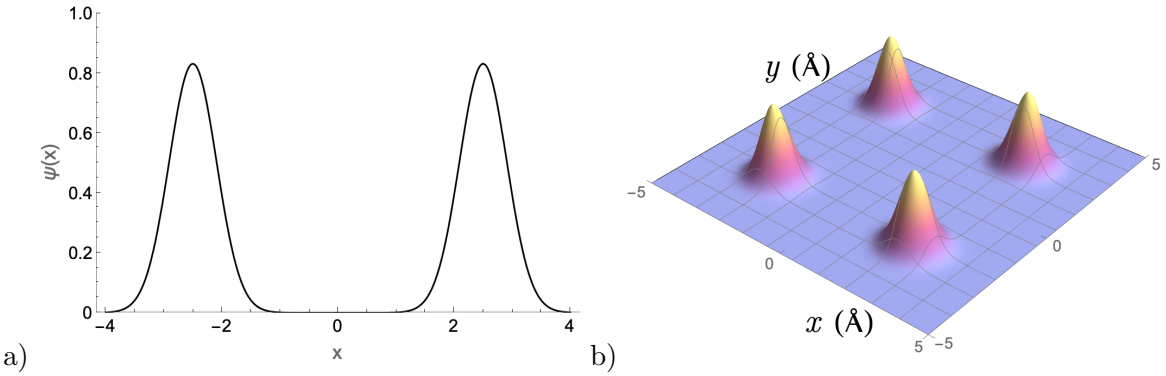

a) b)

Figure C.1: a) The "Schrodinger cat" wavefunction that corresponds to a double Gaussian density matrix. In this case, $b_1 = 3$ and $b_2 = 2.5A$. b) The density matrix corresponding to the wavefunction in a).

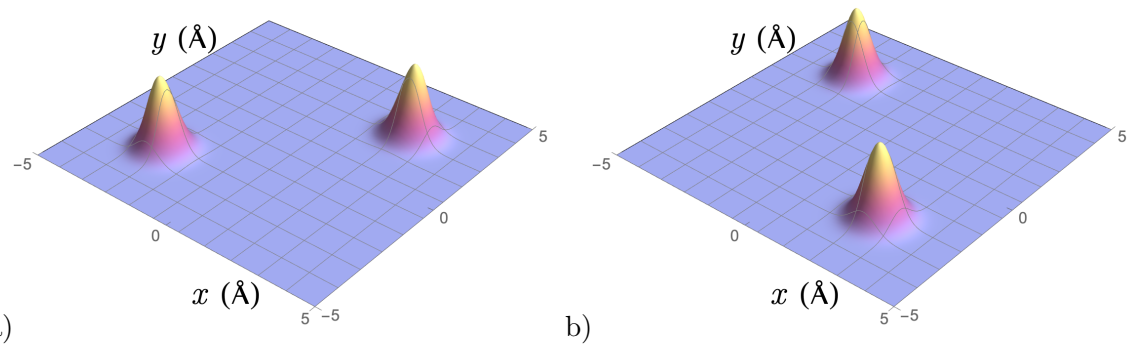

a) b)

Figure C.2: a) The classical, or on-diagonal, components of the double Gaussian initial condition: $e^{-b_1(x\pm b_2)^2}e^{-b_1(y\pm b_2)^2}$. b) The coherent, or off-diagonal, components of the double Gaussian initial condition: $e^{-b_1(x\pm b_2)^2}e^{-b_1(y\mp b_2)^2}$.

In rotated variable space, the double Gaussian is written as

$$\begin{aligned}\rho_0(u,v) = \frac{\sqrt{b_1}}{\sqrt{2\pi}\left(1+e^{-2b_1b_2^2}\right)}&\left(e^{-\frac{b_1}{4}(2u-v-2b_2)^2}+e^{-\frac{b_1}{4}(2u-v+2b_2)^2}\right)\\ &\times\left(e^{-\frac{b_1}{4}(2u+v-2b_2)^2}+e^{-\frac{b_1}{4}(2u+v+2b_2)^2}\right).\end{aligned} \tag{C.21}$$

Each term in this sum is Gaussian in u, so can be Fourier transformed using the identities in Eq. (C.14). This gives

$$\rho_0(K,v) = \frac{1}{2\sqrt{2\pi}\left(1+\mathrm{e}^{-2b_1b_2^2}\right)}\Big(\mathrm{e}^{-\frac{K^2}{8b_1}+ib_2K-\frac{b_1v^2}{2}}+\mathrm{e}^{-\frac{K^2}{8b_1}-ib_2K-\frac{b_1v^2}{2}} \\ +\mathrm{e}^{-\frac{K^2}{8b_1}-\frac{b_1(2b_2+v)^2}{2}}+\mathrm{e}^{-\frac{K^2}{8b_1}-\frac{b_1(2b_2-v)^2}{2}}\Big). \tag{C.22}$$

Here, the first two terms (containing a term linear in K) represent the classical states, or on-diagonal Gaussians, and the second two terms represent the coherent states, or off-diagonal Gaussians. Now, we replace v by v_0 in each of the four terms. We obtain a sum,

$$\rho_0(K,v_0) = \frac{1}{2\sqrt{2\pi}\left(1+\mathrm{e}^{-2b_1b_2^2}\right)}\sum_i \mathrm{e}^{C_2^iK^2+C_1^iK+C_0^i}, \tag{C.23}$$

where the index i takes values p$\pm$ to refer to the populations (classical states) and c$\pm$ to refer to the coherent states. The values of the coefficients are

$$\begin{aligned}
C_2^{\mathrm{p}\pm} &= -\frac{1}{8b_1} - \frac{b_1\hbar^2}{8M^2\gamma^2(1+2R_\Omega)^2}\left(1-\mathrm{e}^{-2\gamma(1+2R_\Omega)t}\right)^2 \\
C_1^{\mathrm{p}\pm} &= \pm ib_2 + \frac{b_1\hbar(x-y)}{2M\gamma(1+2R_\Omega)}\mathrm{e}^{-2\gamma(1+2R_\Omega)t}\left(1-\mathrm{e}^{-2\gamma(1+2R_\Omega)t}\right) \\
C_0^{\mathrm{p}\pm} &= -\frac{1}{2}b_1(x-y)^2\mathrm{e}^{-4\gamma(1+2R_\Omega)t}, \\
C_2^{\mathrm{c}\pm} &= -\frac{1}{8b_1} - \frac{b_1\hbar^2}{8M^2\gamma^2(1+2R_\Omega)^2}\left(1-\mathrm{e}^{-2\gamma(1+2R_\Omega)t}\right)^2 \\
C_1^{\mathrm{c}\pm} &= \frac{b_1\hbar\left(1-\mathrm{e}^{-2\gamma(1+2R_\Omega)t}\right)\left((x-y)\mathrm{e}^{-2\gamma(1+2R_\Omega)t}\pm 2b_2\right)}{2M\gamma(1+2R_\Omega)} \\
C_0^{\mathrm{c}\pm} &= -\frac{1}{2}b_1((x-y)\mathrm{e}^{-2\gamma(1+2R_\Omega)t}\pm 2b_2)^2,
\end{aligned} \tag{C.24}$$

where as before I have replaced $v = x - y$.

Now, the exact time-dependent solution in Fourier space can be written as

$$\begin{aligned}
\rho(K,v,t) &= \frac{1}{2\sqrt{2\pi}\left(1+\mathrm{e}^{-2b_1b_2^2}\right)}\left(\sum_i \mathrm{e}^{C_2^iK^2+C_1^iK+C_0^i}\right)\times \mathrm{e}^{E_2K^2+E_1K+E_0} \\
&= \frac{1}{2\sqrt{2\pi}\left(1+\mathrm{e}^{-2b_1b_2^2}\right)}\sum_i \mathrm{e}^{(E_2+C_2^i)K^2+(E_1+C_1^i)K+(E_0+C_0^i)}.
\end{aligned} \tag{C.25}$$

This is a sum of Gaussians in K, with the coefficients formed by summing the coefficients of

the time-dependent and initial condition parts of the solution. Therefore, taking the inverse Fourier transform is straightforward, and we obtain

$$\rho(x,y,t) = \frac{\mathrm{e}^{E_0}}{2\sqrt{2\pi}\left(1+\mathrm{e}^{-2b_1b_2^2}\right)} \sum_i \frac{1}{\sqrt{-2(E_2+C_2^i)}} \mathrm{e}^{C_0^i - \frac{(E_1+C_1^i - \frac{i(x+y)}{2})^2}{4(E_2+C_2^i)}}, \tag{C.26}$$

with the coefficients given in Eqs. (C.17) ans (C.24).

Appendix D

Benchmarking Coherence Measures

The l_1-norm of coherence has been used throughout as the default coherence measure. This is largely because it is easier to compute than other measures. In addition, it has been shown to be the most general measure of coherence [39]. However, for thoroughness, it is sensible to benchmark the results of the l_1-norm coherence against the relative entropy of coherence, which is the other very widespread coherence measure. This is to ensure that the two crucial dynamical features are obtained using both measures: firstly, that the short-term decoherence process should not be significantly affected by non-Markovian corrections, and secondly, that the coherence resurgence should be present.

The relative entropy of coherence is defined using the incoherent baseline method by

$$C_{\text{ent}}(t) = S\left(\tilde{\rho}^{\text{M}}_{\text{decoh}}(t)\right) - S\left(\tilde{\rho}(t)\right), \tag{D.1}$$

with the von Neumann entropy defined in terms of the purity μ as

$$\begin{aligned} S\left(\tilde{\rho}(t)\right) &= -k_B \text{Tr}\left(\tilde{\rho}\ln\tilde{\rho}\right) \\ &= k_B\left(\frac{1-\mu}{2\mu}\ln\frac{1+\mu}{1-\mu} - \ln\frac{2\mu}{1+\mu}\right). \end{aligned} \tag{D.2}$$

We begin by comparing the l_1-norm of entropy with the relative entropy of coherence over the short timescale ($t < 10$fs) dynamics.

In Figures D.1-D.3, the relative entropy of coherence has been scaled such that $C_{\text{ent}}(0) = C_{l_1}(0)$. It seems that the relative entropy of coherence is slightly more sensitive to the resurgence

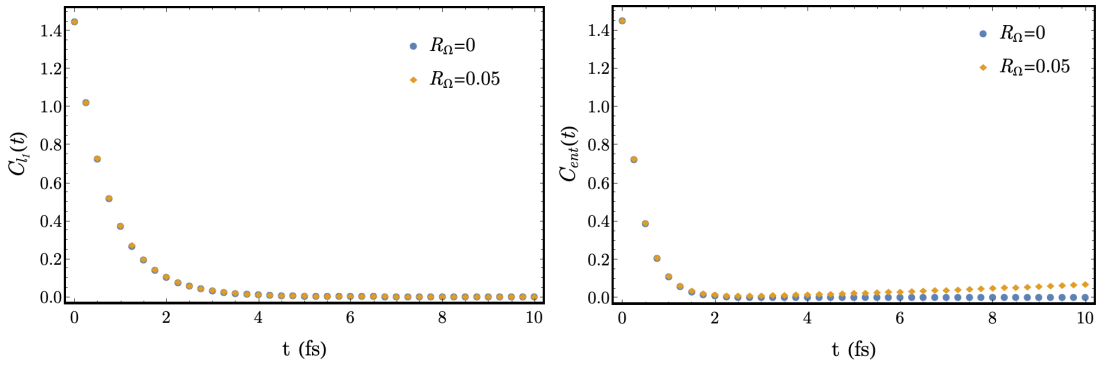

Figure D.1: Benchmarking between l_1-norm of coherence (left) and relative entropy of coherence (right) for the evolution over 10fs of a system with $\gamma = \frac{kT}{10\hbar}$, $T = 320$K in the Markovian and non-Markovian cases.

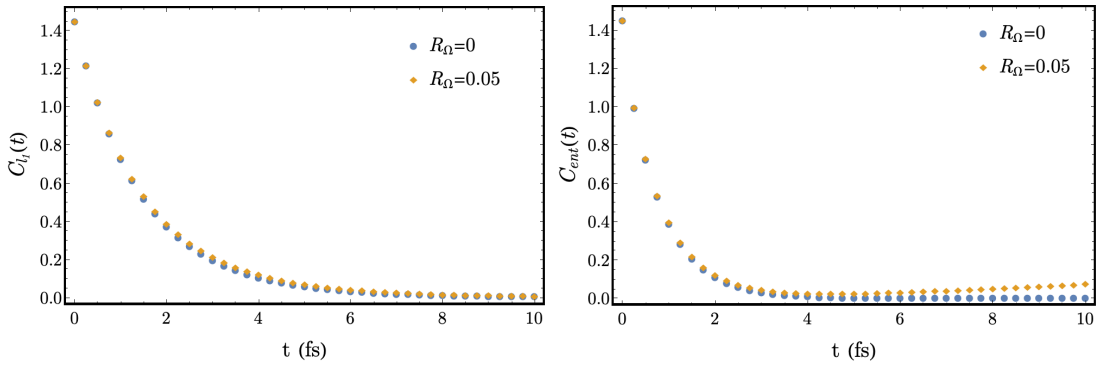

Figure D.2: Benchmarking between l_1-norm of coherence (left) and relative entropy of coherence (right) for the evolution over 10fs of a system with $\gamma = \frac{kT}{20\hbar}$, $T = 320$K in the Markovian and non-Markovian cases.

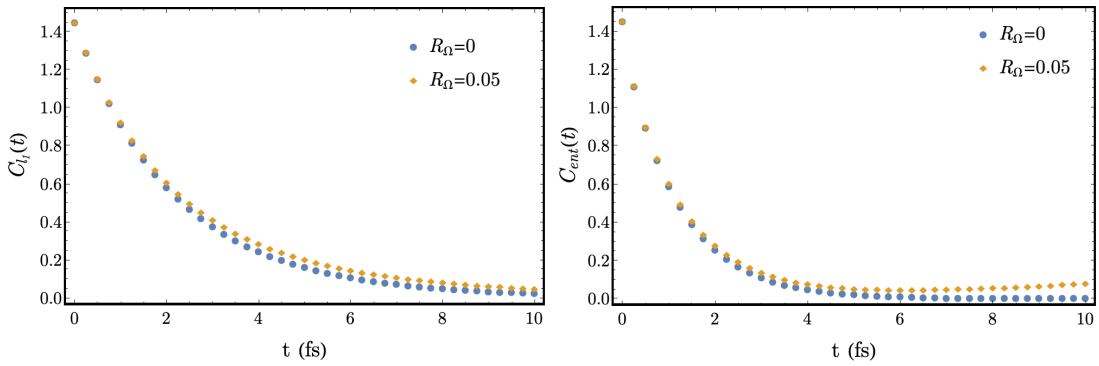

Figure D.3: Benchmarking between l_1-norm of coherence (left) and relative entropy of coherence (right) for the evolution over 10fs of a system with $\gamma = \frac{kT}{30\hbar}$, $T = 320$K in the Markovian and non-Markovian cases.

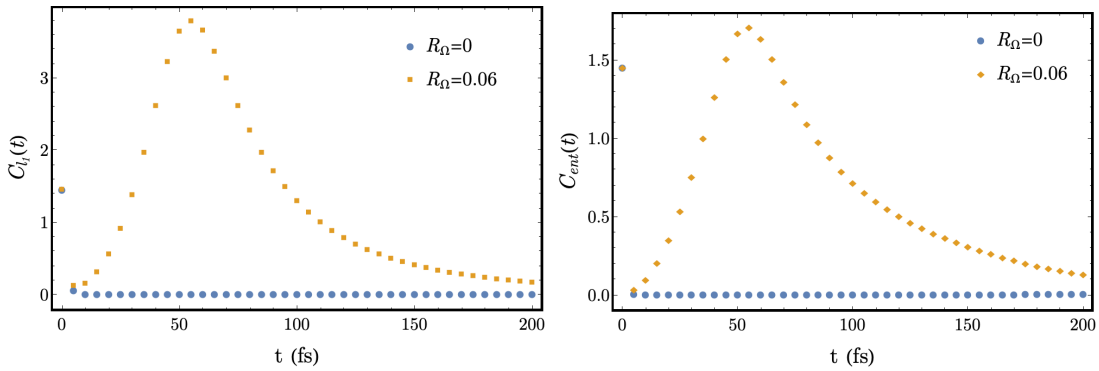

Figure D.4: Benchmarking between l_1-norm of coherence (left) and relative entropy of coherence (right) for the evolution over 200fs of a system with $\gamma = \frac{kT}{30\hbar}$, $T = 320$K in the Markovian and non-Markovian cases. In both cases, the coherence resurgence occurs at the same time, although the magnitude is different.

than the l_1 norm, as there is a slight increase visible in the non-Markovian relative entropy cases which is not present in the l_1-norm case. However, the two coherence measures agree on the main feature of the decoherence, which is that there is no non-Markovian deviation in the main decoherence process, observed over 2fs.

Secondly, we need to benchmark the longer coherence calculations, showing the coherence resurgence which is a main conclusion of this thesis.

In Figure D.4, the relative entropy has again been scaled such that $C_{\text{ent}}(0) = C_{l_1}(0)$. The main feature we are interested in, i.e. the coherence resurgence, is present in both cases. Although the magnitude is not the same, this is not expected. The resurgence peak occurs at the same time, which is all we need.

Although the match between the l_1-norm coherence and the relative entropy of coherence is not perfect, they agree on the main features of the decoherence process and this lends credibility to the conclusions drawn using the l_1-norm of coherence. Additionally, the coherence resurgence is observed in the relative entropy of coherence as well as the l_1-norm of coherence. The magnitudes are not the same but this is not problematic, as we do not draw strong conclusions about the precise value of the coherence, preferring to use more unambiguously defined quantities such as the von Neumann entropy. This benchmarking simply affirms that our conclusions are applicable to general coherence measures, and are not an artifact of our specific choice of the l_1-norm of coherence.

Appendix E

Heat Flow in the non-Markovian Master Equation

The heat flow is conventionally given by

$$\dot{E}_S = \mathrm{Tr}(\dot{\rho} H_S). \tag{E.1}$$

For the free particle case, we have that $H_S = \frac{1}{2M}\hat{p}^2$. We therefore substitute this, as well as the operator form of the master equation (Equation 5.3.11), giving

$$\begin{aligned}\dot{E}_S &= \mathrm{Tr}\left(\frac{1}{2M}\left(\frac{1}{i\hbar}[H_S,\rho] - \frac{i\gamma_R}{\hbar}[q,\{p,\rho\}] - \frac{2M\gamma kT}{\hbar^2}[q,[q,\rho]] + \frac{4RkT}{\hbar^2}[q,[p,\rho]]\right)\hat{p}^2\right) \\ &= -\frac{i}{2M\hbar}\mathrm{Tr}\left([H_S,\rho]\hat{p}^2\right) - \frac{i\gamma_R}{2M\hbar}\mathrm{Tr}\left([q,\{p,\rho\}]\hat{p}^2\right) - \frac{\gamma kT}{\hbar^2}\mathrm{Tr}\left([q,[q,\rho]]\hat{p}^2\right) + \frac{RkT}{M\hbar^2}\mathrm{Tr}\left([q,[p,\rho]]\hat{p}^2\right).\end{aligned} \tag{E.2}$$

We proceed term-wise through the evaluation of this expression, using the techniques described in detail in Appendix F.

For the first term (Hamiltonian), we can use the cyclic property of the trace to obtain 0. Setting $H_S = \frac{\hat{p}^2}{2m}$ and multiplying out the term gives

$$\mathrm{Tr}\left((\hat{p}^2\tilde{\rho} - \tilde{\rho}\hat{p}^2)\hat{p}^2\right) = \mathrm{Tr}\left(\hat{p}^2\tilde{\rho}\hat{p}^2\right) - \mathrm{Tr}\left((\tilde{\rho}\hat{p}^2)\hat{p}^2\right). \tag{E.3}$$

According the cyclic property of the trace, i.e. that $\mathrm{Tr}(AB) = \mathrm{Tr}(BA)$, the two terms are equal and so cancel out.

For the second term (relaxation), we evaluate the matrix elements directly to obtain

$$\langle x|[q,\{p,\rho\}]\hat{p}^2|y\rangle = -i\hbar^3\Big(x\frac{\partial^3}{\partial x\partial y^2} - x\frac{\partial^3}{\partial y^3} - 2\frac{\partial^2}{\partial x\partial y} - y\frac{\partial^3}{\partial x\partial y^2} + 2\frac{\partial^2}{\partial y^2} + y\frac{\partial^3}{\partial y^3}\Big)\rho(x,y). \quad \text{(E.4)}$$

After taking the trace by setting $x = y$ and integrating, we are left with

$$-\frac{i\gamma_R}{2M\hbar}\mathrm{Tr}\left([q,\{p,\rho\}]\hat{p}^2\right) = -\frac{\gamma_R\hbar^2}{M}\int \mathrm{d}x\left(\frac{\partial^2}{\partial y^2} - \frac{\partial^2}{\partial y\partial x}\right)\tilde{\rho}(x,y). \quad \text{(E.5)}$$

The conventional interpretation of this expression is that the integrand should be evaluated directly, then the substitution $x = y$ is made before the integration is performed. However, we are able to remove some terms before the substitution is formally made due to their $(x - y)$ dependence - we can see that this will not contribute to the trace.

The fourth term (orthogonal) is addressed in the same way (and we address it before the third because it shares the same operators in a different combination). For the matrix elements, we obtain

$$\langle x|[q,\{p,\rho\}]\hat{p}^2|y\rangle = -i\hbar^3\Big(x\frac{\partial^3}{\partial x\partial y^2} + x\frac{\partial^3}{\partial y^3} - 2\frac{\partial^2}{\partial x\partial y} - y\frac{\partial^3}{\partial x\partial y^2} - 2\frac{\partial^2}{\partial y^2} - y\frac{\partial^3}{\partial y^3}\Big)\rho(x,y) \quad \text{(E.6)}$$

Therefore, we obtain

$$\frac{RkT}{M\hbar^2}\mathrm{Tr}\left([q,[p,\rho]]\hat{p}^2\right) = -\frac{iR\hbar kT}{M}\int \mathrm{d}x\left(\frac{\partial^2}{\partial y^2} + \frac{\partial^2}{\partial y\partial x}\right)\tilde{\rho}(x,y). \quad \text{(E.7)}$$

Similarly, it is intended that the integrand be evaluated before the trace is taken. This contribution is imaginary and therefore we require that the integral is 0; this is because the heat flow is an observable and cannot be complex. Computation of this term confirms that it does cancel.

Finally, the third term (decoherence) has matrix elements

$$\langle x|[q,[q,\rho]]\hat{p}^2|y\rangle = -\hbar^2\Big((x-y)^2\frac{\partial^2}{\partial y^2} - 4(x-y)\frac{\partial}{\partial y} + 2\Big)\tilde{\rho}(x,y). \quad \text{(E.8)}$$

This simplifies when we take the trace to

$$\begin{aligned} -\frac{\gamma kT}{\hbar^2}\mathrm{Tr}\left([q,\{p,\rho\}]\hat{p}^2\hat{p}^2\right) &= 2\gamma kT\int \mathrm{d}x\tilde{\rho}(x,x) \\ &= 2\gamma kT, \end{aligned} \tag{E.9}$$

due to the property $\mathrm{Tr}(\tilde{\rho}) = 1$.

It is clear that the dominant term in the energy flow will be from the decoherence term: the relaxation term is $O(\hbar^4)$ and so can be discarded as negligible. Therefore, we can say that

$$\dot{E}_S = 2\gamma kT + O(\hbar^2); \tag{E.10}$$

the heat flow is constant in the dominant term.

Appendix F

Wigner Transforms of Orthogonal and Potential Terms

In this Appendix, we derive the Wigner transform of the orthogonal term,

$$\hat{L}_{\mathrm{O}} = \frac{4kT}{\hbar^2}[\hat{q},[\hat{p},\tilde{\rho}]], \tag{F.1}$$

and the potential term,

$$\hat{L}_{\mathrm{V}}\tilde{\rho} = \frac{1}{2\hbar^2}[\hat{q},\{\tilde{\rho},[\hat{p},\hat{\mathrm{V}}_R]\}], \tag{F.2}$$

which appear in the operator form of the non-Markovian master equation. This is done by applying the definition of the Wigner transform,

$$W_{\tilde{\rho}}(q,p,t) = \frac{1}{\hbar}\int \mathrm{d}u \ \exp\Big\{i\frac{pu}{\hbar}\Big\}\left\langle q-\frac{u}{2}|\tilde{\rho}|q+\frac{u}{2}\right\rangle, \tag{F.3}$$

to the terms that arise when the operator brackets are multiplied out.

F.1 Preliminaries

As mentioned in the main text, we use the identities

$$\langle x|\hat{q}|y\rangle = x\delta(x-y) \tag{F.1}$$

$$\langle x|\hat{\mathrm{v}}_R|y\rangle = \hat{\mathrm{v}}_R(x)\delta(x-y) \tag{F.2}$$

and

$$\langle x|\hat{p}|y\rangle = -i\hbar\frac{\partial}{\partial x}\delta(x-y) = i\hbar\frac{\partial}{\partial y}\delta(x-y) \tag{F.3}$$

to evaluate the Wigner transform. Therefore, we can make the substitution

$$\langle q-\frac{u}{2}|\hat{q}|A_1\rangle = \left(q-\frac{u}{2}\right)\delta(A_1-q+\frac{u}{2}), \tag{F.4}$$

for instance. Additionally, we define the useful derivative identity

$$\partial_{q\pm\frac{u}{2}} = \frac{1}{2}\partial_q \pm \partial_u. \tag{F.5}$$

. We make frequent use of integration by parts to evaluate derivatives of δ-functions, for example

$$\int \mathrm{d}A_2\,\langle x|\tilde{\rho}|A_2\rangle\,\frac{\partial}{\partial A_2}\delta(A_2-y) = -\frac{\partial}{\partial y}\,\langle x|\tilde{\rho}|y\rangle\,. \tag{F.6}$$

F.2 Wigner Transform of the Orthogonal Term

When we expand the commutator relation of the orthogonal term we find

$$[\hat{q},[\hat{p},\tilde{\rho}]] = \hat{q}\hat{p}\tilde{\rho} - \hat{q}\tilde{\rho}\hat{p} - \hat{p}\tilde{\rho}\hat{q} + \tilde{\rho}\hat{p}\hat{q}. \tag{F.1}$$

We proceed term-by-term finding the Wigner transforms:

$$\begin{aligned}(\hat{q}\hat{p}\tilde{\rho})_W &= \frac{1}{\hbar}\int \mathrm{d}u\,\exp\Big\{-i\frac{pu}{\hbar}\Big\}\int \mathrm{d}A_1\mathrm{d}A_2\,\langle q-\frac{u}{2}|\hat{q}|A_1\rangle\,\langle A_1|\hat{p}|A_2\rangle\,\langle A_2|\tilde{\rho}|q+\frac{u}{2}\rangle \\ &= -\frac{1}{\hbar}(i\hbar)\int \mathrm{d}u\,\exp\Big\{-i\frac{pu}{\hbar}\Big\}\int \mathrm{d}A_1\mathrm{d}A_2\left(q-\frac{u}{2}\right)\delta\left(A_1-q+\frac{u}{2}\right)\frac{\partial}{\partial A_2}\delta\left(A_2-A_1\right)\langle A_2|\tilde{\rho}|q+\frac{u}{2}\rangle \\ &= \frac{1}{\hbar}(i\hbar)\int \mathrm{d}u\,\exp\Big\{-i\frac{pu}{\hbar}\Big\}\left(q-\frac{u}{2}\right)\left(\frac{1}{2}\partial_q-\partial_u\right)\langle q-\frac{u}{2}|\tilde{\rho}|q+\frac{u}{2}\rangle\,.\end{aligned} \tag{F.2}$$

The commutator structure means we can write down a corresponding expression,

$$-(\hat{p}\tilde{\rho}\hat{q})_W = -\frac{1}{\hbar}(i\hbar)\int \mathrm{d}u\,\exp\Big\{-i\frac{pu}{\hbar}\Big\}\left(q+\frac{u}{2}\right)\left(\frac{1}{2}\partial_q-\partial_u\right)\langle q-\frac{u}{2}|\tilde{\rho}|q+\frac{u}{2}\rangle\,, \tag{F.3}$$

by making the replacement $\left(q-\frac{u}{2}\right)\to\left(q+\frac{u}{2}\right)$. Similarly for the other "commutator pair" we can write down

$$\begin{aligned}-\left(\hat{q}\tilde{\rho}\hat{p}\right)_W &= \frac{1}{\hbar}\int \mathrm{d}u \exp\Big\{-i\frac{pu}{\hbar}\Big\}\int \mathrm{d}A_1\mathrm{d}A_2 \left\langle q-\frac{u}{2}|\hat{q}|A_1\right\rangle \left\langle A_1|\tilde{\rho}|A_2\right\rangle \left\langle A_2|\hat{p}|q+\frac{u}{2}\right\rangle \\ &= -\frac{1}{\hbar}(i\hbar)\int \mathrm{d}u \exp\Big\{-i\frac{pu}{\hbar}\Big\}\int \mathrm{d}A_1\mathrm{d}A_2 \left(q-\frac{u}{2}\right)\delta\left(A_1-q+\frac{u}{2}\right)\left\langle A_1|\tilde{\rho}|A_2\right\rangle \frac{\partial}{\partial A_2}\delta\left(A_2-q-\frac{u}{2}\right) \\ &= \frac{1}{\hbar}(i\hbar)\int \mathrm{d}u \exp\Big\{-i\frac{pu}{\hbar}\Big\}\left(q-\frac{u}{2}\right)\left(\frac{1}{2}\partial_q+\partial_u\right)\left\langle q-\frac{u}{2}|\tilde{\rho}|q+\frac{u}{2}\right\rangle\end{aligned} \tag{F.4}$$

and

$$\left(\tilde{\rho}\hat{p}\hat{q}\right)_W = -\frac{1}{\hbar}(i\hbar)\int \mathrm{d}u \exp\Big\{-i\frac{pu}{\hbar}\Big\}\left(q+\frac{u}{2}\right)\left(\frac{1}{2}\partial_q+\partial_u\right)\left\langle q-\frac{u}{2}|\tilde{\rho}|q+\frac{u}{2}\right\rangle. \tag{F.5}$$

Summing these terms gives us

$$\begin{aligned}\left[\hat{q},\left[\hat{p},\tilde{\rho}\right]\right]_W &= -\frac{1}{\hbar}(i\hbar)\int \mathrm{d}u \exp\Big\{-i\frac{pu}{\hbar}\Big\}u\ \partial_q\left\langle q-\frac{u}{2}|\tilde{\rho}|q+\frac{u}{2}\right\rangle \\ &= -(i\hbar)^2\frac{1}{\hbar}\int \mathrm{d}u\ \partial_p \exp\Big\{-i\frac{pu}{\hbar}\Big\}\partial_q\left\langle q-\frac{u}{2}|\tilde{\rho}|q+\frac{u}{2}\right\rangle.\end{aligned} \tag{F.6}$$

The derivatives can simply be moved outside of the integral to leave

$$\begin{aligned}\left[\hat{q},\left[\hat{p},\tilde{\rho}\right]\right]_W &= \hbar^2\ \partial_p\partial_q\frac{1}{\hbar}\int \mathrm{d}u \exp\Big\{-i\frac{pu}{\hbar}\Big\}\left\langle q-\frac{u}{2}|\tilde{\rho}|q+\frac{u}{2}\right\rangle \\ &= \hbar^2\partial_p\partial q W.\end{aligned} \tag{F.7}$$

Therefore,

$$\begin{aligned}\left(\hat{L}_{\mathrm{O}}\right)_W &= \frac{4kT}{\hbar^2}\left(\hbar^2\partial_p\partial q W\right) \\ &= 4kT\partial_p\partial q W.\end{aligned} \tag{F.8}$$

F.3 Wigner Transform of the Potential Term

We use the same approach to calculate the Wigner transform of the potential term. The calculation is slightly more involved because there are more terms to calculate:

$$\left[\hat{q},\{\tilde{\rho},\left[\hat{p},\hat{\mathrm{V}}_R\right]\}\right] = \hat{q}\rho\hat{p}\hat{\mathrm{V}}_R - \hat{q}\rho\hat{\mathrm{V}}_R\hat{p} + \hat{q}\hat{p}\hat{\mathrm{V}}_R\rho - \hat{q}\hat{\mathrm{V}}_R\hat{p}\rho - \rho\hat{p}\hat{\mathrm{V}}_R\hat{q} + \rho\hat{\mathrm{V}}_R\hat{p}\hat{q} - \hat{p}\hat{\mathrm{V}}_R\rho\hat{q} + \hat{\mathrm{V}}_R\hat{p}\rho\hat{q}. \tag{F.1}$$

However, once again we can use the commutator structure to slightly simplify things. Proceeding term by term as before, we calculate

$$\begin{aligned}(\hat{q}\tilde{\rho}\hat{p}\hat{\mathrm{V}}_R)_W &= \frac{1}{\hbar}\int \mathrm{d}u\ \mathrm{e}^{-i\frac{pu}{\hbar}} \int \mathrm{d}A_1\mathrm{d}A_2\mathrm{d}A_3 \left\langle q-\frac{u}{2}|\hat{q}|A_1\right\rangle \left\langle A_1|\tilde{\rho}|A_2\right\rangle \left\langle A_2|\hat{p}|A_3\right\rangle \left\langle A_3|\hat{\mathrm{V}}_R|q+\frac{u}{2}\right\rangle \\ &= \frac{1}{\hbar}(i\hbar)\int \mathrm{d}u\ \mathrm{e}^{-i\frac{pu}{\hbar}}\mathrm{V}_R(q+\frac{u}{2})(q-\frac{u}{2})(\frac{1}{2}\partial_q+\partial_u)\left\langle q-\frac{u}{2}|\tilde{\rho}|q+\frac{u}{2}\right\rangle,\end{aligned} \tag{F.2}$$

where we have used the same process as for the orthogonal term but omitted some details of the calculation. The other half of the commutator pair is

$$-(\tilde{\rho}\hat{p}\hat{\mathrm{V}}_R\hat{q})_W = -\frac{1}{\hbar}(i\hbar)\int \mathrm{d}u\ \mathrm{e}^{-i\frac{pu}{\hbar}}\mathrm{V}_R(q+\frac{u}{2})(q+\frac{u}{2})(\frac{1}{2}\partial_q+\partial_u)\left\langle q-\frac{u}{2}|\tilde{\rho}|q+\frac{u}{2}\right\rangle. \tag{F.3}$$

We proceed through the rest of the terms:

$$\begin{aligned}-(\hat{q}\tilde{\rho}\hat{\mathrm{V}}_R\hat{p})_W &= -\frac{1}{\hbar}\int \mathrm{d}u\ \mathrm{e}^{-i\frac{pu}{\hbar}} \int \mathrm{d}A_1\mathrm{d}A_2\mathrm{d}A_3 \left\langle q-\frac{u}{2}|\hat{q}|A_1\right\rangle \left\langle A_1|\tilde{\rho}|A_2\right\rangle \left\langle A_2|\hat{\mathrm{V}}_R|A_3\right\rangle \left\langle A_3|\hat{p}|q+\frac{u}{2}\right\rangle \\ &= -\frac{1}{\hbar}(i\hbar)\int \mathrm{d}u\ \mathrm{e}^{-i\frac{pu}{\hbar}}(q-\frac{u}{2})(\frac{1}{2}\partial_q+\partial_u)\left[\mathrm{V}_R(q+\frac{u}{2})\left\langle q-\frac{u}{2}|\tilde{\rho}|q+\frac{u}{2}\right\rangle\right]\end{aligned} \tag{F.4}$$

and

$$(\tilde{\rho}\hat{\mathrm{V}}_R\hat{p}\hat{q})_W = \frac{1}{\hbar}(i\hbar)\int \mathrm{d}u\ \mathrm{e}^{-i\frac{pu}{\hbar}}(q+\frac{u}{2})(\frac{1}{2}\partial_q+\partial_u)\left[\mathrm{V}_R(q+\frac{u}{2})\left\langle q-\frac{u}{2}|\tilde{\rho}|q+\frac{u}{2}\right\rangle\right], \tag{F.5}$$

$$\begin{aligned}(\hat{q}\hat{p}\hat{\mathrm{V}}_R\tilde{\rho})_W &= \frac{1}{\hbar}\int \mathrm{d}u\ \mathrm{e}^{-i\frac{pu}{\hbar}} \int \mathrm{d}A_1\mathrm{d}A_2\mathrm{d}A_3 \left\langle q-\frac{u}{2}|\hat{q}|A_1\right\rangle \left\langle A_1|\hat{p}|A_2\right\rangle \left\langle A_2|\hat{\mathrm{V}}_R|A_3\right\rangle \left\langle A_3|\tilde{\rho}|q+\frac{u}{2}\right\rangle \\ &= -\frac{1}{\hbar}(i\hbar)\int \mathrm{d}u\ \mathrm{e}^{-i\frac{pu}{\hbar}}(q-\frac{u}{2})(\frac{1}{2}\partial_q-\partial_u)\left[\mathrm{V}_R(q-\frac{u}{2})\left\langle q-\frac{u}{2}|\tilde{\rho}|q+\frac{u}{2}\right\rangle\right]\end{aligned} \tag{F.6}$$

and

$$-(\hat{p}\hat{\mathrm{V}}_R\tilde{\rho}\hat{q})_W = \frac{1}{\hbar}(i\hbar)\int \mathrm{d}u\ \mathrm{e}^{-i\frac{pu}{\hbar}}(q+\frac{u}{2})(\frac{1}{2}\partial_q-\partial_u)\left[\mathrm{V}_R(q-\frac{u}{2})\left\langle q-\frac{u}{2}|\tilde{\rho}|q+\frac{u}{2}\right\rangle\right], \tag{F.7}$$

and finally

$$
\begin{aligned}
(\hat{q}\hat{\mathrm{V}}_R\hat{p}\tilde{\rho})_W &= \frac{1}{\hbar}\int \mathrm{d}u\ \mathrm{e}^{-i\frac{pu}{\hbar}} \int \mathrm{d}A_1\mathrm{d}A_2\mathrm{d}A_3\, \langle q-\frac{u}{2}|\hat{q}|A_1\rangle \langle A_1|\hat{\mathrm{V}}_R|A_2\rangle \langle A_2|\hat{p}|A_3\rangle \langle A_3|\tilde{\rho}|q+\frac{u}{2}\rangle \\
&= \frac{1}{\hbar}(i\hbar)\int \mathrm{d}u\ \mathrm{e}^{-i\frac{pu}{\hbar}}\mathrm{V}_R(q-\frac{u}{2})(q-\frac{u}{2})(\frac{1}{2}\partial_q+\partial_u)\,\langle q-\frac{u}{2}|\tilde{\rho}|q+\frac{u}{2}\rangle
\end{aligned}
\tag{F.8}
$$

and

$$
-(\hat{\mathrm{V}}_R\hat{p}\tilde{\rho}\hat{q})_W = -\frac{1}{\hbar}(i\hbar)\int \mathrm{d}u\ \mathrm{e}^{-i\frac{pu}{\hbar}}\mathrm{V}_R(q-\frac{u}{2})(q+\frac{u}{2})(\frac{1}{2}\partial_q+\partial_u)\,\langle q-\frac{u}{2}|\tilde{\rho}|q+\frac{u}{2}\rangle\,. \tag{F.9}
$$

When we sum these terms, we see that they simplify dramatically, leaving us with

$$
\begin{aligned}
[\hat{q},\{\tilde{\rho},[\hat{p},\hat{\mathrm{V}}_R]\}]_W = \frac{1}{\hbar}(i\hbar)\int \mathrm{d}u\ \mathrm{e}^{-i\frac{pu}{\hbar}} u\Big[\frac{1}{2}\partial_q\Big(\mathrm{V}_R(q+\frac{u}{2})+\mathrm{V}_R(q-\frac{u}{2})\Big)+\partial_u\Big(\mathrm{V}_R(q+\frac{u}{2})-\mathrm{V}_R(q-\frac{u}{2})\Big)\Big] \\
\times\,\langle q-\frac{u}{2}|\rho|q+\frac{u}{2}\rangle\,.
\end{aligned}
\tag{F.10}
$$

We use the Taylor series to address the potential terms, leading to an infinite sum in phase space:

$$
\mathrm{V}_R(q\pm\frac{u}{2}) = \sum_{n=0}\frac{1}{n!}\frac{\partial^n}{\partial q^n}\mathrm{V}_R(q)\left(\pm\frac{u}{2}\right)^n. \tag{F.11}
$$

We can therefore calculate the derivatives,

$$
\begin{aligned}
\mathrm{V}_R(q+\frac{u}{2})+\mathrm{V}_R(q-\frac{u}{2}) &= \sum_{n=0}\frac{1}{n!}\mathrm{V}_R^{(n)}(q)[(1)^n+(-1)^n]\Big(\frac{u}{2}\Big)^n \\
&= \sum_{n=0}\frac{2}{(2n)!}\mathrm{V}_R^{(2n)}(q)\Big(\frac{u}{2}\Big)^{2n} \\
\implies \frac{1}{2}\partial_q\Big[\mathrm{V}_R(q+\frac{u}{2})+\mathrm{V}_R(q-\frac{u}{2})\Big] &= \sum_{n=0}\frac{1}{(2n)!}\mathrm{V}_R^{(2n+1)}(q)\Big(\frac{u}{2}\Big)^{2n}
\end{aligned}
\tag{F.12}
$$

and

$$
\begin{aligned}
\mathrm{V}_R(q+\frac{u}{2})-\mathrm{V}_R(q-\frac{u}{2}) &= \sum_{n=0}\frac{1}{n!}\mathrm{V}_R^{(n)}(q)[(1)^n-(-1)^n]\left(\frac{u}{2}\right)^n \\
&= \sum_{n=0}\frac{2}{(2n+1)!}\mathrm{V}_R^{(2n+1)}(q)\left(\frac{u}{2}\right)^{2n+1} \\
\implies \partial_u\left[\mathrm{V}_R(q+\frac{u}{2})-\mathrm{V}_R(q-\frac{u}{2})\right] &= \sum_{n=0}\frac{1}{(2n)!}\mathrm{V}_R^{(2n+1)}(q)\left(\frac{u}{2}\right)^{2n}.
\end{aligned}
\tag{F.13}
$$

Therefore, we have

$$
\begin{aligned}
[\hat{q},\{\rho,[\hat{p},\hat{v}]\}]_W &= \sum_{n=0}\frac{8}{(2n)!}\mathrm{V}_R^{(2n+1)}(q)\frac{1}{\hbar}\left(\frac{i\hbar}{2}\right)\int \mathrm{d}u\ \mathrm{e}^{-i\frac{pu}{\hbar}}\left(\frac{u}{2}\right)^{2n+1}\langle q-\frac{u}{2}|\rho|q+\frac{u}{2}\rangle \\
&= \sum_{n=0}\frac{8}{(2n)!}\mathrm{V}_R^{(2n+1)}(q)\left(\frac{i\hbar}{2}\right)\left(\frac{-i\hbar}{2}\right)^{2n+1}\frac{\partial^{2n+1}}{\partial p^{2n+1}}\frac{1}{\hbar}\int \mathrm{d}u\ \mathrm{e}^{-i\frac{pu}{\hbar}}\langle q-\frac{u}{2}|\rho|q+\frac{u}{2}\rangle \\
&= 2\hbar^2\sum_{n=0}\frac{1}{(2n)!}(-\hbar^2)^n\left(\frac{1}{2}\right)^{2n}\frac{\partial^{2n+1}\mathrm{V}_R(q)}{\partial q^{2n+1}}\frac{\partial^{2n+1}W}{\partial p^{2n+1}},
\end{aligned}
\tag{F.14}
$$

and the Wigner transform of the potential term is then

$$
\left(\hat{L}_{\mathrm{V}}\right)_W = \sum_{n=0}\frac{1}{(2n)!}(-\hbar^2)^n\left(\frac{1}{2}\right)^{2n}\frac{\partial^{2n+1}\mathrm{V}_R(q)}{\partial q^{2n+1}}\frac{\partial^{2n+1}W}{\partial p^{2n+1}}. \tag{F.15}
$$

In the $\hbar\to 0$ limit, this goes to

$$
\lim_{\hbar\to 0}\left(\hat{L}_{\mathrm{V}}\right)_W = \frac{\partial \mathrm{V}_R(q)}{\partial q}\frac{\partial W}{\partial p}. \tag{F.16}
$$

Bibliography

[1] T. Farrow, V. Vedral, *Optics Communications* **2015**, *337*, 22–26.

[2] W. H. Zurek, *Reviews of Modern Physics* **2003**, *75*, 715.

[3] J. D. Trimmer, *Proceedings of the American Philosophical Society* **1980**, 323–338.

[4] E. P. Wigner in *Philosophical Reflections and Syntheses*, Springer, **1995**, pp. 247–260.

[5] W. H. Zurek, *Annalen der Physik* **2000**, *9*, 855–864.

[6] W. H. Zurek, *Physical Review D* **1981**, *24*, 1516.

[7] W. H. Zurek, *Physical Review D* **1982**, *26*, 1862.

[8] M. Schlosshauer, *Reviews of Modern physics* **2005**, *76*, 1267.

[9] H.-P. Breuer, F. Petruccione, et al., *The theory of open quantum systems*, Oxford University Press on Demand, **2002**.

[10] U. Weiss, *Quantum dissipative systems*, *Vol. 13*, World scientific, **2012**.

[11] S. F. Huelga, M. B. Plenio, *Contemporary Physics* **2013**, *54*, 181–207.

[12] Y. Kim, F. Bertagna, E. M. D'Souza, D. J. Heyes, L. O. Johannissen, E. T. Nery, A. Pantelias, A. Sanchez-Pedreño Jimenez, L. Slocombe, M. G. Spencer, et al., *Quantum Reports* **2021**, *3*, 80–126.

[13] F. Caruso, A. W. Chin, A. Datta, S. F. Huelga, M. B. Plenio, *The Journal of Chemical Physics* **2009**, *131*, 09B612.

[14] A. Chin, J. Prior, R. Rosenbach, F. Caycedo-Soler, S. F. Huelga, M. B. Plenio, *Nature Physics* **2013**, *9*, 113–118.

[15] G. S. Engel, T. R. Calhoun, E. L. Read, T.-K. Ahn, T. Mančal, Y.-C. Cheng, R. E. Blankenship, G. R. Fleming, *Nature* **2007**, *446*, 782–786.

[16] G. D. Scholes, G. R. Fleming, L. X. Chen, A. Aspuru-Guzik, A. Buchleitner, D. F. Coker, G. S. Engel, R. Van Grondelle, A. Ishizaki, D. M. Jonas, et al., *Nature* **2017**, *543*, 647–656.

[17] W. Wiltschko, R. Wiltschko, *Science* **1972**, *176*, 62–64.

[18] R. Wiltschko, W. Wiltschko, *Biosensors* **2014**, *4*, 221–242.

[19] T. Ritz, P. Thalau, J. B. Phillips, R. Wiltschko, W. Wiltschko, *Nature* **2004**, *429*, 177–180.

[20] B. Adams, I. Sinayskiy, F. Petruccione, *Scientific Reports* **2018**, *8*, 1–10.

[21] M. Tiersch, U. E. Steiner, S. Popescu, H. J. Briegel, *The Journal of Physical Chemistry A* **2012**, *116*, 4020–4028.

[22] P.-O. Löwdin, *Reviews of Modern Physics* **1963**, *35*, 724.

[23] D. Devault, *Quarterly Reviews of biophysics* **1980**, *13*, 387–564.

[24] J. Hopfield, *Proceedings of the National Academy of Sciences* **1974**, *71*, 3640–3644.

[25] O. Pusuluk, T. Farrow, C. Deliduman, K. Burnett, V. Vedral, *Proceedings of the Royal Society A: Mathematical Physical and Engineering Sciences* **2018**, *474*, 20180037.

[26] C. Marletto, D. Coles, T. Farrow, V. Vedral, *Journal of Physics Communications* **2018**, *2*, 101001.

[27] C. Y. Lee, W. Choi, J.-H. Han, M. S. Strano, *Science* **2010**, *329*, 1320–1324.

[28] V. Salari, J. Tuszynski, M. Rahnama, G. Bernroider in Journal of Physics: Conference Series, *Vol. 306*, IOP Publishing, **2011**, p. 012075.

[29] F. H. C. Crick, J. D. Watson, *Proceedings of the Royal Society of London. Series A. Mathematical and Physical Sciences* **1954**, *223*, 80–96.

[30] L. Slocombe, J. Al-Khalili, M. Sacchi, *Physical Chemistry Chemical Physics* **2021**, *23*, 4141–4150.

[31] A. O. Caldeira, A. J. Leggett, *Physica A: Statistical Mechanics and its Applications* **1983**, *121*, 587–616.

[32] A. Kolli, E. J. O'Reilly, G. D. Scholes, A. Olaya-Castro, *The Journal of Chemical Physics* **2012**, *137*, 174109.

[33] A. Kolli, A. Nazir, A. Olaya-Castro, *The Journal of Chemical Physics* **2011**, *135*, 154112.

[34] F. Tacchino, A. Succurro, O. Ebenhöh, D. Gerace, *Scientific Reports* **2019**, *9*, 1–13.

[35] X.-M. Lu, X. Wang, C. Sun, *Physical Review A* **2010**, *82*, 042103.

[36] N. Werren, PhD thesis, **2019**.

[37] S. Lally, N. Werren, J. Al-Khalili, A. Rocco, *Physical Review A* **2022**, *105*, 012209.

[38] B. L. Hu, J. P. Paz, Y. Zhang, *Physical Review D* **1992**, *45*, 2843.

[39] T. Baumgratz, M. Cramer, M. B. Plenio, *Physical Review Letters* **2014**, *113*, 140401.

[40] Á. Rivas, S. F. Huelga, M. B. Plenio, *Reports on Progress in Physics* **2014**, *77*, 094001.

[41] A. Rivas, S. F. Huelga, *Open quantum systems*, *Vol. 10*, Springer, **2012**.

[42] H. D. Zeh, *Foundations of Physics* **1970**, *1*, 69–76.

[43] I. Rotter, J. Bird, *Reports on Progress in Physics* **2015**, *78*, 114001.

[44] D. Porras, F. Marquardt, J. Von Delft, J. I. Cirac, *Physical Review A* **2008**, *78*, 010101.

[45] M. Kostin, *The Journal of Chemical Physics* **1972**, *57*, 3589–3591.

[46] K. Yasue, *Annals of Physics* **1978**, *114*, 479–496.

[47] H. Dekker, *Physical Review A* **1977**, *16*, 2126.

[48] I. Senitzky, *Physical Review* **1960**, *119*, 670.

[49] G. Ford, M. Kac, P. Mazur, *Journal of Mathematical Physics* **1965**, *6*, 504–515.

[50] G. Ford, M. Kac, *Journal of Statistical Physics* **1987**, *46*, 803–810.

[51] G. Ford, R. O'Connell, *Physical Review Letters* **2006**, *96*, 020402.

[52] R. Kubo, *Reports on Progress in Physics* **1966**, *29*, 255.

[53] H. Risken in *The Fokker-Planck Equation: Methods of Solution and Applications*, Springer Berlin Heidelberg, Berlin, Heidelberg, **1996**, pp. 63–95.

[54] W. C. Kerr, A. Graham, *The European Physical Journal B-Condensed Matter and Complex Systems* **2000**, *15*, 305–311.

[55] S. I. Denisov, W. Horsthemke, P. Hänggi, *The European Physical Journal B* **2009**, *68*, 567–575.

[56] C. Addis, G. Brebner, P. Haikka, S. Maniscalco, *Physical Review A* **2014**, *89*, 024101.

[57] S. Groeblacher, A. Trubarov, N. Prigge, G. Cole, M. Aspelmeyer, J. Eisert, *Nature Communications* **2015**, *6*, 1–6.

[58] C. Kittel, P. McEuen, P. McEuen, *Introduction to solid state physics*, *Vol. 8*, Wiley New York, **1996**.

[59] H.-P. Breuer, E.-M. Laine, J. Piilo, B. Vacchini, *Reviews of Modern Physics* **2016**, *88*, 021002.

[60] V. Vedral, *Reviews of Modern Physics* **2002**, *74*, 197.

[61] A. Winter, D. Yang, *Physical Review Letters* **2016**, *116*, 120404.

[62] A. Streltsov, G. Adesso, M. B. Plenio, *Reviews of Modern Physics* **2017**, *89*, 041003.

[63] W. H. Zurek, *Progress of Theoretical Physics* **1993**, *89*, 281–312.

[64] M. Schlosshauer, *Physics Reports* **2019**, *831*, 1–57.

[65] S. Lloyd, PhD thesis, Rockefeller University, **1988**.

[66] M. A. Schlosshauer, *Decoherence: and the quantum-to-classical transition*, Springer Science & Business Media, **2007**.

[67] A. Beige, D. Braun, B. Tregenna, P. L. Knight, *Physical Review Letters* **2000**, *85*, 1762.

[68] M. S. Byrd, D. A. Lidar, *Physical Review Letters* **2002**, *89*, 047901.

[69] T. Albash, D. A. Lidar, *Physical Review A* **2015**, *91*, 062320.

[70] J. McFadden, J. Al-Khalili, *Proceedings of the Royal Society A* **2018**, *474*, 20180674.

[71] A. Marais, B. Adams, A. K. Ringsmuth, M. Ferretti, J. M. Gruber, R. Hendrikx, M. Schuld, S. L. Smith, I. Sinayskiy, T. P. Krüger, et al., *Journal of the Royal Society Interface* **2018**, *15*, 20180640.

[72] G. Homa, J. Z. Bernád, L. Lisztes, *The European Physical Journal D* **2019**, *73*, 1–13.

[73] G. Lindblad, *Communications in Mathematical Physics* **1976**, *48*, 119–130.

[74] V. Gorini, A. Kossakowski, E. C. G. Sudarshan, *Journal of Mathematical Physics* **1976**, *17*, 821–825.

[75] S. Kohler, T. Dittrich, P. Hänggi, *Physical Review E* **1997**, *55*, 300.

[76] L. Diósi, *Physica A: Statistical Mechanics and its Applications* **1993**, *199*, 517–526.

[77] P. Pechukas, *Physical Review Letters* **1994**, *73*, 1060.

[78] R. Karrlein, H. Grabert, *Physical Review E* **1997**, *55*, 153.

[79] R. Alicki, *Physical Review Letters* **1995**, *75*, 3020.

[80] J. M. Dominy, A. Shabani, D. A. Lidar, *Quantum Information Processing* **2016**, *15*, 465–494.

[81] S. Nakajima, *Progress of Theoretical Physics* **1958**, *20*, 948–959.

[82] R. Zwanzig, *The Journal of Chemical Physics* **1960**, *33*, 1338–1341.

[83] S. Vinjanampathy, J. Anders, *Contemporary Physics* **2016**, *57*, 545–579.

[84] R. Alicki, R. Kosloff in *Thermodynamics in the Quantum Regime*, Springer, **2018**, pp. 1–33.

[85] J. Millen, A. Xuereb, *New Journal of Physics* **2016**, *18*, 011002.

[86] S. Deffner, S. Campbell, *Quantum Thermodynamics: An introduction to the thermodynamics of quantum information*, Morgan & Claypool Publishers, **2019**.

[87] M. Popovic, M. T. Mitchison, J. Goold, *arXiv preprint arXiv:2107.14216* **2021**.

[88] M. B. Plenio, V. Vitelli, *Contemporary Physics* **2001**, *42*, 25–60.

[89] K. Funo, H. Quan, *Physical Review Letters* **2018**, *121*, 040602.

[90] H. Kwon, H. Jeong, D. Jennings, B. Yadin, M. S. Kim, *Physical Review Letters* **2018**, *120*, 150602.

[91] A. Deville, Y. Deville, *The European Physical Journal H* **2013**, *38*, 57–81.

[92] L. Del Rio, J. Åberg, R. Renner, O. Dahlsten, V. Vedral, *Nature* **2011**, *474*, 61–63.

[93] E. Y. Chua, *Philosophy of Science* **2021**, *88*, 145–168.

[94] M. Hemmo, O. Shenker, *Philosophy of Science* **2006**, *73*, 153–174.

[95] R. Landauer, *IBM Journal of Research and Development* **1961**, *5*, 183–191.

[96] C. H. Bennett, *Studies In History and Philosophy of Science Part B: Studies In History and Philosophy of Modern Physics* **2003**, *34*, 501–510.

[97] R. P. Feynman, A. R. Hibbs, D. F. Styer, *Quantum mechanics and path integrals*, Courier Corporation, **2010**.

[98] N. Huggett, R. Weingard, *Synthese* **1995**, *102*, 171–194.

[99] M. Fannes, B. Nachtergaele, A. Verbeure, *EPL (Europhysics Letters)* **1987**, *4*, 963.

[100] A. T. Dorsey, M. P. Fisher, M. S. Wartak, *Physical Review A* **1986**, *33*, 1117.

[101] H. Dekker, *Physica A: Statistical Mechanics and its Applications* **1987**, *146*, 375–386.

[102] L. Magazzù, A. Carollo, B. Spagnolo, D. Valenti, *Journal of Statistical Mechanics: Theory and Experiment* **2016**, *2016*, 054016.

[103] A. O. Caldeira, A. J. Leggett, *Annals of Physics* **1983**, *149*, 374–456.

[104] R. P. Feynman, F. L. Vernon, *Annals of Physics* **1963**, DOI 10.1016/0003-4916(63)90068-X.

[105] K. Modi, *Scientific Reports* **2012**, *2*, 1–5.

[106] A. Smirne, H.-P. Breuer, J. Piilo, B. Vacchini, *Physical Review A* **2010**, *82*, 062114.

[107] K. Möhring, U. Smilansky, *Nuclear Physics A* **1980**, *338*, 227–268.

[108] J. Carmona, J. Cortés, *Physical Review D* **2001**, *65*, 025006.

[109] S. Roy, A. Venugopalan, *arXiv preprint quant-ph/9910004* **1999**.

[110] J. Weinbub, D. Ferry, *Applied Physics Reviews* **2018**, *5*, 041104.

[111] R. Cabrera, D. I. Bondar, K. Jacobs, H. A. Rabitz, *Physical Review A* **2015**, *92*, 042122.

[112] C. W. Gardiner et al., *Handbook of stochastic methods*, *Vol. 3*, springer Berlin, **1985**.

[113] B. Delamotte, *American Journal of Physics* **2004**, *72*, 170–184.

[114] V. Bach, T. Chen, J. Fröhlich, I. M. Sigal, *Journal of Functional Analysis* **2007**, *243*, 426–535.

[115] K. G. Wilson, *Reviews of Modern Physics* **1983**, *55*, 583.

[116] J. Polchinski, *arXiv preprint hep-th/9210046* **1992**.

[117] K. G. Wilson, *Reviews of Modern Physics* **1975**, *47*, 773.

[118] J. Bain, *Effective field theories*, na, **2013**.

[119] A. Bonanno, V. Branchina, H. Mohrbach, D. Zappala, *Physical Review D* **1999**, *60*, 065009.

[120] K.-I. Aoki, A. Horikoshi, *Physical Review A* **2002**, *66*, 042105.

[121] J. Kovács, B. Fazekas, S. Nagy, K. Sailer, *Annals of Physics* **2017**, *376*, 372–381.

[122] K.-I. Aoki, *International Journal of Modern Physics B* **2000**, *14*, 1249–1326.

[123] Á. Rivas, S. F. Huelga, M. B. Plenio, *Physical Review Letters* **2010**, *105*, 050403.

[124] M.-D. Choi, *Linear Algebra and its Applications* **1975**, *10*, 285–290.

[125] P. Strasberg, M. Esposito, *Physical Review E* **2019**, *99*, 012120.

[126] Á. Rivas, *Physical Review Letters* **2020**, *124*, 160601.

[127] M. Popovic, B. Vacchini, S. Campbell, *Physical Review A* **2018**, *98*, 012130.

[128] S. Bhattacharya, A. Misra, C. Mukhopadhyay, A. K. Pati, *Physical Review A* **2017**, *95*, 012122.

[129] S. Marcantoni, S. Alipour, F. Benatti, R. Floreanini, A. Rezakhani, *Scientific Reports* **2017**, *7*, 1–8.

[130] H.-P. Breuer, E.-M. Laine, J. Piilo, *Physical Review Letters* **2009**, *103*, 210401.

[131] E.-M. Laine, J. Piilo, H.-P. Breuer, *Physical Review A* **2010**, *81*, 062115.

[132] C. L. Latune, I. Sinayskiy, F. Petruccione, *Physical Review A* **2020**, *102*, 042220.

[133] J. J. Park, H. Nha, S. W. Kim, V. Vedral, *Physical Review E* **2020**, *101*, 052128.

[134] G. Lindblad, *Communications in Mathematical Physics* **1975**, *40*, 147–151.

[135] C. Fleming, A. Roura, B. Hu, *Annals of Physics* **2011**, *326*, 1207–1258.

[136] I. De Vega, D. Alonso, *Reviews of Modern Physics* **2017**, *89*, 015001.

[137] H.-P. Breuer, *Physical Review A* **2004**, *70*, 012106.

[138] L. Ferialdi, *Physical Review Letters* **2016**, *116*, 120402.

[139] L. Ferialdi, *Physical Review A* **2017**, *95*, 020101.

[140] S. Maniscalco, F. Petruccione, *Physical Review A* **2006**, *73*, 012111.

[141] L. Diósi, W. T. Strunz, *Physics Letters A* **1997**, *235*, 569–573.

[142] D. Alonso, I. de Vega, *Physical Review A* **2007**, *75*, 052108.

[143] E. S. Fraga, G. Krein, L. F. Palhares, *Physica A: Statistical Mechanics and its Applications* **2014**, *393*, 155–172.

[144] H. Kleinert, S. Shabanov, *Physics Letters A* **1995**, *200*, 224–232.

[145] Y. Tanimura, R. Kubo, *Journal of the Physical Society of Japan* **1989**, *58*, 101–114.

[146] G. Guarnieri, J. Nokkala, R. Schmidt, S. Maniscalco, B. Vacchini, *Physical Review A* **2016**, *94*, 062101.

[147] F. Grossmann, W. Koch, *The Journal of Chemical Physics* **2009**, *130*, 034105.

[148] S. Einsiedler, A. Ketterer, H.-P. Breuer, *Physical Review A* **2020**, *102*, 022228.

[149] H. Khesbak, O. Savchuk, S. Tsushima, K. Fahmy, *Journal of the American Chemical Society* **2011**, *133*, 5834–5842.

[150] S. T. Van Der Post, C.-S. Hsieh, M. Okuno, Y. Nagata, H. J. Bakker, M. Bonn, J. Hunger, *Nature Communications* **2015**, *6*, 1–7.

[151] S.-Y. Sheu, D.-Y. Yang, H. Selzle, E. Schlag, *Proceedings of the National Academy of Sciences* **2003**, *100*, 12683–12687.

[152] C. Zhong, F. Robicheaux, *Physical Review A* **2016**, *94*, 052109.

[153] H. Wang, M. Hofheinz, M. Ansmann, R. Bialczak, E. Lucero, M. Neeley, A. O'Connell, D. Sank, M. Weides, J. Wenner, et al., *Physical Review Letters* **2009**, *103*, 200404.

[154] M. Lostaglio, K. Korzekwa, D. Jennings, T. Rudolph, *Physical Review X* **2015**, *5*, 021001.

[155] S. Kallush, A. Aroch, R. Kosloff, *Entropy* **2019**, *21*, 810.

[156] X. Cai, Y. Zheng, *The Journal of Chemical Physics* **2018**, *149*, 094107.

[157] L. Mazzola, J. Piilo, S. Maniscalco, *Physical Review Letters* **2010**, *104*, 200401.

[158] B. Bylicka, M. Tukiainen, D. Chruściński, J. Piilo, S. Maniscalco, *Scientific Reports* **2016**, *6*, 1–7.

[159] D. Chruściński, A. Kossakowski, Á. Rivas, *Physical Review A* **2011**, *83*, 052128.

[160] C. Hörhammer, H. Büttner, *Journal of Statistical Physics* **2008**, *133*, 1161–1174.

[161] G. Thomas, N. Siddharth, S. Banerjee, S. Ghosh, *Physical Review E* **2018**, *97*, 062108.

[162] M. Debiossac, D. Grass, J. J. Alonso, E. Lutz, N. Kiesel, *Nature Communications* **2020**, *11*, 1–6.

[163] S. Hesabi, D. Afshar, *Physics Letters A* **2021**, 127482.

[164] N. Ashcroft, N. Mermin, *New York* **1976**.

[165] U. Kleinekathöfer, *The Journal of Chemical Physics* **2004**, *121*, 2505–2514.

[166] W. Cui, Z. R. Xi, Y. Pan, *Physical Review A* **2008**, *77*, 032117.

[167] H. Wang, X. Song, D. Chandler, W. H. Miller, *The Journal of Chemical Physics* **1999**, *110*, 4828–4840.

[168] H.-M. Zou, R. Liu, D. Long, J. Yang, D. Lin, *Physica Scripta* **2020**, *95*, 085105.

[169] M. Thoss, H. Wang, W. H. Miller, *The Journal of Chemical Physics* **2001**, *115*, 2991–3005.

[170] W. Luxemburg, *The American Mathematical Monthly* **1971**, *78*, 970–979.

[171] J. Spiechowicz, J. Łuczka, *Scientific Reports* **2021**, *11*, 1–12.

[172] B. Spreng, G.-L. Ingold, U. Weiss, *Physica Scripta* **2015**, *2015*, 014028.

[173] C. Karlewski, M. Marthaler, *Physical Review B* **2014**, *90*, 104302.

[174] J. Iles-Smith, A. G. Dijkstra, N. Lambert, A. Nazir, *The Journal of Chemical Physics* **2016**, *144*, 044110.

[175] S. A. Adelman, *The Journal of Chemical Physics* **1976**, *64*, 124–130.

[176] P. Schramm, R. Jung, H. Grabert, *Physics Letters A* **1985**, *107*, 385–389.

[177] H. Dekker, *Physics Reports* **1981**, *80*, 1–110.

[178] W. Unruh, W. H. Zurek, *Physical Review D* **1989**, *40*, 1071.

[179] J. Halliwell, T. Yu, *Physical Review D* **1996**, *53*, 2012.

[180] R. Dillenschneider, E. Lutz, *Physical Review E* **2009**, *80*, 042101.

[181] P. Ullersma, *Physica* **1966**, *32*, 56–73.

[182] B. Ahmadi, S. Salimi, A. Khorashad, *Scientific Reports* **2021**, *11*, 1–9.

[183] R. Alicki, M. Horodecki, P. Horodecki, R. Horodecki, *Open Systems & Information Dynamics* **2004**, *11*, 205–217.

[184] J. J. Park, K.-H. Kim, T. Sagawa, S. W. Kim, *Physical Review Letters* **2013**, *111*, 230402.

[185] S. W. Kim, T. Sagawa, S. De Liberato, M. Ueda, *Physical Review Letters* **2011**, *106*, 070401.

[186] B. Çakmak, *Physical Review E* **2020**, *102*, 042111.

[187] K. Korzekwa, M. Lostaglio, J. Oppenheim, D. Jennings, *New Journal of Physics* **2016**, *18*, 023045.

[188] M. O. Scully, M. S. Zubairy, G. S. Agarwal, H. Walther, *Science* **2003**, *299*, 862–864.

[189] P. Kammerlander, J. Anders, *Scientific Reports* **2016**, *6*, 1–7.

[190] A. Godbeer, J. Al-Khalili, P. Stevenson, *Physical Chemistry Chemical Physics* **2015**, *17*, 13034–13044.

[191] M. M. Ali, W.-M. Huang, W.-M. Zhang, *Scientific Reports* **2020**, *10*, 1–16.

[192] M. Thorwart, E. Paladino, M. Grifoni, *Chemical Physics* **2004**, *296*, 333–344.

[193] D. Gribben, A. Strathearn, J. Iles-Smith, D. Kilda, A. Nazir, B. W. Lovett, P. Kirton, *Physical Review Research* **2020**, *2*, 013265.

[194] A. Garg, J. N. Onuchic, V. Ambegaokar, *The Journal of Chemical Physics* **1985**, *83*, 4491–4503.

[195] I. S. Gradshteyn, I. M. Ryzhik, *Table of integrals, series, and products*, Academic press, **2014**.